

University of Nottingham
UK | CHINA | MALAYSIA

Department of Architecture and Built Environment

Faculty of Engineering

Investigation of Open Cycle Thermochemical Energy Storage System in Building Application

Thesis by

Yanan ZHANG (BEng, MSc)

ID: 14284459

Supervisors: Prof. Saffa Riffat, Dr. Guohui Gan

Thesis submitted to the University of Nottingham

For the degree of Doctor of Philosophy

2020

ABSTRACT

In this study, it is aimed to design, develop and evaluate a high-performance thermochemical energy storage (TES) system for building sectors, which is based on material, reactor and process investigations. The TES system can be integrated with and driven by any kind of low temperature sustainable energy sources (e.g. solar energy, wind energy, and waste heat recovery system) to reduce fossil fuel consumption and greenhouse gas (GHG) emissions. In achieving the aims, eight aspects have been set out as followed: 1) A comprehensive literature survey on potential TES materials; 2) Evaluation of the cooling and heat storage capacity of the proposed materials using IES; 3) Selection of salt hydrate mixture and host matrix sorbents; 4) By using SDT-Q600, MIP and SEM to perform material characterisation analysis; 5) Set up some small scale experiments to analyse the characteristics of selected composites; 6) Test the thermochemical performance in a designed small-scale reactor; 7) Design and test a TES prototype in lab under UK weather condition; 8) Economic, environmental and techno-social analyses of the designed TES system.

In the initial experimental work, the three candidates were tested in the lab-scaled rig. V-$CaCl_2$-LiCl showed the highest water uptake of 0.12g/g in the 1st discharging cycle, but in the 2nd discharging process was much lower. The water uptake of V-$MgSO_4$-LiCl was 0.1g/g in 1st reaction process which was twice as the 2nd cycle that means V- $MgSO_4$-LiCl is not suitable for multiple cycles, moreover, the small water loss in charging process led to low regeneration efficiency. V-$MgSO_4$-$CaCl_2$ with weight ratio of 1:1:2 showed good potential for using in open THS systems. Although the water uptake was less, the air outlet temperature can reach as high as 46.1 °C and the water uptake in 2nd cycle stayed very similar with discharging cycle 1. Thus,

V- $MgSO_4$-$CaCl_2$ with weight ratio of 1:1:2 was chosen as the testing TES material in prototype. An open TES prototype with 16 kg V-$MgSO_4$-$CaCl_2$ was numerically and experimentally investigated. In the original prototype, the system showed poor performance in the discharging/reaction process because of some design flaws with lower relative humidity level and the highest air supply temperature was 37.44 °C with reaction COP of 1.05-1.2. Then the designed prototype was modified and optimized by changing the holding plate and placing humidifier in front of centrifugal fan. After that the prototype gave satisfactory results with air outlet temperature was as high as 43.1 °C to supply 2.88 kWh heating energy with COP of 1-1.51. It will be used for short-term TES storage as the system can easily provide enough heating demand daily usage.

The economic and environmental analyses results showed that TES system shows a quick payback period of 6.4 years and a large reduction of 2136.7kg/year on CO_2 emissions compared with conventional natural gas heating system. Technically and economically, the system has proven to be effective in reducing fossil fuel consumption and CO_2 emission, so it is only a matter of time before these systems are installed in houses in the UK and globally.

LIST OF PUBLICATIONS

JOURNAL PAPER:

Jarimi, H., Aydin, D., Zhang, Y., Ding, Y., Ramadan, O., Chen, X., ... & Riffat, S. (2017). *Materials characterization of innovative composite materials for solar-driven thermochemical heat storage (THS) suitable for building application.* International Journal of Low-Carbon Technologies, 13(1), 30-42.

Jarimi, H., Aydin, D., Yanan, Z., Ozankaya, G., Chen, X., & Riffat, S. (2018). *Review on the recent progress of thermochemical materials and processes for solar thermal energy storage and industrial waste heat recovery.* International Journal of Low-Carbon Technologies, 14(1), 44-69.

Jarimi, H., Aydin, D., Zhang, Y., Ding, Y., Ramadan, O., Chen, X., ... & Riffat, S. (2018). *Corrigendum: Materials characterization of innovative composite materials for solar-driven thermochemical heat storage (THS) suitable for building application.* International Journal of Low-Carbon Technologies.

Yuan Yuan*, Yanan Zhang and Saffa Riffat (2018), *A New Composite Adsorbent Material for Water Moisture Adsorption.* Renewable Bioresources, 6(1).

Kutlu, C., Zhang, Y., Elmer, T., Su, Y., & Riffat, S. (2020). *A Simulation Study on Performance Improvement of Solar Assisted Heat Pump Hot Water System by Novel Controllable Crystallisation of Supercooled PCMs.* Renewable Energy.

CONFERENCE PAPER:

Yanan Zhang, Yate Ding, Hasila Jarimi, Omar Ramadan, Saffa Riffat. (2017). *A state-of-the-art review on thermochemical cooling system,* SET2017 – 16th International Conference on Sustainable Energy Technologies, Italy, Bologna.

Omar Ramadan, Yate Ding, Hasila Jarimi, Yanan Zhang and Saffa Riffat. (2017). *Synthesis and Characterization of Salt in Matrix composite materials for open cycle thermochemical heat storage for building applications,* SET2017 – 16th International Conference on Sustainable Energy Technologies, Italy, Bologna.

Hasila Jarimi, Aydin Devrim, Ding Yate, Ramadan Omar, Yanan Zhang and Saffa Riffat. (2017). *Thermochemical heat storage materials,* SET2017 – 16th International Conference on Sustainable Energy Technologies, Italy, Bologna.

Yanan Zhang, Yate Ding, Auwal Dodo, Saffa Riffat. (2018). *Open system and materials of thermochemical energy storage in built environment,* SET2018 – 17th International Conference on Sustainable Energy Technologies, Wuhan, China.

Yuan Yijun, Yanan Zhang, Saffa Riffat. (2018). *A new composite adsorbent material for water moisture adsorption,* SET2018 – 17th International Conference on Sustainable Energy Technologies, Wuhan, China.

Auwal Dodo, Yanan Zhang, Yate Ding, Saffa Riffat. (2018). *Innovative Open Sorption Thermochemical Energy Storage System for Building Applications,* SET2018 – 17th International Conference on Sustainable Energy Technologies, Wuhan, China.

Yanan Zhang, Yate Ding, Auwal Dodo, Saffa Riffat. (2018). *Thermochemical Heating/Cooling Storage Materials in Energy System for Built Environment,* SEEDS2018 – Sustainable Ecological Engineering Design for Society, Dublin, Ireland.

Yanan ZHANG, Cagri KUTLU, Sam GLEDHILL, Adam DICKEN, Zafer URE, Theo ELMER, Andrew CUNNINGHAM, Kitty CUNNINGHAM, Lizhi ZHANG, Guozhong YANG, Huaguan ZHANG, Saffa RIFFAT (2019). *Novel technology of solar assisted domestic hot water (DHW) system with supercooled PCMs - The characteristics analysis of a selected PCM*, SET2019 – 18th International Conference on Sustainable Energy Technologies, Kuala Lumpur, Malaysia.

Yanan ZHANG, Auwal DODO, Yijun Yuan, Saffa RIFFAT (2019). *A prototype of thermochemical heat storage system for space heating in building*, SET2019 – 18th International Conference on Sustainable Energy Technologies, Kuala Lumpur, Malaysia.

ACKNOWLEDGEMENT

First of all, I would like to express my sincere gratitude to my advisor Professor Saffa Riffat for the continuous support of my Ph.D. study and every step of my research, for his patience, motivation, and immense knowledge. He is not only the supervisor of my study, but also the mentor of my life. I am very proud of being your student and thank you for your great support and guidance. I also want to thank my additional supervisor Dr. Gan Guohui; thanks for his support for my academic research.

I want to special thank my parents. Like in every stage of my life, they gave me as far as possible financial support, spiritual support and infinite care during my four years Ph.D. studies. They make me to grow up and learn in a sweetest family filled with love, and give me indispensable support for my academic, growth and life. They taught me how to give, how to help others, and how to love people. They are ordinary people, but also great people.

Further thanks to Dr. Siddig Omer, Dr. Hasila Jarimi, Dr. Auwal Dodo, Dr. Yate Ding Dr. Omar Ramadan, Prof. Zafer Utlu and Dr. Devrim Aydin for sharing their knowledge and helping me both technically and academically. Also, I would like to thank Ms Zeny Amante Roberts and Ms Celia Berry, and the staff of the Department of Architecture and Built Environment for their sincere help. I also wish to acknowledge the Newton Fund Institutional Links (Award ref 216229499) and Engineering and Physical Sciences Research Council (Award ref AAM118072-EOI) for supporting our project. I am greatly indebted to all friends in Nottingham for their precious friendship. Their companion painted bright colours to my life.

Last but not least, I would especially like to thank Dr. Xiao LI, he is my husband, my friend and my love, who supports my spiritual life, who maintains my family relationship, who prepares dinner for me every day without any complain. He is my strongest support; without him I would not be able to complete my journey. His courage and conviction is always my motivation.

TABLE OF CONTENTS

ABSTRACT ..... **I**

LIST OF PUBLICATIONS ..... **III**

ACKNOWLEDGEMENT ..... **VI**

TABLE OF CONTENTS ..... **VIII**

NOMENCLATURE ..... **XIII**

LIST OF FIGURES ..... **XVII**

LIST OF TABLES ..... **XXV**

1 INTRODUCTION **1**

1.1 Background Information 1

1.2 Energy Consumption And Demand Investigate 3

1.3 Topic Of The Study 5

1.4 Aims And Objectives Of The Research 6

1.5 Novelty of The Research 8

1.6 Thesis Structure 10

2 LITERATURE REVIEW ON THERMOCHEMICAL ENERGY STORAGE **14**

2.1 Introduction 14

2.2 Thermal Energy Storage System 14

2.3 Classification Of Thermal Energy Storage 15

2.4 Phase Change Materials 18

2.4.1 Background information 18

2.4.2 Classification and applications of PCMs 20

2.4.3 PCM Applications in thermal energy storage 21

2.5 Thermochemical Energy Storage 22

2.5.1 Closed thermal energy storage system for heating application 27

2.5.2 Closed thermochemical energy storage system for cooling application 29

2.5.3 Open thermal energy storage system 34

2.5.4 Open thermochemical cooling storage system 46

2.6 SUMMARY 63

3 RESEARCH METHODOLOGY 66

3.1 BACKGROUND INVESTIGATION AND LITERATURE REVIEW 66

3.2 DESIGN AND MODELLING WORK 66

3.3 SMALL SCALE TESTING WORK IN LAB 66

3.4 LABORATORY SCALE RIG TESTING AND DEVELOPMENT 66

3.5 PROTOTYPE TESTING AND MODIFICATION 67

3.6 LIMITATION OF WORK 67

4 INITIAL EXPERIMENTS FOR CHARACTERISTICS ANALYSIS OF SALT IMPREGNATED TES MATERIALS.. 68

4.1 INTRODUCTION 68

4.2 TES MATERIALS SAMPLES PREPARATION 69

4.2.1 Vermiculite base materials preparation 69

4.2.2 Silica gel based composite: Potassium Formate - Silica Gel 73

4.3 TES MATERIALS CHARACTERISTICS STUDIES 77

4.3.1 TA instruments simultaneous TGA / DSC (SDT-Q600) for TES materials energy density test and analysis 77

4.3.2 Scanning Electron Microscope (SEM) test and analysis 82

4.3.3 Synthesised samples: Al_2O_3 - LiCl 83

4.3.4 Synthesised samples: Al_2O_3 - $CaCl_2$ 85

4.4 SORPTION TEST AND ANALYSIS FOR TES MATERIALS 87

4.4.1 Method 87

4.4.2 Calibration 88

4.4.3 Sorption test 89

4.4.4 Results and analysis 89

4.5 THERMAL HEATING STORAGE TEST - HEATING BOX TEST WITH SOLID CACL2 92

4.6 THERMOCHEMICAL COOLING CAN TEST AND ANALYSIS 96

4.7 Experiment Designs for An Open Thermochemical Cooling Storage System 99

4.7.1 Introduction of the experiment 99

4.7.2 Aims 99

4.7.3 Experiment rig set-up and methodology 101

4.7.4 Results and analysis 108

4.7.5 Comparison of the Experiments and Conclusion 110

4.8 Summary 110

5 COMPUTER SIMULATION FOR THERMOCHEMICAL HEATING/COOLING STORAGE SYSTEM 112

5.1 Introduction 112

5.2 Modelling House 112

5.3 Solar Heat Gain and Total Heat Gain of the Modelling House 116

5.4 Modelling of the Heating and Cooling Load of the House 125

5.4.1 Thermochemical heating energy simulation results and analysis 125

5.4.2 Thermochemical cooling energy simulation results and analysis 125

5.4.3 Analysing thermochemical heating and cooling storage materials and sizing 126

5.5 Simulated Thermochemical Heat Storage Evacuated Tube for Materials Tests and Analysis 127

5.5.1 Introduction 127

5.5.2 Simulated experimental cycle 131

5.6 Result and Analysis 135

5.7 Summary 136

6 SALT IMPREGNATED TES MATERIALS TESTS IN OPEN CYCLE THERMOCHEMICAL ENERGY STORAGE RIG 138

6.1 Introduction 138

6.2 Aim 138

6.3 Experimental Design 139

6.4 Experiment Process and Results 143

6.4.1 V-$CaCl_2$-LiCl (weight ratio 1:2:1) 144

6.4.2 V-$MgSO_4$-LiCl (weight ratio 1:2) 149

6.4.3 V-$MgSO_4$-$CaCl_2$ (weight ratio 1:1) *153*

6.4.4 V-$MgSO_4$-$CaCl_2$ (weight ratio 1:2) *157*

6.5 CALIBRATION 162

6.6 ANALYSIS 162

6.7 SUMMARY 166

7 THE PROTOTYPE OF AN OPEN CYCLE FOR THERMOCHEMICAL HEAT STORAGE SYSTEM 167

7.1 INTRODUCTION 167

7.2 EXPERIMENT DESIGNS FOR THE PROTOTYPE OF OPEN THERMOCHEMICAL HEAT STORAGE SYSTEM 172

7.2.1 Experiment rig set-up *172*

7.2.2 Results and analysis *176*

7.2.3 Summary of the Real Prototype *178*

7.3 THE MODIFIED PROTOTYPE AND THE RESULT 178

7.3.1 The description of the modified prototype *178*

7.3.2 Result and analysis *181*

7.4 SUMMARY 189

8 ECONOMIC AND ENVIRONMENTAL ANALYSIS 191

8.1 INTRODUCTION 191

8.2 ECONOMIC ANALYSIS 192

8.2.1 Capital cost and payback period *192*

8.2.2 Life cycle cost saving *194*

8.3 ENVIRONMENTAL ANALYSIS 197

8.4 SUMMARY 198

9 CONCLUSION, RECOMMANDATIONS AND FUTURE WORKS 199

9.1 SUMMARY OF THE WORK 199

9.2 CONCLUSIONS 200

9.3 RECOMMENDATION AND FUTURE WORK 204

9.3.1 Development of the open TES system with solar PV driven *204*

9.3.2 Proposed solar driven thermochemical energy storage system (SeasonalStorage) 205

9.3.3 Long Term Thermochemical Energy Storage System 207

REFERENCES 209

APPENDIX A: TA INSTRUMENT ANALYSIS RUNNING RESULTS FOR SDT-Q600 222

APPENDIX B: SCANNING ELECTRON MICROSCOPY PHOTOS 235

NOMENCLATURE

Symbol	Term	Unit
C	Total Heat Loss Coefficient	kW/K
C_0	Initial Investment	£
C_p	Specific Heat Capacity	J/kg·K
C_t	Net Cash Inflow During the Period	£
D	Degree Days	°C·days
E	Heating Energy Demand	kWh
E_f	An Energy Consumption	kWh
G	Solar Irradiance	kW/m^2
m_c	Mass of Working Fluid	kg
NPV	Net Present Value	£
P	Ambient Pressure	MPa
P_c	Critical Pressure	MPa
P_T	Total Power Input	W, kW
P_w	Water Vapor Pressure	MPa
P_{ws}	Saturated Water Vapor Pressure	MPa
Q	Thermal Power, Power Input	W, kW
r	Discount Rate	%
RH	Relative Humidity	%
T	Temperature of The Working Fluid	K
T_c	Critical Temperature	K
ΔH_c	Reaction Enthalpy Per kg	kJ/kg

Greek Letter	Term	Unit
ŋ	Efficiency	%
α	Solar Absorptance	
Δ	Difference	
λ	Thermal Conductivity	W/m/K
ρ	Density	kg/m^3
τ	Cover Glass Tube Transmittance	%
υ	Kinematic Viscosity	m^2/s

Subscripts and Superscripts

0	Initial Cycle
a	Air
c	Critical
in	Inlet
out	Outlet
t	Number of Cycles
w	Water, Water Vapour
ws	Saturated Water Vapour

Abbreviations

Abbreviation	Term
AC	Active Carbon
ACF	Activated Carbon Fibre
ACS	Adsorption Cooling System
AEE INTEC	AEE - Institute for Sustainable Technologies

AR	Area Ratio
AT	Attapulgite
BC	Before Christ
CAGR	Compound Annual Growth Rate
CFCs	Chlorofluorocarbons
CHP	Combined Heat and Power
CNK	Cankiri Region
COP	Coefficient of Performance
DCHE	Desiccant Coated Heat Exchanger
DHW	Domestic Hot Water
DRH	Deliquescence Relative Humidity
DSC	Differential Scanning Calorimetry
EG	Expanded Graphite
EMC	A Chemical Heat Storage Composite Material
EU	European Union
GHG	Greenhouse Gas
HCFC	Hydrochlorofluorocarbons
HFC	Hydrofluoro Carbons
HP	Heat Pump
HRD	Heat Recovery Device
IDCS	Integrated Desiccant Air Conditioning System
IES	Integrated Environmental Solutions
IRR	Internal Rate of Return
KCOOH	Potassium Formate
LCoE	Levelized Cost of Energy

LHS	Latent Heat Storage
LLP	Lalapaşa-Edirne Region
MIP	Mercury Intrusion Porosimetry
MOF	Metal-Organic Framework
NPV	Net Present Value
PCM	Phase Change Material
PID	Proportional–Integral–Derivative
PR	Productivity Rate
PV	Photovoltaic
RH	Relative Humidity
RSD	Reşadiye-Tokat Region
SCP	Specific Cooling Power
SDC	Solid Desiccant Cooling
SDT	Simultaneous Dsc and Tga
SEM	Scanning Electron Microscopy
SG	Silica Gel
SHS	Sensible Heat Storage
TES	Thermochemical Energy Storage
TGA	Thermogravimetric Analysis
THS	Thermochemical Heat Storage
TSRDC	Two-Stage Rotary Desiccant Cooling
V	Vermiculite
VCRS	Vapour Compression System
VE	Virtual Environment
WSS	Wakkanai Siliceous Shale

LIST OF FIGURES

Figure 1-1 Chemical storage classification. [3, 9] 2

Figure 1-2 Sorption thermal storage classification. [3] 3

Figure 1-3 (a) UK electricity generation by source, terawatt hours (TWh), 1996-2018; (b) Shares of UK electricity generation (%)[11]. 4

Figure 1-4 Flowchart of research work. 13

Figure 2-1 Classification of thermal energy storage. [28] [29] 16

Figure 2-2 Global Energy Storage Database[66]. 23

Figure 2-3 Energy density of PCM, sorption and chemical reaction process. [71] [9, 73, 74] 25

Figure 2-4 Processes of closed thermochemical energy storage system. [77] 27

Figure 2-5 A closed cycle of $CaCl_2$ solar heating system. [82] 29

Figure 2-6 Solar thermal absorption cooling system (STACS). [89] 30

Figure 2-7 Operation principle of closed adsorption system[97]. 32

Figure 2-8 Solar photovoltaic vapour compression system [100]. 33

Figure 2-9 Charging and discharging process in open thermochemical energy storage system. [77, 103] 35

Figure 2-10 Sorption process on silica gel with $CaCl_2$ [3] [105]. 36

Figure 2-11 Solar driven open sorption thermochemical heat storage system [107]. 40

Figure 2-12 Photographs of prototype thermochemical storage system, (a) before and (b) after insulation [107]. 41

Figure 2-13 Schematic representation of thermochemical reactor storage system setup [107]. 42

Figure 2-14 Classification of chemical heat pumps [141, 142]. 43

Figure 2-15 Schematic drawing of the prototype SOLUX [144]..... 44
Figure 2-16 Photographs of the prototype SOLUX in construction [144]. 45
Figure 2-17 Principles of the magnesium oxide/water chemical heat pump: (a) heat storage operation and (b) heat supply operation. [147]..... 46
Figure 2-18 Exergy efficiency with relative humidity and ambient temperature. [163] 50
Figure 2-19 Schematic diagram of solar thermal and electric driven desiccant air conditioning system. [173]..... 52
Figure 2-20 Main types of solid and liquid desiccants. [175]..... 53
Figure 2-21 Systematic diagram of solid desiccant cooling system. [176] 54
Figure 2-22 Classification of advanced desiccant materials. [185]..... 57
Figure 4-1: 600g pure vermiculite is put in a mesh tray for drying..... 73
Figure 4-2 (a) Potassium formate solution; (b) Potassium formate solution with a thin layer of crystal. 75
Figure 4-3 Dried potassium formate solid and powder..... 75
Figure 4-4 Grinded mixture of silica gel with potassium formate..... 76
Figure 4-5 (a) Sorption test of silica gel with potassium formate; (b) Silica gel with potassium formate mixture after 7 days in the water pot..... 76
Figure 4-6 SDt-Q600 for materials energy density analysis..... 77
Figure 4-7 The inside detail of SDT-Q600..... 78
Figure 4-8 Al_2O_3 based SIM composite..... 80
Figure 4-9 Small pieces of materials paste on the holder for SEM. 81
Figure 4-10 Al_2O_3 based materials were cut into small pieces for SDT-Q600. 81
Figure 4-11 SEM photos of SIM samples..... 82
Figure 4-12 SEM photos of Al_2O_3 – LiCl under different magnification. 83

Figure 4-13 Al_2O_3-LiCl SDT-Q600 energy density analysis - 001. 84
Figure 4-14 Al_2O_3-LiCl SDT-Q600 energy density analysis - 002. 84
Figure 4-15 SEM photos of Al_2O_3 - $CaCl_2$ under different magnification. 85
Figure 4-16 Al_2O_3-$CaCl_2$ SDT-Q600 energy density analysis 001. 86
Figure 4-17 Al_2O_3-$CaCl_2$ SDT-Q600 energy density analysis 002. 86
Figure 4-18 Sorption testing set. 87
Figure 4-19 Mass change readings of V-$CaCl_2$-LiCl. 90
Figure 4-20 Mass change readings of V-$MgSO_4$-$MgCl_2$. 90
Figure 4-21 Mass change readings of V-$MgSO_4$-$CaCl_2$. 91
Figure 4-22 Mass change readings of V-$MgSO_4$-LiCl. 91
Figure 4-23 Each part of the $CaCl_2$ box test. 93
Figure 4-24 Details in the $CaCl_2$ test box with thermocouples. 94
Figure 4-25 Temperature change in $CaCl_2$ heating text box. 95
Figure 4-26 Cooling can test with urea. 97
Figure 4-27 Diagram of the cooling can test with Urea. 97
Figure 4-28 Urea cooling can test temperature change. 98
Figure 4-29 Heat pipes with fins at each end. 100
Figure 4-30 Diagram of the cooling box with heat pipes. 102
Figure 4-31 Cooling test box with heat pipes. 103
Figure 4-32 Cooling provider box with fan on the top and a sensor on the fan to record the cooled air temperature. 103
Figure 4-33 Heat pipes were insulated well to protect heat. 104
Figure 4-34 Sensor was put inside composite to record temperature changing. 104
Figure 4-35 Composites after test in reaction box (full of moisture). 107
Figure 4-36 The heat pipe in reaction box after testing. 107

Figure 4-37 Readings record for all the 5 sensors. 108
Figure 4-38 Temperature between material and inlet temperature (ambient temperature). 108
Figure 4-39 Temperature between ambient temperature (air inlet T) and cooled air outlet temperature. 109
Figure 5-1 Draw of the house. 113
Figure 5-2 IES 3-D model [224] 114
Figure 5-3 IES 3-D model [224] 114
Figure 5-4 IES 3-D model [224] 115
Figure 5-5 House heat loss diagram. 115
Figure 5-6 House induction system. 116
Figure 5-7 Monthly heat gain. 123
Figure 5-8 Daily heating demand. 125
Figure 5-9 Daily cooling demand. 125
Figure 5-10: Schematic drawing of the simulated test rig (Reaction/discharging process) 127
Figure 5-11: Schematic drawing of the simulated test rig (Regeneration/charging process) 128
Figure 5-12: Schematic sectional drawing of solar evacuated tube attached with copper pipe and flexible tube. 128
Figure 5-13 Flow diagram of the simulated solar powered TES system 130
Figure 5-14 Hourly solar irradiation in each month. 132
Figure 5-15 Daily average solar irradiation energy gain in each month of the simulated TES system. 133

Figure 5-16 The simulated TES system monthly total solar irradiation energy gain. 133
Figure 5-17 Daily sunlight hours in Nottingham..... 134
Figure 5-18 Daily average sunlight hours in Nottingham..... 134
Figure 5-19 Daily solar irradiation and heating demand with different materials comparison..... 136
Figure 6-1 Open system for thermochemical energy storage materials test rig.. 140
Figure 6-2 The inside details of the thermochemical energy storage test rig..... 141
Figure 6-3 TES materials testing tray and load cell..... 141
Figure 6-4 TES materials testing tray and thermocouple/sensor. 142
Figure 6-5 Discharging cycle in open loop thermochemical energy storage system. 143
Figure 6-6 Charging cycle in open loop thermochemical energy storage system. 143
Figure 6-7 Temperature record of V-$CaCl_2$-LiCl in 1st discharging process. 144
Figure 6-8 V-$CaCl_2$-LiCl in the mesh tray after 1st discharging process. 145
Figure 6-9 V-$CaCl_2$-LiCl weight change in the 1st reaction process..... 145
Figure 6-10 V-$CaCl_2$-LiCl water uptake change with times in the 1st discharging process..... 146
Figure 6-11 Mesh tray with V-CaCl2-LiCl after charging for one hour..... 146
Figure 6-12 V-$CaCl_2$-LiCl weight change with times in the charging process. 147
Figure 6-13 Temperature record of V-CaCl2-LiCl in 2nd discharging process.... 147
Figure 6-14 V-$CaCl_2$-LiCl weight change with times in the 2nd discharging process. 148

Figure 6-15 V-$CaCl_2$-LiCl water uptake change with times in the 2nd discharging process. 149
Figure 6-16 Temperature record of V-$MgSO_4$-LiCl in 1st discharging process. .. 149
Figure 6-17 V-$MgSO_4$-LiCl in the mesh tray after 1st discharging process. 150
Figure 6-18 V-$MgSO_4$-LiCl weight change in the 1st reaction process. 150
Figure 6-19 V-MgSO4-LiCl water uptake change with times in the 1st discharging process. 151
Figure 6-20 V-$MgSO_4$-LiCl in the mesh tray after charging for 2 hours. 151
Figure 6-21 V-$MgSO_4$-LiCl weight change in the charging process. 152
Figure 6-22 Temperature record of V-$MgSO_4$-LiCl in 2nd discharging process. . 152
Figure 6-23 V-$MgSO_4$-LiCl weight change in the 2st discharging process. 153
Figure 6-24 V-$MgSO_4$-LiCl water uptake change with times in the 2nd discharging process. 153
Figure 6-25 Temperature record of V-$MgSO_4$-$CaCl_2$ (weight ratio 1:1) in 1st discharging process. 154
Figure 6-26 V-$MgSO_4$-$CaCl_2$ (weight ratio 1:1) weight change in the 1st discharging process. 154
Figure 6-27 Water uptake in the 1st discharging process. 155
Figure 6-28 V-$MgSO_4$-$CaCl_2$ (weight ratio 1:1) weight change in the charging process. 155
Figure 6-29 Temperature record of V-$MgSO_4$-$CaCl_2$ (weight ratio 1:1) in 2nd discharging process. 156
Figure 6-30 V-$MgSO_4$-$CaCl_2$ (weight ratio 1:1) weight change in the 2nd discharging process. 156
Figure 6-31 Water uptake in the 2nd discharging process. 157

Figure 6-32 V-$MgSO_4$-$CaCl_2$ in the mesh tray after 1st discharging process. 158
Figure 6-33 Temperature record of V-$MgSO_4$-$CaCl_2$ in 1st discharging process. 158
Figure 6-34 Weight changing record of V-MgSO4-CaCl2 in 1st discharging process. 159
Figure 6-35 Water uptake of V-MgSO4-CaCl2 in 1st discharging process. 159
Figure 6-36 V-$MgSO_4$-$CaCl_2$ weight change in the charging process. 160
Figure 6-37 Temperature record of V-$MgSO_4$-$CaCl_2$ in 2nd discharging process. 160
Figure 6-38 V-MgSO4-$CaCl_2$ water uptake change with times in the 2nd discharging process. 161
Figure 6-39 V-MgSO4-$CaCl_2$ water uptake change with times in the 2nd discharging process. 161
Figure 6-40 Charging and discharging process in open thermochemical energy storage system. 163
Figure 6-41 Different materials characteristics. 163
Figure 6-42 Flow chart of numerical model illustrating the analysis parameter... 164
Figure 6-43 Discharging and charging COP of each material. 165
Figure 6-44 Productivity rate and system efficiency with different materials. 165
Figure 7-1 (a)The detail of TES open cycle prototype; (b) the detail of modified TES open cycle prototype 170
Figure 7-2 The reaction chamber and the holding plate. 171
Figure 7-3 The inside detail of the prototype. 171
Figure 7-4 Open system for thermochemical energy storage materials test rig. . 174
Figure 7-5 Temperature an relative humidity record in charging and discharging process of the prototype. 176

Figure 7-6 Air inlet relative humidity and air outlet temperature record. 176
Figure 7-7 COP of discharging/reaction process. 177
Figure 7-8 The modified prototype discharging process. 178
Figure 7-9 Modified prototype reaction chamber and PID controller. 180
Figure 7-10 PID controller and two dataloggers (one for temperature record and one for relative humidifier record). 181
Figure 7-11 The modified components. 181
Figure 7-12 Temperature record for discharging process test in cycle 1. 182
Figure 7-13 Temperature record for discharging process test in cycle 2. 183
Figure 7-14 Air inlet and outlet relative humidity variation in cycle 1. 184
Figure 7-15 Air inlet and outlet relative humidity variation in cycle 2. 184
Figure 7-16 Water content in discharging process of cycle 1 and cycle 2. 185
Figure 7-17 COP variations in each discharging cycle. 187
Figure 7-18 Relative humidity level in charging/regeneration process. 188
Figure 7-19 Absolute humidity in charging process. 188
Figure 7-20 Temperature variation in charging process. 189
Figure 7-21 COP in charging/regeneration process. 189

LIST OF TABLES

Table 2-1 Previous studies about sorption host materials. 37

Table 2-2 Recent studies of thermochemical cooling materials and performance. 58

Table 4-1 Thermochemical energy storage materials mixture weight ratio. 71

Table 4-2 SDT-Q600 analysis results.(Details of the TA analysis figures will be showed in Appendix) 79

Table 4-3 LoadCell calibration for sorption LoadCell readings. 88

Table 4-4 Sorption test results. 92

Table 4-5 Temperature and time detail of each part. 95

Table 4-6 Temperature changing record of the urea cooling can. 98

Table 5-1 U values of the house and heat loss coefficient. 117

Table 5-2 Dimension of each room. 118

Table 5-3 Typical heat gains. 119

Table 5-4 Monthly heat gains. 122

Table 5-5 Monthly base inside temperature, degree days and energy demand. 124

Table 5-6 TES materials energy storage density and potential sizing. 126

Table 5-7 Performances of different composites. 135

Table 6-1 Thermochemical energy storage test rig calibration. 162

Table 7-1 Components information. 175

Table 7-2 Some parameter performance of the system. 187

Table 8-1 Capital cost for TES systems 193

Table 8-2 The net present value (NPV) analysis method calculation. 195

1 INTRODUCTION

1.1 BACKGROUND INFORMATION

The increasing pollution and bills of fossil fuels cause increasing interest in green energy and clean power to reduce GHG emissions, such as solar energy, biomass, wind power, tidal power and etc. Currently a very important solution to reduce fossil fuel consumption is to use as much renewable energy as possible. Energy system covers a wide range of activities consisting renewable energy generation to help domestic and commercial consumers to reduce energy. It is a key part of community to reduce carbon footprint and energy consumption. However, it is a main gap between sustainable energy supply and consumer demand, improvement should be done for sustainable energy systems [1]. Energy storage system can fill the gap between energy demands and provide by effectively storing excessive energy. Energy stored in 'battery' during changing process and provides energy when needed. Water gravitational potential energy takes part in 'battery' role in tidal power system and solar PV battery is a direct way to store solar energy [2].

Sensible heat storage (SHS) system and latent heat storage (LHS) system are main thermal energy storage technologies. Heat can store in the sensible heat storage materials by the temperature difference and energy density will depend on the materials specific heat as well [3]. For example, water and rock can store heat during the daytime and release heat in the evening. A common latent heat storage technology stores thermal energy through materials phases change process at different temperature [3, 4]. The phase change materials (PCMs), such as water/ice, salts and paraffin, can generate heat/cool by changing phase. In Zalba et al. [5] and Sharma et al. [6] studies, results show that PCMs have a 5-14 times higher latent

heat storage than sensible heat storage materials. However, there is a novel energy storage method – thermochemical heat storage (THS) – is already a promising system to be used with much researches and development ongoing [1, 7, 8].

Large amount of energy is stored in the reversible chemical reactions and thermochemical sorption process. In N'Tsoukpoe et al. studies, thermochemical heat storage is identified as chemical storage. However, electrochemical and electromagnetic will not be included (Figure 1-1) [9].

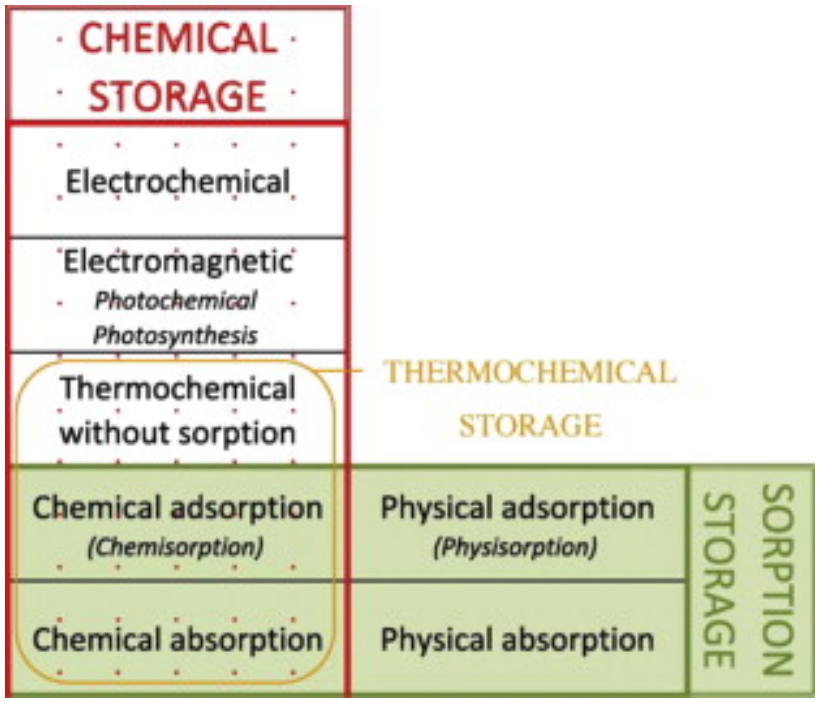


Figure 1-1 Chemical storage classification. [3, 9]

In Yu et al. studies, sorption thermal storage can be divided into four categories by considering the storage mechanisms: liquid absorption, solid adsorption, chemical reaction and composite materials (Figure 1-2) [3].

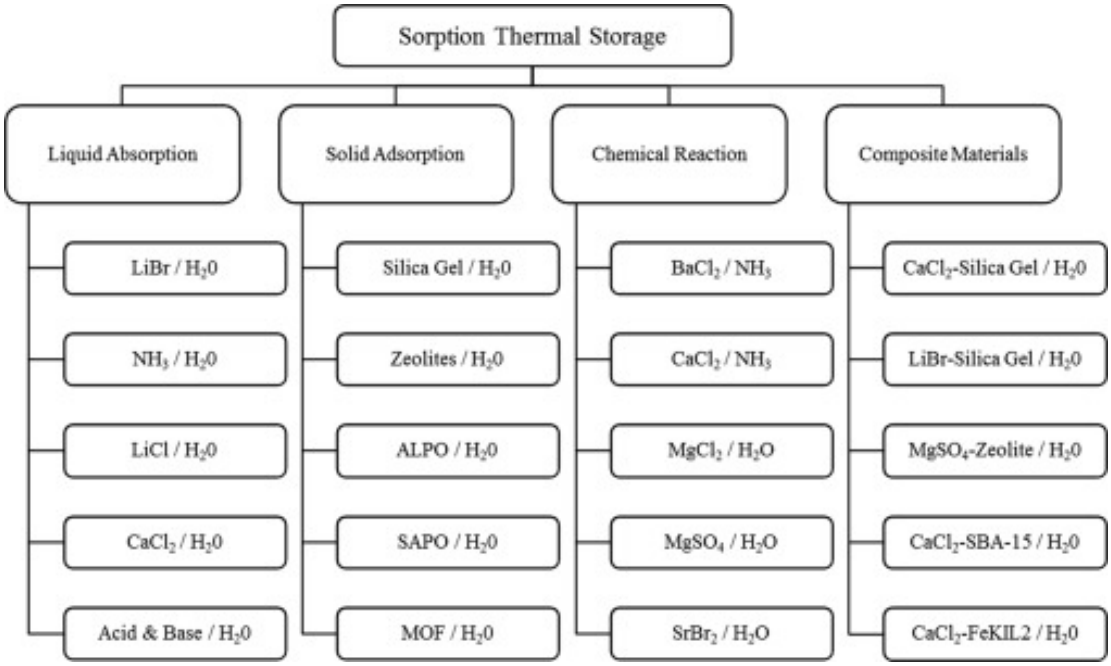


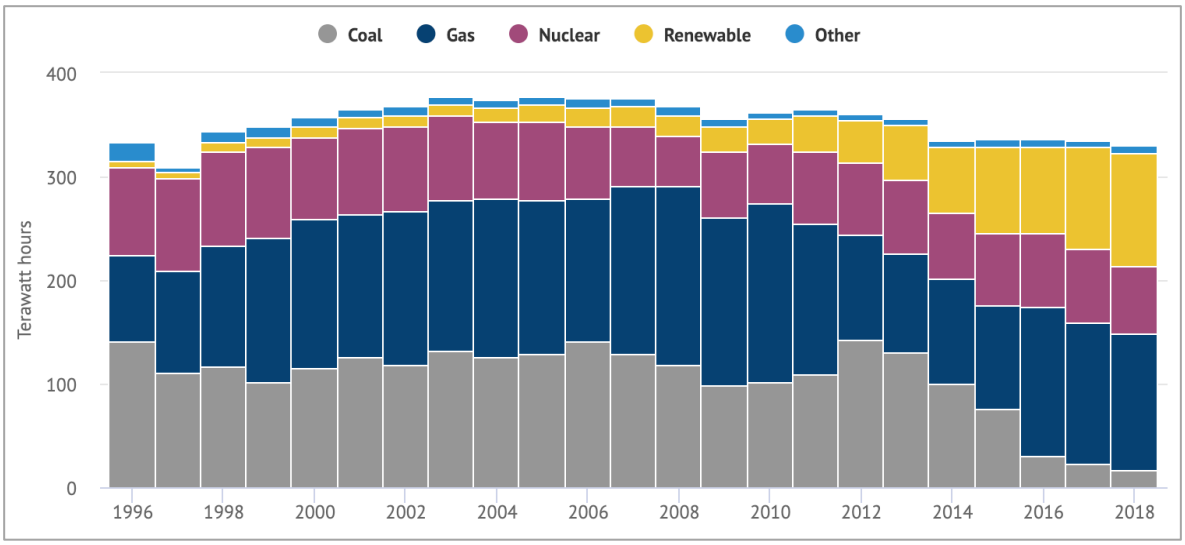
Figure 1-2 Sorption thermal storage classification. [3]

McBain gave a conception of sorption with both adsorption and absorption process [10]. He said that adsorption process happened quickly on the surface of the materials when it contracts with water vapour, then the absorption process happened afterwards slowly into the interior solid materials. Sorption thermal storage includes sorption (discharging) process and desorption (charging) process. Sorption process happens when sorbent contract with sorbate (e.g. water or other liquid). Sorption thermal storage can be either adsorption or absorption which depends on the process. Sorption process needs heat source (solar collector or waste heat recovery system) to remove sorbate (release water vapour to ambient) from sorbent (thermochemical heat storage materials). To achieve long-term storage, solar energy can dry materials to store heat in warm summer and use in cold winter.

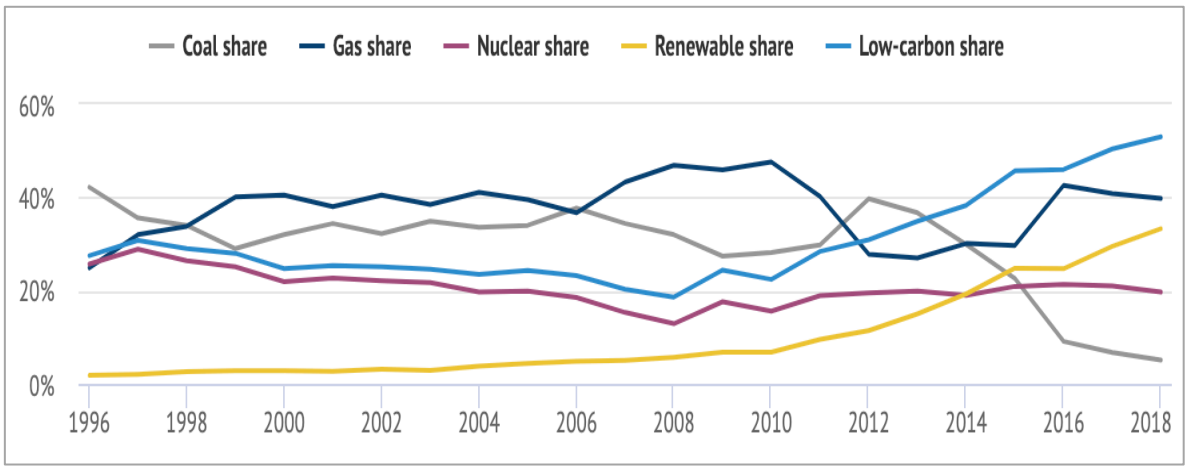
1.2 Energy Consumption And Demand Investigate

In 2018, the UK's renewable energy power generation reached a record high in market, which accounts 1/3 of mixed energy power generation; while coal power

generation fell by 1/4[11]. In last year, the UK set a record for renewable and low-carbon energy, which accounts for 33% and 53% of the UK's electricity generation, respectively. Along with this, power generation from natural gas and coal has declined.



(a)



(b)

Figure 1-3 (a) UK electricity generation by source, terawatt hours (TWh), 1996-2018; (b) Shares of UK electricity generation (%)[11].

Currently, more than 46% of UK energy consumption occurred in building systems creating 36% of GHG emissions. The average UK house energy consumption for hot

water and space heating is 20,720 kWh per annual, of which 20% (about 4,000 kWh) is for hot water and 80% (about 16,500 kWh) is for space heating, which is 16 % higher than the EU27 average of 17,793 kWh/dw [12]. About 30% of UK's energy consumption and 25% of GHG emissions occurred in domestic sector, it is because of the rely on fossil fuels, and most of the consumption is for space heating and hot water. 85% of heating load comes from natural gas consumption in centrally heated houses and 50% in non-centrally heated houses. The households emit around 2t CO_2 per household per year, which represents around 1/10 of average UK household's carbon footprint. As National Grid says that currently the biggest challenge is "decarbonising the energy sector" for the UK [13]. Greenhouse gas emissions are expected to increase in the domestic residential sector, and natural gas is expected to increase by 17% from 2016 to 2035 for cooking and heating [14].

1.3 TOPIC OF THE STUDY

Developing replacement low-carbon heating technologies is an urgent requirement to tackle the escalating climate crisis in the world. Renewable energy can reduce/eliminate GHG emissions and provide a cleaner environment. Therefore, the use of sustainable energy for space heating is an issue that needs to be solved urgently. In my study, open thermochemical energy storage system was built for space heating and cooling in building. Thermochemical energy storage composites materials with high energy density and low regeneration temperature are adsorbent/desiccant in the system, which is ideally using for the energy storage in building applications, especially in the small compact house with limited space. Several tests were taken for TES materials characteristics analysis to select the best or optimal absorbent for the prototype. For example, water absorption test of TES

materials, regeneration temperature test and analysis, energy and bulk density tests and salt adhesion test for host matrix, etc.

1.4 Aims And Objectives Of The Research

On the basis of research background, this PhD research is aimed to investigate a novel thermochemical energy storage (TES) system suitable for heating and cooling in building applications/built environment, which can be integrated with and driven by any kind of low temperature sustainable energy sources. In comparison to the typical desiccant system, this PhD research will explore the use of exothermic and endothermic thermochemical energy storage system for practical building application which will eliminate the need of complicated system and issues regarding desiccant leakage. Meanwhile, for the thermochemical heat storage system, the aim of this PhD research is to propose innovative composite materials to optimise the performance of a THS system. It will be performed by investigating innovative salts mixture into composite materials by combining with suitable highly porous materials as composite THS materials. The TES system has the potential of reducing fossil energy usage in space heating to achieve zero carbon target in building applications: (1) Develop new energy sources to replace traditional fossil fuel energy sources to reduce GHG emissions; (2) This novel energy storage technology can maximize the use of sustainable energy technologies; (3) Use seasonal energy storage device to balance energy supply and demand. The TES system has been devised to address several drawbacks experienced by typical closed TES system. It will also use low temperature for regeneration/charging process, which will be replaced by renewable energy sources in the future development.

In achieving the aims, a number of specific objectives have been set out as detailed below:

1) To evaluate the heating and cooling demand of a building in the UK using IES.

2) To conduct a comprehensive literature survey on various of thermochemical heating and cooling materials, and that can be further optimised for thermochemical heat storage application.

3) To select salt hydrate mixture and host matrix sorbents and prepare of composite sorbent material and procedure optimisation.

4) To perform material characterisation analysis for new composite thermochemical materials for both cooling and heating application. The characterisation analysis includes energy density analysis using SDT-Q600, materials density with MIP and materials structure with SEM.

5) To select the most promising TES materials using the following analytics:

- Energy density from DSC analysis;
- Sorption capacity from isotherm sorption testing;
- Higher mass loss within certain temperature range (TGA analysis).

6) To design and develop a suitable small-scale reactor to test the following thermochemical performance:

- Thermal cyclic;
- The influence of absolute humidity, relative humidity and air inlet temperature to the thermal energy output during discharging and discharging;
- To evaluate materials performance, e.g. materials capacity, energy density.

7) To evaluate the cooling and heat storage capacity of the proposed materials and an analysis will be performed to justify the potential of the materials in meeting cooling and heating demand of a building which has been evaluated using IES.

8) To design a thermochemical energy storage system for both heating and cooling, and the performance will be simulated for a building application under UK yearly weather condition.

9) Construction, laboratory and field testing and performance measurement of an experimental system.

10) Economic, environmental and techno-social analyses of the designed TES system.

1.5 NOVELTY OF THE RESEARCH

The thermochemical energy storage system aims to address the drawbacks related to other common types of thermochemical energy storage (TES) systems. The vacuum-sealed TES systems under high vacuum, within which a small amount of non-condensable gases could dramatically reduce or even stop the thermochemical sorption process. The vacuum-sealed TES system is expensive as it requires pressure vessels which can stand a high level of vacuum. Sealing of connection pipes and heat exchangers within the system is also challenging. As the performance of the reactor decreases dramatically with non-condensable gases, a vacuum pump is required to completely de-air the sealed thermochemical material. To address the above-mentioned drawbacks, an open-air loop TES system with internal heating/cooling is proposed in order to achieve an optimal temperature rise across the thermochemical reactor. Unlike vacuum-sealed system, the closed air loop TES system does not require pressure vessels and other associated complexity. In the

open cycle thermochemical energy storage system, the thermochemical energy storage material granules can be packed in an inexpensive metal or plastic container, and easy to replace in the TES system. The open TES system can obtain a temperature rise of about 20 °C in a discharging process, the temperature is lower than the conventional closed system because the thermal capacity of air flow is high compared to the thermochemical reaction heat, which is produced by sorption of moisture from air flow, however, the 20 °C temperature rising is warm enough for the direct space heating supply.

The TES system will use environmental-friendly and safe TES materials as composites, and will be compact for enabling installation either on the ground or underground beside a house. The system size can be tailored depending on the required period of heating autonomy. This novel TES system has the following innovative aspects:

- The open loop operates at atmospheric condition without pressure fluctuation, which is safe to use in domestic;
- The TES system can meet the mismatch between energy demand and supply;
- Using a mixture of salts with high energy density and different water absorption ability as TES composites can increase the reaction efficiency of the reactant and energy storage density. And for different composites, the regeneration/charging temperature of the materials is sometimes lower than individual salt regeneration temperature.
- The mesh tube with fins will be embedded in the thermochemical reactor as TES materials holder and a heat exchanger to offer a heat transfer enhancement of salt hydrate thermochemical materials.

- Low regeneration temperature of the TES composites allows low temperature heating source (e.g. solar thermal collector and waste heat recovery system). And it will work well in the areas with less sun radiation.

The novel open loop TES system uses innovative composite adsorbent materials to achieve higher energy storage density than other energy storage systems. They offer opportunities for gaining intellectual property by the filing of patent applications. It is timely in terms of its considerable capability of saving energy and reducing the amount of CO_2 released to the environment.

1.6 THESIS STRUCTURE

The thesis includes eight chapters, following the introduction chapter 1, the work is described as followed sections:

Stage 1:

Chapter 1: Some general background introductions are provided first, and then the aims, objectives and methods of the entire work are introduced in detail.

Stage 2:

Chapter 2: The classification of energy storage technologies has been studied and the advantages of thermochemical energy storage technologies over other energy storage methods have been studied. Thermochemical energy storage has the largest energy storage density and realizes short-term/long-term and seasonal thermal energy storage through electrostatic attraction between chemical bonds. This chapter introduces the principle, technology and some recent developments of thermochemical energy storage, and the advancement in recent years and future development.

Chapter 3: In this research methodology chapter, a brief introduction and investigation conducted for each step of the project will be given.

Stage 3:

Chapter 4: Some initial experiments will be done to investigate the performances and characteristics of TES materials and selected the optimal TES materials for the next step testing. The initial tests include materials selection, synthesis, characterization analysis and small experiments of candidate TES materials. Through initial experiments analysis, the composite is compared with a single salt to select the candidate that is most suitable for the TES system.

Chapter 5: Through comparative analysis with other heat storage materials, the applicability of TES materials in British buildings is theoretically studied. The 1st simulation was using Integrated Environmental Solutions Virtual Environment (IES-VE) software to simulate heating and cooling load in a low-carbon house in the UK, and the 2nd one was a solar evacuated tubes collector TES system to analyse the feasibility of the thermochemical energy storage system in building applications.

Stage 4:

Chapter 6: An open thermochemical energy storage system is design, developed, set-up and tested for some candidate TES materials. Within the study, different composites at same air flow rate, relative humidity level and regeneration temperature on heat storage process performance was investigated. Based on the results, one TES composite (V-$MgSO_4$-$CaCl_2$) was selected to be the candidate in the prototype.

Chapter 7: In this chapter, a new TES prototype is introduced and described, and tested in lab under real climatic conditions. A novel tube with fins heat exchange

system is designed for the TES prototype to solve the issue of contact reaction of moisture air and the TES materials. The TES tank (reaction body) contains composite TES material granules distributed between fins on the tube, which serves as the embedded heat exchanger for internal heating/cooling to significantly increased surface area and heat transfer. The fins on the mesh tube can increase the contact surface between materials and air to improve the charging and discharging efficiency. After the first test in prototype, the relative humidity could not reach the designed level, which caused the outlet temperature was much lower than the desired temperature. We then modified the experimental prototype and tested the prototype for 2 cycles. The comparison of results will be described in detail in this chapter.

Stage 5:

Chapter 8: An economic and environmental analysis of the TES system is performed in this chapter. And come with a conclusion to prove the feasibility of TES system to replace the existing traditional energy system technically and economically in the future.

Chapter 9: In this chapter, a general conclusion and discussion based on theoretical and experimental research will be presented. This section will also give some further work and suggestion by introducing some future project and some issues identified in the project.

A flow chart of the schematic of research work will be shown in the following figure.

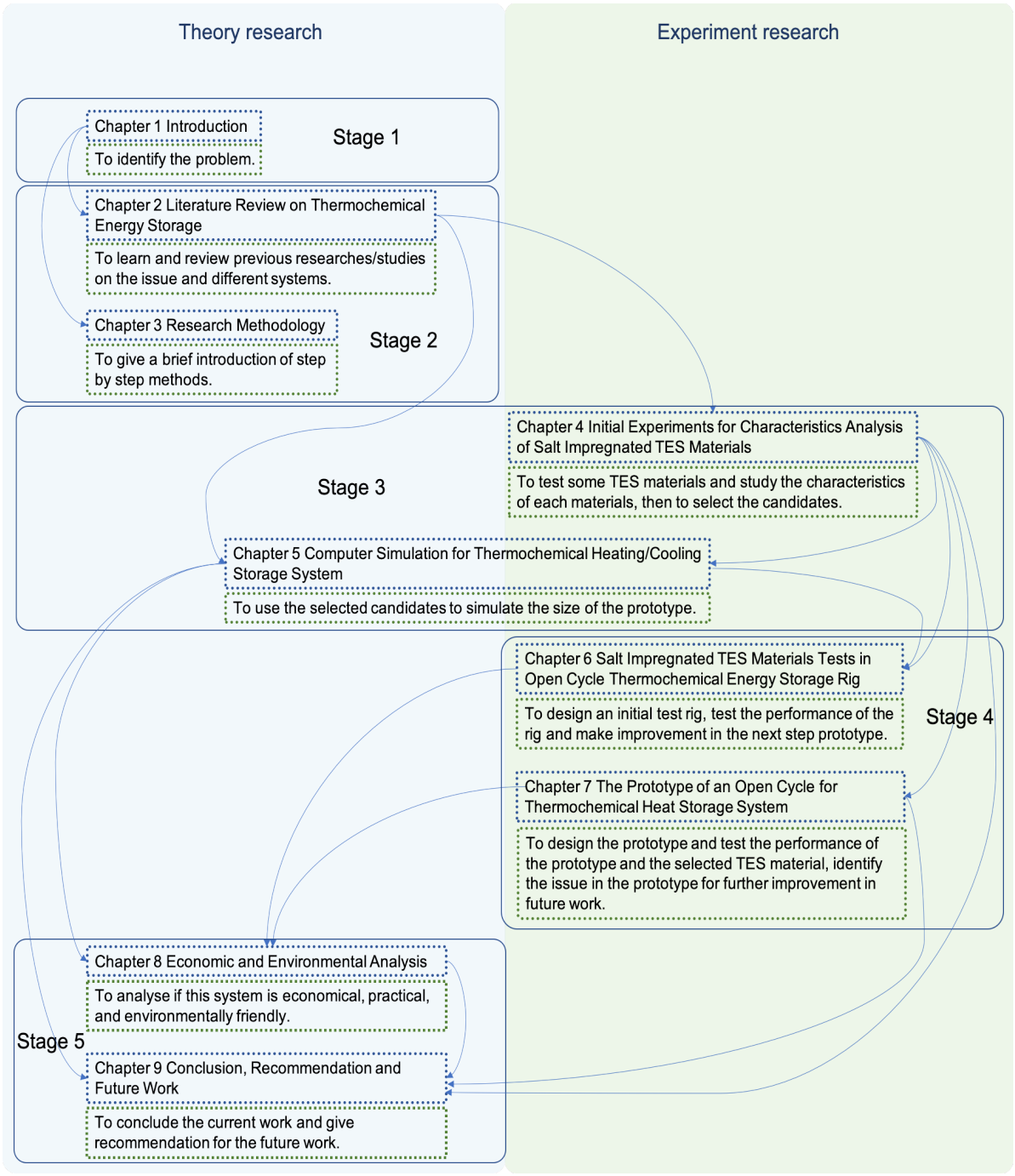


Figure 1-4 Flowchart of research work.

2 LITERATURE REVIEW ON THERMOCHEMICAL ENERGY STORAGE

2.1 INTRODUCTION

In EU, space heating occupied more than 68% of total energy use [15]. Novel energy technologies should be worked out and developed to reduce energy demand and save CO_2 emissions. High energy density materials are required in the system as well as good heat transfer reactor. Arce et al. gave a report that thermal energy storage system in the whole EU saves thermal energy of 10 $MGWh_{th}$ [16]. Sensible heat storage, latent heat storage and thermochemical heat storage are three main methods of thermal energy storage system [17]. Thermochemical energy storage (TES) materials normally have highest energy density in those three thermal heat storage materials [15, 18]. Thermochemical energy storage system mainly includes two types: closed and open cycle. In this section, closed and open cycle will be stated with previous studies. Closed cycle mainly includes vapour compression system (VCRS) for cooling, the sorption absorption cooling system, and adsorption cooling system which is most for cooling system [19].

2.2 THERMAL ENERGY STORAGE SYSTEM

Thermal Energy Storage (TES) is a technology that stores thermal energy by heating or cooling a thermal storage medium to store energy for later using in heating, cooling, and power generation applications [20]. In the year 1780 BC, an icehouse was first built in Mesopotamian town [21]. That was the 1st record people using energy storage. In China, the earliest documented technology for storing winter ice appeared before 1100 BC [22]. In the year 450s, an ice pot was built as a fridge for fruit or vegetable storage. But because the ice storage cost was very high, ice pot would be used only when people did sacrifice or some important events. In Tang dynasty (the year of 700

to 900), people started using saltpater for cooling. It is mineral rock with potassium chlorite or calcium chlorite, which can absorb much heat when contact with water. In Qing dynasty (the year 1600 to 1900), ice house was very common and people can buy some ice cream with lower price. That is the earliest record to show energy storage for mismatch between energy availability and demand. There is plenty of solar energy in summer or in the daytime, but energy demand is much higher in winter or at night. That's the reason why TES is necessary. In recent years, TES technology is particularly using in building and industrial processes [23]. In building application, TES is often used as a heating element for space heating or hot water supply, and sometimes it is used as heat storage media in passive houses. In the industry, TES can store industrial waste heat to achieve waste heat recovery. TES includes a variety of technologies that use different methods to store the available thermal energy. In general, TES system consists of a storage media in a tank, a packaged cooler or combined refrigeration system, piping, pumps, and controllers [24]. TES systems themselves cannot save energy. However, TES applications enable the development of more efficient, integrated energy systems, and improve the performance and thermal reliability of the system. TES makes it possible to more effectively utilize clean energy sources and waste heat recovery for both heating and cooling [25].

2.3 CLASSIFICATION OF THERMAL ENERGY STORAGE

Depending on the different status of materials, TES can be divided into three categories : sensible heat storage (store heat in water or rock), latent heat storage (store heat in phase change materials), and chemical reaction heat storage (store heat with chemical reaction) [26] [27] [28].

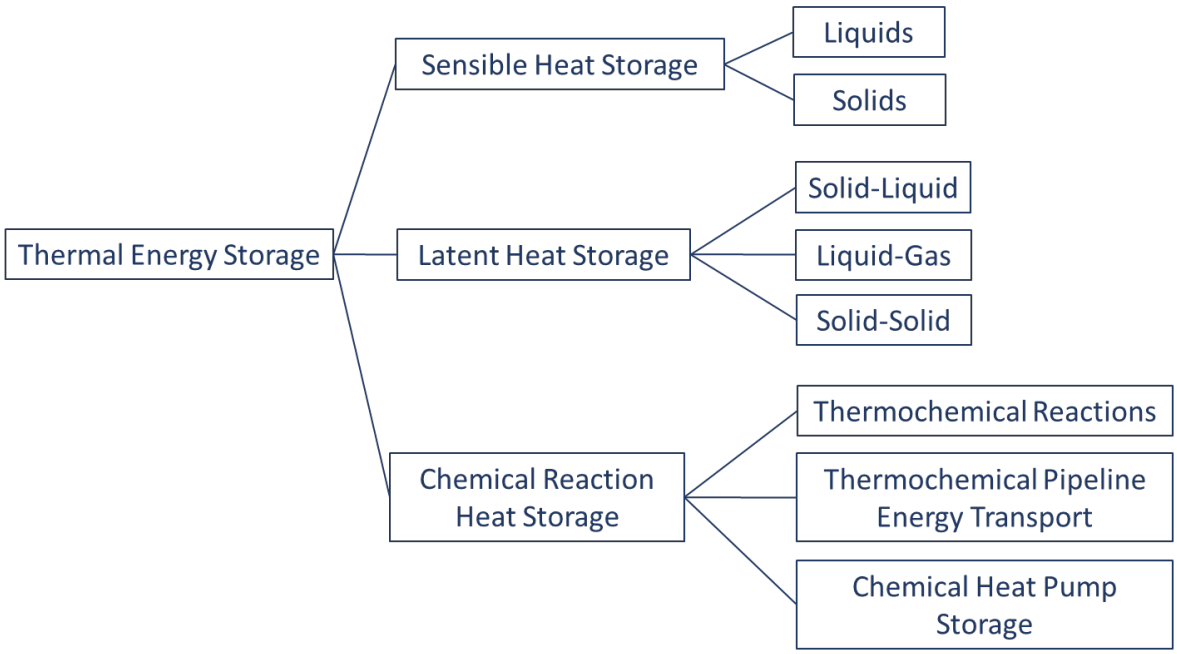


Figure 2-1 Classification of thermal energy storage. [28] [29]

The heat absorbed or released by an object during heating or cooling, without phase changing, is called "sensible heat". Sensible heat is heat by changing the temperature of an object without changing some variables. So, sensible heat is the heat that can be felt. The sensible heat of an object is shown by its temperature. As the temperature increases, the sensible heat content also increases. Domestic hot water tanks are the most common sensible heat storage system [30]. In N.Nallusamy's study, the water used as heat transfer fluid media acts as SHS material to absorb heat from the solar collector and transfer it to the TES tank [31]. A combined sensible and LHS concept TES system has been developed to avoid the disadvantage of variation in water outlet temperature and use at an average water outlet temperature of 45 °C for domestic applications [32].

Latent heat storage, also known as phase change energy storage, uses materials to absorb or release heat during phase change to store or release energy [33] [34]. Latent heat energy storage is based on the principle that materials must absorb or

release the latent heat of phase change during solidification / melting, condensation / gasification, sublimation / sublimation, and other forms of phase change, so it can also be called phase change energy storage [35]. Phase transitions can be solid-liquid, liquid-gas, gas-solid, and solid-solid [36]. Among them, liquid-solid phase transitions are the most common. Examples include melting ice or boiling water. When solids become liquids (melt) or liquids become gases (evaporation), the loosening of intermolecular attractive forces requires energy [37]. From the perspective of energy density, the amount of cold stored by latent heat is much larger than that stored by sensible heat. Latent heat storage material not only has a high energy density, but also uses a simple device, small size, flexible design, Easy to use and manage [38]. In addition, there is a great advantage: in the phase change energy storage process, the material is approximately constant temperature, which can be used to control the temperature of the system [39].

Chemical reaction storage is the storage of chemical reaction heat through chemical substances, the endothermic reaction stores energy, and the reverse reaction releases energy [40]. In chemical energy storage, compound A is converted into a high-enthalpy substance B, C through a positive endothermic reaction, that is, the thermal energy is stored in substance B, C; when a reversible reaction occurs, substances B and C are chemically synthesized into A, and the thermal energy is Was released again. The basic purpose of energy storage is to overcome the temporal or regional differences between energy supply and demand [41]. This difference is caused by sudden changes in energy demand (such as peak changes in energy use caused by seasonal changes) and primary energy and energy conversion devices. Thermochemical energy storage has the largest energy storage density of the three (about 10 times the sensible heat storage and 5 times the latent

heat storage) and realizes short-term / long-term and seasonal storage of thermal energy through electrostatic attraction between chemical bonds [42]. In addition, the decomposition products can be stored at room temperature for a long period of time by using a catalyst or separating the products [43]. This reduces the investment in corrosion resistance and insulation, and is easy to transport over long distances, especially for liquids or gases.

2.4 PHASE CHANGE MATERIALS

2.4.1 Background information

Phase change materials (PCMs) are materials that can change under physical conditions (solid-liquid, liquid-gas, solid-gas, solid-solid, etc.), and the temperature difference between the environment and the system [44]. Or light, electric field, magnetic field, chemical energy, etc. are driving forces, and the function of absorbing and releasing heat energy or recording function of shape memory recovery function is realized, and in the phase change process, the chemical properties of the material are unchanged, and the temperature can be slightly changed [45]. As the energy storage phase change material, the main conditions that should be satisfied are: suitable phase transition temperature; large enough phase change enthalpy; stable performance, can be used repeatedly; small expansion and contraction rate during phase change; good thermal conductivity, phase change speed is fast; the phase change is reversible; the degree of subcooling is small; the raw materials are cheap and easy to obtain [46]. Phase change materials (PCM) are materials with high energy density that are used as energy storage media in latent heat energy storage. It has been divided into two categories: inorganic compounds (eg, hydrates, salts, metals and alloy salts) and organic compounds (e.g. paraffin, fatty acids/esters and

polyols) [47]. Latent heat storage can be achieved by liquid → solid, solid → liquid, solid → gas and liquid → gas phase change. However, only solid-state → liquid and liquid → solid-state changes are applicable to PCM. Initially, it is similar to sensible heat storage (SHS) materials, where the temperature of the solid-liquid PCM rises when heat is absorbed. However, when the PCM reaches the temperature of the melting temperature (phase transition temperature), they absorb a large amount of heat at an almost constant temperature [48]. PCM continuously absorbs heat, but the temperature does not increase significantly until all materials become liquid. When the ambient temperature drops, the PCM solidifies and releases the stored latent heat [49].

The phase change energy storage material utilizes the heat exchange to the external environment during the phase change process, so that the energy is stored in the form of phase change [50]. Since the amount of latent heat of phase change is much larger than the sensible heat, it can have a large energy storage density. Phase change energy storage materials are combined with building materials to produce phase change energy storage building materials [38] [51]. As we all know, building energy storage is usually dominated by sensible heat and latent heat storage [52]. Compared with sensible heat storage, the use of latent heat storage can increase the building's heat storage by several tens of times, or even hundreds of times, so phase change energy storage building materials. The advantage over traditional building materials is that their ability to regulate and control the ambient temperature is greatly enhanced [38] [53]. When the temperature is high during the daytime, the phase change energy storage building material absorbs the external heat absorption; when the temperature drops at night, the stored heat is released again, which effectively complements the external temperature. The phase change energy storage material

can realize the transfer of heat in time and space, reduce the environmental temperature fluctuation, increase the ambient temperature comfort, effectively reduce the frequency of air conditioner use, and reduce the building energy consumption [54]. In the aerospace field, phase change materials can be used to protect astronauts and spacecraft. In the field of refrigeration, phase change technology can be used to replace compressors for cooling, saving more than 60% [55]. In the field of clothing, phase change energy storage materials are implanted. In fiber, it can greatly change people's quality of life. Without using any energy, ordinary clothes can be turned into micro-air conditioners [56]. In the fields of “shifting peaks and valleys” of electricity, recycling of waste heat and waste heat, and solar energy utilization, create a variety of facilities to improve energy efficiency [57].

2.4.2 Classification and applications of PCMs

According to chemical composition of PCM, it can be divided into inorganic, organic and composite PCMs. Inorganic PCMs include crystalline hydrated salt (poor reversibility), molten salt, metal alloy and other inorganic substances; organic PCMs include paraffin, carboxylic acid, ester, polyol and other organic substances; mixed PCMs are mainly mixtures of organic and inorganic PCMs [58] [59]. Suitable phase change temperature can be obtained by mixing different PCMs.

The current issue of PCMs include supercooling, phase separation, volume change during phase change, corrosion of containers, leakage of liquid phase; low melting point, low flammability, low thermal conductivity of organic phase change materials [44]. In order to solve the leakage and corrosion during solid-liquid phase change, capsule phase change materials were produced. In order to increase surface area/volume ratio, micro/nano encapsulated phase change materials and their applications were integrated [26]. The combination of PCMs is a combination of

phase change materials and polymer materials, which avoids the problem of low latent heat of solid-solid phase change materials and avoids liquid leakage of solid-liquid phase change materials [38]. Metal foam PCMs should meet the following requirements: desirable phase transition temperature; sufficient phase change latent heat; stable performance, can be used repeatedly; small expansion and contraction during phase change; good thermal conductivity, fast phase transition; good reversibility of phase change, cheap and easy to obtain raw materials, etc. The method for improving the thermal conductivity of the PCM is to add a filler with a high thermal conductivity such as metal, ceramic material or pyrolytic graphite to the PCM [60]. The fillers normally have the following structural forms: powder, fibre, fin and honeycomb; the materials of the three or different phase change temperatures are placed in the order of the phase change temperature, and a suitable phase change temperature point can be obtained, and the heat conduction speed is accelerated.

2.4.3 PCM Applications in thermal energy storage

Renewable energy sources (e.g. solar, wind, tidal energy, etc.) have been widely used. However, these renewable energy sources are intermittent. Thermal energy storage technology can match the gap between energy supply and demand to overcome the shortages of sustainable energy. And also, PCMs can provide a constant temperature during the phase change process, making it widely used in solar energy, construction, textile, industrial heat recovery and other fields [61].

Phase change heat storage materials are used for heat storage, which are environmentally friendly, efficient, energy-saving, safe and many other advantages [30]. They are very suitable for solar heating system heat storage to replace traditional heating equipment. In the waste heat utilization system of industrial heating equipment, the traditional heat storage device usually uses refractory

material as the heat storage material for absorbing residual heat [62] [63]. Since the heat absorption only depends on the sensible heat capacity change of the refractory material, the heat storage chamber has a volume. The disadvantages of large, high cost, large thermal inertia, and gradual decline in output power are difficult to apply in the industrial heating field [64]. The phase change heat storage system is a new type of waste heat utilization system that can replace the traditional heat storage device [20]. It mainly uses the absorption and release of latent heat in the solid/liquid two-state change process to realize the storage and output of thermal energy, latent heat and sensible heat. The comparison of the phases not only contains more energy, but the release of latent heat is carried out at a constant temperature. Compared with the conventional heat storage chamber, the volume change heat storage system can be reduced by 30% to 50%; therefore, replacing the traditional heat storage device with the phase change heat storage system can not only overcome the shortcomings of the original heat accumulator [61]. The heating system can still operate stably after adopting energy-saving equipment and is beneficial to the wide application of waste heat utilization technology in industrial heating process.

2.5 THERMOCHEMICAL ENERGY STORAGE

Currently, in the UK approximately 70% of heating supply is derived from fossil fuels[65]. Under the consideration about the surging fuel price and the negative effects of greenhouse gas emissions, it is a global challenge to spare no effort to employ renewable energy technologies effectively to face with the energy resources depletion. Thermal energy storage (TES) technology is now being utilized all over the world. As shown in Figure 2-2, TES displays rapid growth in recent years [66]. In current global market [67], thermal energy storage installed capacity is about 2040 MW in 2013 and is anticipated to reach 6000 MW by 2020, expanding at a compound

annual growth rate of 17% from 2014 to 2020. Global thermal energy storage market is projected to reach USD 1818.8 million by 2020. In any industrial energy consumption, TES system can replace about 50% of conventional energy source. It can also optimise the energy system overall efficiency [68]. TES system can reduce energy demand in peak hours result in lower carbon dioxide emissions and bring down energy consumption by end-consumers.

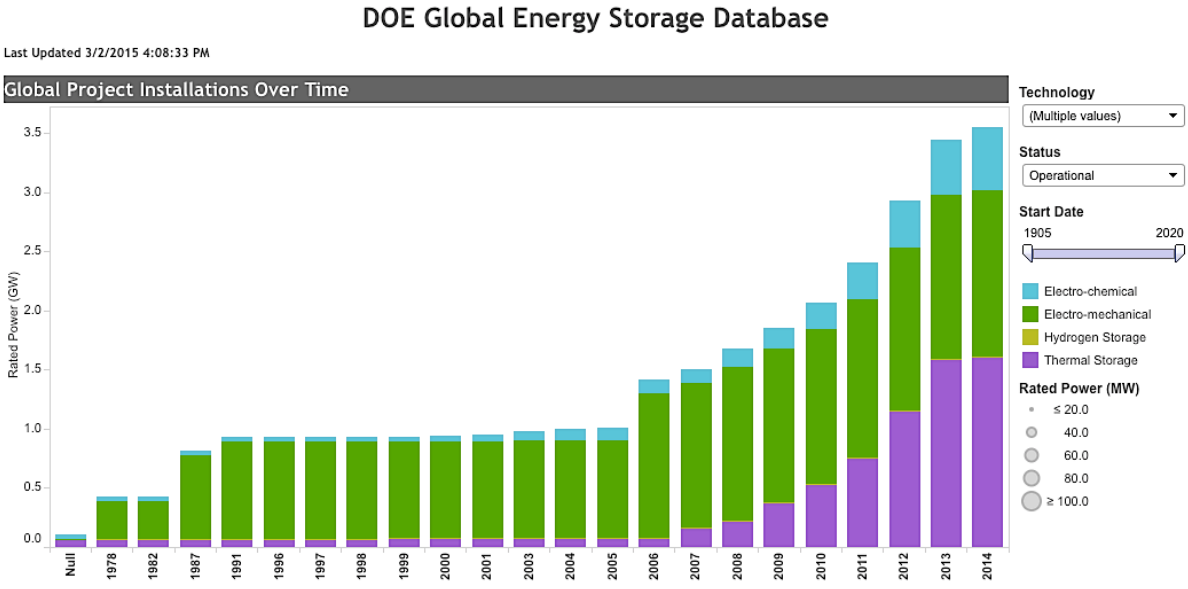


Figure 2-2 Global Energy Storage Database[66].

Thermochemical heat storage (THS) technology can store and discharge energy by reversible chemical reactions. It shows higher heat storage density and better long-term preservation ability than other thermal energy storage system [69]. Moreover, the easier operation process due to no condenser and evaporator in the system, and there is no need to consider about the system pressure make THS system more competitive in heat storage market. However, the ambient temperature and relative humidity will be significant influence factors in the THS system working process. Long-term heat storage in the ambient temperature and limited commercialization of product are main challenges in the growth global thermochemical heat storage

market for the forecasted period. THS is one of the most promising storage technologies for the future, especially THS hybrid system combined with solar technology [70]. In the recent decades, whole Europe is witnessing growing investment in solar thermal heat storage which is expected to benefit market growth. Asia-Pacific is the fastest growing market with a CAGR of 22.3%. Solar collector with thermochemical energy storage technologies can shift power generation to hours when solar resources are not available to provide backup power during night-time. Thus, additional installation of solar collector will create growth opportunity for thermochemical storage system. Thermochemical energy storage will be gaining importance as means to achieve higher efficient and environment-friendly energy system.

The energy density of thermochemical materials is two times higher than latent thermal energy storage, and 8-10 times higher than sensible energy storage materials (Figure 2-3) [71]. Thermochemical heat storage (THS) includes sorption reaction system and chemical reaction system to generate heat or cool. Large heat can be stored in reversible chemical reactions process and sorption storage processes [3]. The concept of ‘sorption’ first came out by MacBain in 1909, molecules sorption on surface was described as a prerequisite to any surface mediated chemical process [10]. Because of the high energy densities and long-term preservation ability, sorption thermal storage has attracted much attention for solar heat storage in recent years [7, 8, 72].

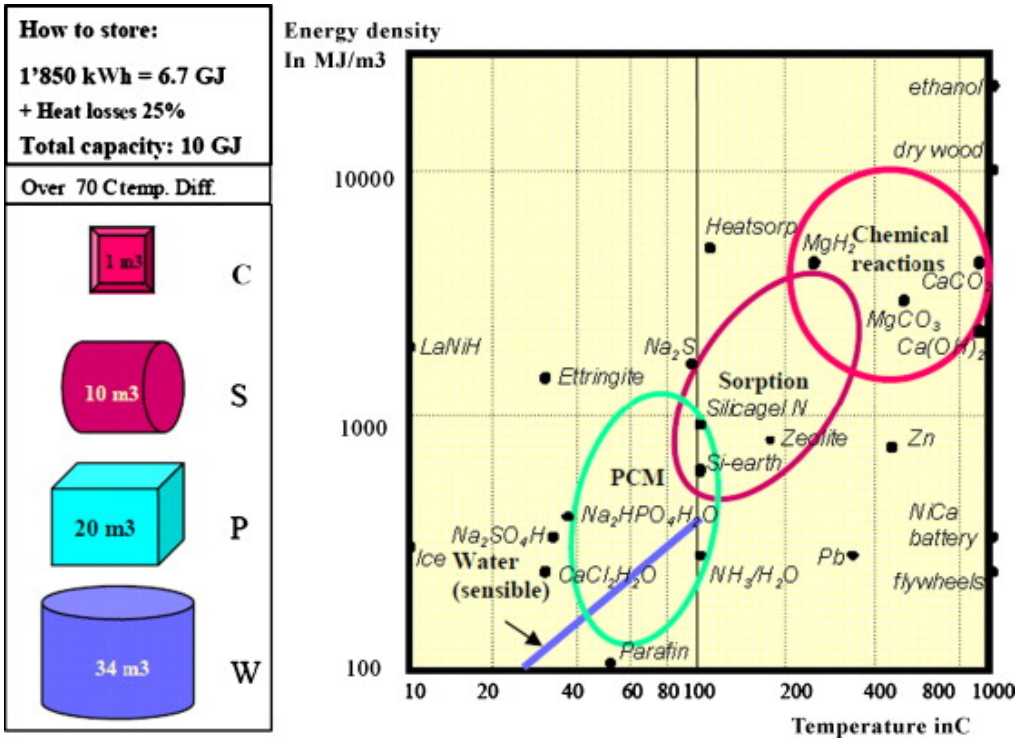


Figure 2-3 Energy density of PCM, sorption and chemical reaction process. [71] [9, 73, 74]

Among the main parameters that influence the performance of a THS is the choice of thermochemical materials [75]. In selecting the appropriate materials, key considerations include:

- High energy storage density;
- Low charging or regeneration temperature;
- High water or sorbate uptake as measured in (g sorbate/ g sorbent);
- Appropriate heat and mass transfer properties for efficient power output;
- Ease of handling to handle and non-poisonous nature;
- Low-cost price per kW/h of energy stored with thermal stability;
- Suitability for the application.

In a THS system which uses salts as the thermochemical materials, deliquescence relative humidity (DRH) values are of interest, as they indicate the sorption properties

of the THS materials. As comprehensively discussed in Ding and Riffat studies [76], presented in equation (a) is the process whereby the environment reaches the value of deliquescence relative humidity (DRH) or above. At this stage, deliquescence of the salt will occur since the inorganic salts will absorb moisture from humid air and form a solution. Meanwhile, when the value of the relative humidity is below the DRH, the salt may still absorb moist or water vapor, thus becoming hydrated, but it will not create solution. This is described in equations as given in Ding's paper [76].

For RH < DRH: Salt (solid) + H_2O (gas) ↔ hydrated salt (solid) (a)

For RH > DRH: Salt (solid) + H_2O (gas) ↔ solution (liquid) (b)

This thermochemical reaction is a reversible process. Thus, in both reactions presented by (a) and (b), the total amount of heat generated/absorbed during the reaction is given by the latent heat of condensation/evaporation and the thermochemical reaction during the water sorption/desorption process. However, the formation of salt solution in equation (a) implies that a higher amount of heat is generated compared to reaction of equation (b) during the sorption reaction due to the additional water sorption of the THS materials. Similarly, during desorption, if the salt used is in a liquid state, higher enthalpy change is required to regenerate the salt. Although higher energy is produced during the discharging (sorption) stage, the second process suffers from a disadvantage caused by the salt solution.

Another important property of the salts during the sorption reaction process is the hygrothermal stability. This property implies the rate of hydration reaction. Therefore, an innovative approach must be taken in order to optimize the performance of Thermochemical heat storage such that a balance between the enthalpy capacity and the hydration rate (discharging rate) process of the thermochemical materials

could be reached. This includes exploring new composite materials with high energy density and have excellent sorption reaction properties and hygrothermal stability.

2.5.1 Closed thermal energy storage system for heating application

The main processes of closed thermochemical heat system include three parts: Charging, storing and discharging part (Figure 2-4). The closed system includes working fluids and thermochemical materials. The internal substances should be separated from heat transport fluid. Thermal energy in the system from heat resource can be transferred to working fluid [77].

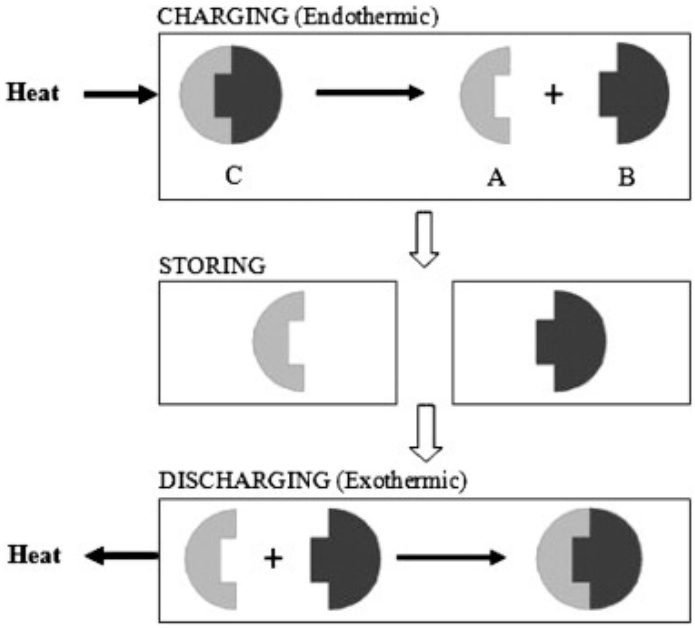


Figure 2-4 Processes of closed thermochemical energy storage system. [77]

An energy balance in the closed systems can be written as:

$m_c C_p (T_1 - T_2) - Q_1 = \Delta H_c$ [77]

- m_c – mass of working fluid, kg;
- C_p – specific heat capacity of the working fluid at constant pressure, J/kg/K;
- T_1 – initial temperature of the working fluid, K;

- T_2 – final temperature of the working fluid, K;
- Q_1 – initial energy, Wt;
- ΔH_c – the enthalpy change in reaction process.

The efficiency of charging process can be shown in the formula below:

$$\eta_{c,cl} = \frac{\Delta H_c}{m_c C_p (T_1 - T_2)} = \frac{\Delta H_c}{Q_{in}} \quad [77]$$

Q_{in} is the energy input during charging part.

This section presents a review of the closed system which can be classified into five categories namely closed chemical heat pump (CHP) for space heating, vapour compression system (VCRS) for cooling, the sorption absorption cooling system, and adsorption cooling system.

2.5.1.1 Closed CHP for space heating

In 1987, Ruiter stated an experiment of closed combined heat and power plant with thermochemical materials [78]. He evaluated the possibility of thermal energy storage by an absorption cycle with over 100% efficiency theoretically. NH_3-H_2O was used in the experiment with a heat storage density of 119 kWh/m^3. In 2007, Bales et al. developed a closed CHP system with NaOH-H_2O to reach an energy density of 250 kWh/m^3 [79]. In 2014, Yang et al. optimised a closed Brayton CHP plant with $CaCl_2$ solution in a single tank to supply sensible and thermochemical sorption heat storage for solar heating (Figure 2-5) [80]. Compared with sensible energy storage $CaCl_2$ solution has a much lower heat loss due to the chemical reaction during discharging process [81]. And also, desiccant $CaCl_2$ is cheaper than $LiCl_2$ and LiBr, which are always selected for cooling applications. The solar charging and discharging processes can be described as the two reactions as followed [82-84]:

Charging process: $CaCl_2 \cdot 9.9H_2O\ (l)\ +\ \Delta H\ \rightarrow\ CaCl_2 \cdot 4.8H_2O\ (l) + 5.1H_2O\ (g)$

Discharging process: $CaCl_2 \cdot 4.8H_2O\ (l) + 5.1H_2O\ (g) \rightarrow CaCl_2 \cdot 9.9H_2O\ (l)\ +\ \Delta H$

Thermal heat energy density depends on the density of $CaCl_2$ solution. The energy density of $CaCl_2$ is 106 kWh/m^3, however, the material energy density can rise to 381 kWh/m^3 when system combined with extra heat source, such as solar thermal collector or waste heat recovery [82].

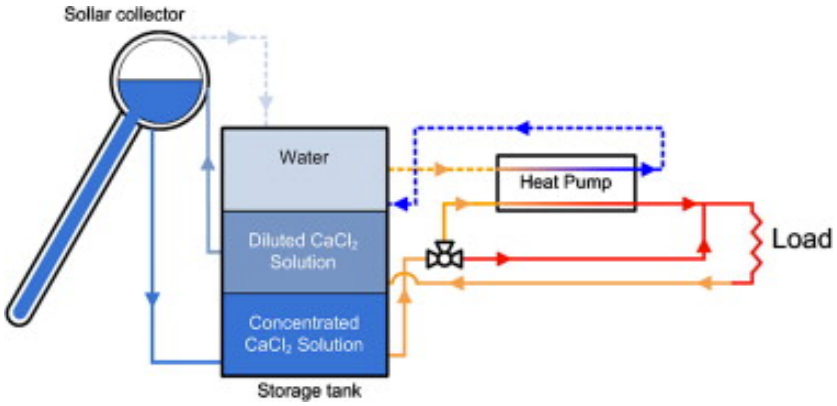


Figure 2-5 A closed cycle of $CaCl_2$ solar heating system. [82]

2.5.2 Closed thermochemical energy storage system for cooling application

2.5.2.1 Absorption cooling system

A solar driven absorption cooling system is a refrigerator that uses solar as heat source to provide energy for driving cooling process. Waste heat can be also used as heat source due to sustainable achievement. With the use of solar energy, consumption of fossil fuel and its peak demand can be reduced. The system can compress refrigerant vapour includes a generator, a pump and an absorber.

The absorption liquid chiller can operate with mediums to absorb liquid and desorb steam, which is the first solar driven absorption refrigeration system introduced by Ferdinand Carre in 1895 [85]. In 1883, Worsøe-Schmidt built a solar driven cooling system with $CaCl_2/NH_3$ as solid absorption [86]. In 1997, Park and Kim used

LiBr/HO(CH_2)OH in their absorption cooling system [87]. In 1998, Ayala and Heard used NH_3/$LiNO_3$ couples where NH_3 is the refrigerant [88]. However, the LiBr/HO(CH_2)OH and NH_3/$LiNO_3$ couples have very low performance; thus, they will not be discussed in detail.

Figure 2-6 shows a domestic solar thermal absorption cooling system reported by Agyenim et al [89]. The absorption system operates at temperature between 75-90 °C. The absorption chiller is 4.5 kW with a vacuum tube solar collector of 12 m^2. The cold storage tank worked with a 6 kW fan coil. Agyenim reported that the average solar performance coefficient of whole system was 0.58, and on the hot sunny day the average peak can reach 800 W/m^2.

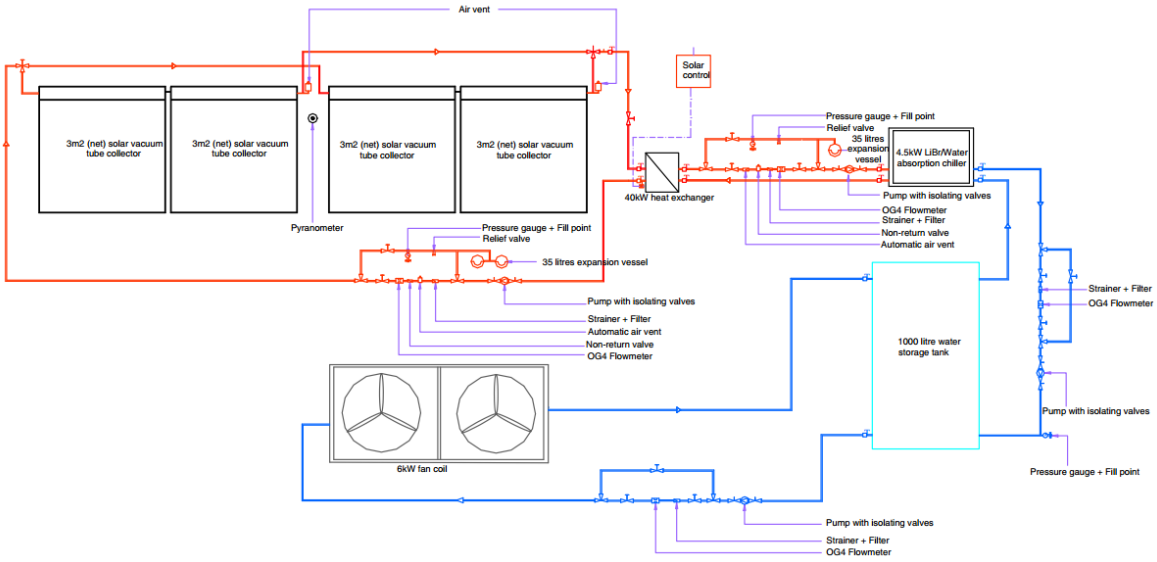


Figure 2-6 Solar thermal absorption cooling system (STACS). [89]

Chiller absorbs heat from thermal storage tank, in which heat provides by solar collector.

The absorption cooling system can be classified into three types:

- Single-effect solar absorption cycle;
- Half-effect solar absorption cycle;

- Double-effect solar absorption cycle.

The hybrid system is another absorption cooling system, it integrates different pairs or systems to achieve higher performance.

2.5.2.2 Adsorption cooling system

Solar powered refrigeration system based on adsorption cycles is simple, quiet in operation, and adaptable to any size systems [90]. In 1848, vapour adsorption technology was firstly introduced by Faraday by using a solid adsorbent [91]. The fundamental experiments on the solar powered adsorption cooling system were carried out using silica-gel/water-vapour combination by Japanese researchers Sakoda and Suzuki in 1984 [92]. The regeneration temperature was around 100 °C. In early 1990s, adsorption cycles were first used in refrigeration system and heat pumps. In 1997, Zhang and Wang developed a waste heat recovery technology driven adsorption cooling system to alternate traditional vapour compression refrigeration to reduce usage of CFCs. And also, it resulted in gas consumption reduction and higher reliability and silent operation [93].

Sami stated an improved dynamic model to study single/double adsorber systems with waste heat recovery technology. The systems included air-cooled evaporator and condenser. Hot oil, superheated steam or exhaust gas can be used as heating fluids in the system for the adsorbers [94]. AEE INTEC in Austria built a closed adsorption prototype to test performance of a solar powered sorption system with silica gel and water for space heating and hot water supply (Figure 2-7)[95, 96]. Solar thermal collector supplied heat energy to dry silica gel. In the sorption process, water evaporator connected with silica gel store to release water vapour for reaction. The energy density of silica gel is 150 kWh/m^3 and the solar collector provided 88 °C heat.

The result showed a 20% lower performance than simulation because of the heat loss between the connection [96, 97].

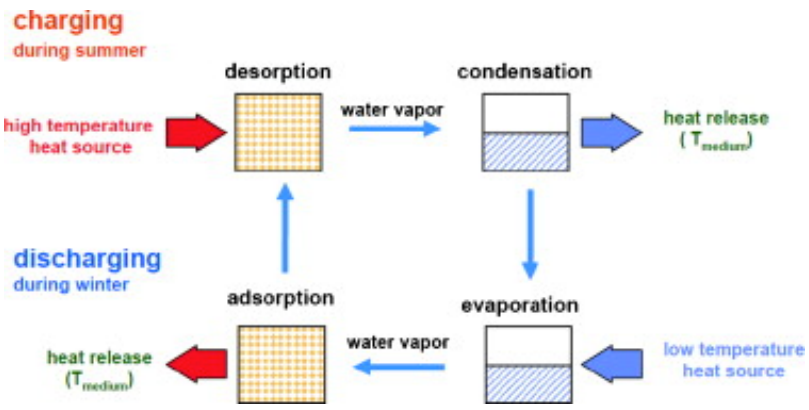


Figure 2-7 Operation principle of closed adsorption system[97].

Base on the employed adsorption pairs, Ahmend classified adsorption cooling system into three types [98]:

- Physical adsorption pairs;
- Chemical adsorption pairs;
- Composite adsorbents.

The most sorption pairs are physical and chemical pairs. And also, some of the hybrid adsorption pairs have higher COP.

2.5.2.3 Vapour compression system

The most common type of closed cooling system is the electrical driven vapour compression system (VCRS). The electrical driven compressor of VCRS may be replaced by the closed cycle vapour absorption system [99] which driven by solar power and waste heat recovery system. Compressor uses in the system to increase the pressure of compressible fluid. Vapour compression refrigeration system (VCRS) is one of the most widely used refrigeration cycles for air-conditioning system of built environment and refrigeration applications.

Solar PV based vapour compression cooling system (Figure 2-8) is energy effective and very simple design. And also, system can be used for remote area, which is far away from electricity grid and cooling capacity can be still modest [85]. However, PV panel efficiency is quite low and the installation cost is very high; thus, it is not cost effective.

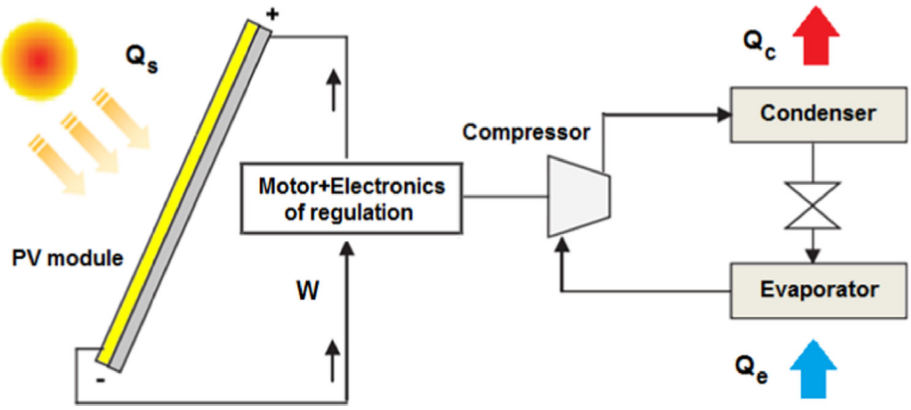


Figure 2-8 Solar photovoltaic vapour compression system [100].

Solar to cooling efficiency (solar electric cooling system overall efficiency) is shown as followed:

- $\eta_{sol-cool} = \eta_{sol-pow} \times \eta_{pow-cool} = \frac{Q_e}{Q_s}$ [100]
- $Q_s = I_p \times A_s$
- $\eta_{pow-cool} = \frac{Q_e}{W}$
- $\eta_{sol-pow} = \frac{W}{I_p \times A_s} = \frac{W}{Q_s}$

In the system, cooling coefficient of performance (COP) was 1.1-3.3 at different evaporator temperatures of -5-15 °C in vapour compression machines. The condenser temperatures ranged between 45-61 °C [100]. The overall efficiency can reach 30% when a VCR system (COP of 3.0) combined with a 10% efficiency solar PV panel. The unit price of the solar panel is €5/Wp, the solar panel would cost about

€1,700 to provide 333 W electricity for 1 kW cooling generation [100]. VCR system is widely used in some medical, food and vaccine transportation and household applications. Solar thermal collectors are also recommended in system to convert heat into useful energy for compressor in system [85].

2.5.3 Open thermal energy storage system

In the closed cycle vapour absorption system, it has a very low thermal COP range of 0.5 in single-effect cycle and up to 1.2 in double-effect cycle that leads to the intensive use of thermal energy [101]. Open systems operate at atmospheric pressure and water vapour is the working fluid, which is released to the ambient environment. Moreover, because of its relative high operation pressure, high operating temperature, expensive and large corrosive chemical solutions, its development has been limited and not a valuable option for small scale heating, e.g. Domestic heating [101, 102]. Therefore, open cycle vapour absorption system is an alternative to closed cycle vapour absorption. It is also known as desiccant air conditioning and evaporative cooling system [101].

The open system includes working fluid and thermochemical materials. Supplied thermal energy is transferred to a transport medium and provides energy necessary for desorption/changing of the thermochemical material. After a storing period, a discharging period occurs during which energy released from synthesis of thermochemical material is absorbed by the working fluid for heating (Figure 2-9).

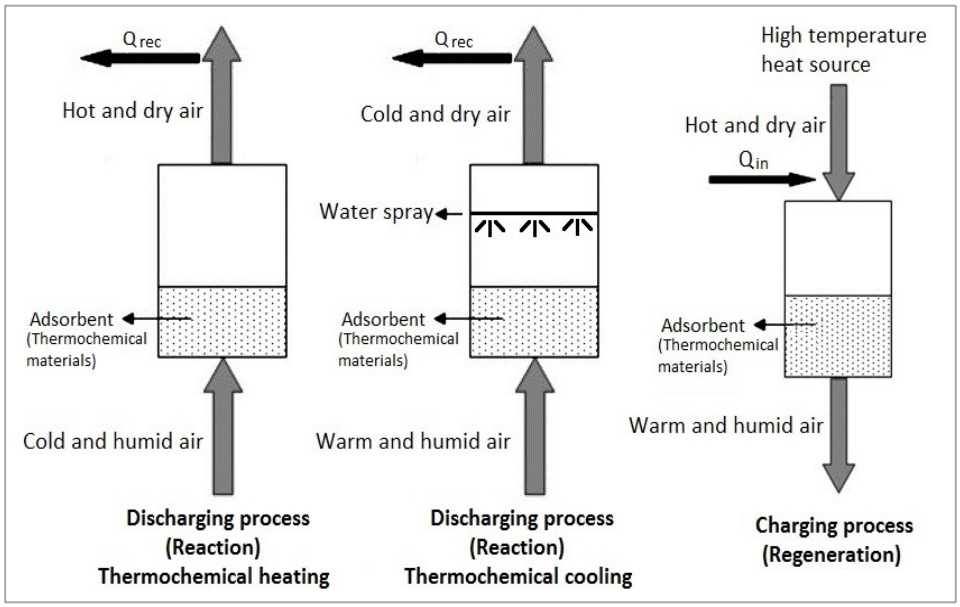


Figure 2-9 Charging and discharging process in open thermochemical energy storage system. [77, 103]

For the thermochemical heating reaction process, thermochemical materials will adsorb water vapour and generate heat when cold and humid air goes into the reactor, then system provides hot and dry air for building. For thermochemical cooling system, warm and humid air goes into reactor and water spray on thermochemical cooling materials at the same time, then cooling system provides cold and dry air for building. In the regeneration process, a high temperature heat source supplies hot and dry air to dry thermochemical materials. Solar energy is a good high temperature heat source for the thermochemical energy storage system for regeneration. At the same time, we aim to using thermochemical materials with lower regeneration temperature for energy saving.

Solar powered refrigeration open cycle system provides cooled and dehumidified air for a comfortable room air condition. Normally, water is used as refrigerant and it is in direct contact with the inside atmosphere. Therefore, the system is an open cycle. There are two types of open cycle of solar refrigeration system: evaporative cooling system and desiccant cooling system. Based on different sorbents, desiccant cooling

system divided into two different technologies: systems with solid and system with liquid sorbents [104]. Open cycle systems can be applied in buildings with ventilation systems or parts of buildings in which the cooling loads can be covered by controlled ventilation.

2.5.3.1 Sorption heat system

Thermochemical sorption heat storage system is an advanced technology to address the balance between energy consumption and energy demand in building service system. In sorption process (Figure 2-10) heat is stored by breaking the binding force between the sorbent and the sorbate in terms of chemical potential.

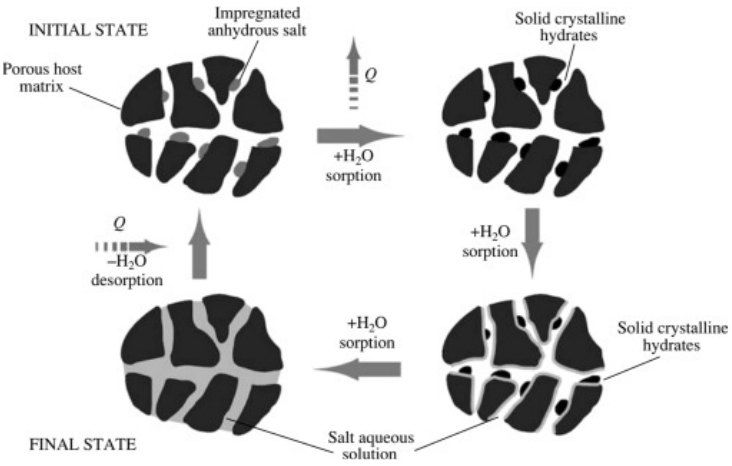
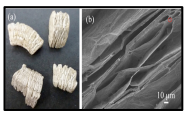
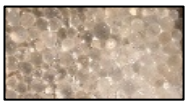


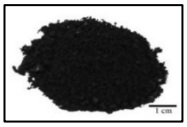
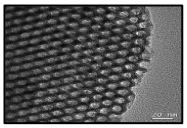
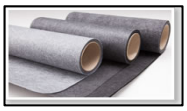
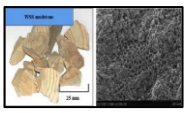
Figure 2-10 Sorption process on silica gel with $CaCl_2$ [3] [105].

Thermochemical materials have a much higher energy density than common sensible and latent heat storage materials, and also, thermochemical heat storage system has a much lower heat loss [1, 73, 106]. Thermochemical heat storage system includes different types: based on physisorption in adsorbing materials (e.g. zeolites), based on absorption in hygroscopic solutions (e.g. NaOH solution) and based on absorption in salts (e.g. salt hydrates) [107].

Recent research in thermochemical heat storage is innovating towards composite material which combines salts and matrix, or salt in matrix [108]. Because of the porosity of the adsorption materials, thermochemical materials such as vermiculite, pillar layered silica, silica gel, zeolite and carbon fibre are also used as host materials. Some previous studies about sorption host materials will be summarised in Table 2-1.

Table 2-1 Previous studies about sorption host materials.

Thermochemical Materials	SSA (m2/g)	Porosity volume	Water uptake	Regeneration temperature	Cost	Image	Ref
Vermiculite	8-10	2.8 cm3/g	0.03 g/g	25.6-48.1℃	0.22-0.4 ($/kg)		[1, 109]
Silica Gel	750-850	1 cm3/g	0.35 g/g	130-150℃	0.88-0.34 ($/kg)		[1, 110, 111]
Zeolite	550-600	0.18-0.47 cm3/cm3; 0.3 cm3/g	0.3 g/g	>200℃	0.21-44 ($/kg)		[1, 112-114]

Activated Carbon Powder	700-1850	0.5-1.5 cm3/g	0.19 g/g	150-180℃	0.5-5 ($/kg)		[1, 115, 116]
Expanded Graphite	18-22	0.073 cm3/g	4%	100-200℃; 65℃ in vacuum condition	1.8-2.5 ($/kg)		[1] [117] [47, 118]
SBA-15	581	1 cm3/g	0.5-0.7	≈ 100℃	117 ($/5g)		[119-121]
Activated Carbon Fibre (ACF)	1237	0.1357 cm3/g; 31.85%	-	-	1.1-1.8 ($/kg)		[1, 122, 123]
Zeolite 13x	680	Pore diameter (Å) = 8	0.24	120-180℃	1.5-5.8 ($/kg)		[124, 125]
Wakkanai Siliceous Shale (WSS)	111.7	Porosity = 60%	-	80℃	-		[126]

Pioneered by Aristov and discussed in Gordeeva and Aristov [127] in synthesising materials, the most common method is impregnating matrix with an aqueous salt solution by following steps: 1) drying the matrix to removed absorbed water; 2)

impregnate the grains with salt solution; 3) filtration; 4) drying the composite matrix to remove the adsorbed water. The method could be further modified into two methods namely: dry (or incipient wetness) impregnation and wet impregnation method [128]. In the 'dry' impregnation method, the wet composite has to be kept for several hours. Although salt solution soaks quite fast into the pore of the host matrices, the process of penetration solution goes into the centre of the matrices is rather slow. By leaving the salts in the wet conditions for several hours, salts are assumed to be located only inside the pores, which means the volume of the salt solutions is equal with the pore volume. When dried, salts will not be formed/observed on the external surface of the porous materials; meanwhile, in the wet method, the volume of the salts solution exceeds the pore volume. After several hours, the excess solution must be removed by filtration or through vacuum desiccator. Nevertheless, a portion of the solution may remain on the external surface after filtration. Therefore, after drying the composite materials, the salt can partially precipitate on the outside of the grains, form large crystals. In order to remove the large crystals, we can use a special humidity/temperature camera to observe the crystals formed on the surface of the materials will absorb water and become solution [129]. The composite materials are taken out when there is no excessive salts solution and then dried in order to get the composite materials without large crystals formed on the surface.

Aristov Aristov, Tokarev [130] gave a method for impregnating matrix with aqueous salt solution and discussed with Gordeeva [62]:

- Dry the matrix to remove moisture;
- Impregnate matrix with salts solution;
- Filtration;

- Dry the composite matrix with salts to remove water.

Too much salts solution leads to crystallization on the surface of the composite materials after dried [131]. The improved incipient wetness method is to mix matrix and salts solution and keep it for several hours to let the solution goes well through the centre of matrix. When mix matric with salt solution, it shows an adequate solution when the liquid just accumulates on the bottom of the container. Crystal will not appear on the surface of composite materials after dried [131].

In the simple solar driven thermochemical energy storage system (Figure 2-11), energy was stored in the hydrated salt in hot summer and released in cold winter. In summer, solar array provides heat to charge the system (dry materials) and water vapour will be released to the ambient environment. In winter, cold and humid air goes into the fan and adsorbed by hydrated salt, then released to the ambient as warm and dry air [107].

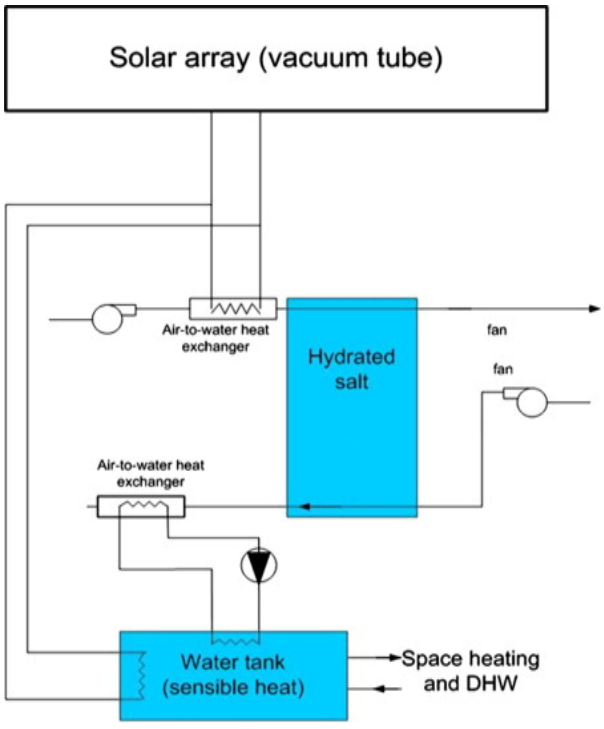


Figure 2-11 Solar driven open sorption thermochemical heat storage system [107].



Figure 2-12 Photographs of prototype thermochemical storage system, (a) before and (b) after insulation [107].

In Zondag et al. research, a prototype was built with a capacity of 17 L $MgCl_2 \cdot 6H_2O$ as sorption materials includes a solar PV heat source, heat exchangers and fan (Figure 2-11) [107]. The energy that can be generated is directly proportional to the moisture flow entering the packed bed. An air flow was about 500 l/min with the pressure of 12 mbar. Results showed that $MgCl_2 \cdot 6H_2O$ has a very high energy density of 0.5 GJ/m^3 and the system can supply about 150 W of thermal energy with only 50 W heat loss for over 40 hours with a COP of 12. The reaction formula is shown below:

$$MgCl_2 \cdot 6H_2O \ + \ \Delta H \ (57\ °C) \ \rightarrow \ MgCl_2 \cdot 4H_2O + 2H_2O \qquad [107]$$

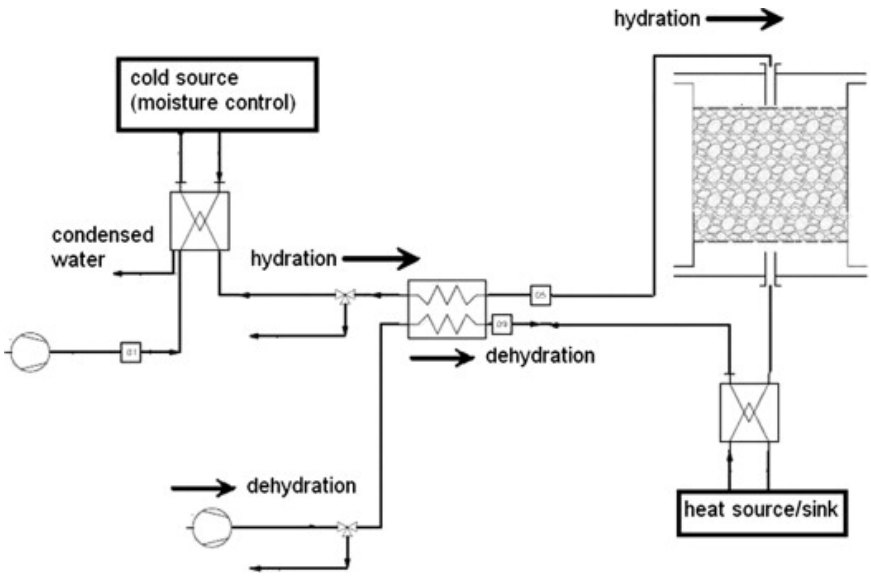


Figure 2-13 Schematic representation of thermochemical reactor storage system setup [107].

Jong et al. stated that thermochemical materials provide a promising solution to achieve a long-term 100% renewable energy economy [132]. The compactness of a long-term storage system is determined by the thermochemical reaction, operating conditions, and system implementation with the necessary additional system components. In their simulation within the MERITS project, Na_2S had a heat storage density of 0.14 GJ/m^3 in the experiment. Development has been done to improve the heat storage density by enhancing vapour and heat transport level [132]. However, Na_2S has the risk of corrosion and reaction and a hazard of H_2S emissions [133-137]. The Australia Group claimed that Na_2S is a dual use material [138].

NaS/H2O was used on the SWEAT prototype by Boer et al. [139]and the energy storage density was measured as 1.1 kWh/kg (1980kWh/m^3) for heating (COP=0.84) and 0.7 kWh/kg for cooling (COP=0.57).

During reaction process, thermochemical materials (sorbate) adsorb moisture from the ambient air directly or a humidifier. In the charging process, heat from solar or other heat source can dry the materials to store energy for later use. The thermochemical heat sorption system is an easy process design operation system;

however, the long-term storage performance of the reactor is the most important part as the moisture adsorption and heat generation act at same time which may cause some heat loss.

2.5.3.2 Chemical heat pumps

Chemical heat pumps (CHP) are those systems use reversible chemical reaction to change the temperature level of the thermal energy, which is stored by chemical energy storage materials. CHP can upgrade low temperature heat source to a higher temperature heat output. CHP system includes two parts: endothermic reactor (lower heat source) and exothermic reactor (hot air outlet) [1]. Low temperature heat source can be from industrial waste heat recovery or solar energy [140]. Because there is no mechanical compression in the system, electricity power is not needed in the chemical heat pump system [1]. The classification of CHP is shown below:

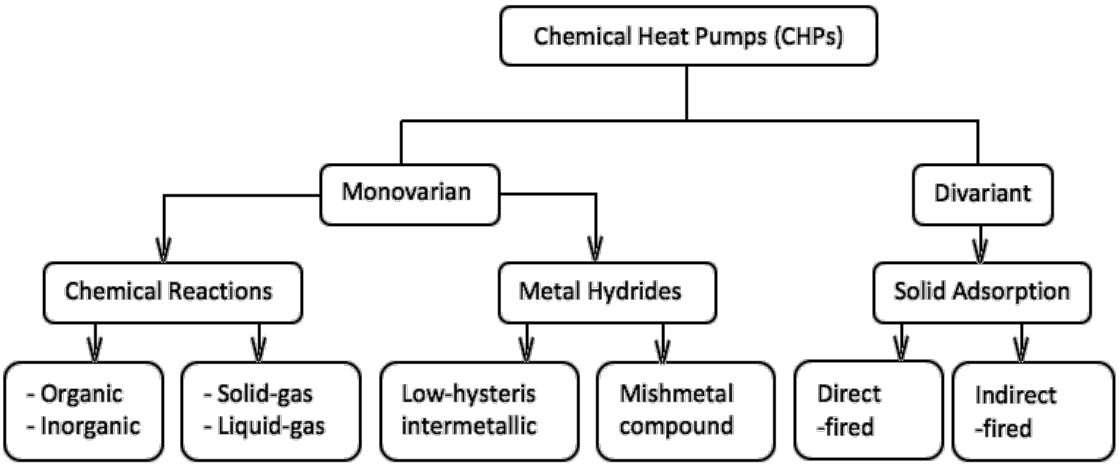


Figure 2-14 Classification of chemical heat pumps [141, 142].

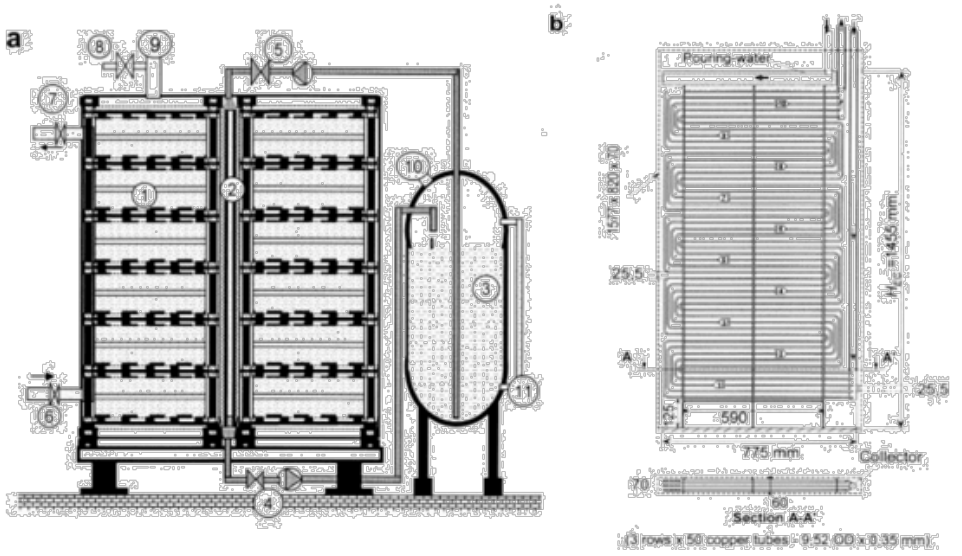
In 2002, Ogura et al. did an experiment by using $CaO/H_2O/Ca(OH)_2$ gas-solid reversible hydration reaction in chemical heat pump system [143]. The hot air produced rate depends on the heat and mass transfer performance of CaO reactor

and heat exchanger. The $CaO/H_2O/Ca(OH)_2$ CHP reaction equations are shown as followed:

$$CaO(s) + H_2O\ (g) \leftrightarrow Ca(OH)_2\ (s) + 104.2\ kJ/mol$$

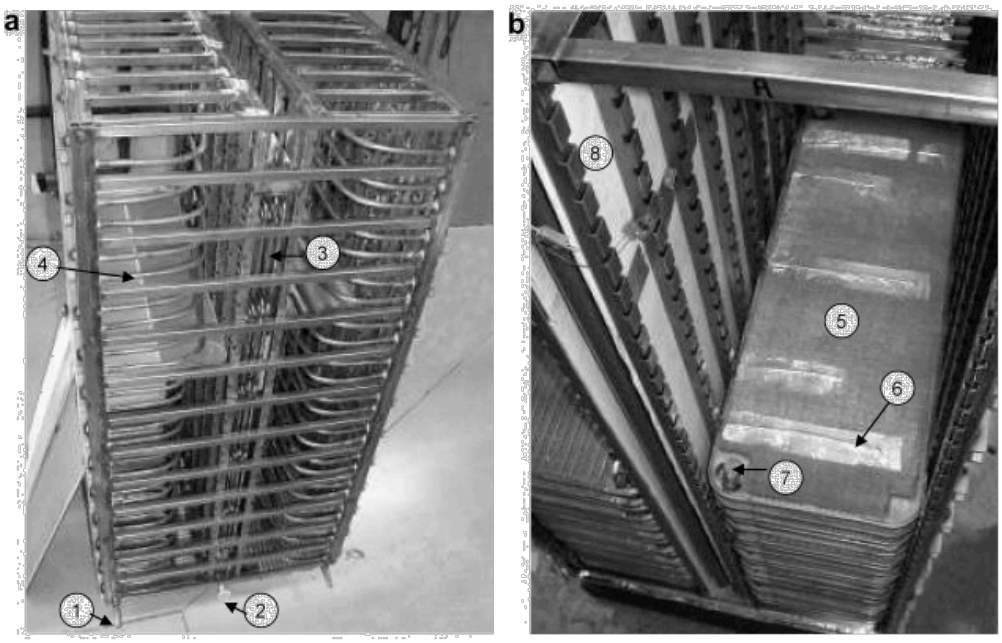
$$H_2O\ (g) \leftrightarrow H_2O\ (l) + 41.7\ kJ/mol$$

In 2008, Mauran et al. [144] built a prototype reactor of chemical heat pump with a total volume of 1 m^3 for solar heating and cooling (Figure 2-15, Figure 2-16). $SrBr_2$ was used as reactant and water as refrigerant fluid in the reaction with 60 kWh for heating and 40 kWh for cooling. The peak energy output is about 2.5-4 kW because a low heat transfer at interface. However, the drawback can be solved by the future development and optimization.



Schematic drawing of the prototype SOLUX. (a) The reactor and its auxiliaries: a module (1), the Evaporator/Condenser (2) between the two stacks of modules, the reactive water stored in the water tank (3), the collection of the pouring-water at the EC bottom and its reintroduction at the top by means of two pumps (4, 5), the inlet and outlet collector (6, 7) of the coolant of the exchanger plates, a vacuum valve (8), the pressure (9, 10) and liquid level (11) measures. (b) Some details of the EC unit constituted by three staggered rows of five parallel tubes which are uniformly wetted with the reactive water by a shower at the top.

Figure 2-15 Schematic drawing of the prototype SOLUX [144].



(a) A view before introducing the modules: Inlet collector of the coolant (1), outlet of the pouring-water (2) at the bottom of the evaporator/condenser (3), tube connection to a plate exchanger (4). (b) View of a module (5) with some temperature measures (6), a detail of inlet connection to a plate exchanger (7) before its welding to the tube (4), and PTFE plate (8) ensuring the containment of water streaming on the EC and its heat insulation at the same time.

Figure 2-16 Photographs of the prototype SOLUX in construction [144].

In Sharonov et al. study, a thermodynamic analysis of a chemical heat pump has been created to identify and compare the idea cycle of chemical and adsorption heat pumps [145]. Results showed that efficiency equal to the Carnot efficiency can be obtained for a chemical heat pump but adsorption heat pump has a lower efficiency due to entropy generation. In Kim et al. research, $CaCl_2$ was added in to the mixture of expanded graphite (EG) and $Mg(OH)_2$ to enhance the thermal conductivity and reactivity of MgO/H_2O chemical heat pump [146]. $CaCl_2$ has high thermal conductivity, moldability and chemically stability, and it can help to enhance the hydration reactivity of MgO due to its high water adsorption ability. An improvement has been done in this design by optimizing the mixing molar ratio between $Mg(OH)_2$ and $CaCl_2$ (Figure 2-17) [147]. Results showed that the molar ratio of $CaCl_2$ and EMC was 0.1 can reach the optimum mixing weight ratio to improve the hydration reacted conversion. EMC also showed better performance by optimizing EG. Myagmarjav et al. developed a

new chemical heat storage materials for MgO/H_2O chemical heat pump called EML [148]. The heat output capacity of EML composite was 1405.3 kJ/kg at a hydration temperature of 110 °C, which was higher than that of pure MgO.

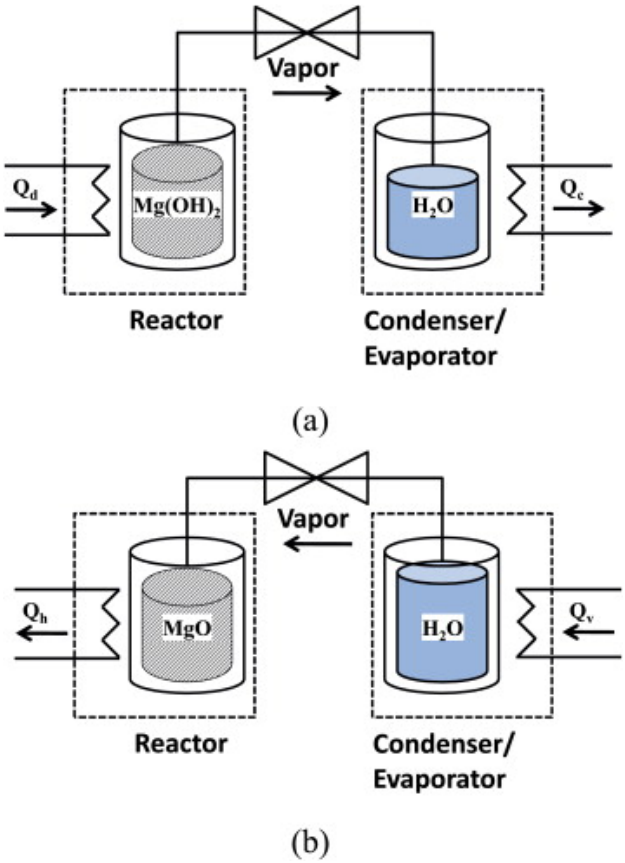


Figure 2-17 Principles of the magnesium oxide/water chemical heat pump: (a) heat storage operation and (b) heat supply operation. [147]

2.5.4 Open thermochemical cooling storage system

A major proportion of the air-conditioning systems available in the market are vapour compression-based systems that not only have low efficiency but also use refrigerants like CFC, HCFC and HFC, which are one of the main sources of ozone layer depletion [149].There are many types of cooling systems that provide cool fresh air for domestic or commercial use. The choice of any system directly affects the amount of energy consumed along with the amount of carbon dioxide emission released to the atmosphere [150]. With the increasing ambient temperature and solar

intensity, energy consumption of conventional vapour compression cycle dramatically increases. An alternative cooling method is closed vapor adsorption systems with the main advantage being utilising solar energy or waste heat for generating cooling. Thereby, fossil fuel consumption and emissions are minimal in this cooling system. However, the thermal COP is in the range of 0.5 in single effect cycles up to 1.2 in double effect cycles, which implies intensive use of thermal energy. The requirement of vacuum conditions and heat exchange mechanisms, complexity of heat/mass transfer, corrosively and leakage problem of adsorbents (e.g. corrosive chemical solutions, LiCl, LiBr, $CaCl_2$) and high cost are the main barriers in taking closed adsorption coolers to the advanced level. Due to the global warming effect and ozone depleting potential of refrigerants alternative air conditioning methods using natural working fluids (e.g. water, air) needs to be sought. A widely researched A/C technology operating with water is the evaporative coolers with Energy Efficiency (COP) range from 8-20 [151]. Researchers at UNOTT reported that the evaporative cooling system has a distinct problem such that in many cases, the resultant temperature of the treated air is far higher than the wet-bulb or dew point limitation, which further reduces its cooling capacity. As a result, in meeting the cooling demand of a building, the size of evaporative (or dew point) cooling systems could be very large and so difficult to be incorporated into buildings. With the latest developments, dew point coolers has also been developed that is able to cool the air up to its dew point without increasing its humidity. However performance of any evaporative cooling system strongly depends on the ambient humidity level [152]. These systems can only be effectively operated in hot and dry climates whereas in humid climates their cooling efficiency remains insufficient. Another alternative to a closed cycle vapour absorption is open cycle desiccant air conditioning with COP_{th} of 0.6-1.2 [153],

and can be classified into liquid and solid desiccant, using water as refrigerant in direct contact with air. Based on exothermic reaction, the desiccant system combines dehumidification using hygroscopic or thermochemical materials as the desiccant, with evaporative cooling. The common desiccant technology applied today uses rotating desiccant wheels, equipped either with nanoporous compounds include silica and alumina based materials such as silica gels, mesoporous silicates, zeolites, zeolite-like molecular sieves, aerogels and etc [154] (in solid desiccant system) or lithium chloride, lithium bromide, tri-ethylene glycol, calcium chloride and potassium formate solutions (in liquid desiccant system) as sorption material [108]. Also recently, more progress is reported in composite materials composed of different host matrix and confined salts. These materials are also investigated in Thermal Energy Storage system and has been actively studied by researchers at UNOTT. In solid desiccant systems, the drying capability is higher than liquid desiccants. However, the system requires relatively higher desiccant regeneration temperature [155]. To date, the application of liquid desiccant air conditioning has been limited particularly in a built environment for small scale applications [156]. Additionally, the main barrier to the practical application of a desiccant system includes the large size of the rotating drum and the complexity of the system such as desiccant solution leakage and equipment corrosion. A novel integrated desiccant air conditioning system (IDCS) was proposed by a group of researchers at DABE, UNOTT which combines the regenerator, dehumidifier and evaporative inter-cooler into a single membrane based heat and mass exchanger using potassium formate ($CHKO_2$) desiccant working fluid. Although the work demonstrates that the novel IDCS concept is viable, mass imbalance between the dehumidifier and regenerator being one of the main issues.

New technologies integrating innovative processes with advanced energy materials are required those are both sustainable, efficient, environmentally friendly and cost-effectively. Cooling with endothermic chemical reactions have received attentions by some researchers, but mainly applied as cooling agent for cold packs and food and beverage containers as patented by Leavitt and Bergida (2015)[157], and Collins P (2013)[158].

2.5.4.1 Evaporative cooling system

Better building envelop insulation causes an increasing demand of cooling. Research shows that a lower 5-7 °C inside room temperature than outside can bring a more comfortable feeling for people [144]. However, traditional air conditioning system leads to a very high electricity consumption and CO_2 emissions. Many processes are already studied by researchers in the world, for example, novel evaporative cooling system and desiccant cooling, or some process based on phase change materials or a chemical reaction.

Solar powered evaporative cooling is a novel cooling system. It makes air cool by increasing its water vapour content. Thus, air temperature drops while the humidity level rises. In Cuce's study, the evaporative cooling system has a great potential to save energy in hot and arid climatic zones [159]. And also, compared to the alternative air-conditioning applications it is a very cost-effective way.

In Kinney's study, three types of evaporative cooling systems have been presented [160]. "Direct" evaporative coolers use a fan to pull outside air through media that are kept thoroughly wet by water that is sprayed or dripped on them. "Indirect" evaporative coolers take advantage of evaporative cooling effects, but cool without raising indoor humidity. A variation called "indirect/direct" evaporative cooling system

adds a second stage of evaporative cooling before the conditioned air enters the dwelling to further lower the temperature of the incoming air.

In 2000, Zhang et al. developed a direct evaporative cooling system in China [161]. The cooling effectiveness range was 67% to 86%. And the maximum COP was 2.88. In 2002, Ibrahim et al. investigated a direct evaporative cooling system equipped with porous ceramic evaporators in residential buildings which can provide 6-8 °C in dry bulb temperature with a 30% rise in relative humidity (RH) with maximum cooling capacity of 224W/m^2 [162].

Taufiq et al. built a direct evaporative cooling system in Malaysia [163]. As shown in Figure 2-18, when environment humidity was at a comfortable level (around 50%-60%), the energy efficiency was 28%-36%; when environment temperature was around 25 °C, the exergy efficiency was at the lowest level of 35%.

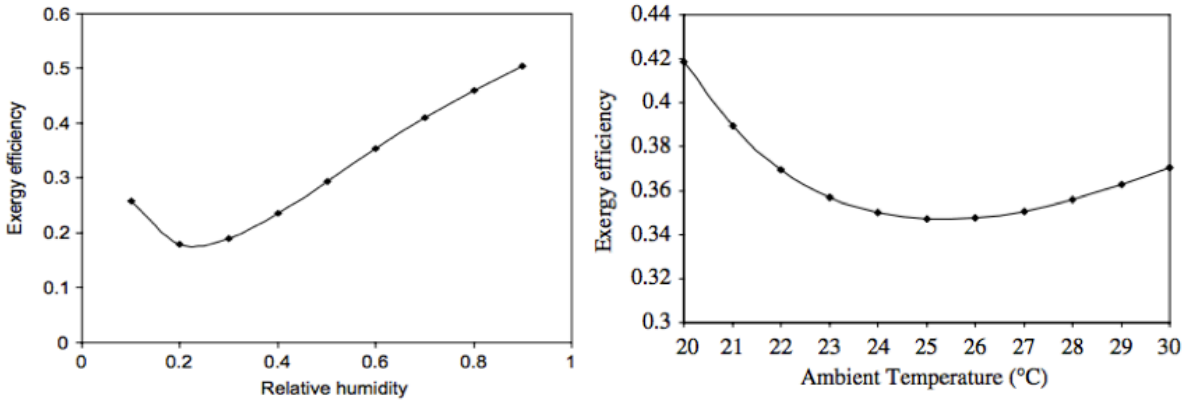


Figure 2-18 Exergy efficiency with relative humidity and ambient temperature. [163]

Kruger, Cruz and Givoni developed a research used indirect evaporative cooling system in two different place in Venezuela and south of Israel [164]. The COP is 0.29 to 0.32 in Venezuela and 0.44 to 0.47 in Israel. In Maheshwari research paper, the energy required of residential cooling system was 1.11 kW leaded to a 40% reduction of energy consumption in peak energy demand [165]. In Hajidavalloo study in 2007,

thermodynamic characteristics of new system are significantly improved, and energy consumption reduces by about 16% with COP rises by about 55% [166].

In 2002, Camargo and Ebinuma [167] presented the principles of operation for direct and indirect evaporative cooling system and the mathematical development of the equations of thermal exchanges, allowing for the determination of heat transfer convection coefficients for primary and secondary air flow. In the paper, the results showed evaporative cooling systems have a very large potential to propitiate thermal comfort and can still be used as an alternative to conventional systems in many tropical regions, save energy and protect the environment. In 1963, Watt [168] developed the first serious analyses of direct and indirect evaporative systems.

Riangvilaikul and Kumar operated their simulation in different climate conditions while the inlet temperature stayed steady at 35 °C [169]. Dew point effectiveness varies from 65% to 86% when the inlet air humidity changes from 6.9 g/kg to 26.4 g/kg; while, wet bulb effectiveness is less sensitive with ranging between 106% and 109%. Idalex developed a perforated cross flow configuration of dew point evaporative cooling system with a cooling cycle called Maisotsenko cycle (M-cycle) and indicated the wet bulb effectiveness of 110-122% and dew point effectiveness of 55-85% [170]. In Caliskan et al. study of M-cycle, the wet-bulb effectiveness was 115% and the dew point effectiveness was 78% with cooling load of 0.64 kW and COP of 2.3 [171]. The primary energy ratio was 0.691. The energy efficiency is 19.14% at a reference temperature of 23.88 °C and showed a maximum exergy destruction rate of 0.1347 kW; while, a minimum exergy destruction rate of 0.1268 kW has been shown at 0 °C reference temperature.

2.5.4.2 Desiccant cooling system

Desiccant cooling system operates on the principle of adsorption dehumidification and evaporative cooling [172]. The thermally driven cooling cycle is a combination of evaporative cooling with air dehumidification by a desiccant. It is a new and potentially clean technology can be used to condition the internal environment of buildings and operates without the use of harmful refrigerants [85]. In 2009, Enteria developed and tested a solar thermal and electric driven desiccant cooling system at Tohoku University in Japan (Figure 2-19) [173]. The result showed that the system can be operated either in daytime or night; therefore, system can store thermal energy during night because of its system design. Thus, it is a very cost effective and reliable hybrid solar driven desiccant cooling system.

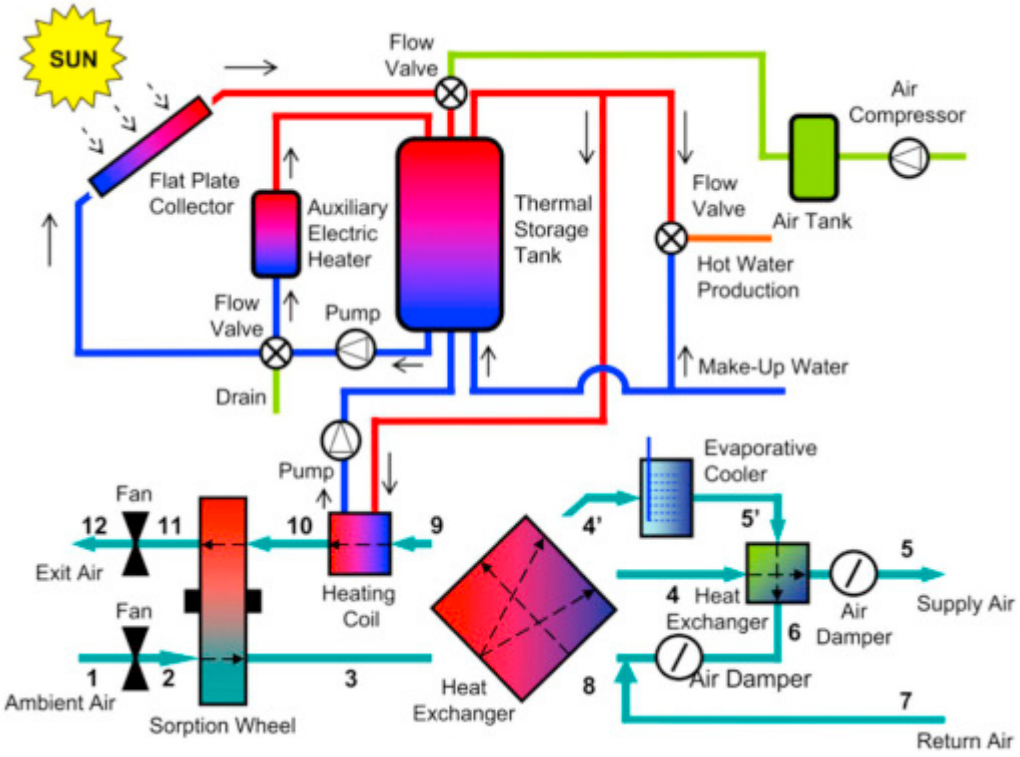


Figure 2-19 Schematic diagram of solar thermal and electric driven desiccant air conditioning system. [173]

Desiccant systems operate at atmospheric pressure and can either be solid adsorption cooling or liquid absorption cooling system [101]. Liquid desiccants have

lower regeneration temperatures, greater dehumidification capacity and a lower air side pressure drop. Solid desiccants systems are compact, simple, less subject to desiccant carryover and corrosion [174]. Figure 2-20 lists the main materials of desiccant.

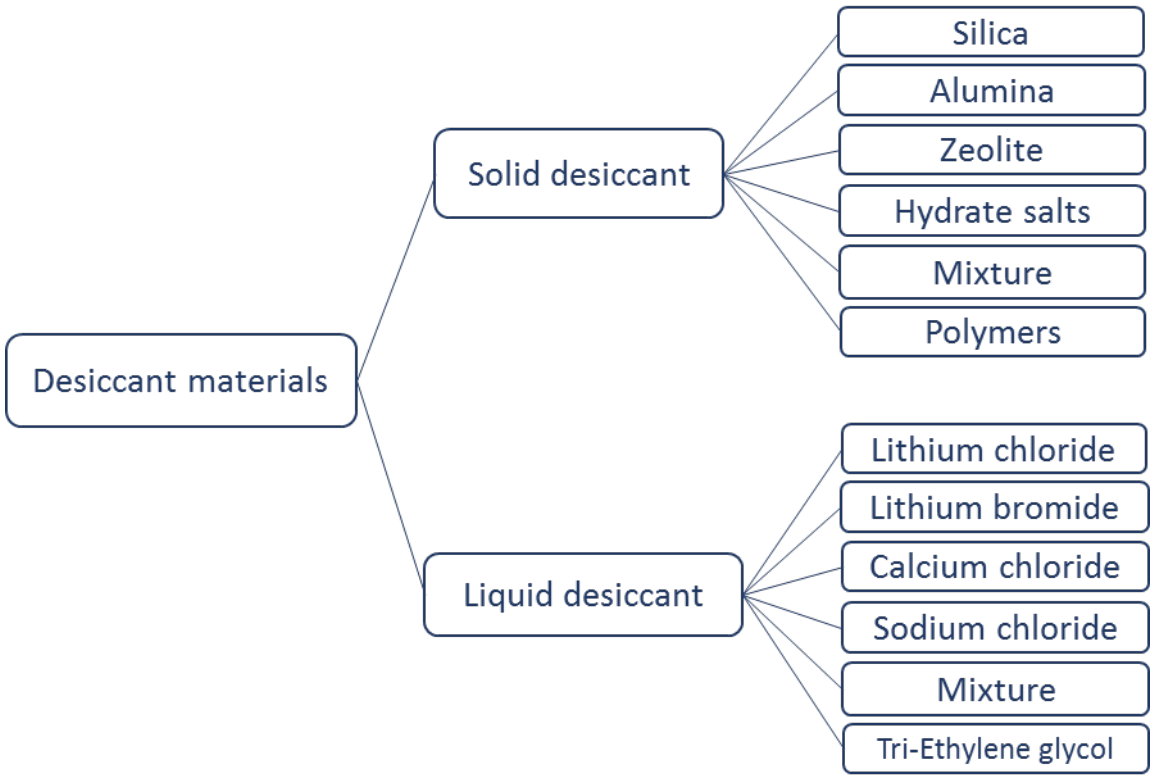


Figure 2-20 Main types of solid and liquid desiccants. [175]

The solar driven solid desiccant cooling system is a simple cooling system. It mainly consists of a desiccant dehumidifier, heat recovery wheel, heating source and evaporative coolers. In its operation the hot and humid air is dehumidified after passing through desiccant dehumidifier, and then this dry air is cooled down in heat recovery wheel (Figure 2-21) [176].

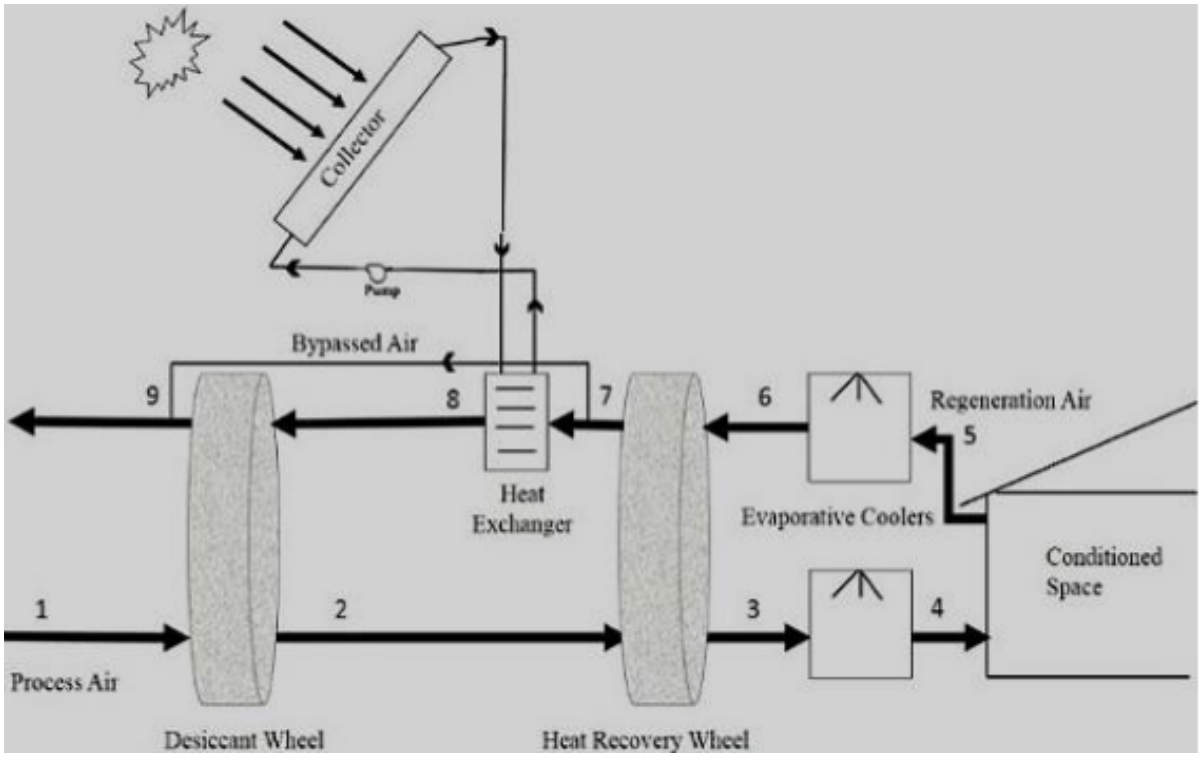


Figure 2-21 Systematic diagram of solid desiccant cooling system. [176]

The evaporative cooler is used to achieve the requirement of indoor air supply conditions. For the operation to be continuous, heat is supplied to regenerate the desiccant wheel. Heat sources in the system can be solar thermal, waste heat recovery or any other sustainable energy. The rotating adsorption wheels are normally made of silica gel, zeolite or lithium chloride as sorption materials [85]. The operation process will be described briefly below:

1-2: Outside air goes through desiccant wheel in rotation to be dehumidified;

2-3: air goes through a heat exchanger to be pre-heated;

3-4: air passes through humidifier to get cooling effect;

5-6: Regeneration air go through the humidifier for regeneration, then new air goes through 3 again;

6-7: air temperature rises;

7-8: air is heated by solar collector and heat exchanger;

8-9: the heated air goes through desiccant wheel to desorb water contained in adsorbent (regeneration process).

Zhao and Dai proposed and tested a new type of solid desiccant dehumidification cycle driven by waste heat recovery device (HRD) with sorptive material coated heat exchanger [177] [178]. Waste heat recovery will be used for regeneration. As a results, the system thermal COP has been improved to 1.2, almost twice of the conventional cycle without HRD. The electrical COP can reach 13.83.

In Muzaffar and Vladimir investigation of performance of solid desiccant evaporative cooling [66] system, the system performance is strongly influenced by the climate conditions [179]. The results showed that the COP of the micro-thermal climate place, mesothermal climate, and dry-summer are average 0.405, 0.89 and 1.01, respectively. While the COP in the day place and humid place are 2.43 and 3.03 respectively.

2.5.4.3 Solid desiccant materials for TES system

Over the last decades, the depletion of fossil fuels and the threat of global warming have challenged building application industry to develop new cooling technologies to replace conventional fossil fuel driven heating and cooling system [180]. Numerous alternative technologies have been developed to substitute conventional air conditioning systems. Solid desiccant technology is one of them. Compared with other systems, solid desiccant cooling systems have several significant advantages [181] [182]:

- SDC systems can be driven by low grade thermal energy, such as waste heat recovery and solar thermal technologies, to reduce large energy consumption;

- Water is used as the refrigerant. And most desiccant materials, such as silica gels and zeolites, are also no harmful to the environment;
- Desiccant materials are efficient and economical for dehumidification;
- SDC systems can be able to handle air with extremely low dew-point temperature;
- SDC systems can treat latent and sensible heat loads independently to avoid great energy waste;
- Compared with liquid desiccant, SDC systems have less corrosion problems.

In overall performance of the whole cooling system, performance of desiccant plays a significant role. Especially in terms of dehumidification and regeneration capacity.

Solid desiccant material is the material can adsorb water vapor in moisture air and it can be regenerated at relatively high temperature. In general, it can be classified into two main categories [183]:

- Materials with porous structure, such as activated alumina, silica gels and zeolites. These materials work based on the different pressure of water vapor between pores and surrounding air. It is a physical adsorption process;
- Materials can form solid crystalline hydrate, such as LiCl, $CaCl_2$ and LiBr. It is a hydration reaction process.

The higher adsorption capacity and better regeneration ability of solid desiccants are expected in cooling cycle. And also, appropriate desiccant materials should also have other characteristics, such as long-term stability, nontoxicity and cost efficient [184].

Therefore, the summary of recent researches and developments on novel solid desiccant materials will be presented. It will include composite desiccants,

nanoporous inorganic materials and polymeric desiccants. The classification of advanced solid desiccant materials is shown in Figure 2-22 [185].

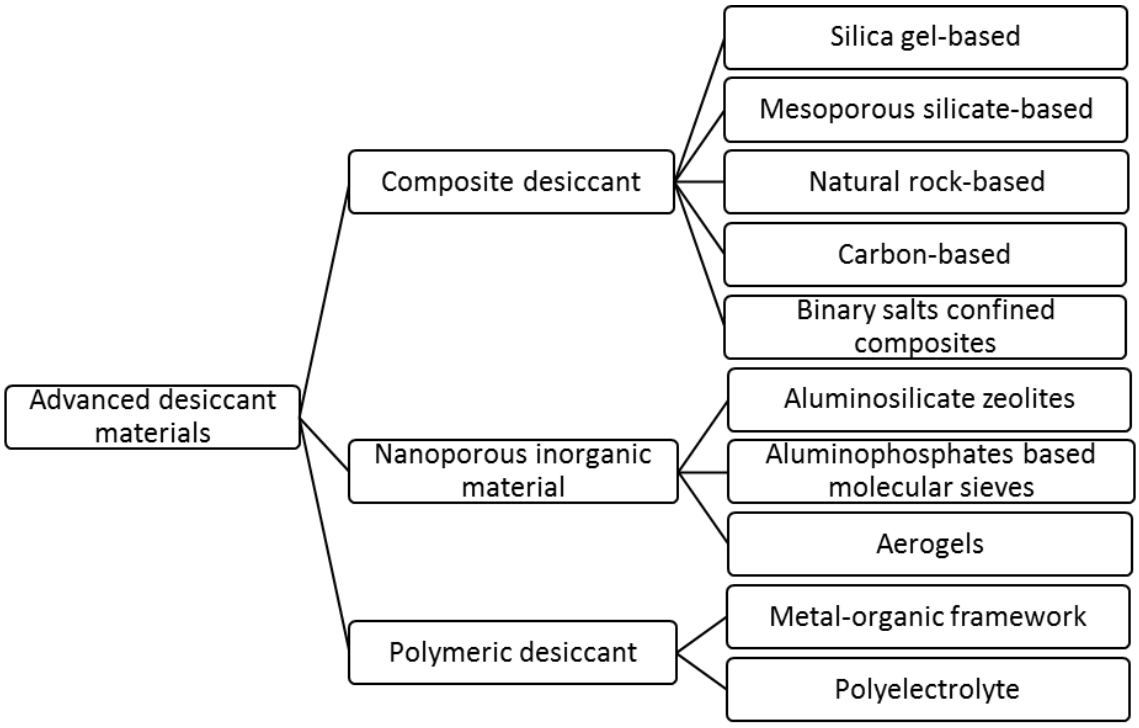


Figure 2-22 Classification of advanced desiccant materials. [185]

2.5.4.4 Endothermic materials for cooling system

Endothermic chemical reaction is an energy absorption process when the endothermic materials adsorb water.

As one of the best endothermic materials, urea was discovered by Friedrich at the first time in 1828 and it presented that urea can be obtained from inorganic starting materials [186]. It adsorbs water while absorbs great energy to show a cold surrounding temperature. In recent studies, there is no research shown on urea cooling system. The equation of urea hydrolysis is shown as followed:

$$(NH_2)_2CO + 2H_2O \xrightarrow{urease} (NH_4)_2CO_3$$ [187]

In 1974, Gossett developed a patent of urea cold pack which had an inner bag to provide an immediate cold [188]. In his patent, urea was used as endothermic

materials for medical cooling. Later in 2016, Kruckman and Chang invented a dry instant cold pack, which includes about 50-55g raw endothermic materials [189]. The raw material is preferably ammonium nitrate, calcium ammonium nitrate [190] or urea and the cold pack can produce a cooling effect within 30 seconds. The melting point of urea is 133 °C [99]; therefore, the regeneration temperature should be very low. However, there is no research shows the urea dehumidify temperature.

Nitrates such as sodium nitrate ($NaNO_3$), calcium nitrate ($Ca(NO_3)_2$), ammonium nitrate (NH_4NO_3) can absorb heat/energy when mixed with water. They are important endothermic materials which can be theoretically used for cooling. In Diarce et al. study, a mixture composed of sodium nitrate and urea for use as a phase change material (PCM) in thermal energy storage systems between 75 and 90 °C [191]. The melting temperature was 85 °C with a latent melting enthalpy of 172 J/g and the mixture also showed sub-cooling during solidification.

Urea and Nitrate salts have the characteristic of water-cooled; however, there is few research did for the endothermic cooling system. Because of the hygroscopic of these endothermic materials, the influence of degradation and temperature shall be considered and tested in the future work.

Some previous studies with materials are shown in Table 2-2:

Table 2-2 Recent studies of thermochemical cooling materials and performance.

Materials	Performance and characteristics	References
Silica gel (SG)/haloids	Regeneration temperatures from 65 °C to 80 °C, 65 °C to 75 °C and 80 °C to 90 °C were recommended for different environmental condition. The experimental results showed	(Ge, Li, Wang, & Dai, 2009) [192]

	that high performance of the system can be achieved with lower regeneration temperature which makes the use of low grade energy feasible.	
SG /LiCl	The specific cooling power was 210-290 W/kg and real cooling COP was 0.32-0.4	(Gordeeva, Freni, Aristov, & Restuccia, 2009) (Gordeeva & Aristov, 2011) [193] [194]
SG/$CaCl_2$	The desired adsorption properties can be achieved by varying the content of the $CaCl_2$ in the pores. They strongly suggested that for a short working cycle the content of salt in the composite adsorbent should not be too high.	(Zhang & Qiu, 2007) [195]
SG/active carbon	It improved the dehumidification ability of carbon black at a relative humidity condition of 40% by combining silica gel with activated carbons.	(Huang et al., 2010) [196]
SG/$CaCl_2$ SG/LiCl SG/$MgCl_2$	Water uptake decreased in the order SG/$CaCl_2$ > SG/LiCl > SG/$MgCl_2$ >> Pure Silica Gel at a condition of 17% salt in silica gel-based composite desiccants. By the meantime, silica gel-based desiccant with 33% $CaCl_2$ showed COP of 0.83 and 0.85g/g water adsorption ability without showing flooding of the sorbent bed.	(Cortés, Chejne, Carrasco-Marín, Pérez-Cadenas, & Moreno-Castilla, 2012) [197]

Silica KSK with 34.5wt% of $LiNO_3$	Maximum bed temperature was only 64.5 °C, both the COP and SCP remained reasonable, 0.155 and 193 W/kg, respectively. A much lower heat source was possible to the regeneration of composite desiccant.	(Aristov, Sapienza, Ovoshchnikov, Freni, & Restuccia, 2012) [198]
$SG/NaSO_4$	The sorption capacity of composite $SG/NaSO_4$ is stated to be 0.85 g/g that exceeds noticeably the linear superposition of the sorption capacity of the $SG/NaSO_4$ mechanical mixture which is 0.66 g/g. The heat storage capacity of the system was stated to be 0.36 kWh/kg	(Sukhyy, Belyanovskaya, Kozlov, Kolomiyets, & Sukhyy, 2014) [199]
SBA-15/$CaCl_2$	At a condition of T = 50 °C and vapor pressure is 0-50 mbar, the material showed a high water sorption capacity exceeds 0.47 g/g when P/P0 is lower than 0.3	(Ponomarenko, Glaznev, Gubar, Aristov, & Kirik, 2010) [200]
SBA-15/LiCl MCM-41/LiCl	Composite desiccant with larger pore size had much higher dynamic sorption quantities and reasonable diffusion rate constant	(Zheng, Wang, Ge, & Hu, 2015) [201]
SBA- 15/$CaCl_2$	Composite desiccant with larger pore size was able to be driven by a lower desorption temperature which was 6 °C lower than composite desiccant with smaller pore size.	[202] [202]

Mesoporous silica with sodium malate; sodium polyacrylate and sodium polystyrene sulfonate	The moisture/toluene selectivity of three composite mesoporous silica are 4.7, 3.2, and 2.8 times than that of MS, respectively. The one with sodium malate showed the best moisture adsorption capacity, and the water uptake was doubled compared to pure mesoporous silica at 25 °C and P/Po of 0.7.	(Pei & Zhang, 2012) [203]
Wakkanai siliceous shale with LiCl, $CaCl_2$ or NaCl	The shale and chlorides composite desiccant can adsorb and desorb 60 g water vapor per hour at the regeneration temperature of 40°C while silica gel and zeolite adsorbed and desorbed only 10 g and 25 g per hour respectively. The shale composite desiccant will achieve the effective use of low temperature exhaust heat for regeneration.	(Nakabayashi et al., 2011) [204]
Vermiculite/$LiNO_3$	The water adsorption load was 0.4 g/g at a temperature range of 33-36 °C in adsorption process and 62-65 °C in regeneration process, corresponding to a remarkable heat storage capacity of 0.9 MJ/kg	(Sapienza et al., 2012) [205]
Actived carbon/LiCl	Dehumidification capacity of all samples increased with higher inlet air humidity. Composite coated heat exchanger can remove more moisture from the process air than mesoporous silica gel. Composite active carbon had the best dehumidification capacity under set simulation conditions.	(Zheng, Wang, & Ge, 2016b) [206]

ACF-$CaCl_2$ and SG-$CaCl_2$	The best sorption performance of water uptake 1.7 g/g, which is three times more than silica gel-$CaCl_2$.	(Wang, Wang, & Wang, 2016) [207]
NaCl/$CaCl_2$/EG	Increased linearly with the addition of EG content and density. And also, it demonstrated that the binary eutectic chloride was restricted in minimum 7 wt% of EG content with no leakage from porous structure of EG in the melting and freezing process. The specific heat capacity of composite PCMs strictly decreased with the increase of EG content.	(Tian, Wang, Ding, Wei, & Huang, 2016)[208]
FAM-Z02(SAPO-34)	Compared the performance of one and two-adsorber bed ACS packed with FAM-Z02 showed that the SCP and COP of the two-adsorber bed ACS increase by 28% and 47%, respectively. And the maximum cooling COP of two-adsorber bed was 0.39 at a regeneration temperature of 70 °C.	(Sharafian, Dan, Huttema, & Bahrami, 2016) [209]
CPO-27 MOF	The water adsorption load of CPO-27(Ni) is 0.47g/g, and the energy density of CPO-27(Ni) was shown as 170 W h/kg.	(Elsayed, Raya, Mahmoud, Elsayed, & Anderson, 2016) [210]
MOF-801	MOF-801-P and MOF-841 are the highest performers based on the three criteria stated above; they are water stable, do not lose capacity after five	(Kim et al., 2016) [211]

adsorption/desorption cycles, and are easily regenerated

at room temperature.

2.6 SUMMARY

A comprehensive review of different thermochemical energy storage materials, systems, and technologies have been presented. Some convectional thermal heat storage technology such as latent and sensible heat storage have been introduced initially. Compared with the traditional energy storage system, it has been concluded that novel thermochemical energy storage materials and open heating/cooling cycles are energy efficient and environment friendly approach for built environment. Numbers of researchers have spent effort on this study by using simulation and doing experiment. Systems and materials performances have been significantly improved in recent years. Thermochemical energy storage can store large load of heating/cooling energy in relative smaller equipment, compared with sensible and latent heat storage system. In this chapter, thermochemical energy storage principle, technologies and some recent advances have been shown. The recent research focus on the development of the absorption and adsorption working pair and the optimal materials and composites with the following properties:

- High energy storage density;
- Low charging or regeneration temperature;
- High water or sorbate uptake as measured in (g sorbate/ g sorbent);
- Appropriate heat and mass transfer properties for efficient power output;
- Ease of handling to handle and non-poisonous nature;
- Low-cost price per kW/h of energy stored with thermal stability;

- Suitability for the application.

Conclusions can be drawn from the literature review on the thermal heat store and thermochemical energy storage system. Further research is necessary to develop the scientific and engineering characteristics of thermochemical energy storage technologies and improve system performance and implementation. A main result of this review has concluded that thermochemical energy storage materials and systems are energy efficient and environment friendly approach for building applications. Further development and improvement in systems design and materials performances will be the key issues of energy storage system in built environment.

The following aspects should be taken into consideration in order to achieve an optimal and energy efficient thermochemical energy storage system for commercialization:

1. System cycle design: The length of TES system cycle is very important for an optimal design. TES system can provide either short-term or long-term (seasonal) energy storage. The main design of TES system is for heating and cooling supply in applications to balance the energy mismatch in a most economical way.

2. Materials development: Compared with other energy storage materials, TES materials have the characteristics of high energy storage density and long storage time. It is important to develop composite materials with higher energy storage density, lower regeneration temperature, higher reaction temperature and lower price.

3. Heat transfer process: Heat transfer systems need to be simple and efficient to provide the occupants of a building with the comfort they need. The heat transfer efficiency of the TES system is the key to directly affecting the efficiency of the entire

system. Therefore, the heat transfer from the TES materials to heating or cooling supply in the system is very worth studying.

4. Regeneration process: The regeneration process determines the duty cycle of a TES system. In the TES heat storage system, solar energy in summer or daytime can be stored in TES material for winter or evening use. The charging source determines that the regeneration temperature of TES materials needs to be lower than that of traditional heat storage materials. Hence, we need to increase the efficiency of the regeneration process with very low energy consumption while increasing the provided regeneration temperature of the system, and reduce the regeneration temperature required for TES materials.

5. Optimise operation to make it simple: In order to commercialize the developed TES system, we need to optimize the entire operating system to make it easier to use and manage in building applications. It also needs to simplify the later possible maintenance and repairs.

3 RESEARCH METHODOLOGY

In this thesis, the methodology is mainly based on the following stages:

3.1 BACKGROUND INVESTIGATION AND LITERATURE REVIEW

The previous and current research about different thermal energy storage and thermochemical energy storage system have been studied and compared. In the literature review, the state-of-the-art of the energy storage cycle, materials and system design have been investigated to understand the development and potential of the project.

3.2 DESIGN AND MODELLING WORK

In this simulation, the applicability of open loop TES in buildings in the UK and worldwide through a comparative analyse with SHS and LHS will be theoretically investigated. Using IES-VE, MATLAB and Excel software to evaluate the material based thermodynamic analysis in the system.

3.3 SMALL SCALE TESTING WORK IN LAB

Some small scaled tests have been designed and investigated for the system and materials performance analysis. To select the optimal materials and the best system design after analysing the small tests results.

3.4 LABORATORY SCALE RIG TESTING AND DEVELOPMENT

The THS system test rig has been designed and developed, it was tested under the laboratory conditions, and the one optimal material has been selected for using in the prototype.

3.5 PROTOTYPE TESTING AND MODIFICATION

A field trial was carried out on a prototype in the laboratory to detect and monitor the real-time performance characteristics of the full-scale open loop THS system and some modification has been done after the 1st cycle test. Another test cycle was taken after modified the prototype.

3.6 LIMITATION OF WORK

This project basically completed the preliminary research on the properties of TES materials and the TES system. However, due to various conditions, there are some limitations to work.

1. Since the prototype is carried out under laboratory conditions, its operating conditions are somewhat different from the real environment. Therefore, there are some inaccurate results.

2. As the experimental project has a two-year period, there is not enough time to develop more TES materials.

3. Due to the limitation of laboratory conditions, the solar PV panel was not connected to the prototype in the end.

4. Due to the limitation of the production process, the entire system cannot be completely insulated, which is also one of the important reasons for the deviation of the results.

In future work, we will refer to the problems in this project and improve the new prototype, to avoid the above limitations to the greatest extent and make the experimental results more accurate.

4 INITIAL EXPERIMENTS FOR CHARACTERISTICS ANALYSIS OF SALT IMPREGNATED TES MATERIALS

4.1 INTRODUCTION

Thermochemical heat storage is mainly based on the reversible chemical reaction process: A + water ↔ B + heat. Similar to other thermal energy storage ways, thermochemical energy storage cycle consists of two main processes: charging and discharging. In my study, before working on the test rig, several thermochemical energy storage materials have been selected for some initial tests based on previous researches. The initial tests focused on energy storage capacity of the prepared TES composite materials. Some new TES composites materials will be prepared based on the initial tests as well. Thus, several initial investigations of TES materials were performed. It aims at:

- Determining the performance of TES materials under the specified operation conditions;
- Analysing the TES materials parameters;
- Using better performance materials to prepare TES composites and analysing the energy storage availability and capacity.

In order to perform technical assessment of the system the exact material specification was needed to be assessed and taken into consideration for the TCES design. The data obtained was weight, temperature, humidification, energy density of the material, see table for detailed description of the measuring equipment.

Components	Purpose
DataTaker d80	Measuring temperature change
Sensirion	Measuring relative humidity of the material
SDT-Q600	Measuring energy density of the material
Kern weight scale de6x10	Measuring the weight of the material

4.2 TES MATERIALS SAMPLES PREPARATION

4.2.1 Vermiculite base materials preparation

Vermiculite is a natural, non-toxic mineral. It is a relatively rare mineral that belongs to the silicate salts. Structurally, vermiculite is a mixed layered silicate crystal. It can swell at high temperature at 300 °C. Vermiculite is widely used as building materials, adsorbents, because it is lightweight materials. And also it is used for active carriers for adsorbents, filter aids, chemicals and fertilizers. Furthermore, as the host matrix, vermiculite has been confirmed slowdown sorption dynamics, allowing the reaction process to be more easily controlled, and suppling energy when it is necessary [212].

The composite thermochemical materials will be salt hydrate mixture stabilised in porous vermiculite. The targeted salts are $CaCl_2$, $MgCl_2$, LiCl and their mixtures in various compositions to be impregnated into porous vermiculite. These salts are highly hygroscopic and will likely dissolve without proper containment within a host matrix. The vermiculite is a laminar aluminium-iron-magnesium silicate and its structure is primarily macroporous with a pore size ranging between 10 nm to 10,000 nm. The macropores can facilitate salt impregnation and also benefit the kinetics of

moisture migration. The internal surface area of vermiculite can be up to 15 m^2/g, which provides a sufficient surface for salts to attach, hence, overcoming the issue of salt dissolution and subsequent aggregation. Pioneered by Aristov and discussed by Gordeeva and Aristov [127] in composite materials, the most common method is impregnating matrix with an aqueous salt solution:

- Dry the hold matrix to remove absorbed water;
- Impregnate with salt solution;
- Filtration;
- Dry the composite matrix to remove the adsorbed water.

An excess of salts solution leads to more crystallization on surface of the composite materials after dried [131]. The improved incipient wetness method is to mix matrix and salts solution and keep it for several hours to let the solution goes well through the centre of matrix. When mix matric with salt solution, it shows an adequate solution when the liquid just accumulates on the bottom of the container. Crystal will not appear on the surface of composite materials after dried [131].

The method is further classified into two methods: dry and wet impregnation method [128]. In the ‘dry’ method, wet composite has to be kept for several hours to let the salts solution goes into the centre of matrix. So the salt solutions volume is assumed equal with the pore volume. Crystal will not be formed on the external surface of the porous materials when drying composite materials; however, in the wet method the volume of the salts solution exceeds the pore volume leads to crystallization occurs on the surface of the composite materials. In order to remove the large crystals on the surface, a special humidity/temperature camera can be used to observe the

crystals formed on the surface of the materials will absorb water and become solution [129].

In our thermochemical energy storage materials preparation, we use 600g vermiculite mixed with 1800g salts solution (different salts ration in 100g vermiculite shown in Table 4-1).

Table 4-1 Thermochemical energy storage materials mixture weight ratio.

	V-$CaCl_2$-$MgSO_4$	V-$CaCl_2$-LiCl	V-$MgCl_2$-$MgSO_4$	V-$MgSO_4$-LiCl
1st salt	$CaCl_2$	$CaCl_2$	$MgCl_2$	$MgSO_4$
2nd salt	$MgSO_4$	LiCl	$MgSO_4$	LiCl
1st salt solution weight, g	200	200	150	150
2nd salt solution weight, g	100	100	150	150
1st salt solubility in water, g/100ml	86	86	54.3	36
2nd salt solubility in water, g/100ml	36	83	36	83
1st salt weight % in solution	46.2	46.2	35.2	26.5
2nd salt weight % in solution	26.5	45.4	26.5	45.4
1st salt weight, g	92.4	92.4	52.8	39.8

2nd salt weight, g	26.5	45.4	39.8	68.1
1st salt weight ratio in mixture, %	42.2	38.8	27.4	19.1
2nd salt weight ratio in mixture, %	12.1	19.1	20.7	32.8
1st salt weight in 600g mixture, g	253.2	232.8	164.4	114.6
2nd salt weight in 600g mixture, g	72.6	114.6	124.2	196.8

Firstly, put 600g vermiculite in a mesh tray (as shown in Figure 4-1) in oven for 2 hours at 200 °C. If temperature increased to above 210 °C, vermiculite will become bigger and change colour to dark (the characteristic will change as well). Then take out vermiculite from oven to cool down for 1 hour, after it cooled down to room temperature, mix 600g dried vermiculite with salt solutions (1800g). Then leave it for at least 24 hours to let the vermiculite adsorb salts solutions completely. Mixture should be put in to oven at 200 °C for another 24 hours to let it completely dry. Drying temperature depends on the materials, for example, some materials can only be dried under 55 °C (e.g. vermiculite with urea). However, these TES composite materials don't have the issue of temperature, so we dry mixture at 200 °C. There is still some moisture remain in the mixture materials at 150 °C, so 200 °C is required.



Figure 4-1: 600g pure vermiculite is put in a mesh tray for drying.

After 24 hours drying, TES composites should be sealed in container to cool down to room temperature for at least 2-3 hours, because salts impregnated in the host matrix can be easy deliquescence, hence, it should be sealed to avoid adsorb moisture in surround environment. Each time before starting a new test, materials should be put into oven at 200 °C for at least 24 hours and then put it in a sealed container for at least 2-3 hours for cooling down.

4.2.2 Silica gel based composite: Potassium Formate - Silica Gel

The composite of silica gel impregnated with potassium formate (KCOOH) has been chosen as a candidate TES material. Silica gel is a granular porous silica hydrate which is prepared by washing and drying sodium silicate with acid, and is mainly used as a desiccant and an adsorbent. Because of the low cost and low desorption temperature, silica gel is wide used in TES materials. Potassium formate is strongly hygroscopic white solid is normally used as desiccant in adsorption research [213]. A novel KCOOH/H_2O pair was used in an absorption heat storage prototype to prove the interest of the KCOOH/H_2O couple in low-temperature heat storage process and

it substantially decreases the investment cost of process [214]. Study on the dehumidification performance of an internal cooling dehumidifier using KCOOH, the simulated model showed mass transfer performance precisely with the relative difference of 6.05% for dehumidification [215]. KCOOH has also been applied as a desiccant in an innovative liquid desiccant dehumidification system with a counter-flow heat and mass exchanger [216].

As solid absorbent material, silica gel is featured with high porosity and no solubility, but very limited capacity of water moisture absorption. The organic salt KCOOH shows higher capacity of water moisture absorption. In this study, we combine both adsorbent materials and salts to synthesise composite materials with high water moisture uptake and without dissolution. Silica gel and KCOOH were selected in this study because they have no corrosive effect on almost of materials, such as aluminium, iron and copper. Moreover, KCOOH is low-cost/cheap in comparison to the typical desiccant such as $CaCl_2$ and LiCl [217], [218]. It is environmentally friendly with non-corrosive and non-toxic, it is biodegradable and environmentally responsible in case of spillage or accidental release [219]. KCOOH also has a negative crystallization temperature [220] high solubility (up to 80% at ambient temperature) and gives consistent humidity reduction [219], [217], [156]. KCOOH desiccant has a low regeneration temperature requirement at around 40-50°C, which can be easily driven by solar collector or waste heat recovery system [217].

The preparation process of the synthetization of KCOOH and silica gel involves the following steps:

Step 1: 1 L of KCOOH saturated solution was dried in the oven at 150°C for 72 h to turn the solution into a powder form (Figure 4-2 and Figure 4-3).

Step 2: 460 g dried KCOOH powder was then prepared to be mixed with Silica gel.

Step 3: At ratio 2:1, 230 g of silica gel was grinded into powder form and mixed with the KCOOH powder (Figure 4-4).

Step 4: To impregnate the KCOOH into the silica gel, the mixture was left in the container for 7 days until the materials turned into a ‘sticky’ or ‘viscous solution’ form (Figure 4-5).

Step 5: The mixture was then dried in the oven at temperature 150°C to complete the impregnation process.

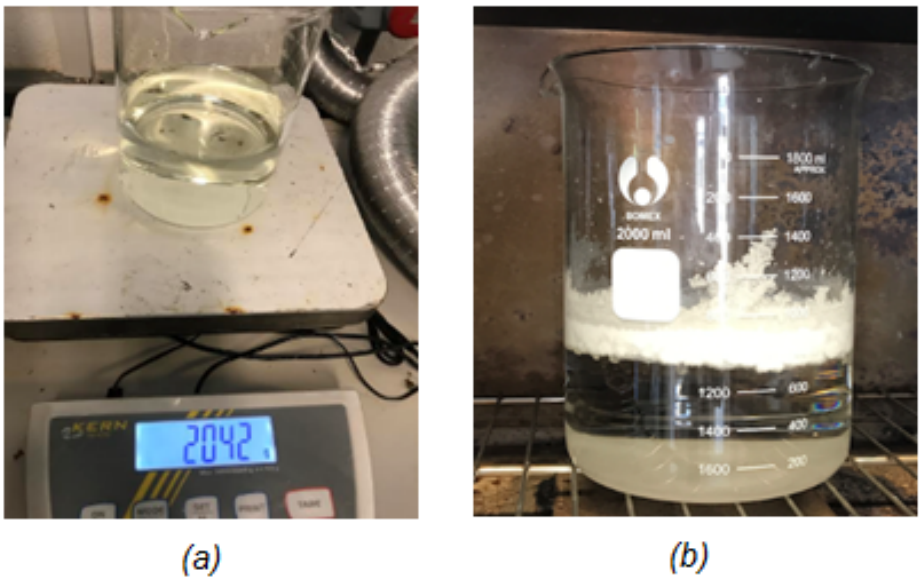


Figure 4-2 (a) Potassium formate solution; (b) Potassium formate solution with a thin layer of crystal.



Figure 4-3 Dried potassium formate solid and powder.

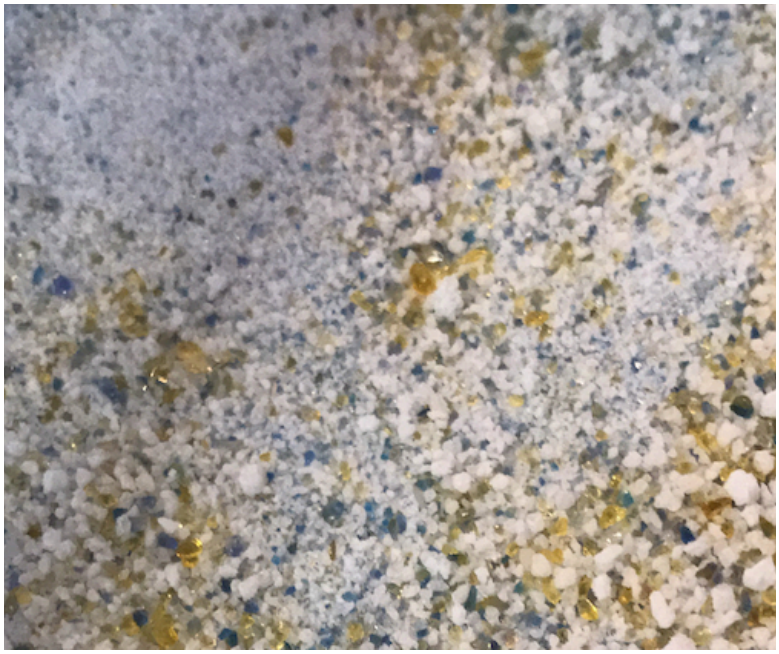


Figure 4-4 Grinded mixture of silica gel with potassium formate.

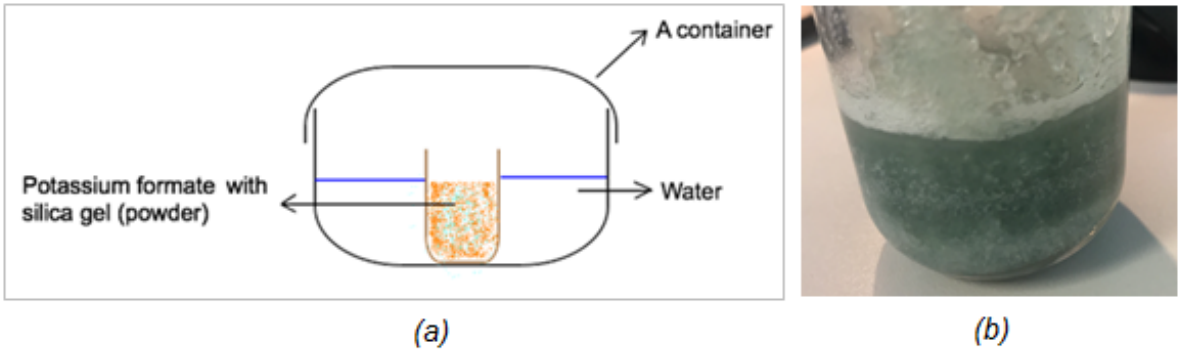


Figure 4-5 (a) Sorption test of silica gel with potassium formate; (b) Silica gel with potassium formate mixture after 7 days in the water pot.

This study discusses energy storage density and water absorption of the composites SG/KCOOH. The experimental results show that the composite adsorbent has greatly improved compared to the individual adsorbent, with values of 1600 kJ/kg and 0.675 kg/kg, respectively. TA-DSC pictures will be shown in the next section.

4.3 TES MATERIALS CHARACTERISTICS STUDIES

4.3.1 TA instruments simultaneous TGA / DSC (SDT-Q600) for TES materials energy density test and analysis

The energy density test is performed on the SDT-Q600 (see Figure 4-6 and Figure 4-7) which allows simultaneous Thermogravimetric Analysis (TGA) and Differential Scanning Calorimetry (DSC). In this test only TGA is required. Simultaneous Differential Scanning Calorimeter (TGA) measures transitions and reactions in materials in the range of ambient temperature to 1500 °C under air or nitrogen flow.

The test materials will include thermochemical heating and cooling storage materials, for example: potassium formate with silica gel, vermiculite with $MgCl_2$+$MgSO_4$, vermiculite with LiCl+$CaCl_2$, vermiculite with $MgCl_2$+$LiNO_3$, vermiculite with $MgSO_4$+$CaCl_2$, vermiculite with $MgSO_4$+$MgCl_2$+$LiNO_3$, vermiculite with urea and vermiculite with $NaNO_3$.

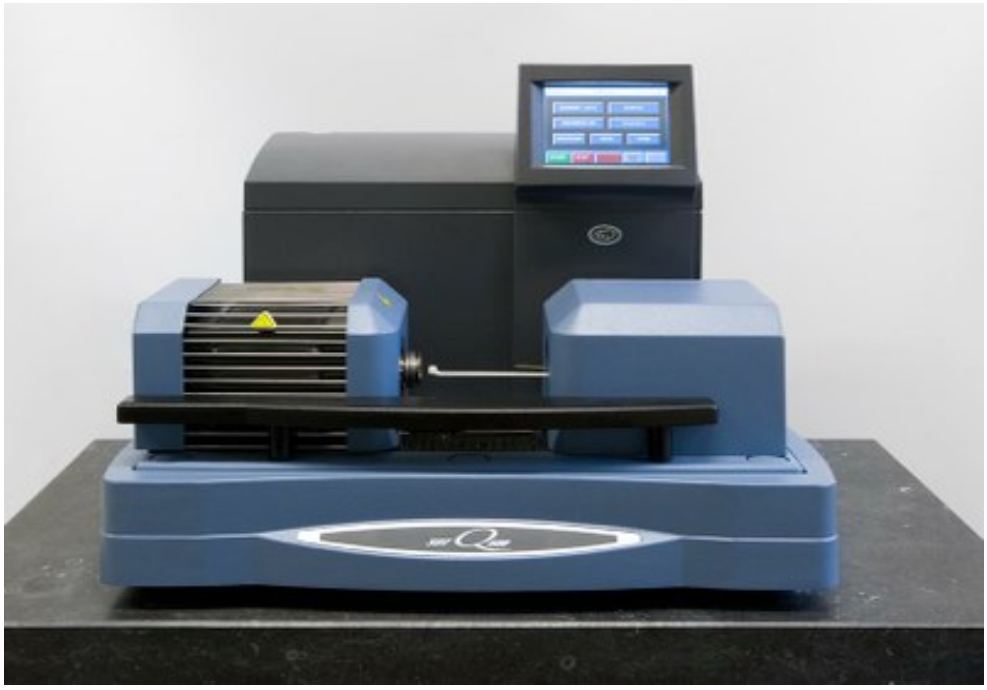


Figure 4-6 SDt-Q600 for materials energy density analysis.

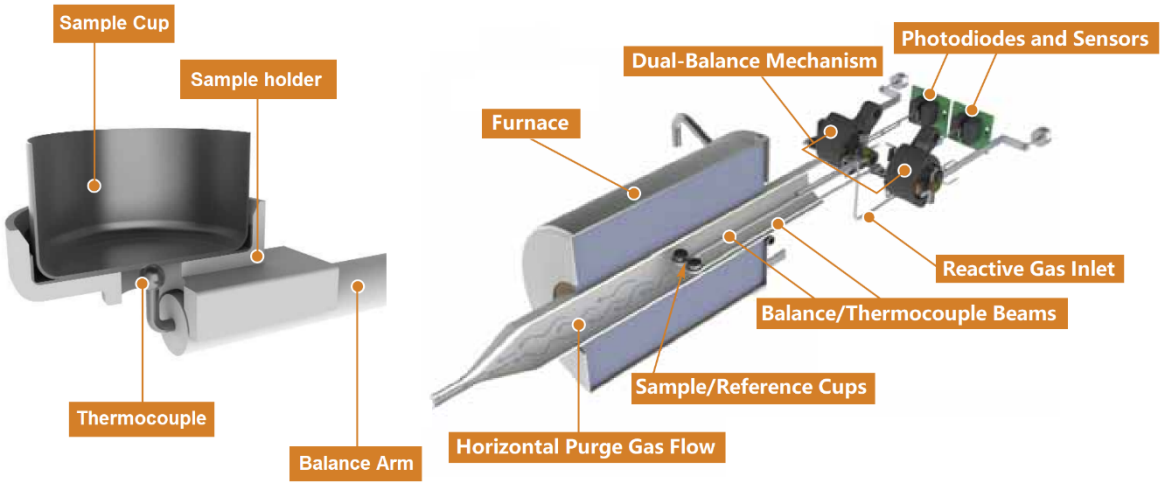


Figure 4-7 The inside detail of SDT-Q600.

4.3.1.1 Vermiculite based sample preparation

The Vermiculite matrix samples should be wetted two hours prior to testing so that the samples relative humidity can reach 95%, and the TES material is holding its maximum amount of water.

4.3.1.2 Testing

Before the test is performed, two empty alumina cups are placed onto the balance. One will be used to hold the sample later and the other is a reference cup. The furnace is sealed and the 'tare' function is used repeatedly until the weight reading of the sample and reference cups become within 0.1mg of one another. This process must be repeated before every sample is tested. The two cups are then heated from ambient temperature to 150°C at a constant rate of 10°C/minute in an inert argon atmosphere and cooled using ambient air whilst the weight of the cups is continuously measured along with heat flow. This gives a baseline measurement.

One cup is now filled with a sample to approximately halfway, and then the cup is placed onto the balance next to the empty reference cup. Once the balance settles slightly, the furnace is sealed, and then the balance is allowed to fully settle inside

the closed furnace. The test starts, and the temperature is increased again from ambient to 150°C at a constant rate in an inert argon atmosphere then cooled using ambient air. Another graph is formed. However, we only want to know information about the sample, not the cup. Therefore, we must subtract the baseline measurement from the test measurement. This can be performed by the SDT Q600 software. To find the energy density of the sample, we take the average integral reading (J/g) in the temperature range of 30-150°C.

4.3.1.3 Results

Table 4-2 SDT-Q600 analysis results.(Details of the TA analysis figures will be showed in Appendix)

	Energy density, kJ/kg	Regeneration temperature, °C
V-$MgSO_4$-LiCl	990.2	74.7
V-$MgSO_4$-$CaCl_2$	1173.5	63
V-$MgSO_4$-$LiNO_3$	1000.8	81.7
V-CaCl2-LiCl	856.4	79
V-$MgSO_4$-$LiNO_3$-$MgCl_2$	748.6	71.7
V-$NaNO_3$	872.3	82
V-Urea	727.85	54.5
Potassium formate with silica gel	442.7	125

According to the TA analysis (SDT-Q600 results analysis software) results for SDT-Q600 test (see Table 4-2), for the thermochemical heating storage materials, V-$MgSO_4$-$CaCl_2$ showed the highest energy density (1173.5 kJ/kg) and lowest regeneration temperature (63 °C). In the SEM analysis, salts can increase the porosity of vermiculite, then we mix three salts ($MgSO_4$, $LiNO_3$, $MgCl_2$) which show very good performance, together to see if there is any better performance shown; however, V-$MgSO_4$-$LiNO_3$-$MgCl_2$ did not give a higher energy density and lower regeneration temperature; hence, it does not say that the more mixed salts in the composites materials, the better performance will show. Because of these characteristics, V-$MgSO_4$-$CaCl_2$ is the optimal material can be selected. For the thermochemical cooling storage materials, V-$NaNO_3$ showed the highest energy density of 872.3 kJ/kg, while V-Urea showed the lowest regeneration temperature at 54.5 °C; however, because the price of $NaNO_3$ is much higher than urea, thus, V-Urea is the better thermochemical cooling storage material.

4.3.1.4 Al_2O_3 based sample preparation

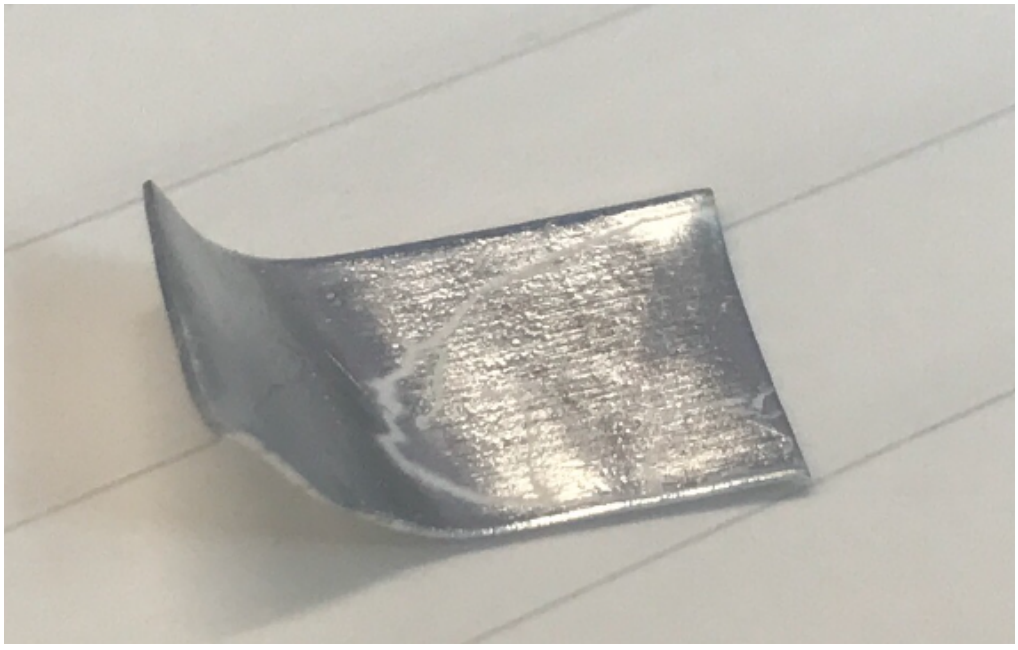


Figure 4-8 Al_2O_3 based SIM composite.

Samples are Al_2O_3 based with impregnated LiCl and $CaCl_2$ solution for 24 hours and let samples dry before test. The characterisation aims to understand the nano structure of the synthesised materials and energy density.

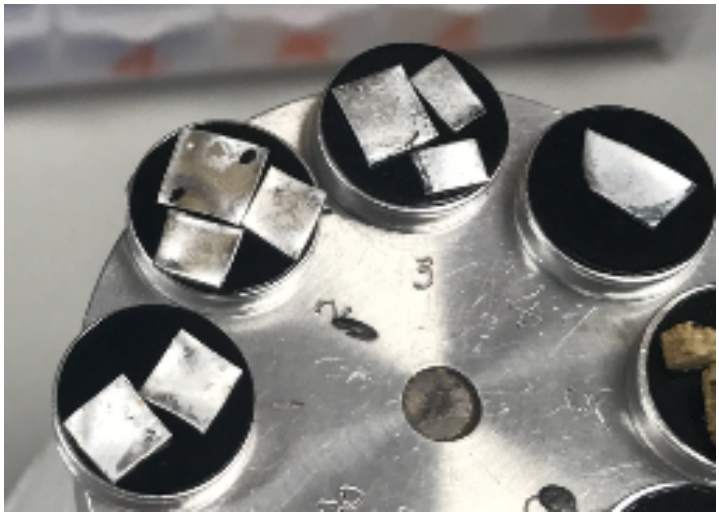


Figure 4-9 Small pieces of materials paste on the holder for SEM.

Dry samples were cut into small pieces (about 4mm*4mm) for SEM analysis. 2 or 3 pieces were necessary for the accuracy of the analysis.

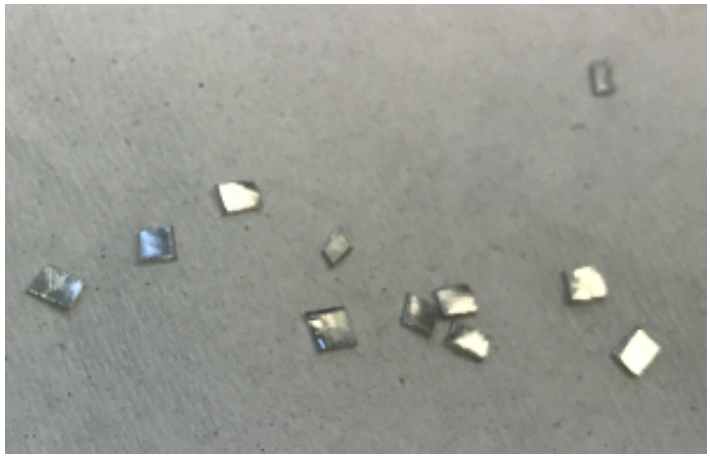


Figure 4-10 Al_2O_3 based materials were cut into small pieces for SDT-Q600.

Samples were cut into very small pieces (2mm*2mm) for energy density analysis with SDT-Q600. Before started testing, water spray was supplied on the samples to make it moisture for SDT-Q600 testing. And about 50-60mg samples filled half of the alumina cup for testing.

4.3.2 Scanning Electron Microscope (SEM) test and analysis

Scanning Electron Microscopes (SEM) can be used to visualise the salt inside of the matrix of a SIM composite. The resolution produced is better than one nanometre. This can be used to make sure that the salt is binding uniformly inside the matrix and therefore maximising surface area and potential for mass and heat transfer. Material characterization allows the SIM samples to be compared for the best overall material in an open loop system can be determined. The increase in porosity of samples after impregnation shows the potential of salt impregnation of host matrices in open cycle THS systems (from SEM photos). Other SEM photos will be shown in the Appendix B.

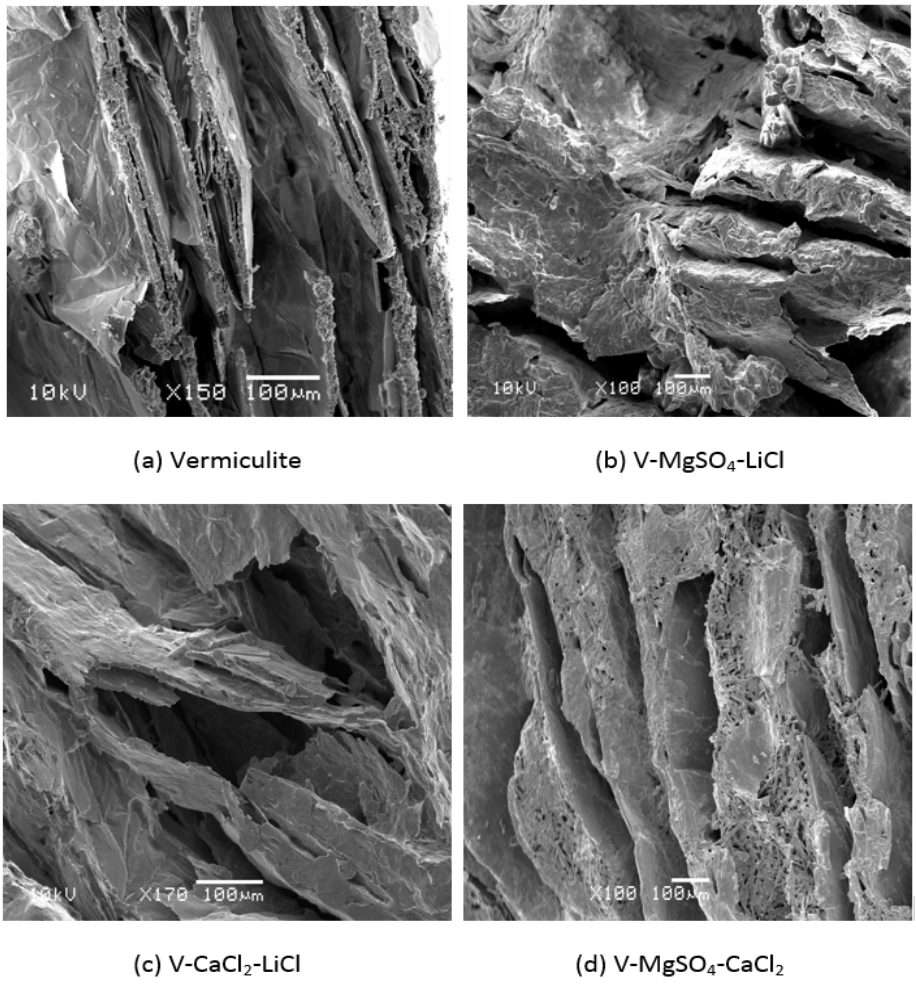


Figure 4-11 SEM photos of SIM samples.

4.3.3 Synthesised samples: Al_2O_3 - LiCl

In the SEM analysis, there is no observed nano structure showed any pore on the surface in all the samples (samples from two different pieces given). Samples photos in different magnification are shown as followed:

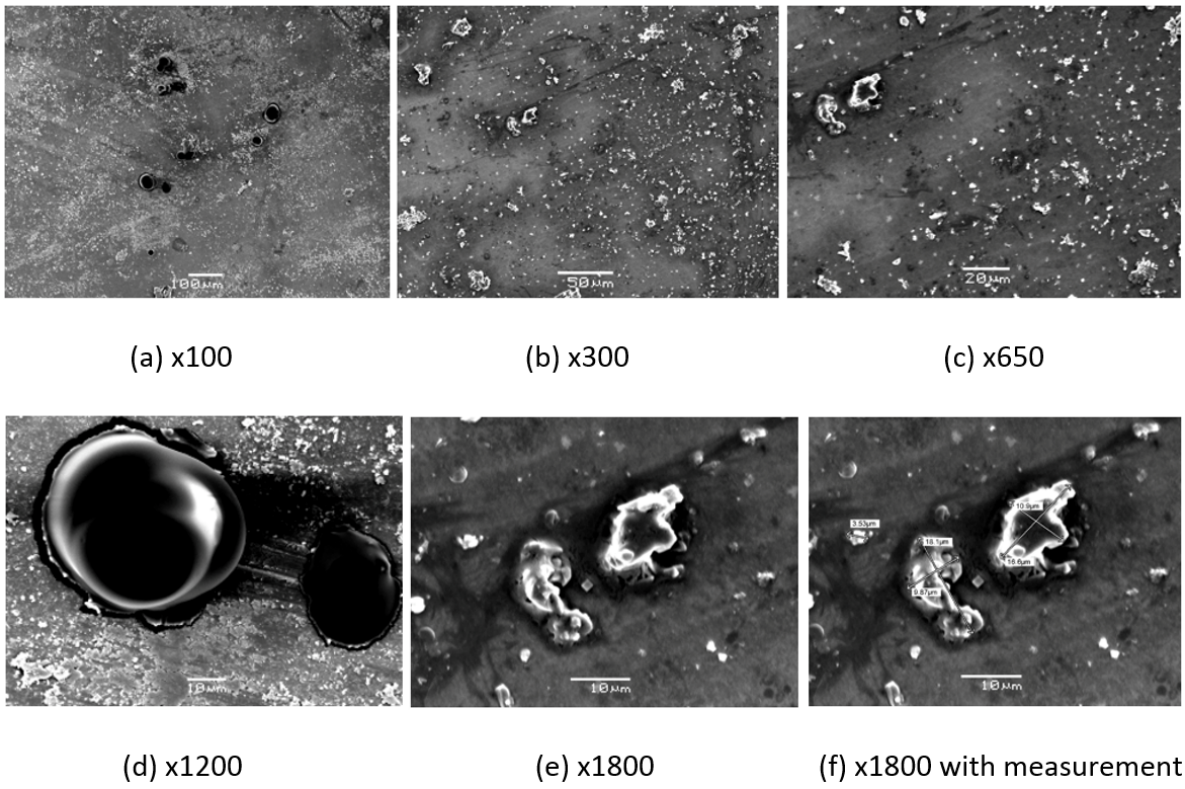


Figure 4-12 SEM photos of Al_2O_3 – LiCl under different magnification.

According to the SEM photos, even in 1800 magnification, there is no pore showed, but only some solid salts on the material surface.

In the SDT-Q600 energy density analysis, water spray supplied 2 hours before testing to make it became moisture with a relative humidity at about 95%. 40-60mg samples were cut into very small pieces for energy density testing. For each sample, each material has been taken tests for twice.

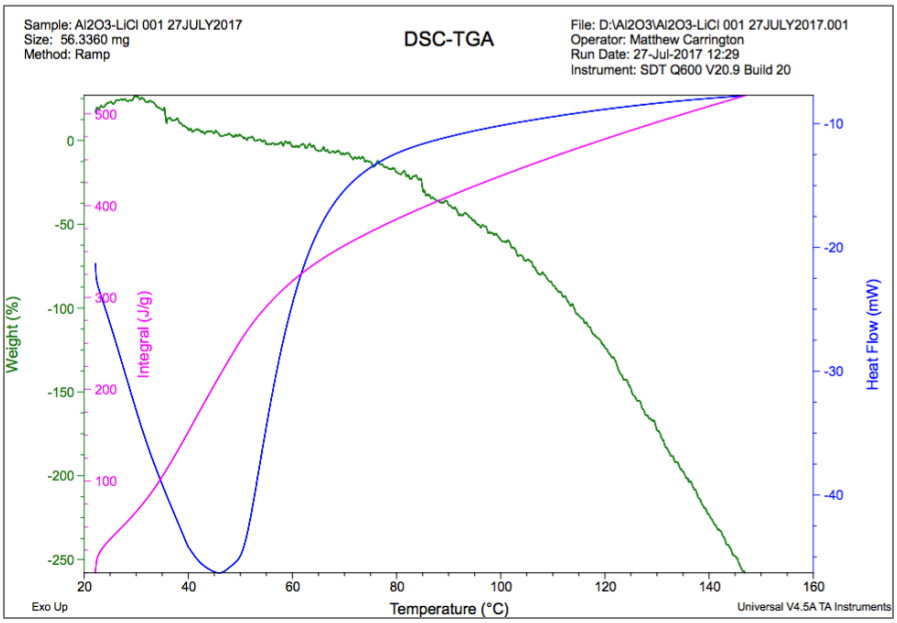


Figure 4-13 Al_2O_3-LiCl SDT-Q600 energy density analysis - 001.

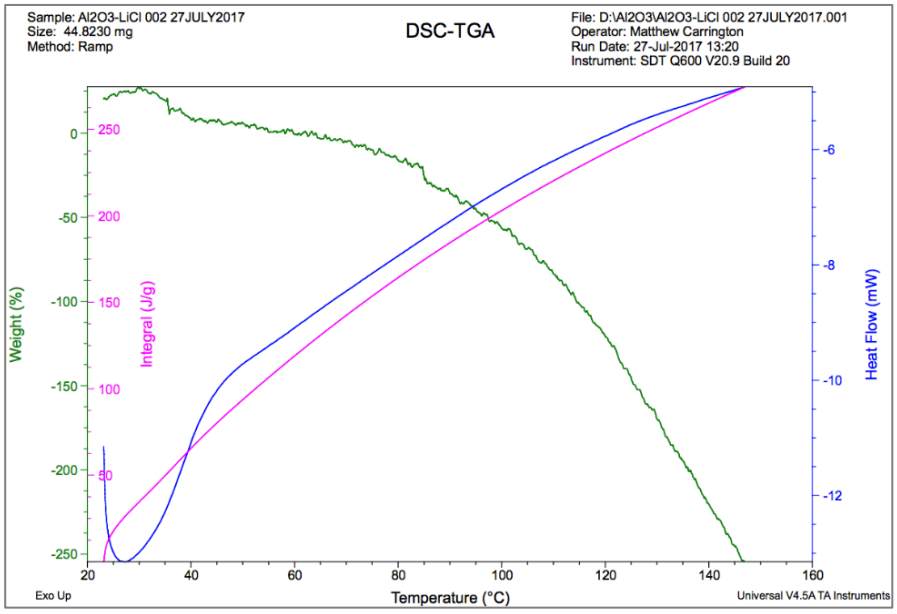


Figure 4-14 Al_2O_3-LiCl SDT-Q600 energy density analysis - 002.

The average energy density is 274.94 J/g based on the average energy density between 30-150°C. However, the average energy density for each test is quite different. So, I think more tests should be done to confirm the results.

4.3.4 Synthesised samples: Al_2O_3 - $CaCl_2$

The SEM analysis showed a very nice pore structure which means the porosity is large. Samples photos in different magnification are shown as followed:

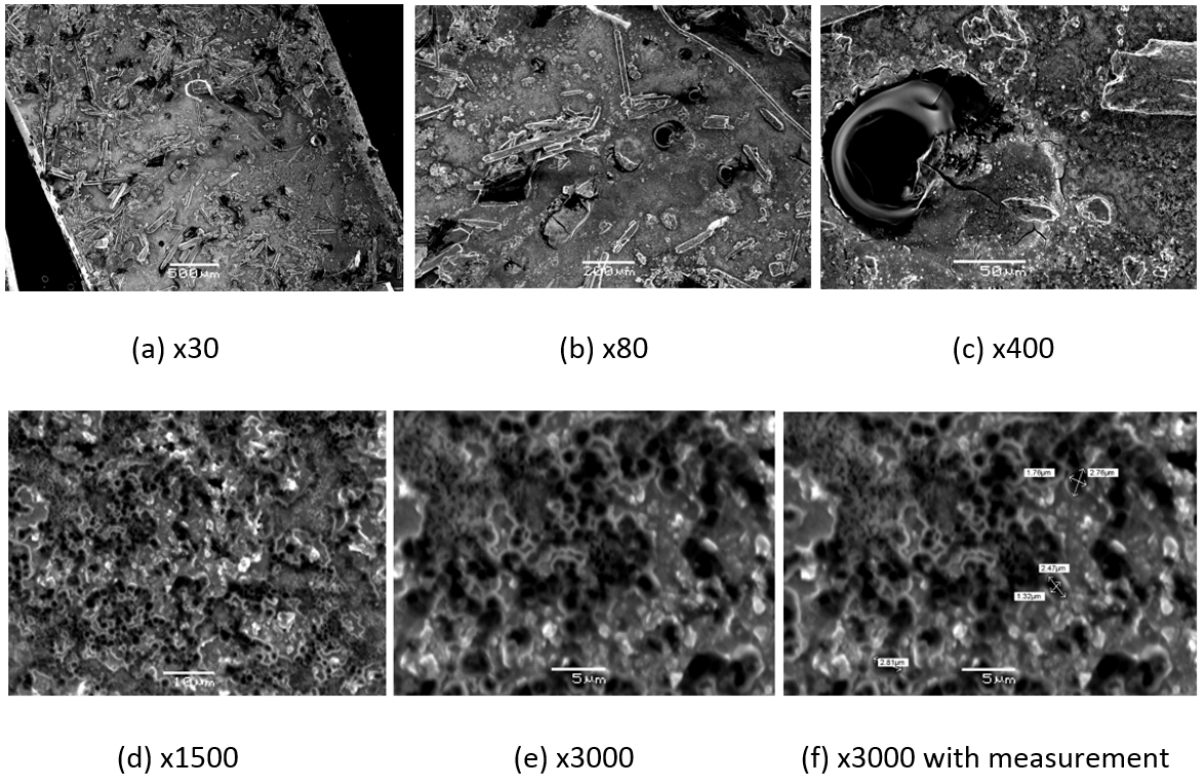


Figure 4-15 SEM photos of Al_2O_3 - $CaCl_2$ under different magnification.

At a magnification of 1500 times, there are some nice pores can be seen obviously and also some measurement of the pore has been label marked. That means the synthesised sample – Al_2O_3 with $CaCl_2$ is a good and feasible material for energy storage.

For the SDT-Q600 energy density analysis, same as the one before, water spray supplied two hours before testing to make samples moisture. Two samples have been tested.

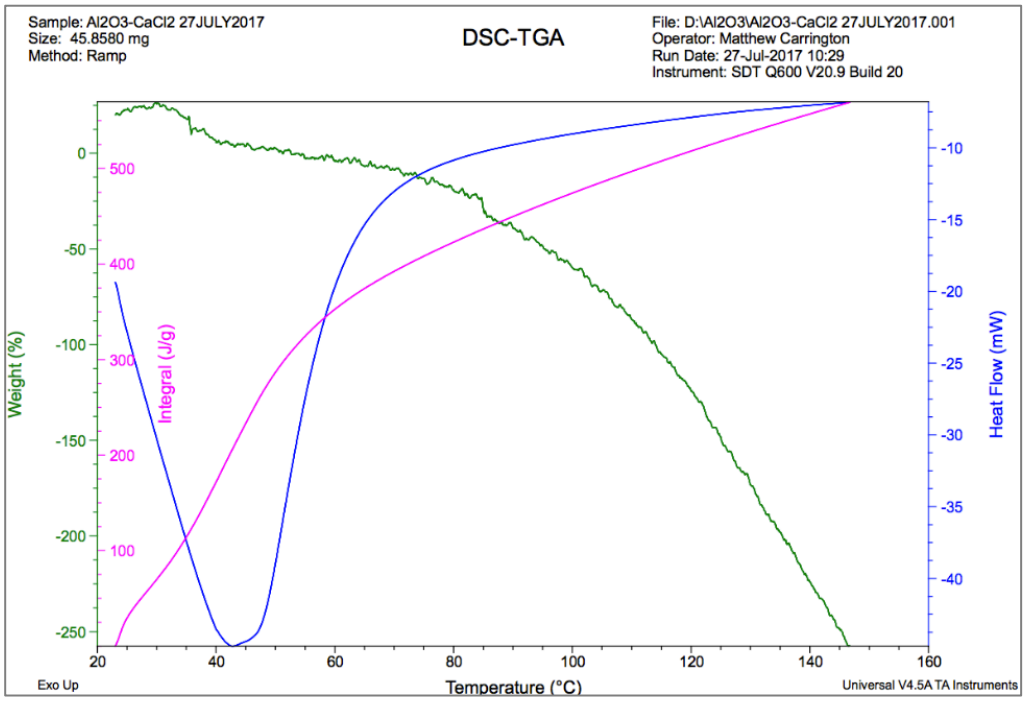


Figure 4-16 Al_2O_3-$CaCl_2$ SDT-Q600 energy density analysis 001.

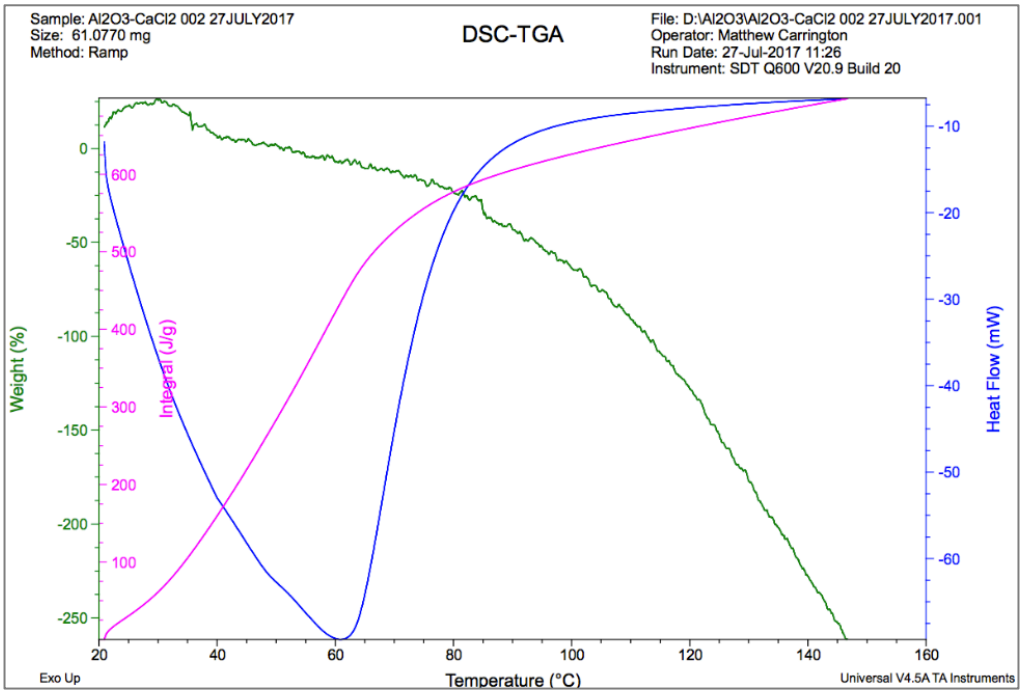


Figure 4-17 Al_2O_3-$CaCl_2$ SDT-Q600 energy density analysis 002.

The average energy density is 463.095 J/g based on the average energy density between 30-150°C. More test should be done to confirm the energy density as well.

According to the analysis of these two samples, Al_2O_3-$CaCl_2$ shows a higher performance than the Al_2O_3-LiCl.

4.4 Sorption Test and Analysis for TES Materials

4.4.1 Method

Sorption experiments with different materials and different salts sorption solution will be done. The adsorption liquids of the four salts solution are KNO_3, $MgSO_4$, $MgCl_2$ and LiCl. The test materials are: vermiculite with $CaCl_2$+LiCl, vermiculite with $MgSO_4$+$MgCl_2$, vermiculite with $MgSO_4$+$CaCl_2$, vermiculite with urea and potassium formate+silica gel.

A sorption test is used to observe the mass of water a sample can adsorb in a set period under differing humidity. In the set up below four cases are used to create four atmospheres, each with a different relative humidity level. These atmospheres are created using solutions of KNO_3, $MgSO_4$, $MgCl_2$ and LiCl (with relative humidity level: 92%, 75%, 40% and 16%) at the bottom of each case.

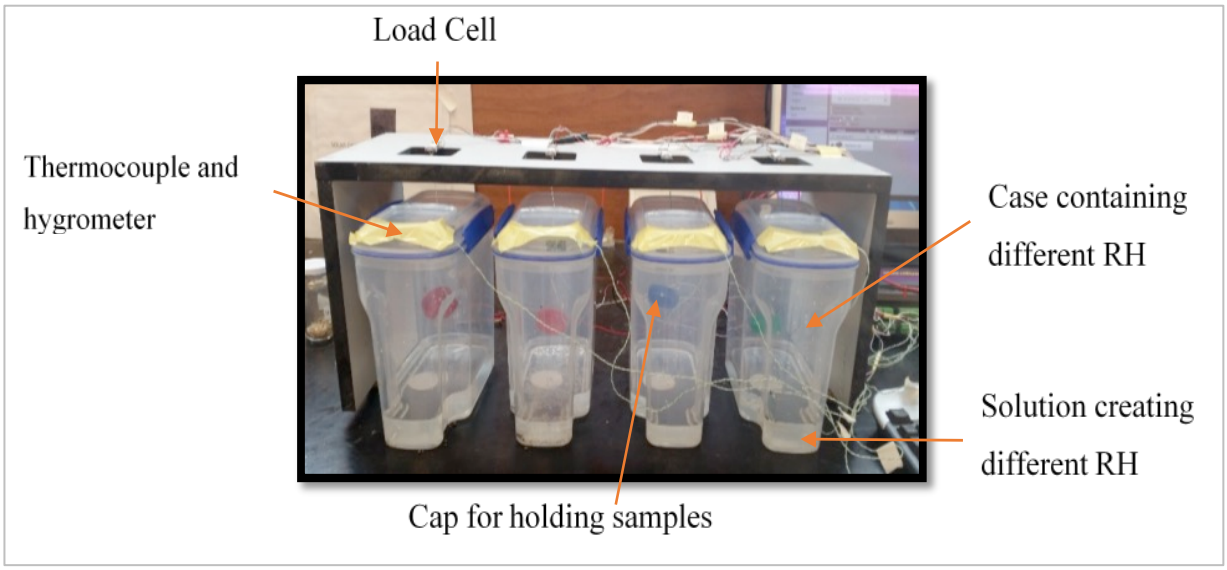


Figure 4-18 Sorption testing set.

4.4.2 Calibration

The load cell must first be calibrated before a sample can be placed into the cap. This is done in two steps:

- A reading is taken from the LoadCell with no sample in each cap. (ie. 0g in container);
- Another three readings are taken with fixed mass in each cap (2.5g, 4g and 5g);
- Every time the mass put in the cap must be left for at least 20 minutes for the LoadCell reading to be stable.

Calibration should be done in each weight sensor (Load Cell) to record an accurate number. Before the test, different loads used in the four cups. Figures show different readings in different load cells.

Table 4-3 LoadCell calibration for sorption LoadCell readings.

	Calibration 1	Calibration 2	Calibration 3	Calibration 4	Formula
Real weight, g	0g	2.5g	4g	5g	X: sensor reading; y: real reading
LoadCell1 reading, g	192	205	213	218	0.196x-37.654=y
LoadCell2 reading, g	56	68	76	81	0.196x-10.933=y
LoadCell3 reading, g	60	49	42	38	13.334-0.221x=y
LoadCell4 reading, g	35	48	55	60	0.198x-6.978=y

Samples to be tested:

- V-$CaCl_2$-LiCl (oven temp. at 200°C)
- V-$MgSO_4$-$MgCl_2$ (oven temp. at 200°C)
- V-$MgSO_4$-$CaCl_2$ (oven temp. at 200°C)
- V-$MgSO_4$-LiCl (oven temp. at 200°C)
- Silica gel with potassium formate (oven temp. at 150°C)
- V-Urea (oven temp. at 55°C)

4.4.3 Sorption test

Once the load cells have been calibrated, each cap can be filled with approximately 2g of sample. Each sample with then start to adsorb moisture from the environment around it and its mass will change. This is logged using a datalogger for at least seven days for each sample, data was recorded every 30 minutes.

4.4.4 Results and analysis

The results show the minimum humidity for complete hydration of each salt in a time period that can be set as required.

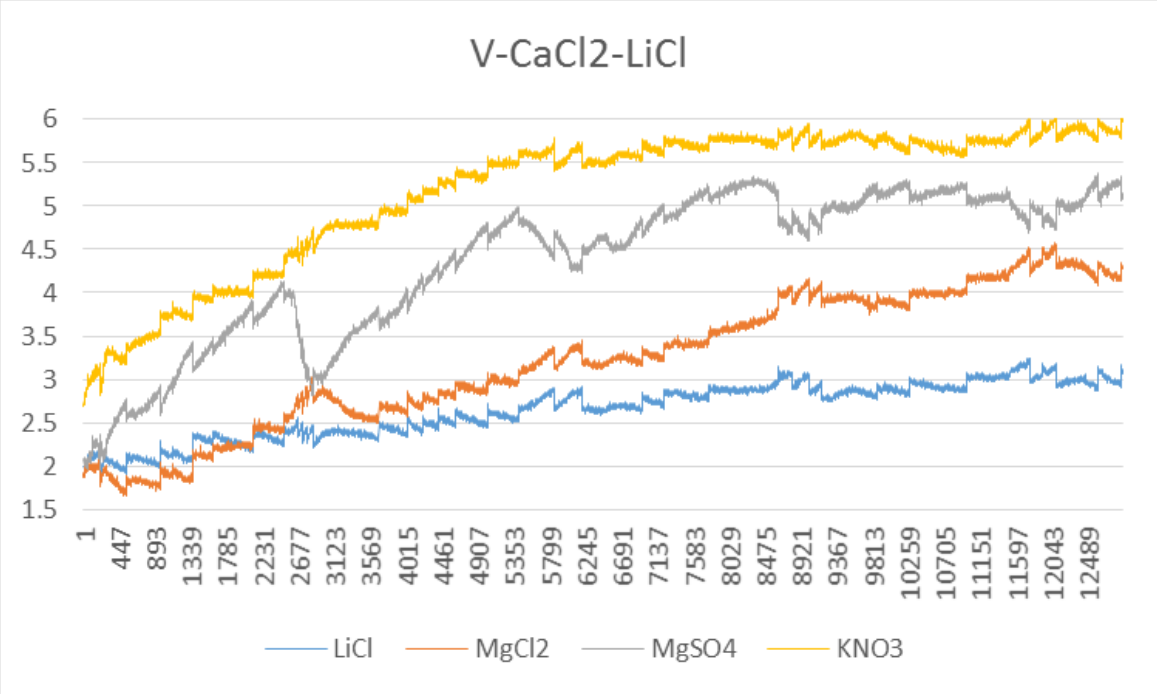


Figure 4-19 Mass change readings of V-$CaCl_2$-LiCl.

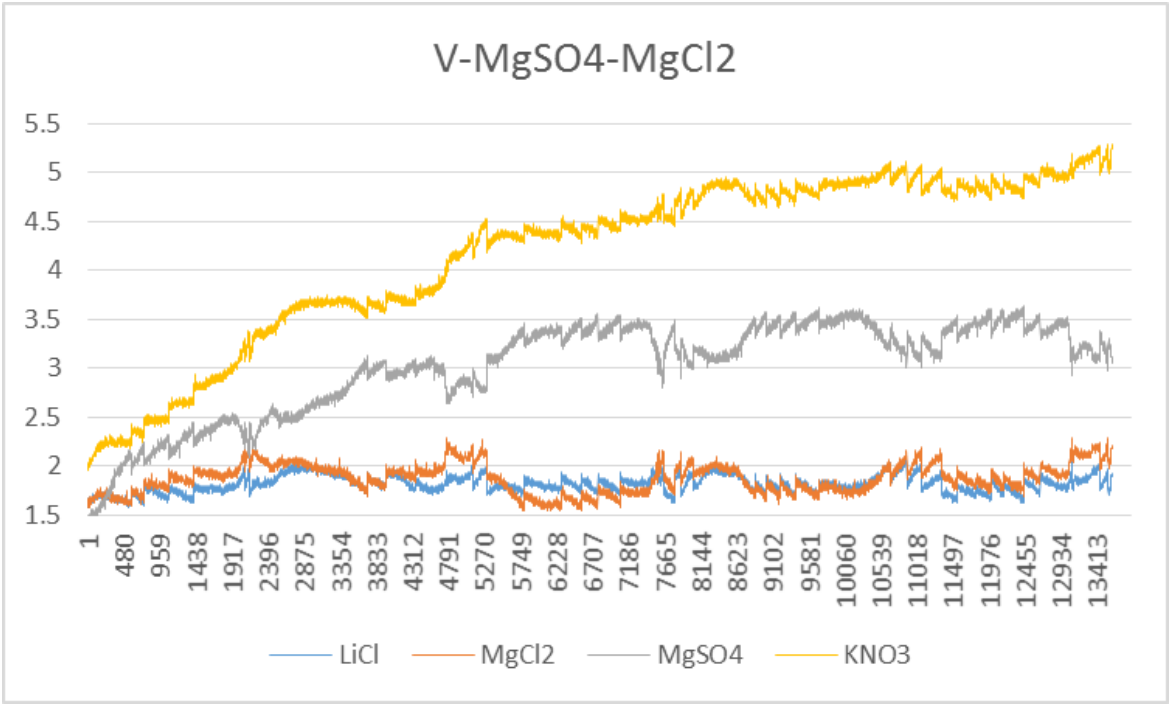


Figure 4-20 Mass change readings of V-$MgSO_4$-$MgCl_2$.

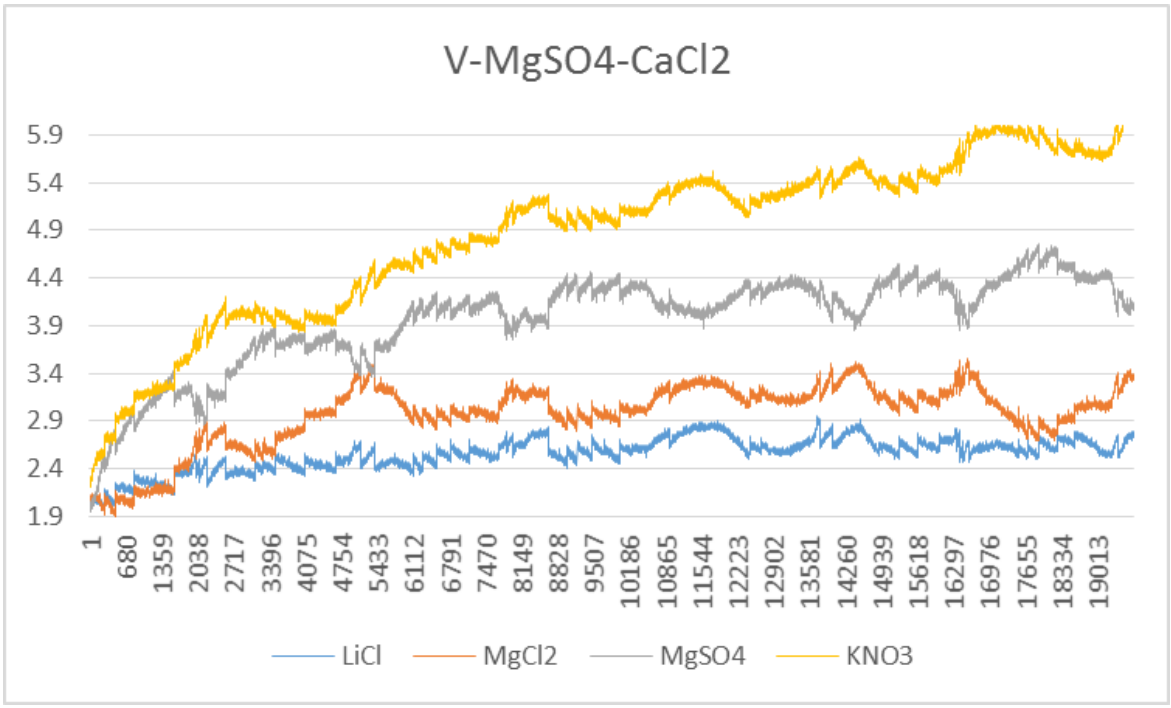


Figure 4-21 Mass change readings of V-$MgSO_4$-$CaCl_2$.

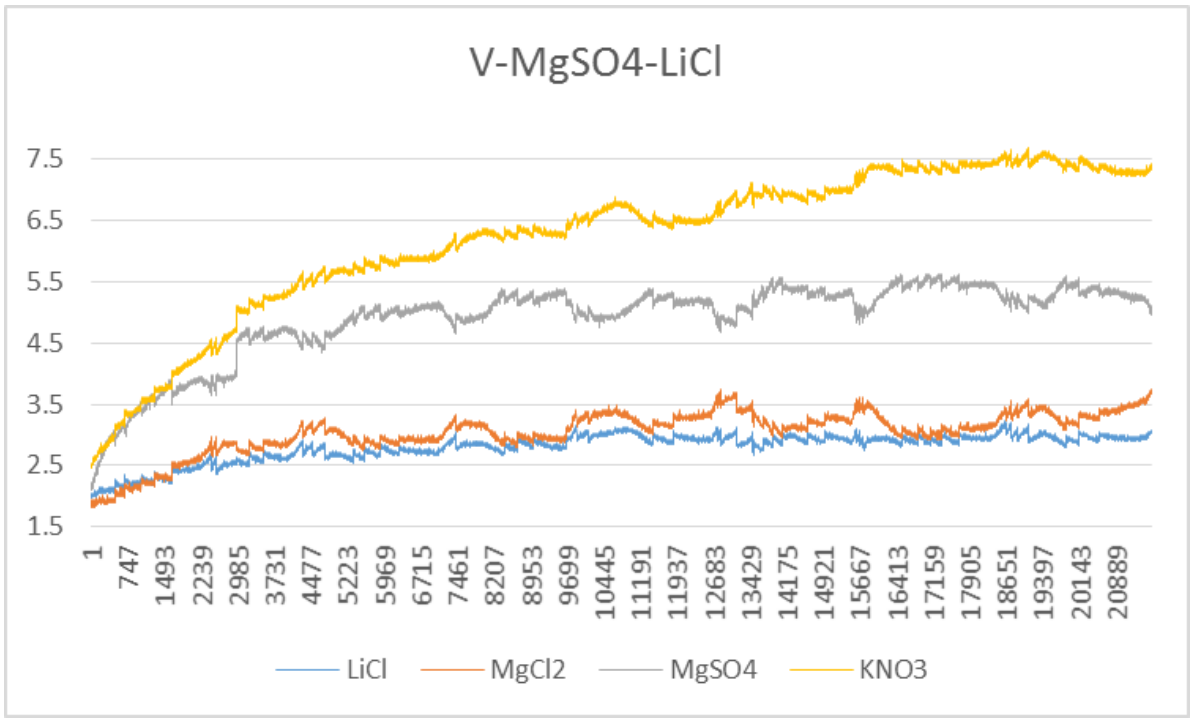


Figure 4-22 Mass change readings of V-$MgSO_4$-LiCl.

Table 4-4 Sorption test results.

Water uptake, g/g	KNO_3, 92%	$MgSO_4$, 75%	$MgCl_2$, 40%	LiCl, 16%
V-$CaCl_2$-LiCl	1.75	1.55	1.15	0.5
V-$MgSO_4$-$MgCl_2$	1.65	1	0.4	0.25
V-$MgSO_4$-$CaCl_2$	2	1.6	1.3	0.4
V-$MgSO_4$-LiCl	2.5	1.8	1	0.45

As it can be seen in the above figures, KNO_3 saturated solution provides the highest relative humidity condition (RH=92%). $MgSO_4$ saturated solution provides second highest humidity condition (RH=75%). LiCl and $MgCl_2$ give a similar lower humidity condition ($MgSO_4$ RH=40% and LiCl RH=17%). According to the results, V-$MgSO_4$-LiCl and V-$MgSO_4$-$CaCl_2$ showed a relative high water uptake, and in the high humidity level condition, materials can normally have more water uptake. Therefore, V-$MgSO_4$-$CaCl_2$ and V-$MgSO_4$-LiCl will be better sorbents with higher water uptake in the thermochemical heat storage system.

4.5 THERMAL HEATING STORAGE TEST - HEATING BOX TEST WITH SOLID CACL2

In this test, an insulated box was made as the built environment testing box. The Built Environment testing box is used for testing $CaCl_2$ as thermal heat storage material. $CaCl_2$ is a very good thermochemical heating material which has a very high energy density and it can heat the room very quick. This experiment will test how quick the material can heat up room and how much $CaCl_2$ is needed for space heating. The problems will be figure out afterwards.



Figure 4-23 Each part of the $CaCl_2$ box test.

The Built Environment box is used for testing $CaCl_2$ as heating material (see Figure 4-23). 1kg solid $CaCl_2$ was filled in an aluminium foil box and sealed properly. A horizontal PVC pipe with two rows of holes was inserted in $CaCl_2$. A 160cm high vertical PVC pipe was installed with a small water tank on the top and connected with the horizontal pipe on the bottom to provide high pressure water. A value on the horizontal pipe to control the water supply speed to provide a suitable water pressure, value was switched at half, so the water speed was neither too quick nor too slow.

Five thermocouples were set to record the temperature of the reactor ($CaCl_2$ heater), the room temperature (built environment box) and the outside temperature (to make sure it has a good insulation) (see Figure 4-24). Two thermocouples were set for room temperature test and two for reactor test to make sure the records are correct (just in case of there might be something wrong in the reaction duration). When everything was ready, poured water from the top water tank (a bottle funnel). 1kg water was injected into the reactor slowly and the reaction started. There were some

small holes on the top of the reactor just in case of the explosion. The outside environment temperature was around 25 °C at the moment.

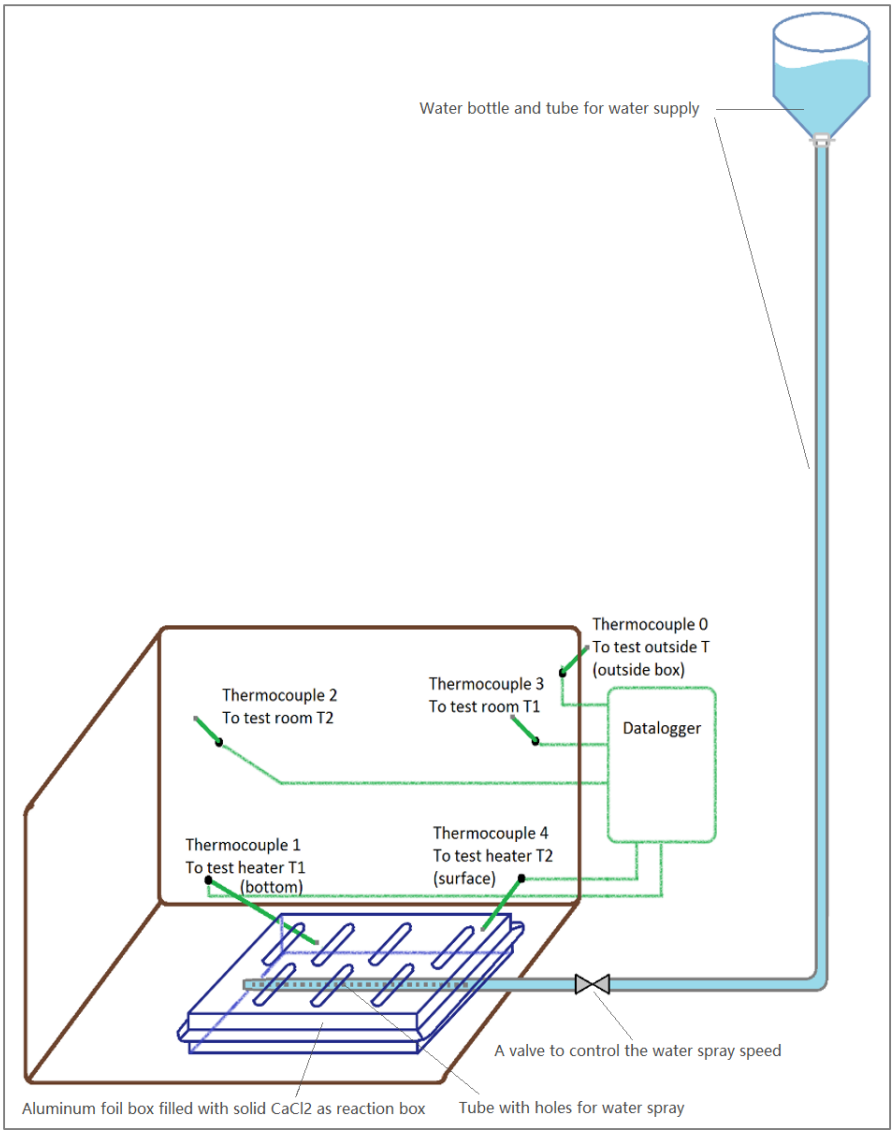


Figure 4-24 Details in the $CaCl_2$ test box with thermocouples.

The whole duration of the reaction was 7 hours. It can be seen from the record, reaction started at 12:12:40 and it just spent 3 mins for the room temperature reached 30 °C (very warm temperature). And it only took 6 mins, the temperature rose to 45 °C. It spent 15 mins to reach the highest temperature. The duration to reach highest temperature in each part will be shown in table.

The highest temperature $CaCl_2$ reactor (heater) can reach was 101.9 °C. And the highest room temperature (built environment box) was 74 °C.

(Details show in the Figure 4-25 and Table 4-5.)

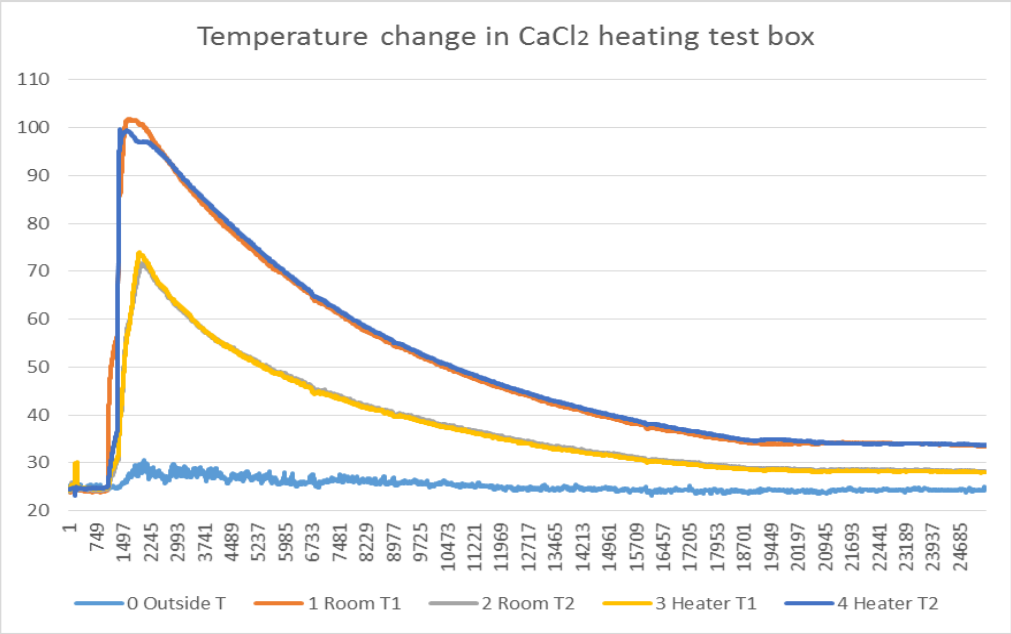


Figure 4-25 Temperature change in $CaCl_2$ heating text box.

Table 4-5 Temperature and time detail of each part.

	Outside T	Room T1	Room T2	Heater T1	Heater T2
Maximum T, °C	30.6	74	71.6	101.9	99.4
Reaction start time	12:12:08	12:12:08	12:12:08	12:12:08	12:12:08
Maximum T time	12:29:00	12:26:59	12:27:36	12:21:48	12:20:42
Duration reach the max T	00:16:52	00:14:51	00:15:28	00:09:40	00:08:34

$CaCl_2$ is a very good thermochemical heating material which has a very high energy density and it can heat the room very quick. However, if the pure $CaCl_2$ is used as

the reaction material, there will be a problem of reuse. So if we want to reuse it, we have to reduce water supply. But it may lead to a lower temperature provide.

4.6 THERMOCHEMICAL COOLING CAN TEST AND ANALYSIS

The purpose of this cooling can test will show a general understand of how quickly the urea can cool down the liquid and the feasibility of the cooling can concept. The simple urea cooling can test components (see Figure 4-26) included a can, half plastic bottle, aluminium heat transfer panel and urea. The idea is to test how quick the cooling can should cool down the drink and how to reuse/regenerate the cooling materials (e.g. urea). Five thermocouples were set to record temperature change of liquid inside can (water), outside can dry part, outside can wet part, inside urea, and on the aluminium heat transfer panel, see Figure 4-27. Because the wet cloth can help to reduce the temperature during the cooling period. So I used a wet cloth on half surface of the can to check.

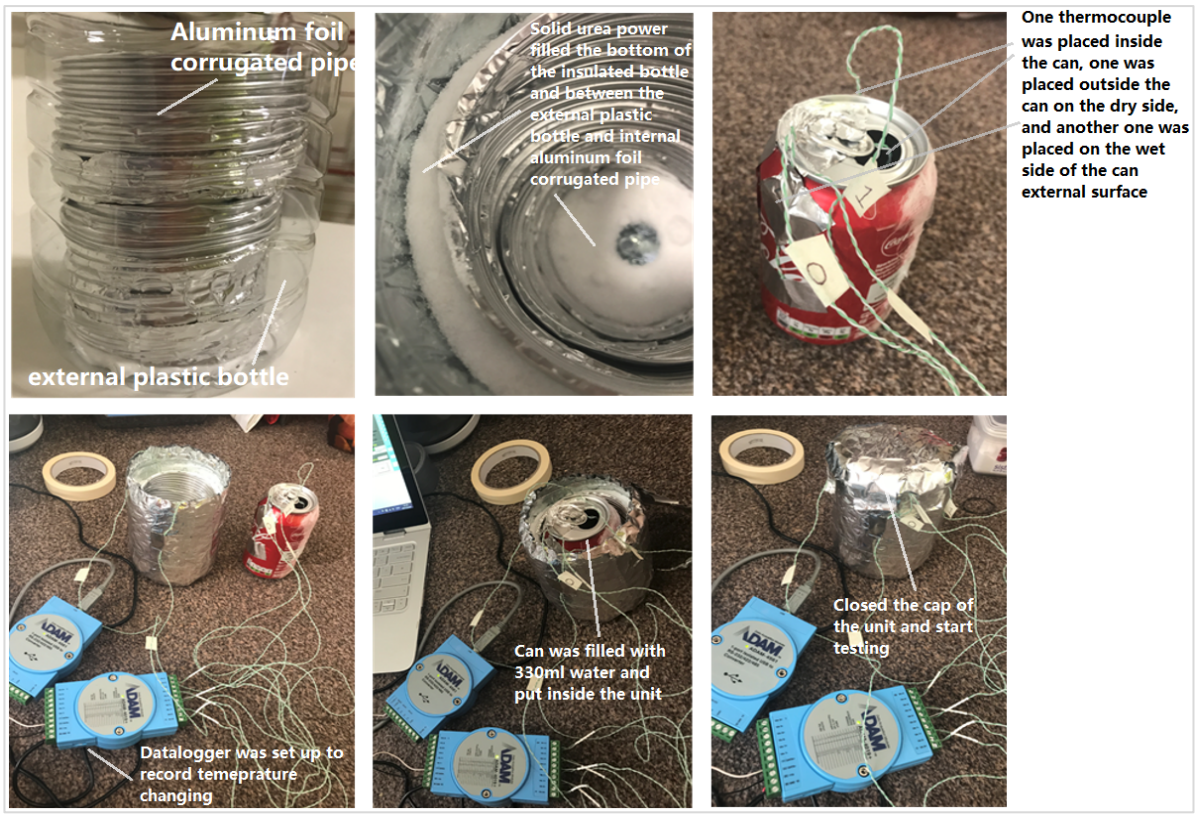


Figure 4-26 Cooling can test with urea.

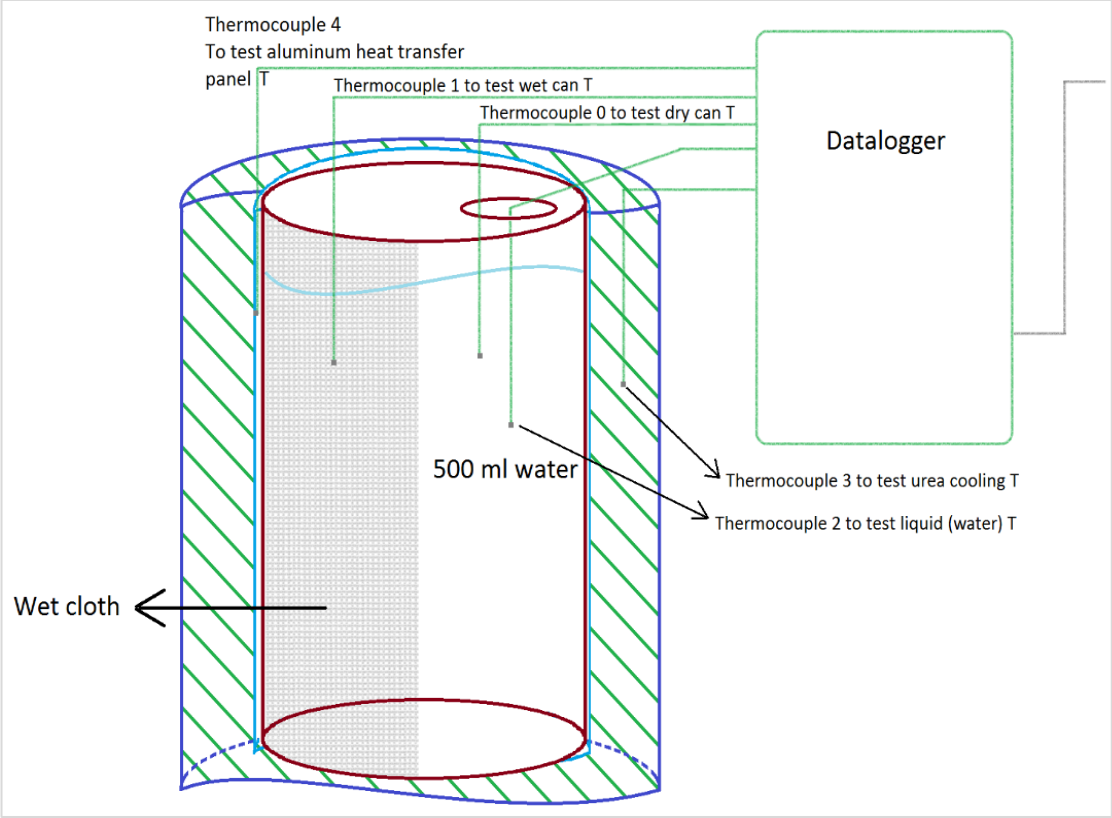


Figure 4-27 Diagram of the cooling can test with Urea.

As shown in the record, the urea can cooling to the lowest temperature in 3 mins and the aluminium heat transfer panel can be cooled to the lowest temperature in 3mins and 26 seconds. However, the liquid can't be cooled so quick, liquid inside can was cooled to the lowest temperature in 23 mins, and the can surface temperature dropped to the lowest temperature cost 18 mins and 20 mins (dry).

Even though the time spent to cool to the lowest temperature costs 23 mins, it can be cooled for long time. The cool duration (15-16 °C) is last 1hour and 17mins.

The temperature change detail is shown in Figure 4-28 and Table 4-6.

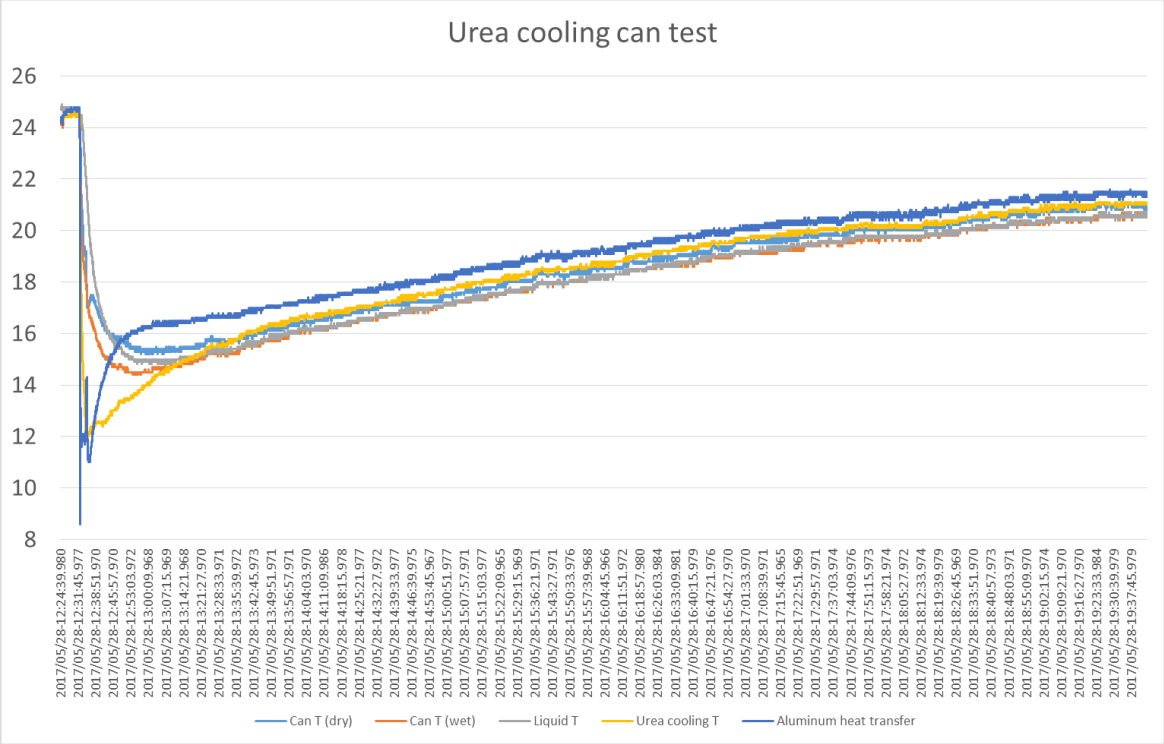


Figure 4-28 Urea cooling can test temperature change.

Table 4-6 Temperature changing record of the urea cooling can.

	Can T (dry)	Can T	Liquid T	Urea cooling T	Aluminium heat transfer panel
Minimum T, °C	15.2	14.5	14.8	11.6	11
Reaction start time	12:32:36	12:32:36	12:32:36	12:32:36	12:32:36
Minimum T time	12:52:49	12:50:43	12:55:41	12:35:27	12:36:02
Duration reach the min T	00:20:13	00:18:07	00:23:05	00:02:51	00:03:26

4.7 Experiment Designs for An Open Thermochemical Cooling Storage System

4.7.1 Introduction of the experiment

This test was a simple thermochemical cooling test for cooling system in built environment, which includes novel composite thermochemical cooling storage materials (endothermic materials) that creates cooling effect when hydrated. Endothermic materials were used as thermochemical cooling storage materials to store cooling in room temperature for a long time life period. Urea was selected as the cooling storage material, which was wildly used for first aid as instant cold pad [221]. An instant cold pack is a device that consists of two bags; one containing water, inside a bag containing ammonium nitrate, calcium ammonium nitrate or urea [222]. When the inner bag of water is broken by squeezing the package, it is allowed to dissolve the solid in an endothermic reaction. This reaction absorbs heat from the surroundings, quickly lowering the temperature [223]. In this test, I used the same reaction mechanism but an open system with heat pipes (with fins on each end of the heat pipes) to provide a good air quality for cooling.

4.7.2 Aims

The conventional technologies use some refrigerants with high ozone depletion potential that harmful for global environment and lead to global warming. The new thinking on renewable energy development will be a solution to meet environmentally friendly and human needs. Solar energy is a fantastic idea because normally cooling demand grows with solar radiation increases in summer. Solar cooling is an innovative, promising alternative to reduce high energy consumption and greenhouse gas emissions. Cooling applications, such as air condition system and refrigeration

system have become a common use chiller for hot weather. In this context, a new cooling technology using water as heat transfer fluid and urea with vermiculite as cooling media was worked out. The idea of thermochemical cooling system with endothermic materials is to develop a technology that stores the abundant solar energy in chemical bond inside of the salt based composites (vermiculite with urea) for space cooling. The composites covered one side of these heat pipes. Water sprayed on the composites to generate cool for space cooling. Using heat pipes can provide a clean air cooling for the buildings and the fins at each end of the heat pipes can give more surface to increase heat transfer (see Figure 4-29). The proposed project focuses on developing composite materials that will not degrade and that provides adequate and steady endothermic performance which can repeat for several cycles (long time life system). The composite materials will consist of a porous host matrix (vermiculite) and a salt (urea) which endothermic dissolves when hydrated.

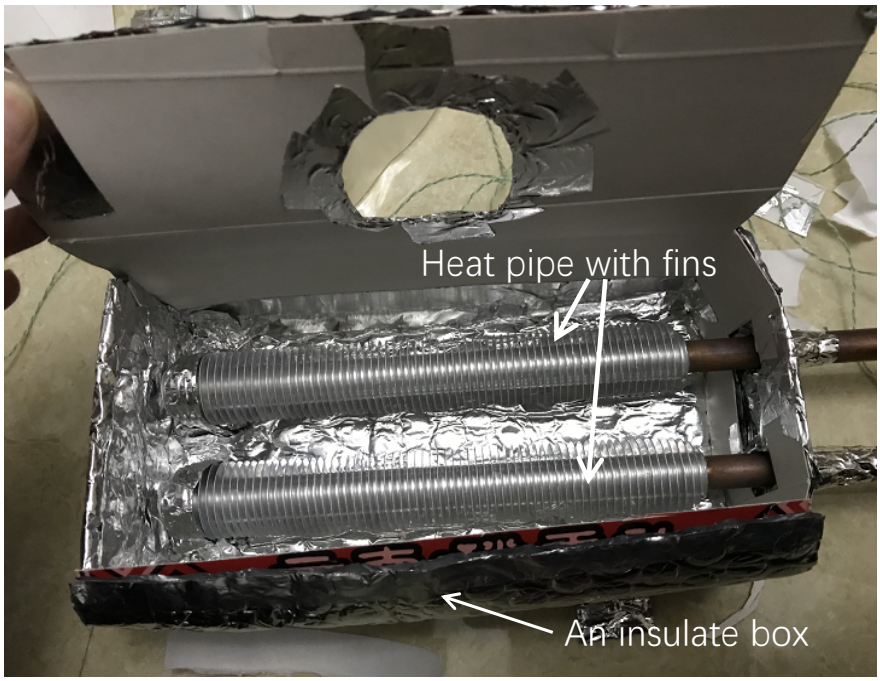


Figure 4-29 Heat pipes with fins at each end.

4.7.3 Experiment rig set-up and methodology

Endothermic chemical reaction is an energy absorption process when the endothermic materials adsorb water.

As one of the best endothermic materials, urea was discovered by Friedrich at the first time in 1828 and it presented that urea can be obtained from inorganic starting materials [186]. It adsorbs water while absorbs great energy to show a cold surrounding temperature. In recent studies, there is no research shown on urea cooling system. The equation of urea hydrolysis is shown as followed:

$$(NH_2)_2CO + 2H_2O \xrightarrow{urease} (NH_4)_2CO_3 \qquad \textit{Eq. 1 [187]}$$

In 1974, Gossett developed a patent of urea cold pack which had an inner bag to provide an immediate cold [188]. In his patent, urea was used as endothermic materials for medical cooling. Later in 2016, Kruckman and Chang invented a dry instant cold pack, which includes about 50-55g raw endothermic materials [189]. The raw material is preferably ammonium nitrate, calcium ammonium nitrate [190] or urea and the cold pack can produce a cooling effect within 30 seconds. The melting point of urea is 133 °C [99]; therefore, the regeneration temperature should be very low. However, there is no research shows the urea dehumidify temperature.

Nitrates such as sodium nitrate ($NaNO_3$), calcium nitrate ($Ca(NO_3)_2$), ammonium nitrate (NH_4NO_3) can absorb heat/energy when mixed with water. They are important endothermic materials which can be theoretically used for cooling. In Diarce et al. study, a mixture composed of sodium nitrate and urea for use as a phase change material (PCM) in thermal energy storage systems between 75 and 90 °C [191]. The melting temperature was 85 °C with a latent melting enthalpy of 172 kJ/kg and the mixture also showed sub-cooling during solidification.

Urea and Nitrate salts have the characteristic of water-cooled; however, there is few research did for the endothermic cooling system. Because of the hygroscopic of these endothermic materials, the influence of degradation and temperature shall be considered and tested in the future work.

In this test, two heat pipes with fins at each end were used as heat transfer media, two insulated boxes covered each side (covered fins inside the box) (see Figure 4-30 and Figure 4-31). One side of the box was filled with composites and one side box with a small fan on the top and 4 small holes on the bottom, this box was used as the cooling provider. 5 sensors were set to record temperature changing (composite, reaction heat pipe, cooling provide heat pipe, cooled air and ambient temperature).

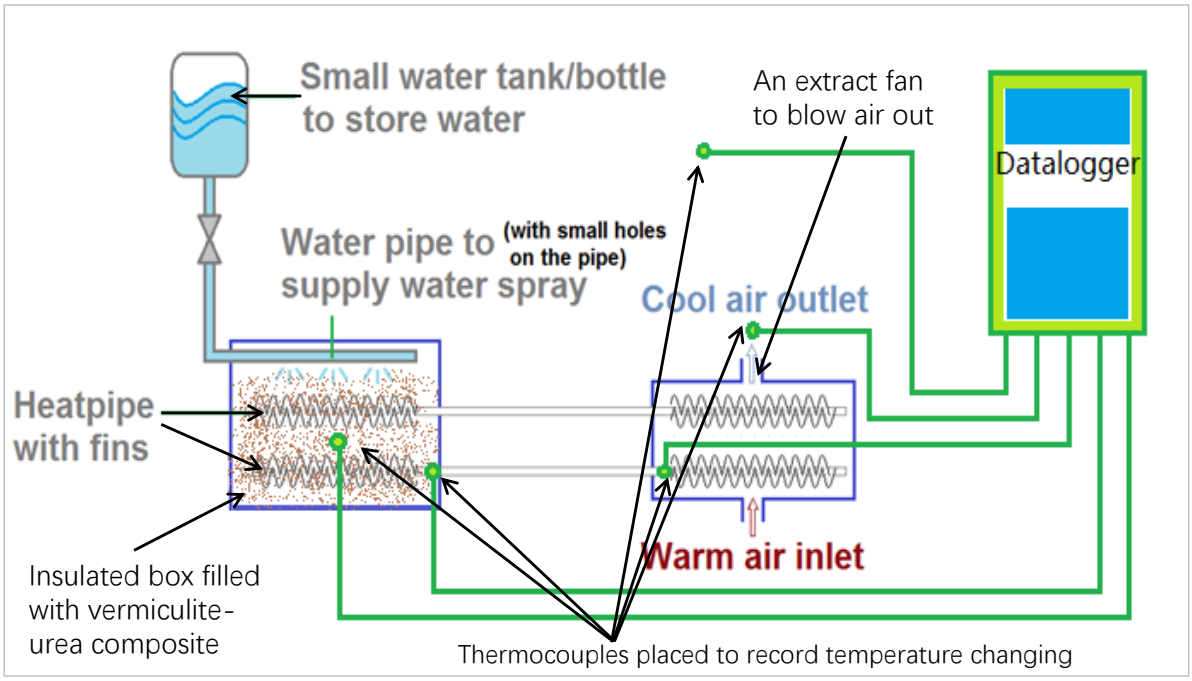


Figure 4-30 Diagram of the cooling box with heat pipes.

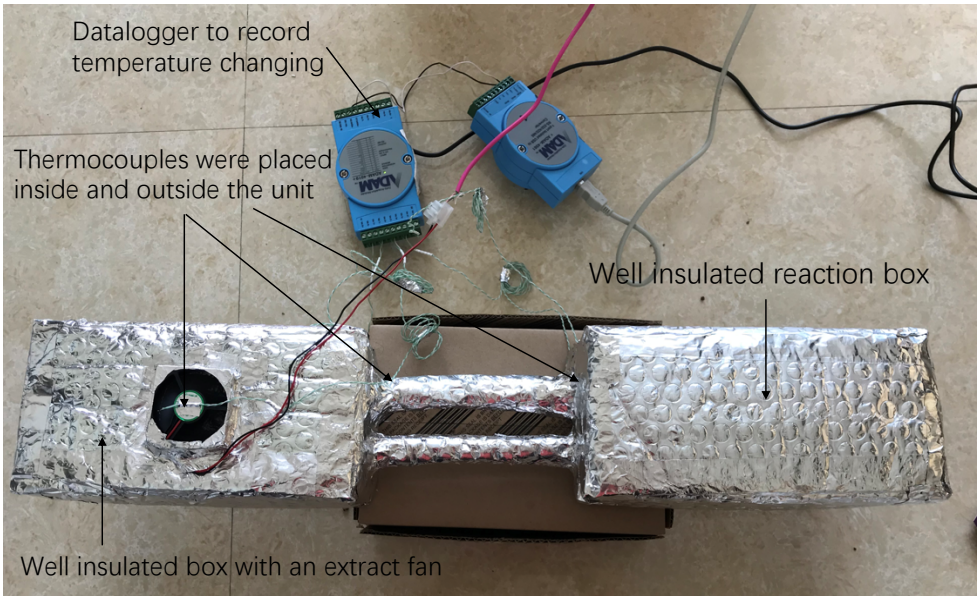


Figure 4-31 Cooling test box with heat pipes.

The whole system was insulated well to guarantee the heat inside the system (Figure 4-31). The test box was set on another box to make sure there was some room under the cooling provider box, because there were four small holes on the bottom of the box to confirm the air transfer (room temperature was 21 °C so the inlet air temperature was 21 °C).

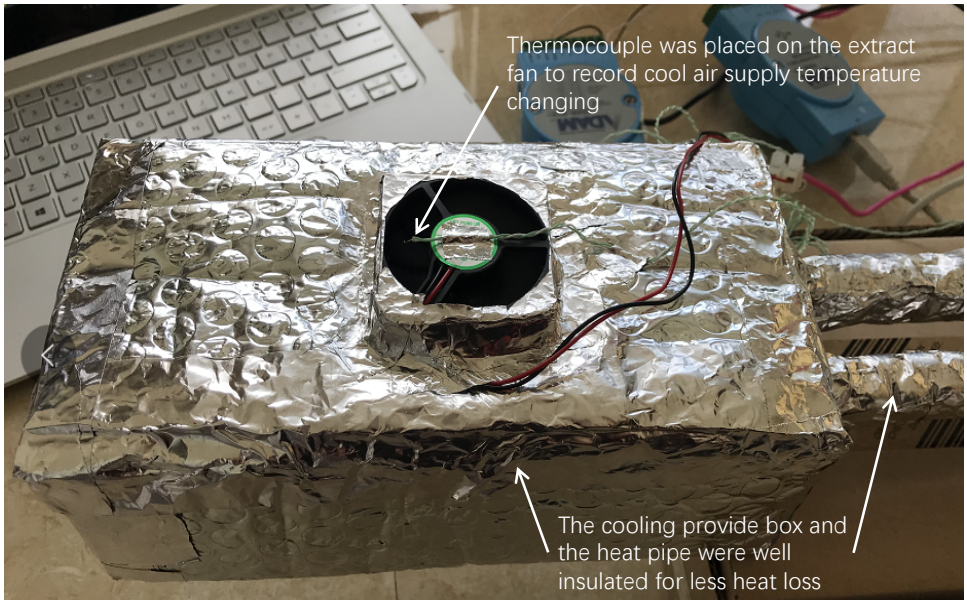


Figure 4-32 Cooling provider box with fan on the top and a sensor on the fan to record the cooled air temperature.

A sensor was set on the fan of the cooling provider box to record the temperature changing of the cooled air (see Figure 4-32). This was recording the air outlet temperature.

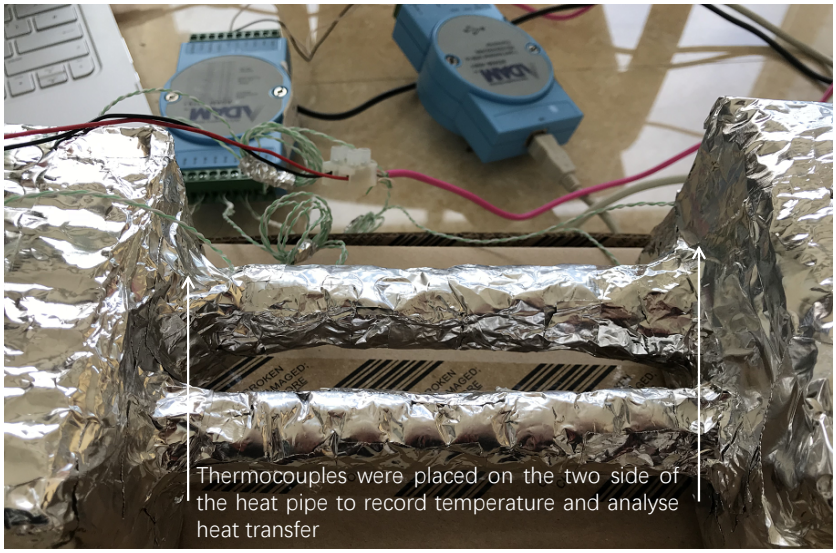


Figure 4-33 Heat pipes were insulated well to protect heat.

The middle part of the heat pipes were insulated well to make sure there was no heat escape from the gap (see Figure 4-33). And there was one sensor set on the reaction part of the heat pipe and one was set on the cooling provider part of the heat pipe to record temperature changing.

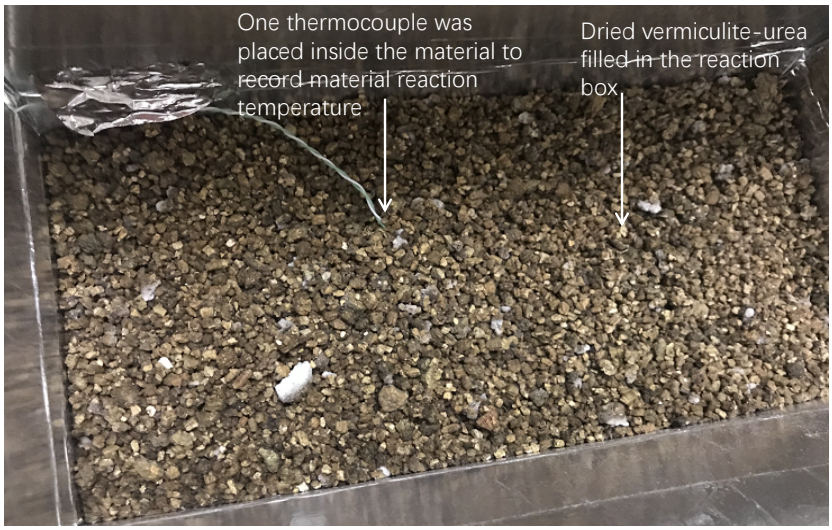


Figure 4-34 Sensor was put inside composite to record temperature changing.

The composite of vermiculite with urea was fully filled in the reaction box covered the heat pipe fins parts (see Figure 4-34). One sensor was put inside the materials to record the temperature changing during reaction process. I used 400g dried vermiculite with urea as the reaction materials.

Materials preparation:

1. Pre-heated oven to 220 °C (do not allow to let the temperature go beyond 240 °C because when the temperature goes above 240 °C, the structure of vermiculite will change, the volume of vermiculite will be 3 times bigger and the characteristics may change as well). Put vermiculite in oven for at least 24 hours to dry.
2. At the same time, prepare urea solution. At 21 °C, 1050g urea can solve in 1000g water. So I put 1050g urea into 1000g water, mixed them well and let them stay for overnight (because when urea and water mixed together, the temperature can drop very low, there was a lot crystal on the bottom of the solution, so we need to let them warm up a bit to solve all the salts, at least 24 hours will be a good idea). On the next day morning, there was only a very little crystal on the bottom of the solution, which means the liquid was saturated well.
3. After dried the vermiculite for 24 hours, I took them out and out the hot materials in a box and sealed the box to make sure there was no gap to let the moisture go inside the box. Cool it down in the box for at least 2-3 hours.
4. Then mixed 500g dried vermiculite with 1.5kg urea solution (weight ratio of matrix material and thermochemical salt was 1:3, which was the best ratio after several test).

5. Let the vermiculite absorb water for at least 24 hours. Because vermiculite has a porous structure, it will take some time to let the liquid go into each hole. So it is better to leave them for overnight at least 24 hours before drying in the oven.
6. After 24 hours, stir the materials well to easy drying in case of the mixture packed together.
7. Put mixture in oven at 55 °C for at least 48 hours to dry. Normally, when we prepare the thermochemical energy storage materials, we dry the materials at 200 °C for 24 hours, however, this time I use urea, if the temperature goes over 55 °C, some ammonia gas can be released. The drying temperature is very low compared with 200 °C, so the longer drying time is needed. After about 46 hours, I checked weight for each hour, the weight never changed, so I assumed that after 48 hours is the best drying time for vermiculite with urea, the lower regeneration temperature materials.
8. Put the dried materials in a sealed box for 3-5 hours to let them cool down to room temperature. If the materials will not be used immediately, for example after one week, then we need to dry them one day before using. The drier the material the more accurate results will be.
9. Before put materials in the test box, check the weight to make sure there is no water moisture goes inside the materials.
10. Then, put 400g dried mixture in the reaction box.
11. Set all the sensors up, and turned on fan, started recording.
12. Using a water spray tube to provide a fine spray on the dried materials.

13. When the outlet heat pipe temperature stopped dropping to increase a little bit, then stopped providing water spray.
14. Checking the water weight before and after water spray and recording the weight. (about 230g)
15. It spent 14 minutes before temperature went to the lowest.
16. Recording the readings for 10 hours. Some figures will be showed later.
17. After all parts were set up, using a water spray to provide fine water mist for the materials. When the temperature stopped dropping, then switched off the water provider. Checked weight before and after the water providing. Recording the readings for 10 hours.



Figure 4-35 Composites after test in reaction box (full of moisture).



Figure 4-36 The heat pipe in reaction box after testing.

After testing, all the TES materials need to be removed, and it is found that there was no water on the bottom of the reaction box, which means water were absorbed completely by the dried materials.

4.7.4 Results and analysis

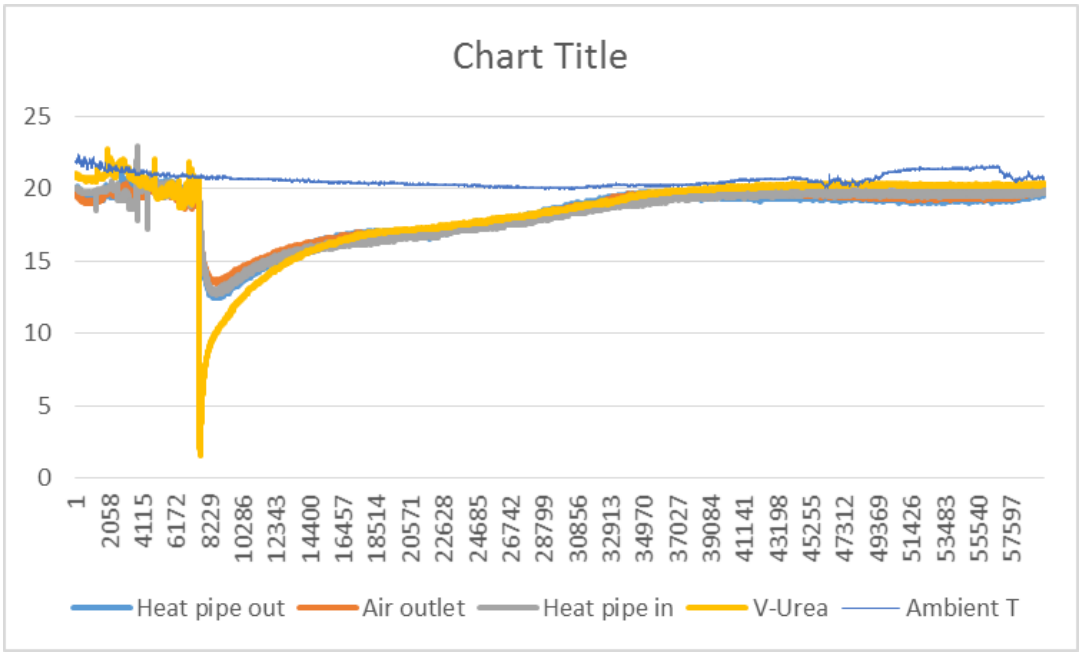


Figure 4-37 Readings record for all the 5 sensors.

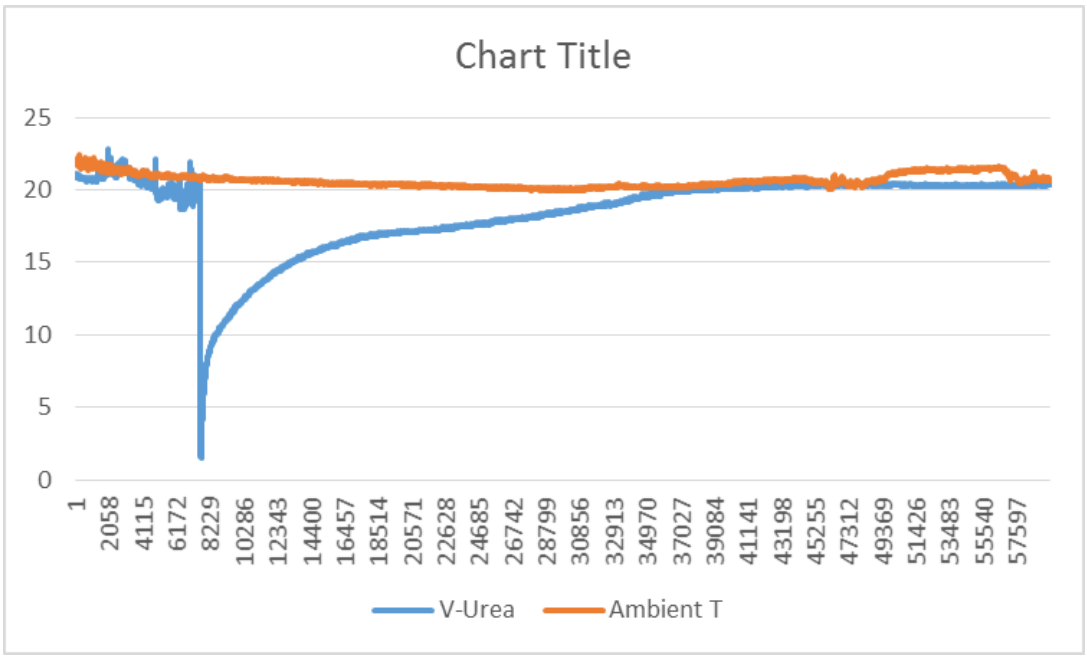


Figure 4-38 Temperature between material and inlet temperature (ambient temperature).

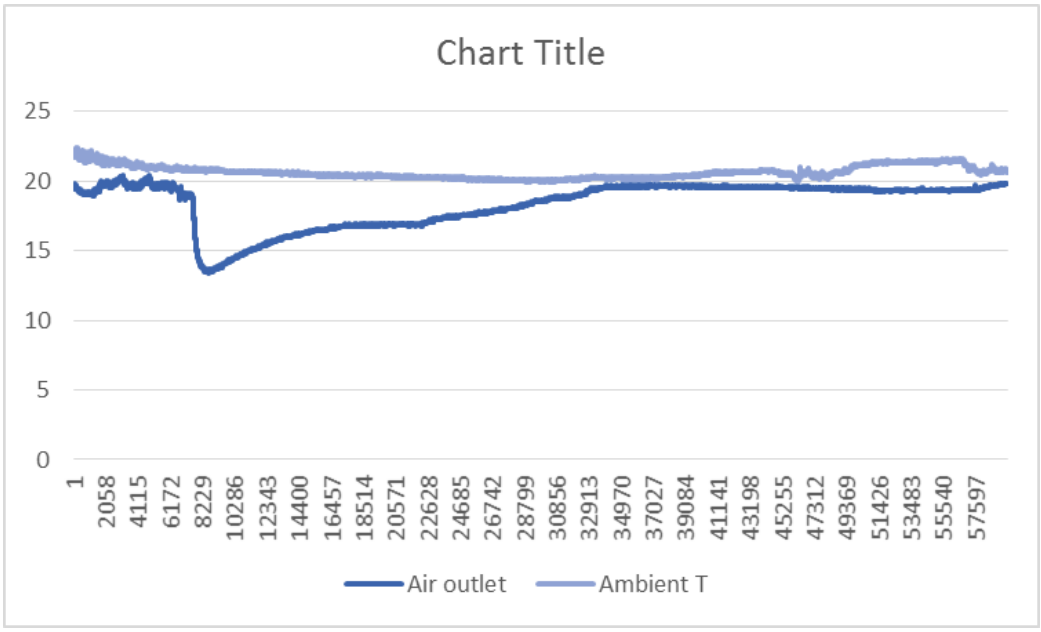


Figure 4-39 Temperature between ambient temperature (air inlet T) and cooled air outlet temperature.

According to the record readings, results showed that the v-urea temperature dropped to the lowest temperature at 1.2 °C after water spray in 5 minutes. And the temperature of cooled air dropped to the lowest temperature at 13.4 °C after 15 minutes, and outlet air temperature stayed under 15 °C for 90 minutes. Outlet air temperature stayed under 17 °C for 4 hours and 20 minutes. The fan velocity is 0.56 m/s and the diameter is 0.05m (equals to $0.00196m^2$ * 0.56m/s * $1.29kg/m^3$ = 0.00142 kg/s, air density is $1.29kg/m^3$). The power of the small fan is 1.2W. The total cooling hour (outlet air temperature is lower than ambient temperature) was 7.3 hours.

Specific heat capacity (C_p) of air is 1.006 kJ/kgC.

Using heat transfer formula, for every second:

$Q_c = Cp*m_a*\Delta T$ = 1.006 kJ/kgC * 0.00142kg * ΔT

ΔT = Ambient Temperature – Outlet air temperature, °C

Using every second reading to calculate the total energy generate: $Q_{c\text{-}total}$ = 128.68 kWs/3600s/h = 0.036 kWh

Small fan energy consumption is E_f = 1.5W*7.3 h = 0.011kWh.

The COP is the ratio of the heat absorbed from surrounding environment to the input work:

$$COP = \frac{E_f}{Q_c} = \frac{0.036kWh}{0.011kWh} = 3.27$$

4.7.5 Comparison of the Experiments and Conclusion

In the cooling box test, 400g dried vermiculite with urea was used as TES materials for cooling air supply. The COP of this simple cooling box system was 3.27, which means vermiculite with urea is a feasible TES material for space cooling system. The energy density of the v-urea is 665 kJ/kg, so 400g dried material ideally can provide 226kJ cooling energy, which equals to 0.06kWh. Therefore, the cooling energy generation (0.036kWh) is 60% of the ideal energy (0.06kWh) of the v-urea, the main reason for it is because of the large heat loss of the cooling reaction box; and the gap and leakage of the box can cause some heat loss as well as the reaction box is not completely closed.

4.8 SUMMARY

Vermiculite and Al_2O_3 based composites have been chosen as the desired TES materials. The preparation was introduced at the beginning. According to the TA tests results, the performance vermiculite with $MgSO_4$-$CaCl_2$ and vermiculite with $MgSO_4$-$LiNO_3$ showed a higher energy density (1173.5 kJ/kg and 1000.8 kJ/kg, respectively) and lower regeneration temperature (63 °C and 81.7 °C, respectively), which were the key features of TES composites. Vermiculite with MgSO4-LiCl and vermiculite with $MgSO_4$-$LiNO_3$-$MgCl_2$ showed low regeneration temperature (74.7 °C and 71.7 °C, respectively) as well, however, these two composites showed lower energy

density (990.2 kJ/kg and 748.6 kJ/kg, respectively), especially the vermiculite with $MgSO_4$-$LiNO_3$-$MgCl_2$. Although the performance of each single salt was good, the performance of the composite showed greatly deficient. V-$CaCl_2$-LiCl has energy density of 856.4 kJ/kg with regeneration temperature of 79 °C. For thermochemical cool storage materials, vermiculite with urea presented good energy density (727.85 kJ/kg) and relative low regeneration temperature at 54.5 °C.

Sorption test was taken with thermochemical heat storage materials to study the water uptake of each composite. Based on the results, V-$MgSO_4$-$CaCl_2$, V-$MgSO_4$-LiCl and V-$CaCl_2$-LiCl showed better sorption performance with higher water uptake. Depended on the tests and analysis in this chapter, it is feasible to use TES materials in building application for space heating and cooling supply. Many TES materials characteristics have been analysed and some of them have been selected to be the preferred materials for the following further testing in the lab-scaled rig. In the next chapter, computer simulation will be done based on the tests results of some TES materials. Further details on the sizing of the thermochemical energy storage system for the building will be shown in the next chapter as well.

5 COMPUTER SIMULATION FOR THERMOCHEMICAL HEATING/COOLING STORAGE SYSTEM

5.1 INTRODUCTION

Gas consumption for heating is the most significant energy use in the domestic house. It is necessary to implement sustainable energy to reduce fossil fuel consumption. Thermochemical heat storage is a new technology that can store heat in the warm weather and release in cold winter. THS is a seasonal technology that use high density thermochemical materials to store heat and solar collector to charge the system. Thermochemical materials can release heat when adsorb moisture; and solar collector will be used to remove the moisture of the materials during charging process. In the report, an old Victorian house in Harrington Drive (Nottingham) will be used as the modelling house. It is mid-terrace house and recent refurbished. The energy consumption of the modelling house will be assumed by considering the EPC of the house. However, the U-Values will be set followed by passive house or zero carbon house standard. The heating base temperature will be 19 °C that means when the inside temperature goes below 19 °C than the heater will be turned on and stopping at 21 °C. And the cooling base temperature will be 28 °C, so the cooling system will start working at 28 °C and stop at 21 °C.

5.2 MODELLING HOUSE

A house located in Harrington drive will be used as the modelling by IES software. The selected house is used as student accommodation in Harrington, Nottingham. The energy consumption simulation will be set followed passive house or zero carbon house standard. The total area of the two floors is 105 m^2. The U-values of the house elements depend on the Building regulation 2010 to build a low carbon modelling.

There are 3 bedrooms inside with one living room, one kitchen and two toilets. Because of the weather in Nottingham, cooling will not be considered in the simulation.

In the simulation, novel heating technology will be installed to instead of the old one. Solid desiccant will be used in the new facility for space heating.

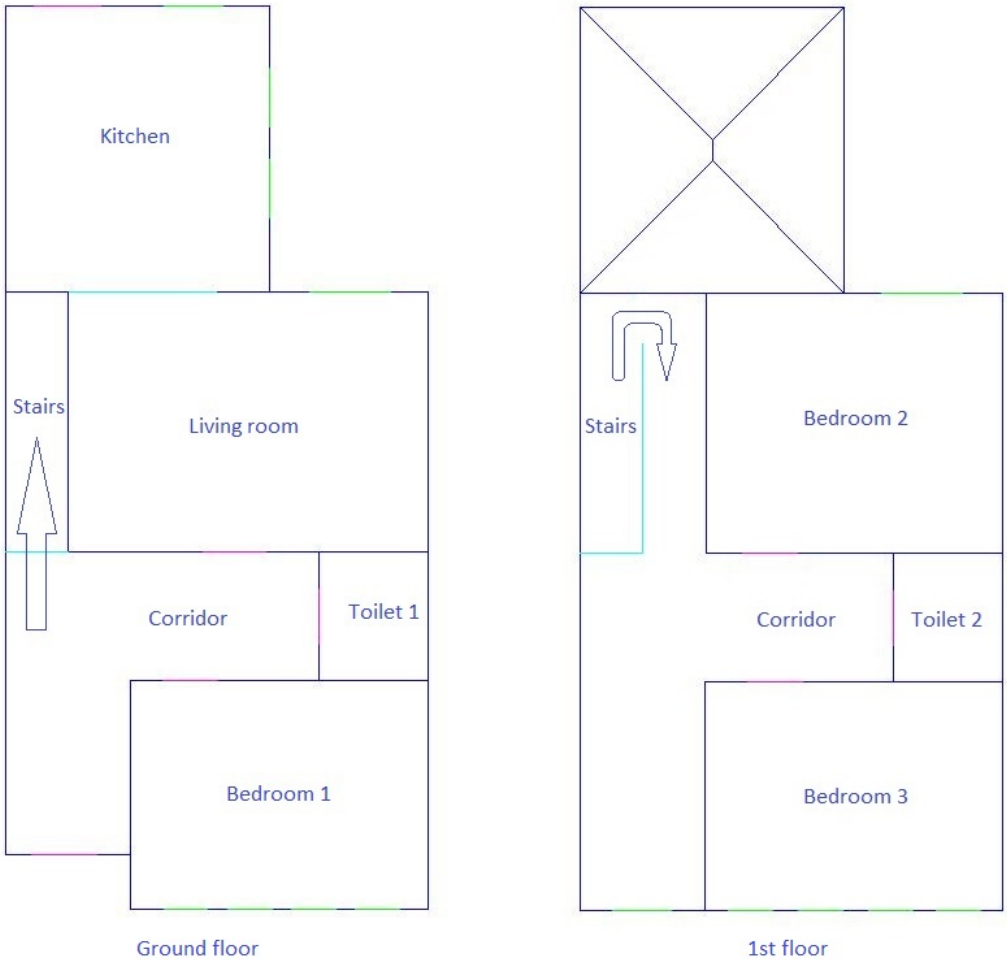


Figure 5-1 Draw of the house.

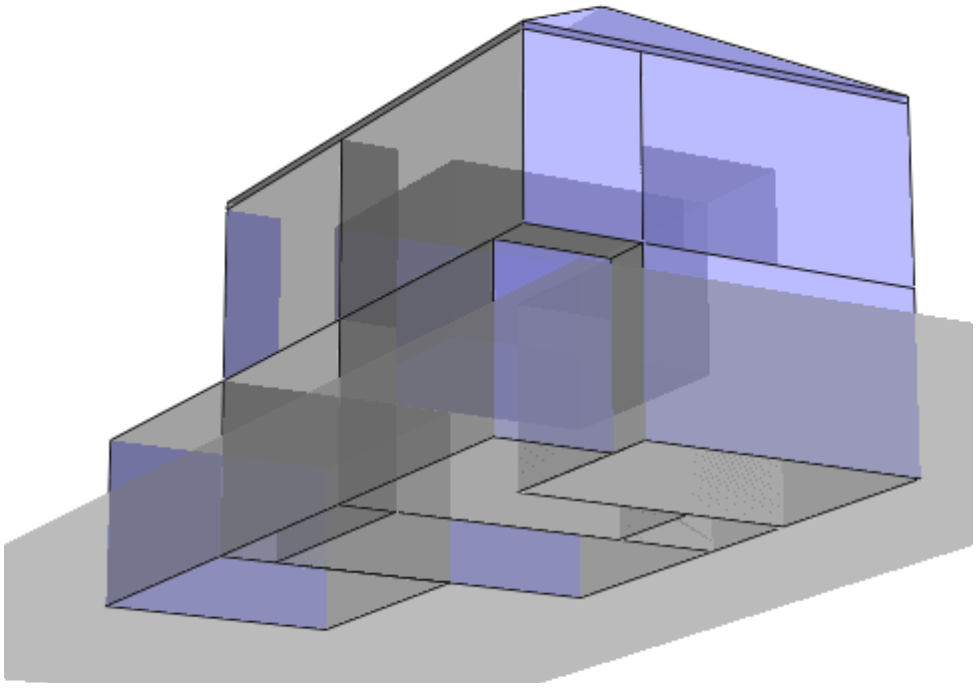


Figure 5-2 IES 3-D model [224]

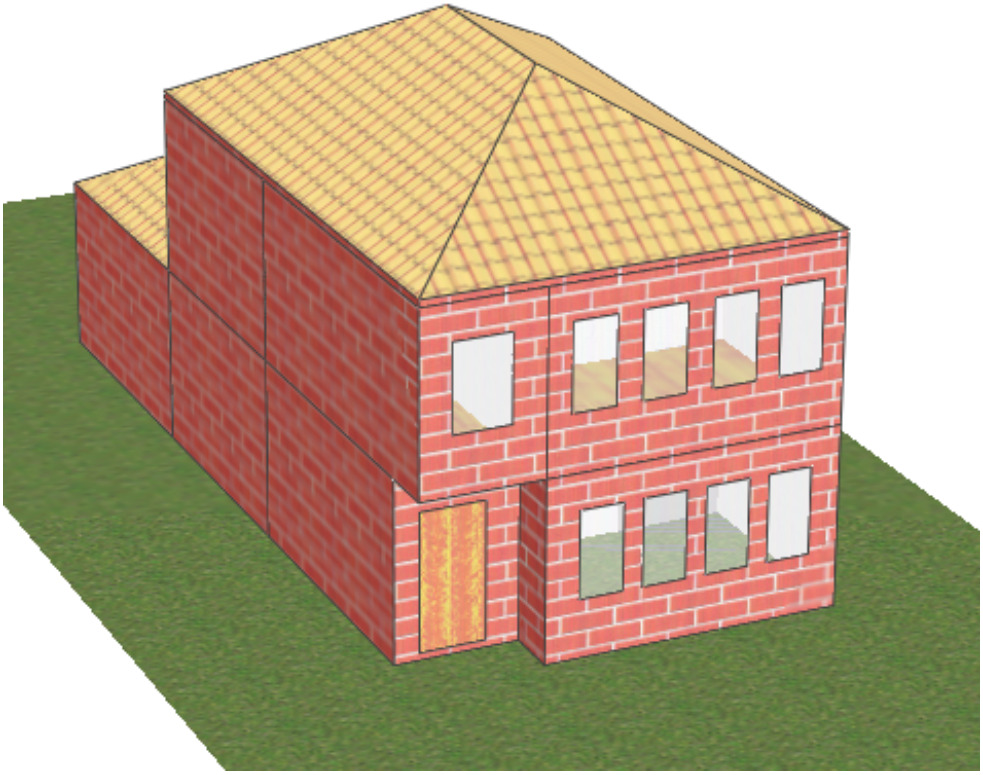


Figure 5-3 IES 3-D model [224]

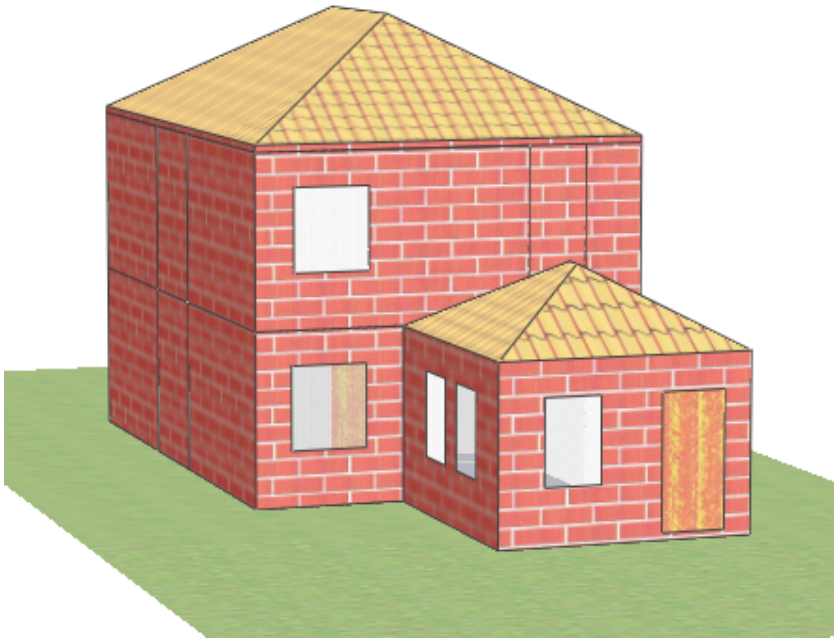
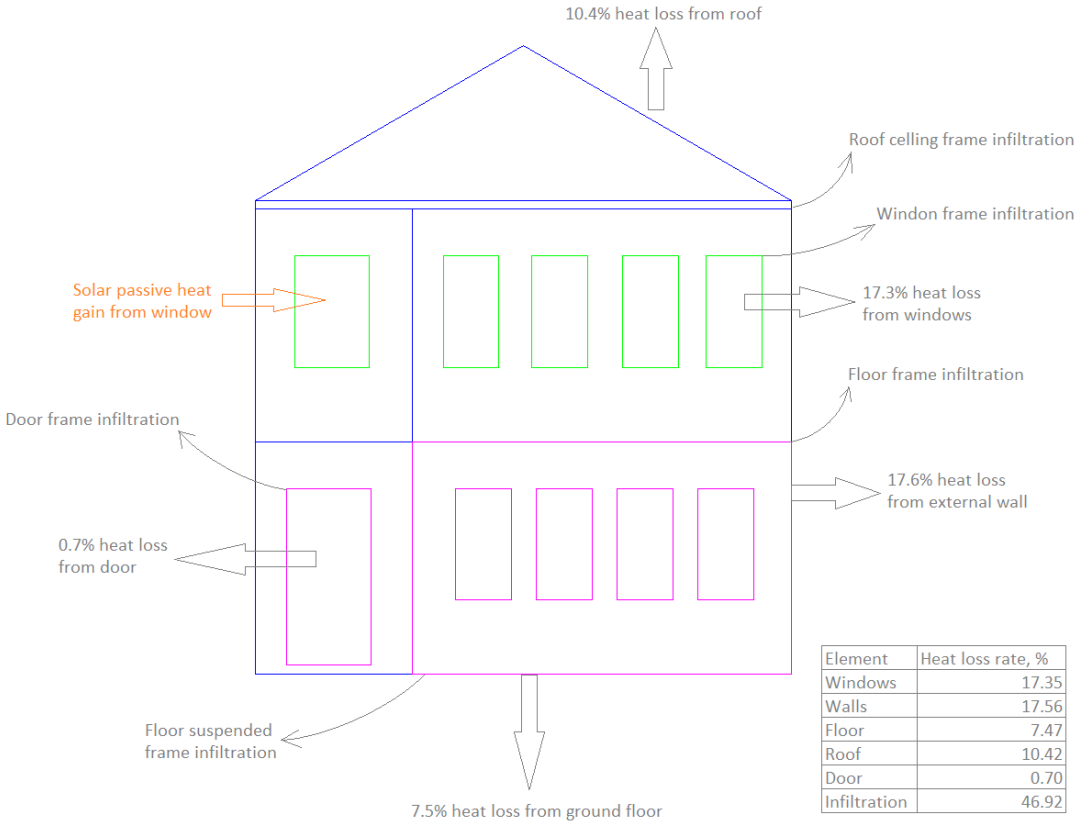


Figure 5-4 IES 3-D model [224]



Element	Heat loss rate, %
Windows	17.35
Walls	17.56
Floor	7.47
Roof	10.42
Door	0.70
Infiltration	46.92

Figure 5-5 House heat loss diagram.

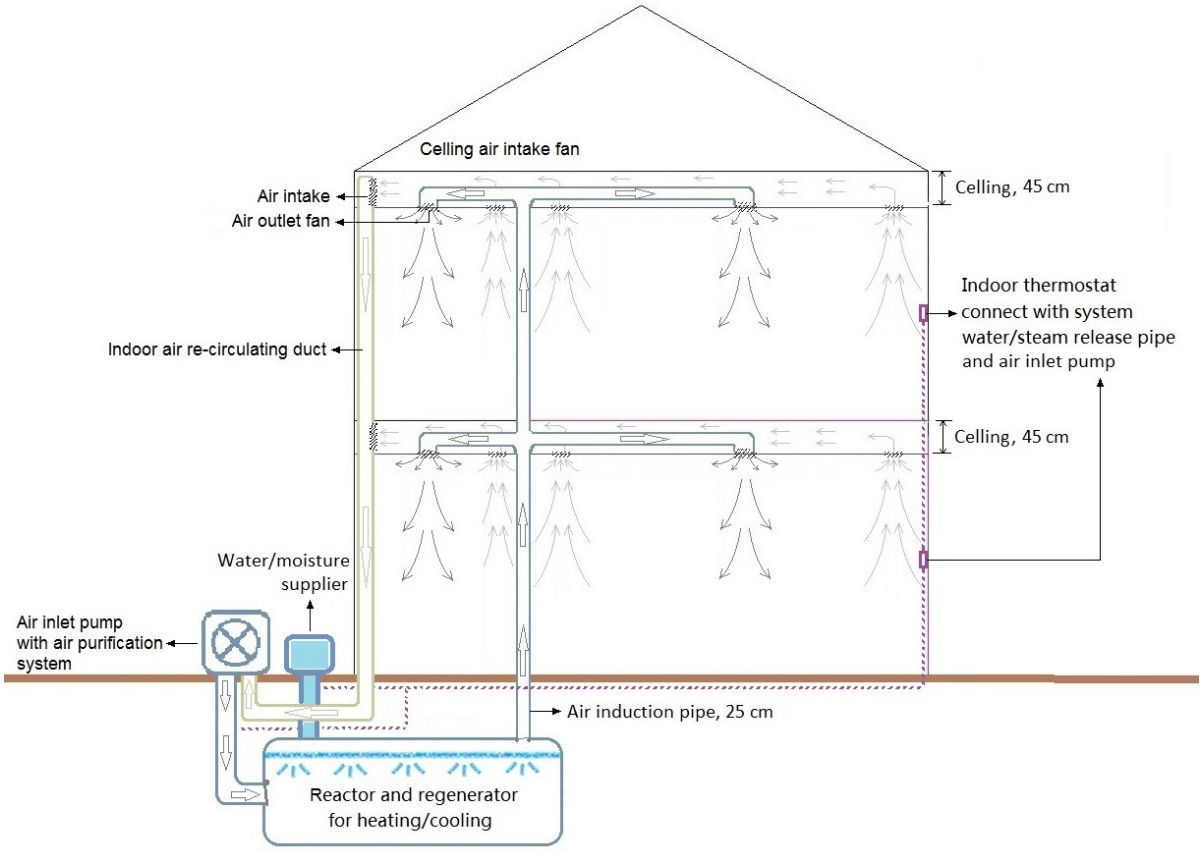


Figure 5-6 House induction system.

5.3 SOLAR HEAT GAIN AND TOTAL HEAT GAIN OF THE MODELLING HOUSE

Firstly, monthly energy consumption will be estimated in detail by analyzing the house EPC 2008. And also, according to the EPC, materials U value will be assumed with an average value. Air flow rate will be less than 0.6 ACH according to BR Part L1A 2010. However, we use the passive house or zero carbon house standard, so we assumed that the ACH is 0.3 ACH. That means 30% air change per hour by building frame. So, the air flow rate is 78.75m^3/hour in the house. The air flow rate is 21.9L/s. Air density is 1.29 g/L; hence, the air mass transfer is 28.2g/s (0.0282kg/s). It depends on the different temperature and different pressure caused by wind. And also, open windows will make the infiltration different.

By using the formula $Q= m*Cp*(T_{in} – T_{out})$, heat loss from the air flow will be calculate. Cp air is 1.006; m is 0.04. The U-value of each element will be set follow the BR Part L 2010 showed as followed:

Table 5-1 U values of the house and heat loss coefficient.

Element	Description	U-Value, W/m²K	Area, m^2	AU, kW/K
Windows	Double glazing	1.2	11.28	0.0135
Walls	Cavity wall	0.1	137	0.0137
Floor	Suspended	0.1	58	0.0058
Roof	Pitched roof	0.13	63	0.0081
Door	half glazed with double glazing	0.16	3.42	0.0005
Total				0.0417
Cp	1.006			
Air flow rate, kg/s	0.04			
m*Cp	0.04			
Total	0.078	kW/K		

Table 5-2 Dimension of each room.

Floor	Room	Floor area, m^2	Volume, m^3	Ext wall area, m^2
Ground floor	Living room	17.455	43.638	14.275
	Kitchen	14.004	35.010	28.450
	Bedroom 1	12.698	31.746	19.850
	Toilet 1	2.625	6.563	4.375
	Corridor 1	11.460	28.651	14.525
First floor	Bedroom 2	12.698	31.746	17.975
	Bedroom 3	14.398	35.994	19.000
	Corridor 2	15.789	39.474	18.550
Total		101.128	252.821	137.000

The detail of house internal heat gain shows in the following table:

Table 5-3 Typical heat gains.

Description	**Typical Heat Gains**
People	
Seated, quiet	Sensible – 65W/person Latent – 30W/person 58W/m^2 (per unit area of body)
Sleeping adults	41W/m^2
Person Cooking	81 – 134 W/m^2
Electrical Equipment	
Lighting	8 - 12 W/m^2
Computer	Electrical Consumption = 100W
	Heat Gain = 20W (computer in energy saving mode) + 55W (monitor) = 75W
TV	Electrical Consumption = 150W
	Heat Gain = 40% of 150W
Kitchen Equipment	

Coffee machine	Electrical consumption = 670W
	210W – Sensible with hood 440W – Sensible without hood
	230W – Latent without hood
Dishwasher	50W – Sensible with hood 50W – Sensible without hood 110W – Sensible without hood
Freezer	Electrical consumption = 810W
	320W – Sensible with/without hood
Microwave oven	Electrical consumption = 600W
	600W – Sensible with/without hood
Refrigerator	Electrical consumption = 1730W
	690W – Sensible with/without hood
Oven	Electrical consumption = 800W
	800W - Sensible
Fridge Freezer	61.4kWh/yr 52.9kWh/yr

Simulations were run via IES-VE for the typical UK house with 3 bedrooms model to get the following results:

- Solar gain;

- Internal heat gain (includes people and electricity appliances heat gain);
- Infiltration (natural and mechanical ventilation);
- Electricity consumption (in the old house and the one after doing some appliances replacement);
- Gas consumption (includes space heating, DHW consumption and cooking consumption).

Heat inside room keeps a comfortable warm living condition for people. Heat gain from outdoor comes from sun radiation in the daytime. When the sun rises, sunlight goes through window to heat the space. And also, building materials could also transmit heat. Inside heat comes from people, computer using, lighting and other appliances using, which depends on people activity period inside house. Solar radiation depends on different locations, house glazing area and construction materials. In this project, the modelled house is located in Nottingham; hence, Nottingham weather data in IES-VE will be applied to get the solar heat gain for the modelled house. Solar heat gain relates to the glazing sunlight transmutability. In the modelled house, the low-e high performance triple glazing with U-Value of 1.8 W/m2/K would reflect about 75% sun radiation.

By using IES heat gain setting, people's behaviour for staying inside room, using equipments and turning on the heating will be set. Then the monthly inside heat gain (people gain) and solar heat gain will be output:

Table 5-4 Monthly heat gains.

PEOPLE HEAT GAIN												
	Jan	Feb	Mar	Apr	May	Jun	Jul	Aug	Sep	Oct	Nov	Dec
Internal heat gain, kW	1.13	1.05	0.96	0.93	0.86	0.57	0.43	0.50	0.93	1.03	1.09	1.10
SOLAR HEAT GAIN												
	Jan	Feb	Mar	Apr	May	Jun	Jul	Aug	Sep	Oct	Nov	Dec
Solar gain, kW	0.50	0.74	0.75	0.92	1.14	1.26	1.44	1.70	1.22	0.84	0.61	0.54
TOTAL HEAT GAIN												
	Jan	Feb	Mar	Apr	May	Jun	Jul	Aug	Sep	Oct	Nov	Dec
Heat gain, kW	1.63	1.78	1.71	1.85	2.00	1.83	1.87	2.20	2.15	1.87	1.69	1.64

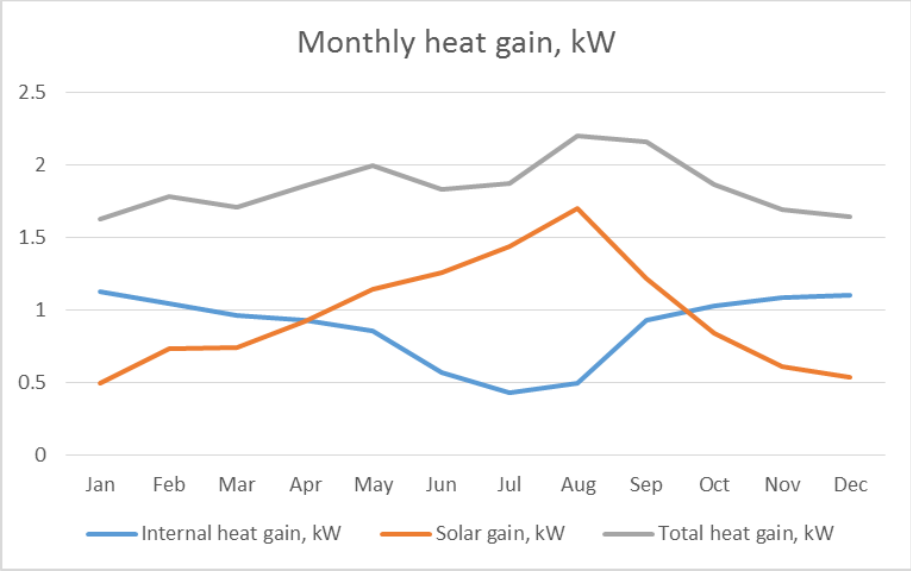


Figure 5-7 Monthly heat gain.

Depending on different monthly heat gain, we got different base temperature T_b for heating.

The base temperature will be calculated by using the formula of:

$T_b = 19 – Q_{gain}/C$

T_b – base temperature for heating, °C;

Q_{gain} – total heat gain from inside building and solar gain, kW;

C – total heat loss coefficient, kW/K.

By using degree days method, the daily and monthly heating demand will be worked out.

Heating demand can be calculated by using the formula:

E = C * degree days * 24 hours/day

E – heating energy demand, kWh;

C – total heat loss coefficient, kW/K;

Degree days – °C, days.

Monthly inside temperature, degree days and monthly heating demand are shown:

Table 5-5 Monthly base inside temperature, degree days and energy demand.

	Jan	Feb	Mar	Apr	May	Jun
T_b, ℃	4.9	3.6	4.3	3.0	1.8	3.2
Degree days, °C Days	38	22	22	8	0	0
Heating, kWh	300.4	173.9	173.9	63.2	0.0	0.0
	Jul	Aug	Sep	Oct	Nov	Dec
T_b, ℃	2.9	0.0	0.4	2.9	4.4	4.9
Degree days, °C Days	0	0	0	0	20	28
Heating, kWh	0.0	0.0	0.0	0.0	158.1	221.4

5.4 MODELLING OF THE HEATING AND COOLING LOAD OF THE HOUSE

5.4.1 Thermochemical heating energy simulation results and analysis

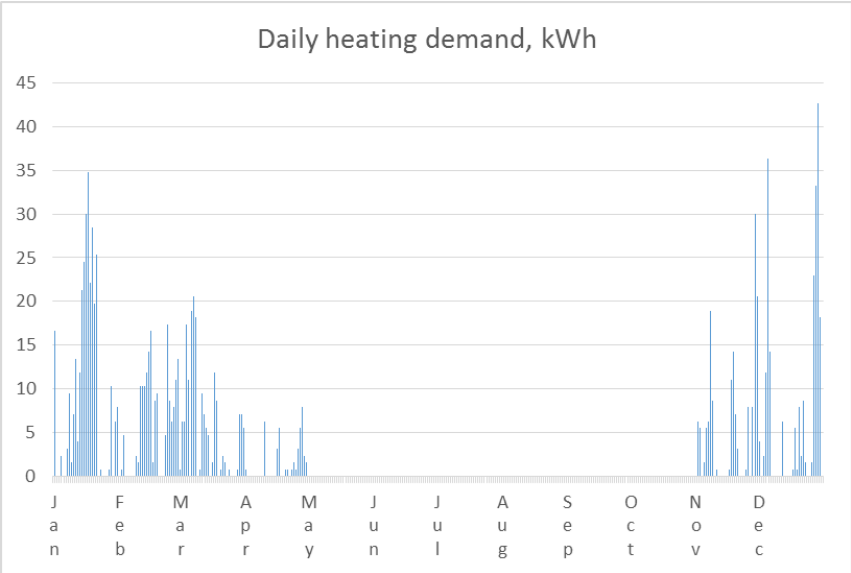


Figure 5-8 Daily heating demand.

In the novel heating system, thermochemical salts will be used for heating. The materials heat storage density will be shown as followed:

In the simulation house, total heating demand is 1091kWh/year or 11.5kWh/m^2/year, which equals to 3927.6MJ/year.

5.4.2 Thermochemical cooling energy simulation results and analysis

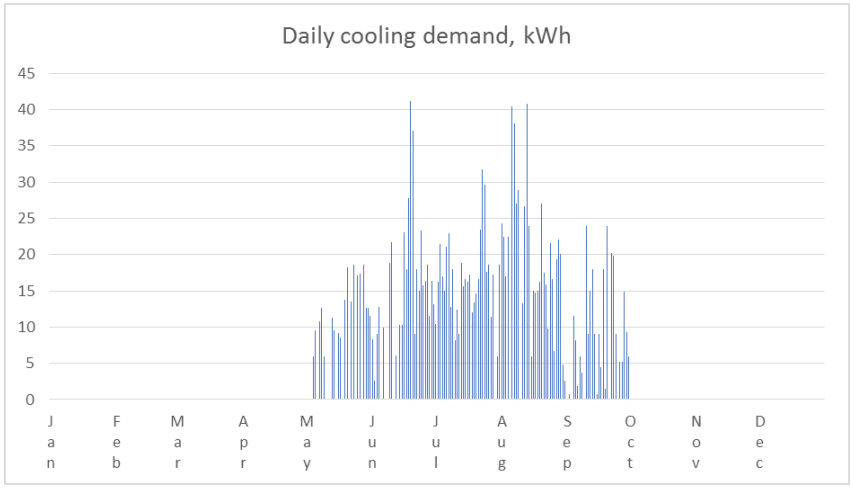


Figure 5-9 Daily cooling demand.

In the thermochemical cooling system, thermochemical salts will be used for cooling. The materials heat storage density will be shown as followed:

In the simulation house, total cooling demand is 1982.6kWh/year or 18.9kWh/m^2/year, which equals to 7137.2MJ/year.

5.4.3 Analysing thermochemical heating and cooling storage materials and sizing

Table 5-6 TES materials energy storage density and potential sizing.

TES composite	Heat storage density, kJ/kg	Mass, ton
V-$MgSO_4$-$CaCl_2$	1173.5	3.34
V-$MgCl_2$-$LiNO_3$	1000.8	3.89
V-$MgSO_4$-LiCl	990.2	3.94
V-$MgSO_4$-$LiNO_3$-$MgCl_2$	748.6	5.21
V-$CaCl_2$	888.2	4.39
V-$NaNO_3$ (TES cooling material)	872.3	8.15
V-Urea (TES cooling material)	727.85	9.77

5.5 Simulated Thermochemical Heat Storage Evacuated Tube for Materials Tests and Analysis

5.5.1 Introduction

In this simulation, the applicability of solar driven TES in buildings in the UK and worldwide through a comparative analyse with SHS and LHS will be theoretically investigated. The rig consists of three solar evacuated tubes (length is 200cm) [224], a copper pipe (diameter is 1cm) and flexible tube (diameter is 1.5cm) are attached to each evacuated tube (see Figure 5-10 – Figure 5-12). Some holes on the copper pipes to provide an access for moisture going through. Flexible tubes are connected with evacuated tubes and release heat to building in reaction process. An ultrasonic humidifier [224] is connected with three copper pipes via flexible plastic tubes to provide moisture in reaction process. Desiccant is filled in the three solar evacuated tubes. Laboratory solar simulator [224] is set beside solar tubes to supply simulated sunlight for regeneration process.

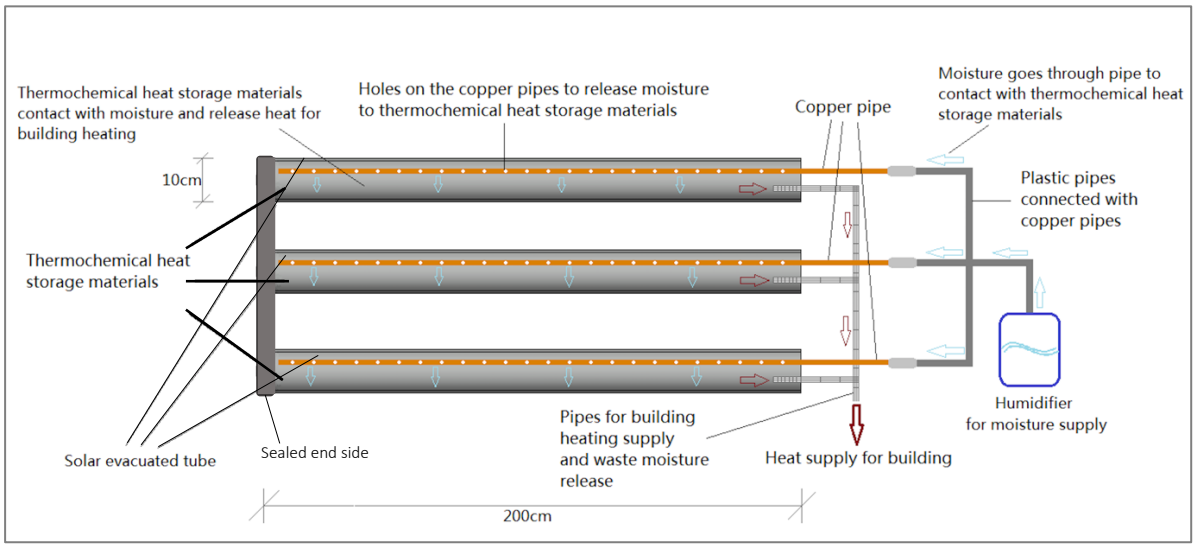


Figure 5-10: Schematic drawing of the simulated test rig (Reaction/discharging process)

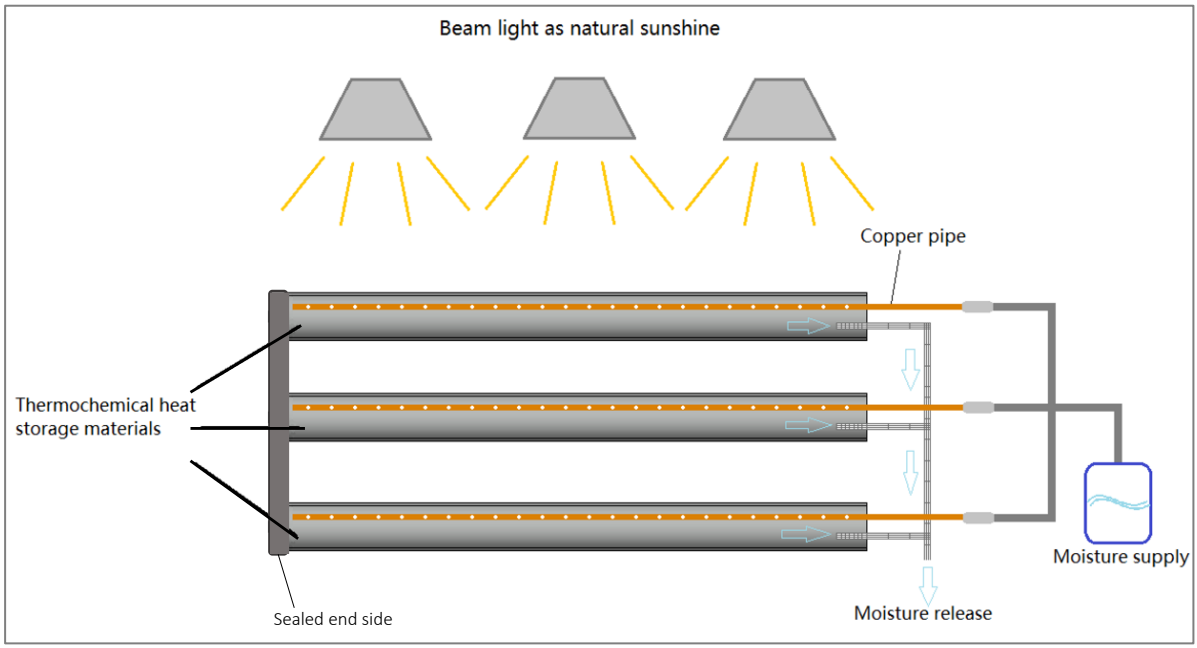


Figure 5-11: Schematic drawing of the simulated test rig (Regeneration/charging process)

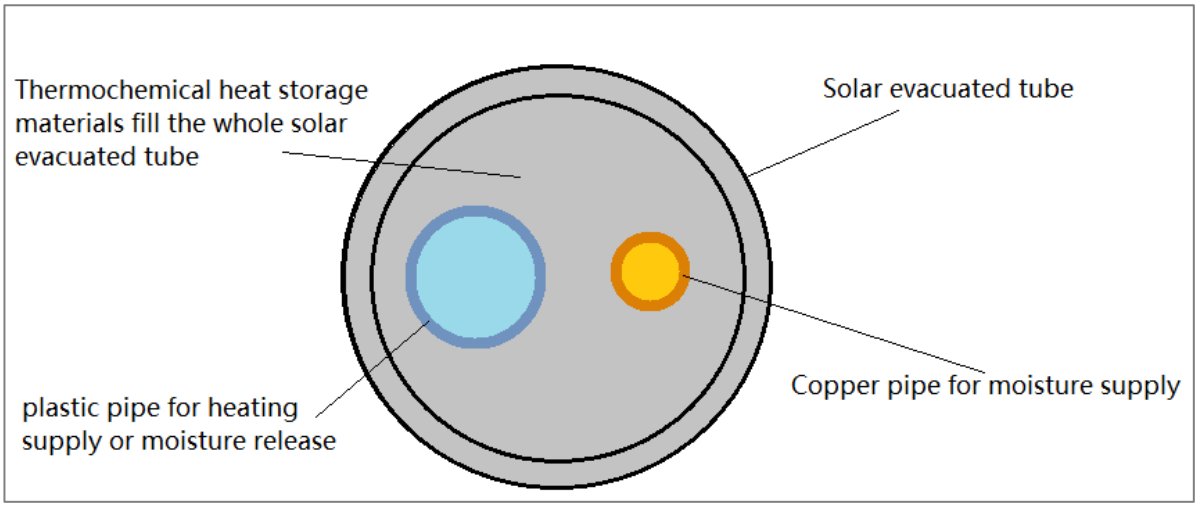


Figure 5-12: Schematic sectional drawing of solar evacuated tube attached with copper pipe and flexible tube.

The reaction (discharging) process involves using high humidity air (moisture provide by humidifier) to react with the desiccant material giving off low level heat (normally <45˚C). Moisture air comes from ultrasonic humidifier through the holes on copper pipes and releases to the solar evacuated tubes which fully filled with desiccant materials. Heat releases (warm and dry air, 40˚C) from desiccant materials when contact with humidity air to provide low temperature heating for building via flexible

tubes on solar evacuated tubes. An air outlet should be set at the end of the flexible tubes for exhaust (heat provide - reaction process and moisture release - regeneration process) to the outside.

In charging (regeneration) process, humidifier is deactivated, valve of the humidifier is switched off, no moisture provided. Laboratory solar simulator is turned on to supply simulated sunlight for heating provide to dry wet desiccant materials. Flexible tubes become an access for moisture releasing to the outside. solar simulator heats up solar evacuated tubes to a high temperature to dry desiccants inside. Moisture air (warm and wet air) removes from the sorption material and leaves the reactor via exhaust port. Charging process lasts until outlet humidity is read as RH=0%. It is expected that this condition will be achieved in t_{chr}<5h.When the material is dry, the cycle may be repeated or the experiment terminated depending on the operators requirements (See: Flow diagram).

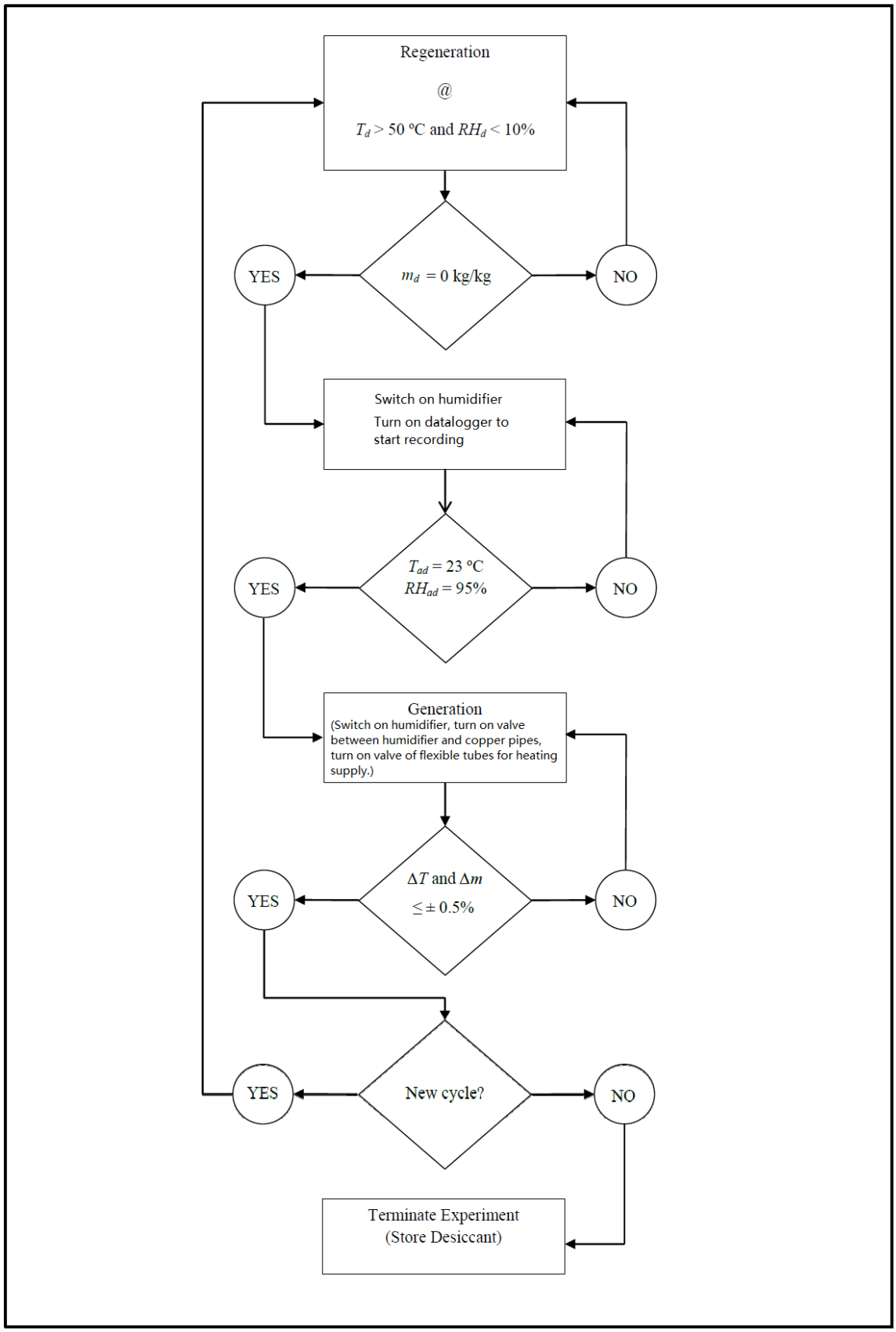


Figure 5-13 Flow diagram of the simulated solar powered TES system

5.5.2 Simulated experimental cycle

1) Switch on the datalogger to start recording.
2) Switch on the humidifier to provide moisture for the desiccant in solar evacuated tubes.
3) Ensure there is adequate water in the humidifier.
4) When the outlet temperature (T_{out}) has returned to the initial outlet temperature [225] deactivate discharging line and activate charging line via valves (switch off humidifier and close the valve between humidifier and evacuated tubes).
5) Turn on the laboratory solar simulator to provide simulated sunlight to heat up evacuated tubes for drying wet desiccants.
6) When the outlet relative humidity is 0%, then turn off lamps and switch off the valve of flexible tubes.
7) Stop both the Sensiron and Data taker. Save the data as a NEW file. Be sure to use sequential file names for further material cycles.

It is assumed that three evacuated tubes are adiabatic, and the total heat absorbed/loss by the glass tubes, the inner glass tubes and the copper tubes [226] of the whole TES system is simulated as 2W/m^{2}K[227]. The total received solar irradiation energy by the simulated TES system is shown as followed:

$$Q_u = Q_T - Q_L \qquad \textit{Eq 1 [226]}$$

Q_u - the useful energy absorbed by the working medium;

Q_T - the total received solar irradiation energy;

Q_L - the total heat loss of the evacuated tube to the environment.

$$Q_T = A * (\tau\alpha) * G \qquad \text{Eq 2 [226]}$$

A - the aperture area of evacuated tube (m^2), 0.6 m^2;

τ - cover glass tube transmittance (dimensionless), 0.91;

α - the solar absorptance of selective coatings (dimensionless), 0.92;

G - solar irradiance (kW/m^2).

In the simulation, the hourly average solar irradiance of each month in Nottingham location is used and shown as followed:

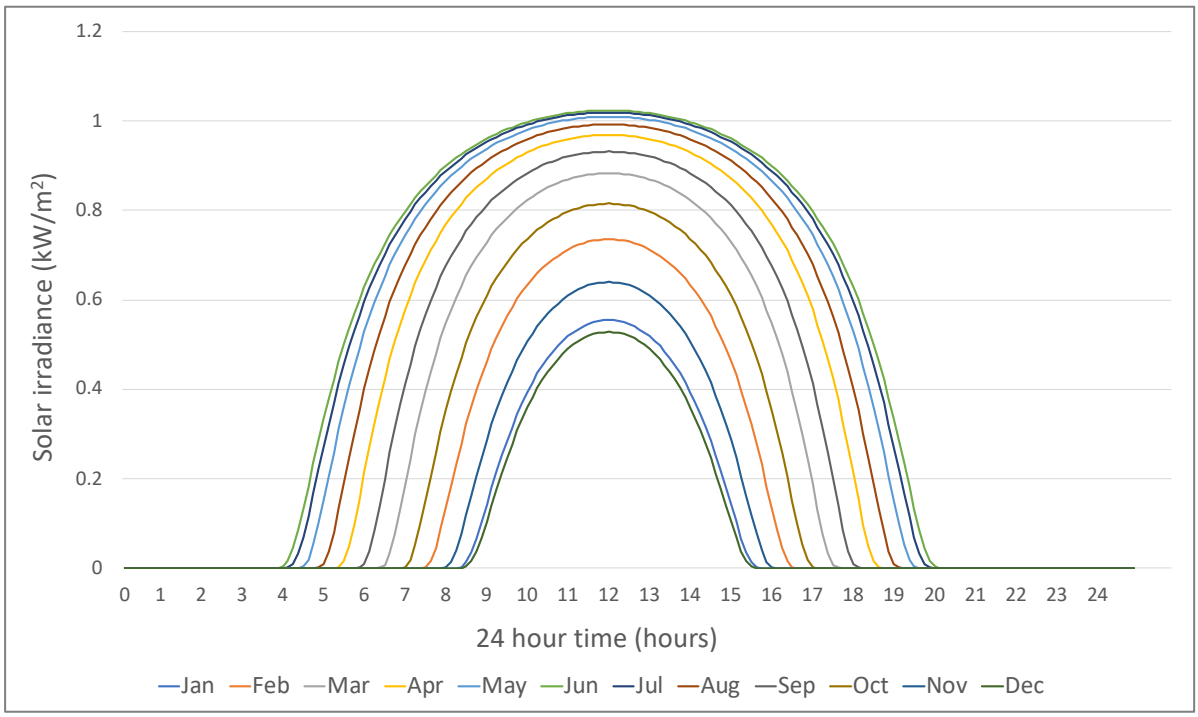


Figure 5-14 Hourly solar irradiation in each month.

Using hourly solar irradiation of each month to calculate daily and monthly solar energy gain, result is shown below:

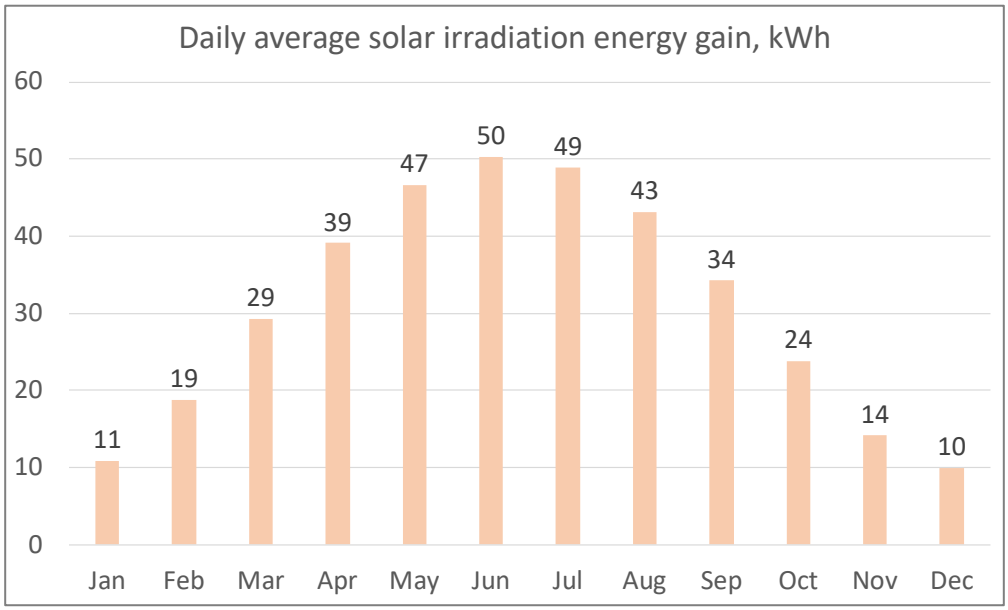


Figure 5-15 Daily average solar irradiation energy gain in each month of the simulated TES system.

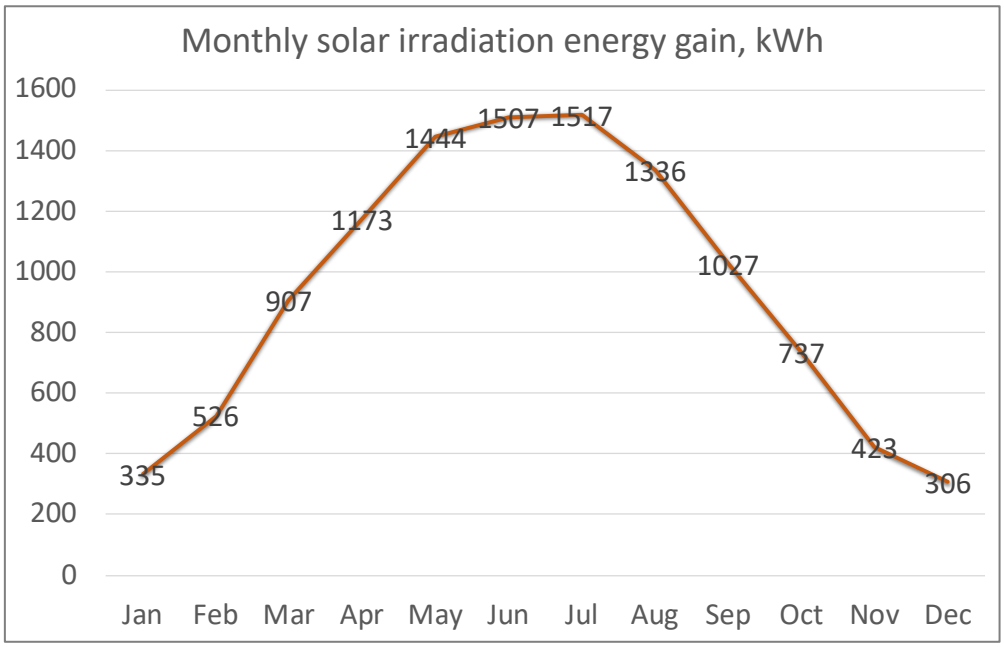


Figure 5-16 The simulated TES system monthly total solar irradiation energy gain.

$$Q_L = A_s * U_L * (T_h - T_a) \qquad \text{Eq 3 [226]}$$

A_s - the total surface area of the simulated system, 0.047 m^2;

U_L - heat loss coefficient of the simulated system, 2 $W/(m^2 \cdot K)$;

T_h - assumed tube working medium average temperature, 80 °C;

T_a - the assumed ambient temperature (°C).

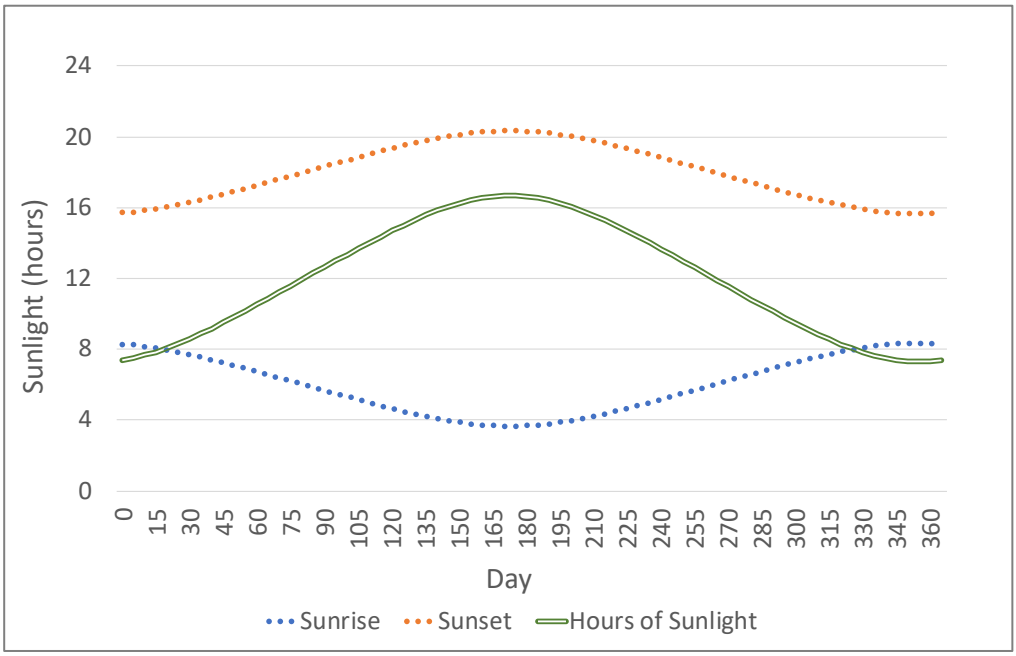


Figure 5-17 Daily sunlight hours in Nottingham.

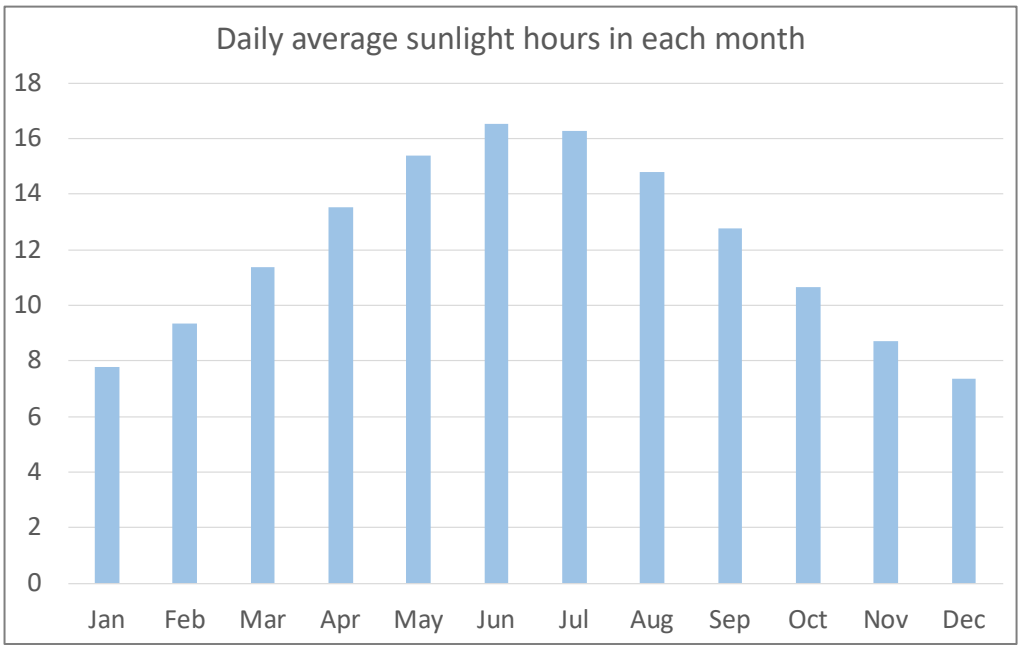


Figure 5-18 Daily average sunlight hours in Nottingham.

The length of the three tubes is 2 m, the internal diameter of the tube is 0.1 cm and the external diameter of the tube is 0.13 cm. The diameter of the copper tube and the outlet flexible tube is 1 cm. Energy density and the porosity of the composites are analysed by using SDT-Q600 and MIP (results shown in Chapter 4). According to the

size and volume of the simulated TES system, some parameters have been worked out.

5.6 Result and Analysis

According to the results in Table 5-7, vermiculite with $MgSO_4$ and $LiNO_3$ showed the highest stored energy capacity. Vermiculite with $MgSO_4$ and $CaCl_2$ showed ability to store large amounts of energy as well. However, the energy density and energy storage ability of the composite of vermiculite with $MgSO_4$, $LiNO_3$ and $MgCl_2$ were very low, it was similar as the latent heat storage. The energy density of a better performance latent heat storage material can be 200 kJ/kg, in this simulated system, the total mass was 75.2kg and the stored energy was 4.2 kWh; while, the sensible heat storage showed a much lower performance with energy storage of 2.19 kWh.

Table 5-7 Performances of different composites.

	V-$MgSO_4$-LiCl	V-$MgSO_4$-$CaCl_2$	V-$MgSO_4$-$LiNO_3$	V-$MgSO_4$-$LiNO_3$-$MgCl_2$
Energy density, kJ/kg	990.2	1173.5	1000.8	748.6
Bulk density, kg/m^3	334.1	515.6	652.9	263.7
Mass, kg	31.41	48.47	61.37	24.79
Stored energy, kWh	8.64	15.80	17.06	5.15
water uptake, kg/kg	0.41	1.46	1.73	0.40

Porosity, cm^3/g	2.300	1.250	0.730	1.030
Porosity, m^3	0.072	0.061	0.045	0.026

Figure 5-19 showed the comparison of daily average heating demand and daily average solar irradiation received by the simulated system. As a short-term heating storage system, stored heat was higher than heating demand. And daily solar irradiation received by evacuated tubes can provide enough regeneration energy for regenerating/charging TES system. Parallel lines displayed energy storage capacity of different materials. Stored energy in TES materials were much higher than latent and sensible heat storage materials.

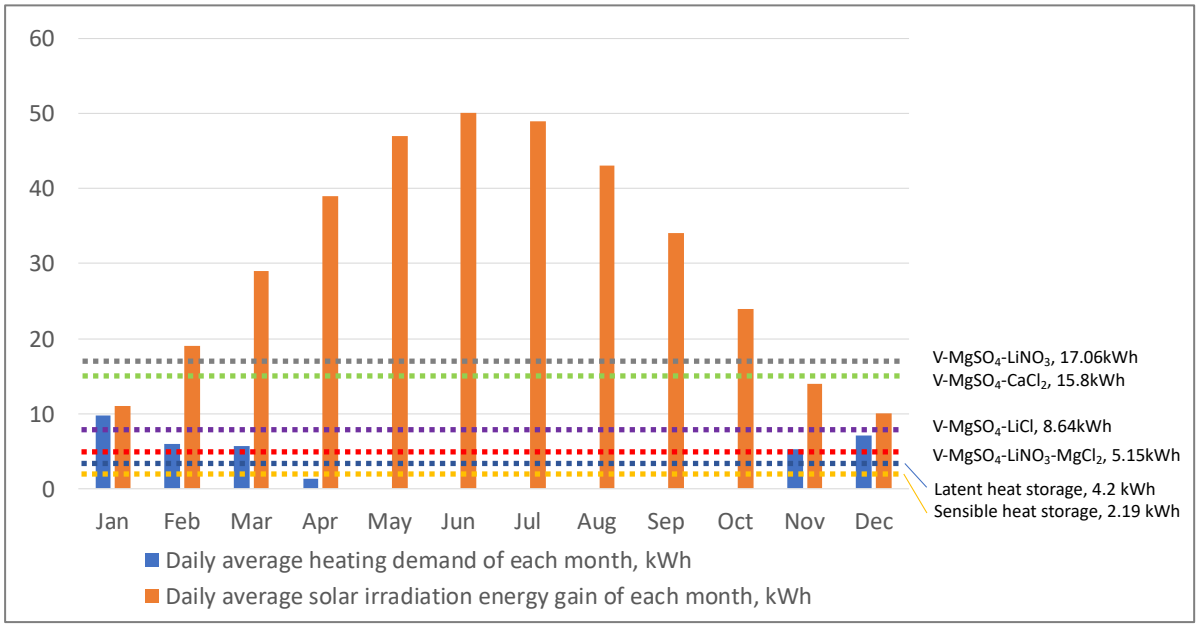


Figure 5-19 Daily solar irradiation and heating demand with different materials comparison.

5.7 SUMMARY

In this chapter, computer simulation of heating and cooling demand in a house and a solar evacuated tube collector TES system have been presented and analysed. A typical low-carbon 3 bedroom house was simulated with heating and cooling load.

Seasonal and daily heating and cooling load of a selected building was simulated via Integrated Environmental Solutions Virtual Environment (IES-VE). According to the energy demands, required heat and cool storage volume for the case of using different thermochemical energy storage materials for solar energy storage was investigated both for short term and seasonal basis. The results show that compared with latent and sensible heat storage, TES materials can be an optimal option for a typical house to meet annual heating/cooling load with limited space due to the high energy density of TES materials. Moreover, the solar evacuated tube collector with TES materials can be another choice for a limited roof space to provide short-term energy storage. In the next chapter, some relevant experiments on materials selection, development and optimisation will be investigated based on the feasibility of the computer simulation.

6 SALT IMPREGNATED TES MATERIALS TESTS IN OPEN CYCLE THERMOCHEMICAL ENERGY STORAGE RIG

6.1 INTRODUCTION

Thermochemical energy storage (TES) is a novel technology for storing energy to provide more efficient and clean energy systems [106]. TES has the potential for high energy density storage. It has the highest potential to achieve the requirement of compact thermochemical energy storage when the space is limited. The research of TES system and materials are currently still undergoing. Some composites materials have been tested and analysed before the rig test to choose the optimal TES materials.

Thermochemical heat storage system uses thermochemical materials act with moisture to generate heat for providing heating in built environment. In my project, an open thermochemical energy storage system has been built for TES materials test. This open system includes power, reaction rig (to store thermochemical materials, it is the reaction place), humidifier (to supply moisture), fan (to supply decent air flow rates) and heater (for regeneration). In the real system for next step, solar PV system will replace power system, fan and heater. Thermochemical heat storage system stores solar energy in the thermochemical materials in summer/day time and release heat in winter/cool night when needed. Regeneration will take place in day time with solar energy system.

6.2 AIM

In this context, a new heating method using thermochemical materials as heat storage media is proposed. The idea of endothermic heating system is to develop a technology that stores the abundant solar energy in matrix with the salt based

composites for space heating. The proposed project focuses on developing composite materials that will not deliquesce and that provides adequate and steady endothermic performance over repeating cycles. The composite materials will consist of a porous host matrix and a salt which endothermically dissolves when hydrated. Some composite materials have already been tested. In this test, four best materials with better performance will be used as heat source to test their performance in the thermochemical heat storage system.

6.3 EXPERIMENTAL DESIGN

A lab-scale open cycle TES system for different materials tests was installed at lab. In Figure 6-1 and Figure 6-2, the open TES system diagram and the detail on the test body are shown. As it can be seen, the test rig consists of (1) the reaction chamber in which the TES materials were hold in the mesh drawer, two sensors were placed on the bottom of the mesh drawer to record weight changing; (2) the humidifier was installed to provide moisture air for TES materials in discharging process; (3) a fan was installed to blow air into the reaction chamber; (4) a heater was installed after fan as a heat source in the regeneration process (the heater will be replaced by solar PV/thermal collector as a renewable heat source in the future step); (5) a PID controller was installed to control the regeneration temperature. All parts were connected with each other under a normal atmospheric pressure, and the air circulating inside was connected to the ambient air.

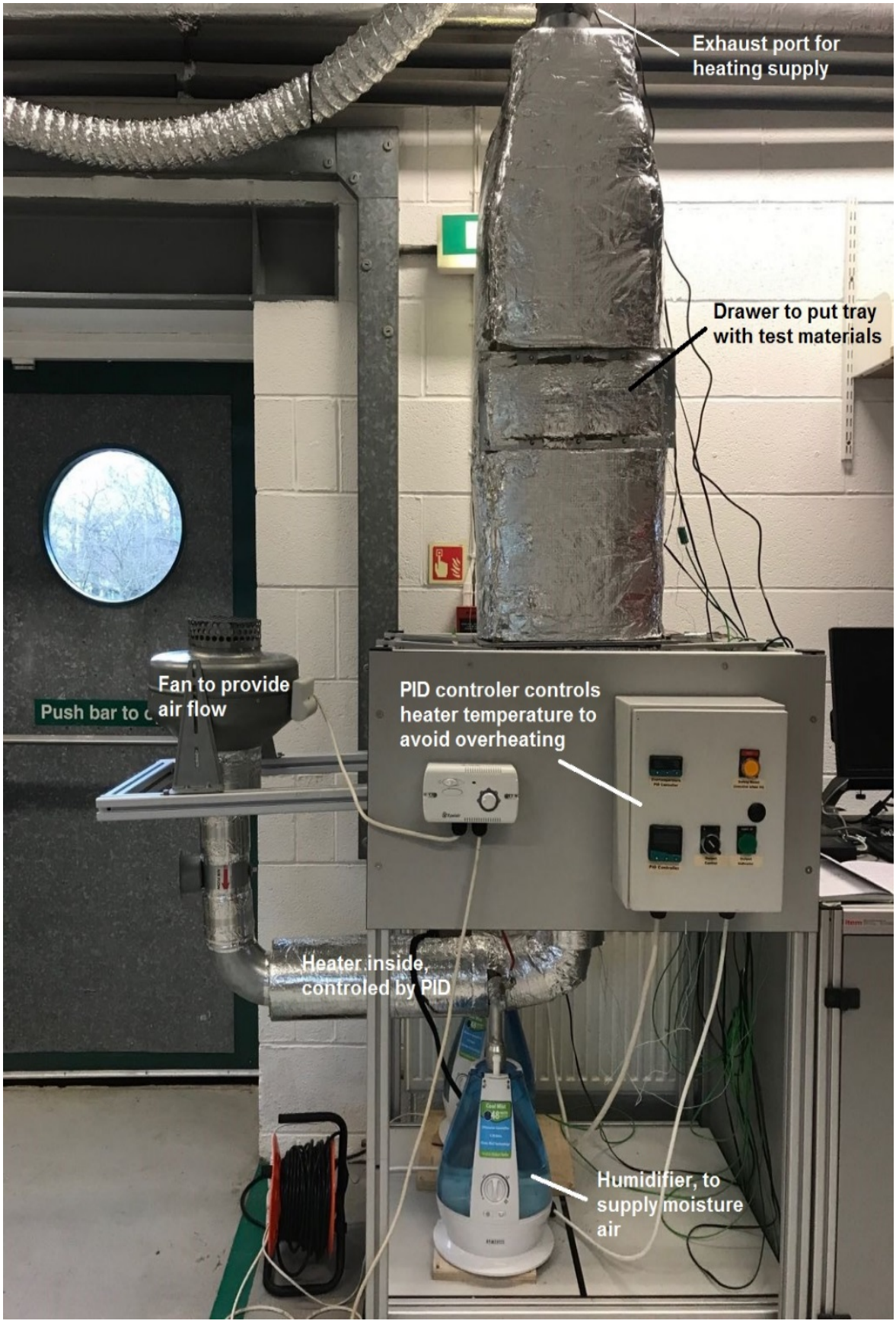


Figure 6-1 Open system for thermochemical energy storage materials test rig.

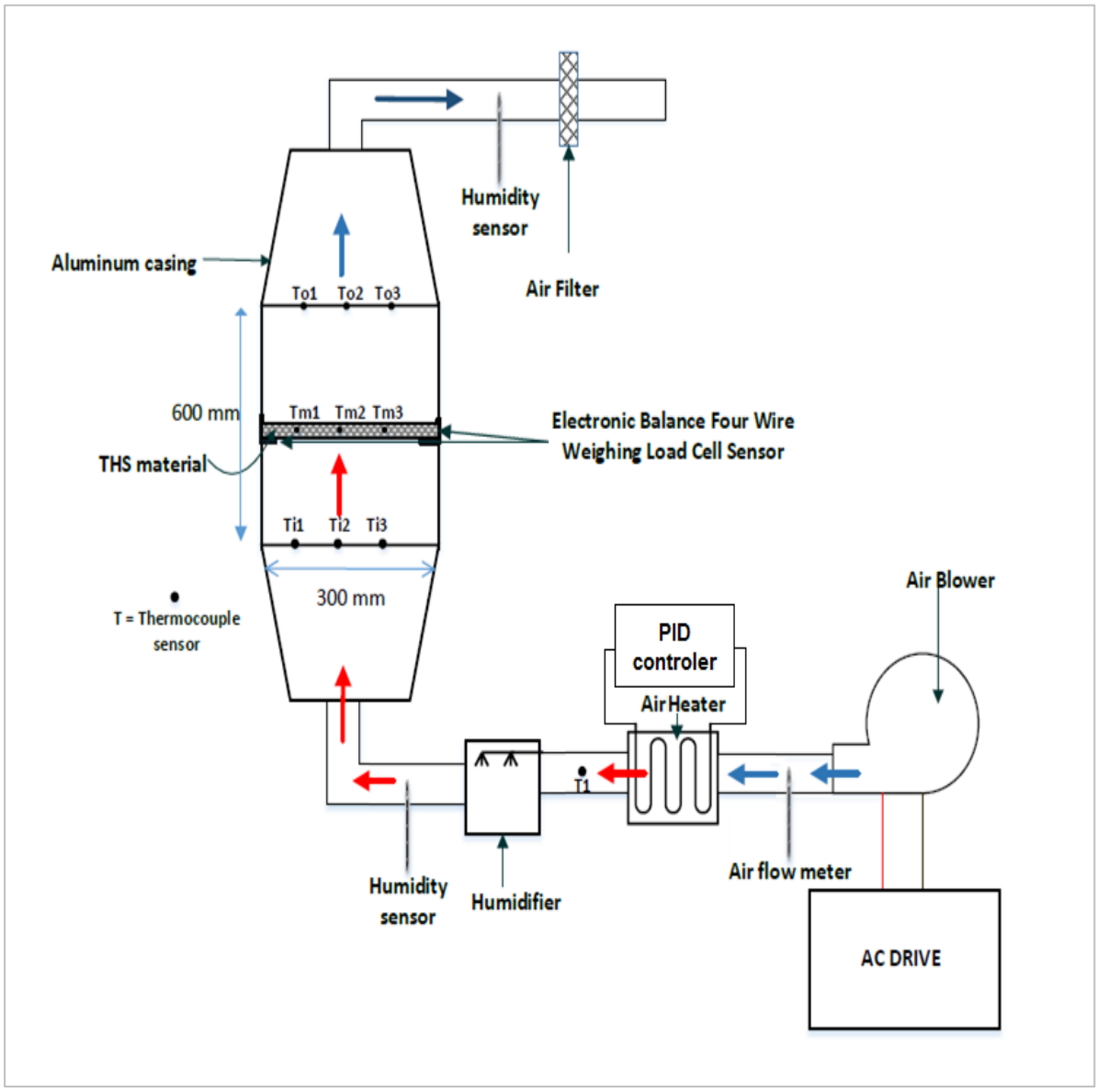


Figure 6-2 The inside details of the thermochemical energy storage test rig.

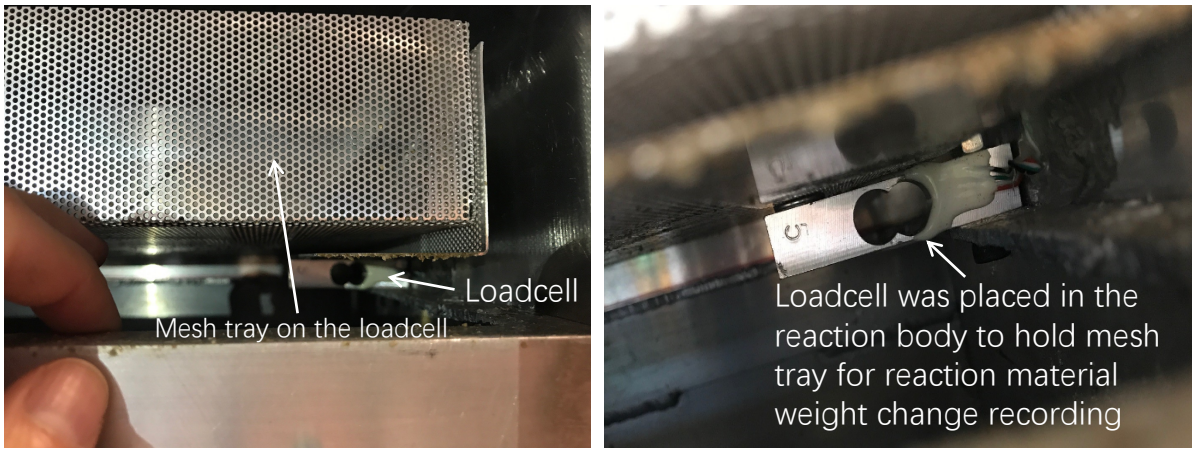


Figure 6-3 TES materials testing tray and load cell.



Figure 6-4 TES materials testing tray and thermocouple/sensor.

This thermochemical energy storage test rig is a simple one just for the TES materials test (Figure 6-1). A fan is for blowing humid air into the reaction body with an air flow rate of 1.6m/s (equals to 0.032kg/s). The humidifier in the rig is used for increasing humidity level to above 90% for reaction process (Figure 6-5). A drawer in the reaction body to put mesh tray with test materials, on each side of the drawer, there is LoadCell for recording mass change of the materials holder tray. The materials holder tray was made from mesh metal plate for moisture air going through the materials easily. The whole test rig is standing for letting moisture pass through the reaction body quickly. In the regeneration/charging process, heater was used for heating the air at 90 °C to dry the wet materials (Figure 6-6). An exhaust port was installed on the top of the reaction body for providing warm and dry air for building in reaction process, and for wet air exhausting in the regeneration process. There were several thermocouples and sensors set before air goes through the material tray, inside the material, after the air goes through the material tray and one on the outlet pipe for recording temperature and humidity level.

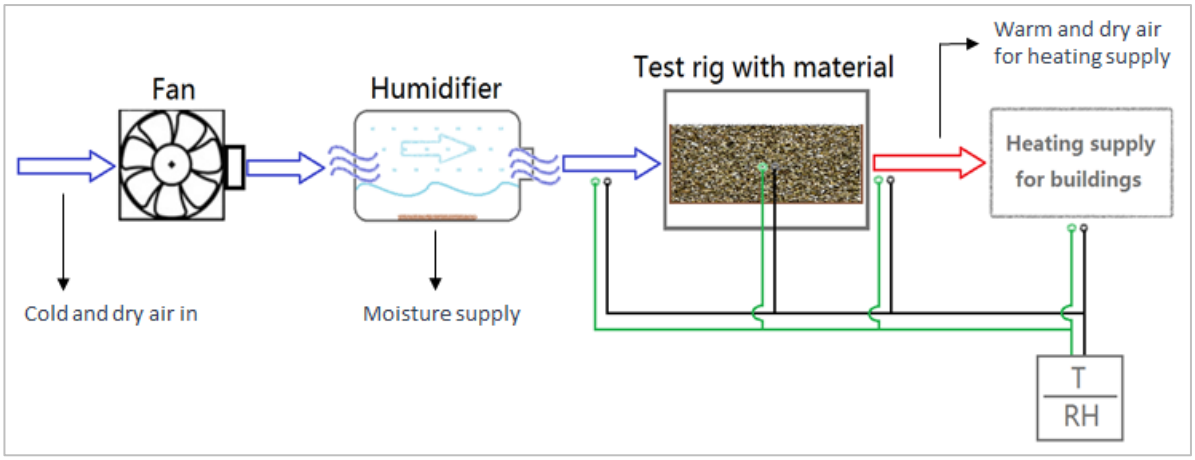


Figure 6-5 Discharging cycle in open loop thermochemical energy storage system.

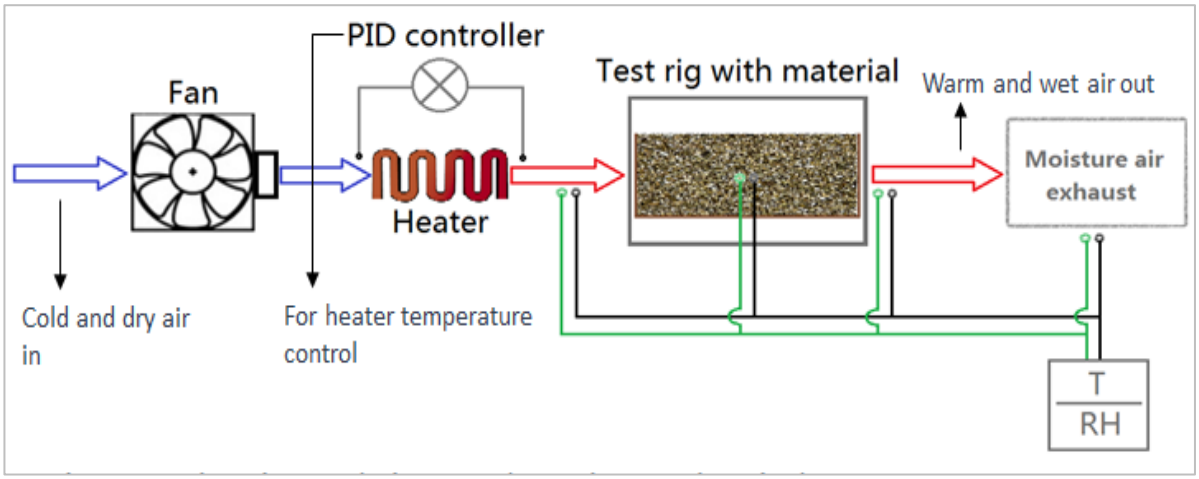


Figure 6-6 Charging cycle in open loop thermochemical energy storage system.

6.4 Experiment Process and Results

All the testing composites were put in oven at 200 °C and dried for 24 hours before testing day to remove water moisture inside materials and make sure it is completely dried. Then in the testing day morning material was taken out and cooled down for 2 hours before starting test cycle to confirm it was completely cool at room temperature.

6.4.1 V-$CaCl_2$-LiCl (weight ratio 1:2:1)

In the 1st discharging process, put dried v-CaCl2-LiCl in the mesh tray and total mass of material with mesh tray was 600g, the 1st discharging process was taken 3 hours. Initial temperature was 20 °C. The temperature record is shown below (Figure 6-7):

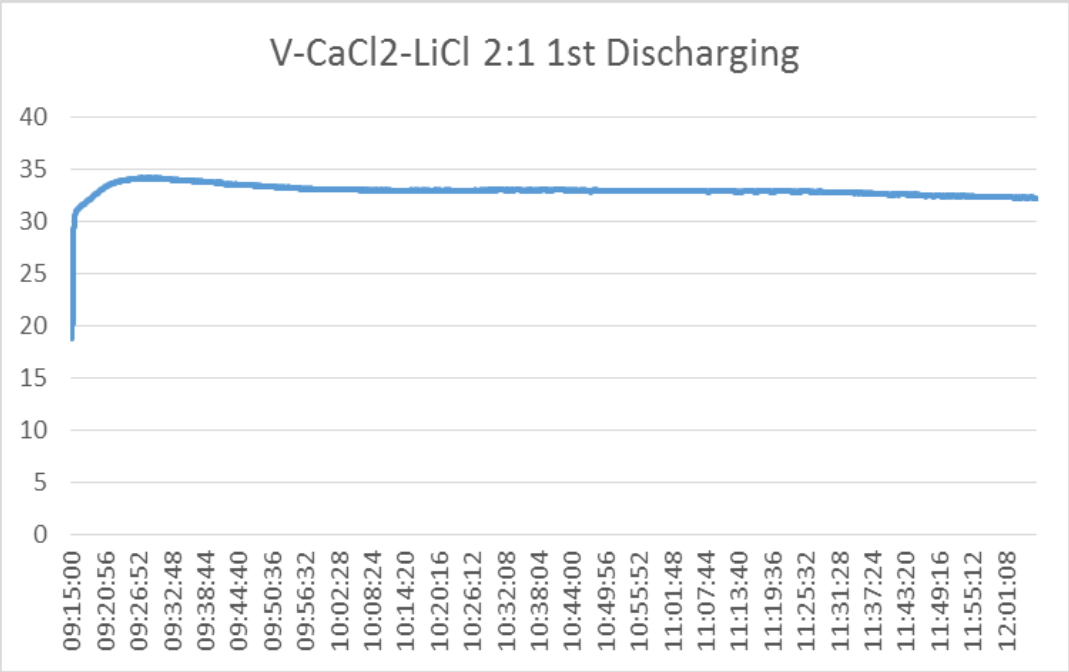


Figure 6-7 Temperature record of V-$CaCl_2$-LiCl in 1st discharging process.

After 14 minutes, it reached the highest temperature at 34.13 °C. Then the air outlet temperature stayed at around 33 °C. After 3 hours, mesh tray was taken out with materials inside to check the weight, the reading was 666g, which means the water vapour uptake of the composite was 66g (see Figure 6-8, Figure 6-9 and Figure 6-10). As the air outlet temperature was very stable, we changed discharging time to 1 hour in the next tests.



Figure 6-8 V-$CaCl_2$-LiCl in the mesh tray after 1st discharging process.

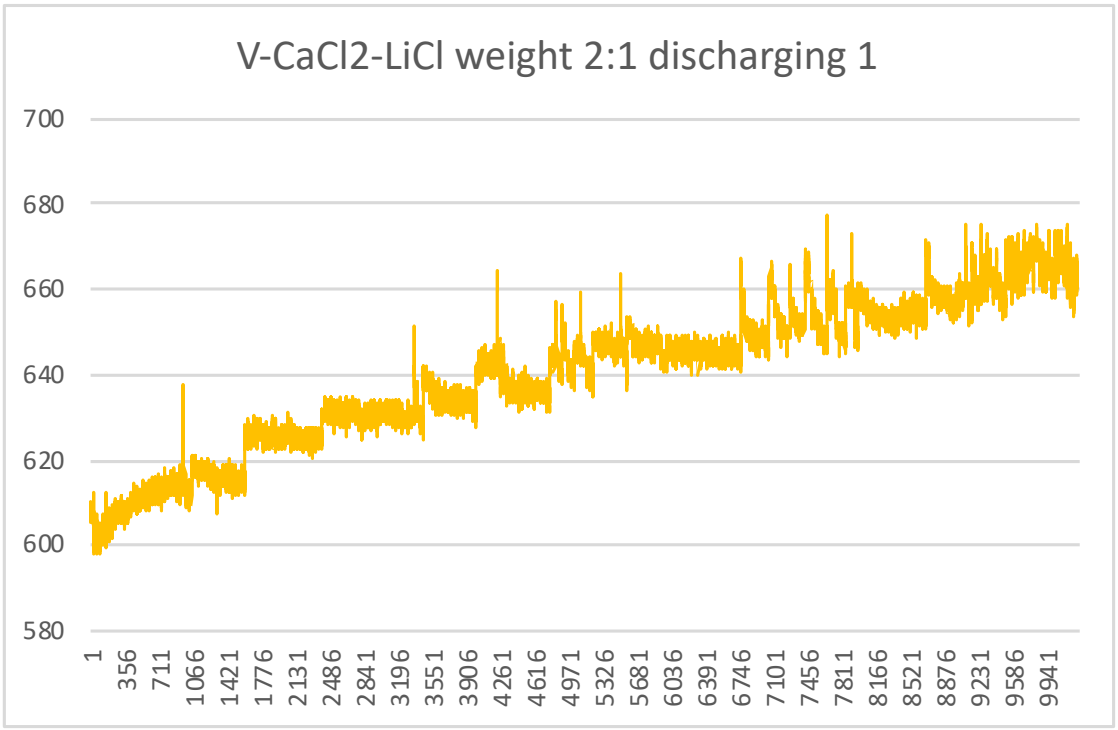


Figure 6-9 V-$CaCl_2$-LiCl weight change in the 1st reaction process.

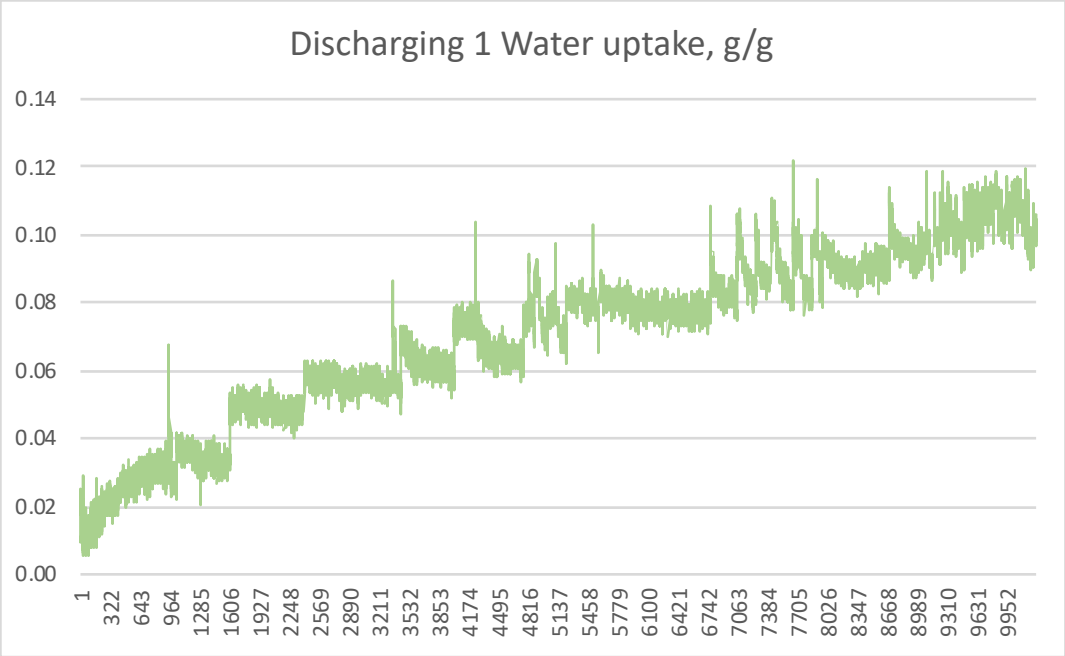


Figure 6-10 V-$CaCl_2$-LiCl water uptake change with times in the 1st discharging process.

The first charging process took 2 hours with an initial weight of 666g (mesh mass was 144g). Material temperature reached 90 °C after 30 minutes. After charging process, the mesh tray with materials were taken out and it showed that the mesh tray with materials weight was 641g after charging process. 25g of water vapour has been removed from wet materials (see Figure 6-11 and Figure 6-12).



Figure 6-11 Mesh tray with V-CaCl2-LiCl after charging for one hour.

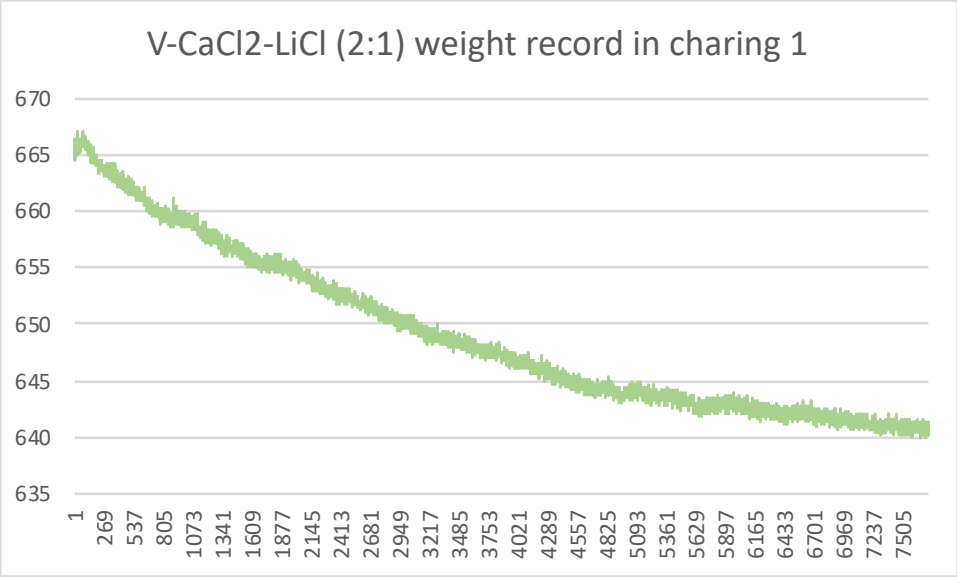


Figure 6-12 V-CaCl$_2$-LiCl weight change with times in the charging process.

After regeneration process, material and the rig were cooled down at room temperature (20 °C) for 1 hours. Then the 2nd discharging started and processed for 1 hour.

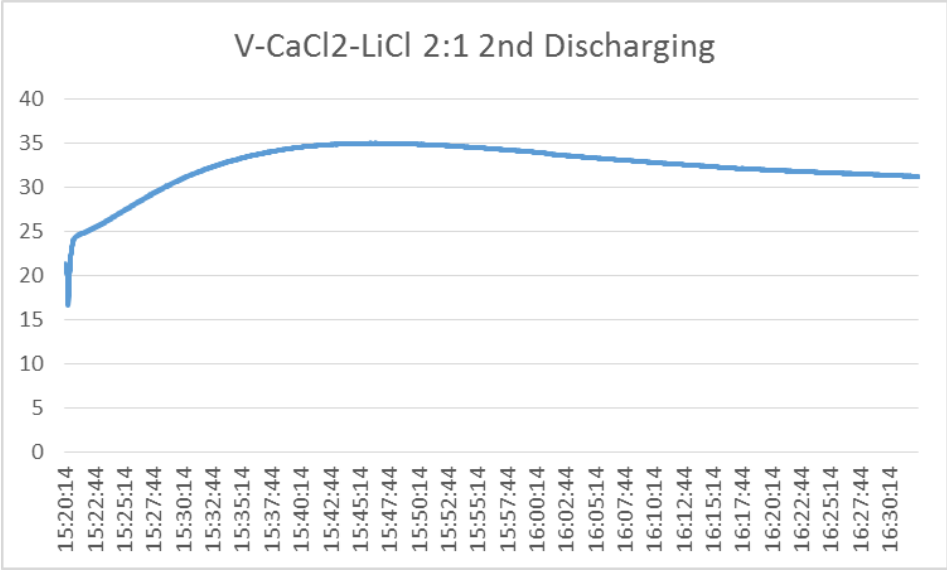


Figure 6-13 Temperature record of V-CaCl2-LiCl in 2nd discharging process.

The highest temperature reached 35.01 °C after 26 minutes, which was surprisingly a bit higher than the highest temperature in the first discharging process. The mass

record was 669g after 1 hour discharging, and the total water uptake was 0.057g/g (see Figure 6-14 and Figure 6-15).

There were some tips need to be noticed in the testing process:

- In the charging process, the rig should be supplied 90 °C air flow temperature before put in the materials.
- Discharging process should be stayed longer to record how long it will take to stay at a high temperature condition and provide warm air.

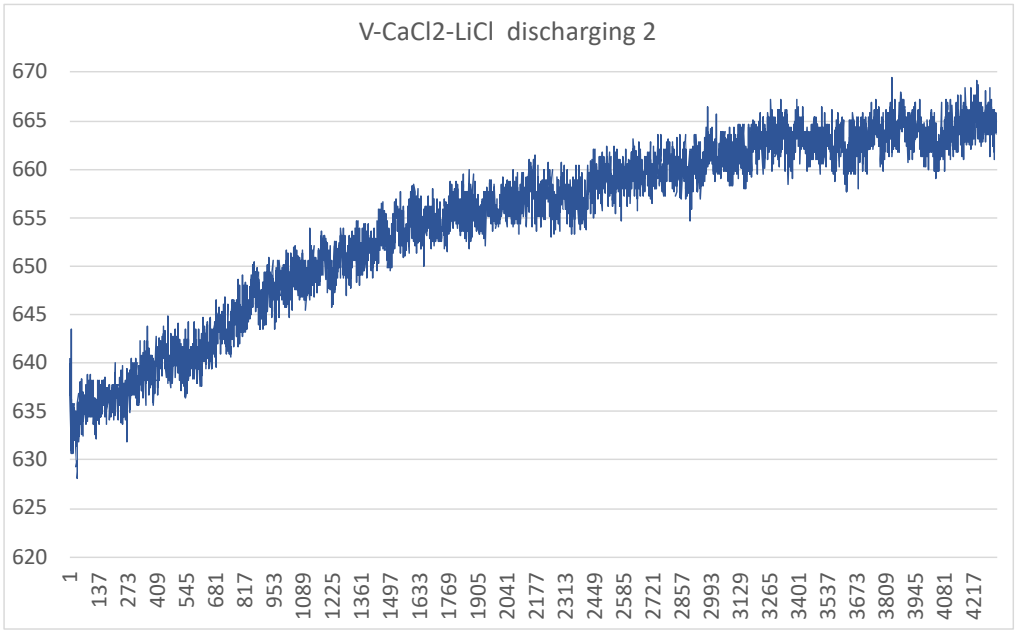


Figure 6-14 V-$CaCl_2$-LiCl weight change with times in the 2nd discharging process.

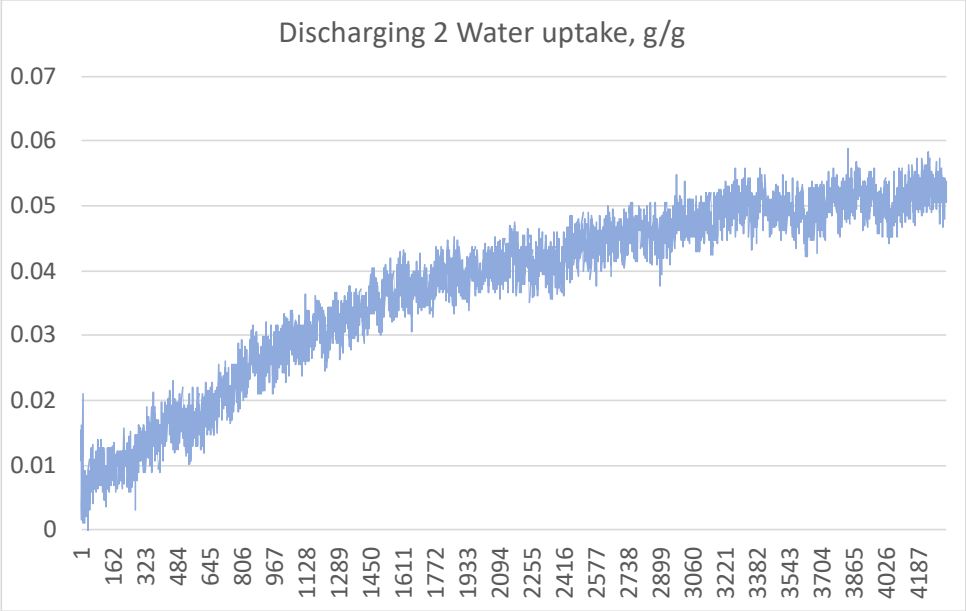


Figure 6-15 V-$CaCl_2$-LiCl water uptake change with times in the 2nd discharging process.

6.4.2 V-$MgSO_4$-LiCl (weight ratio 1:2)

In the 1st discharging process, total mass of mesh tray with material were 600g, the 1st discharging process started at 9:35am and end at 10:35am with the initial air inlet temperature was 20 °C.

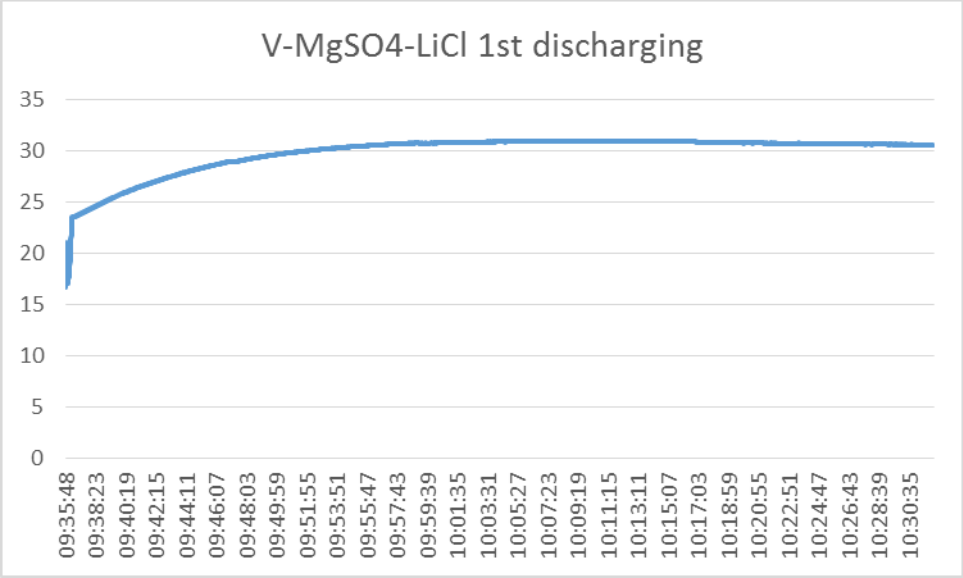


Figure 6-16 Temperature record of V-$MgSO_4$-LiCl in 1st discharging process.

At 10:08am, materials temperature slowly reached 30.9 °C after 33 minutes. However, it can be seen in Figure 6-16 that it can stay above 30 °C for quite a long time. After 1st discharging, the weight was 668g (see Figure 6-17, Figure 6-18), which means there was 68g water vapor uptake in total (0.1g/g) (see Figure 6-19).



Figure 6-17 V-$MgSO_4$-LiCl in the mesh tray after 1st discharging process.

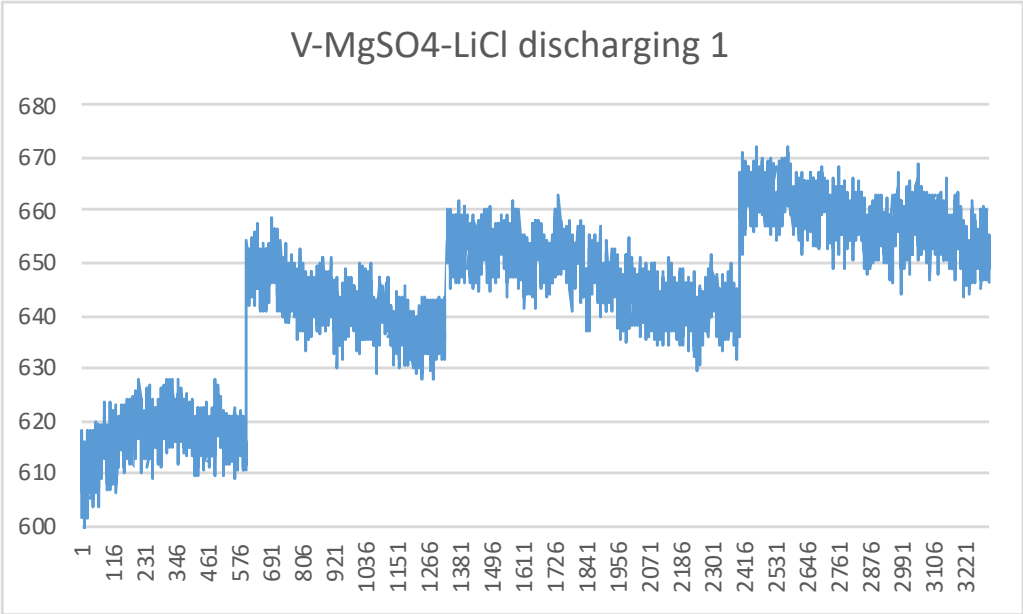


Figure 6-18 V-$MgSO_4$-LiCl weight change in the 1st reaction process.

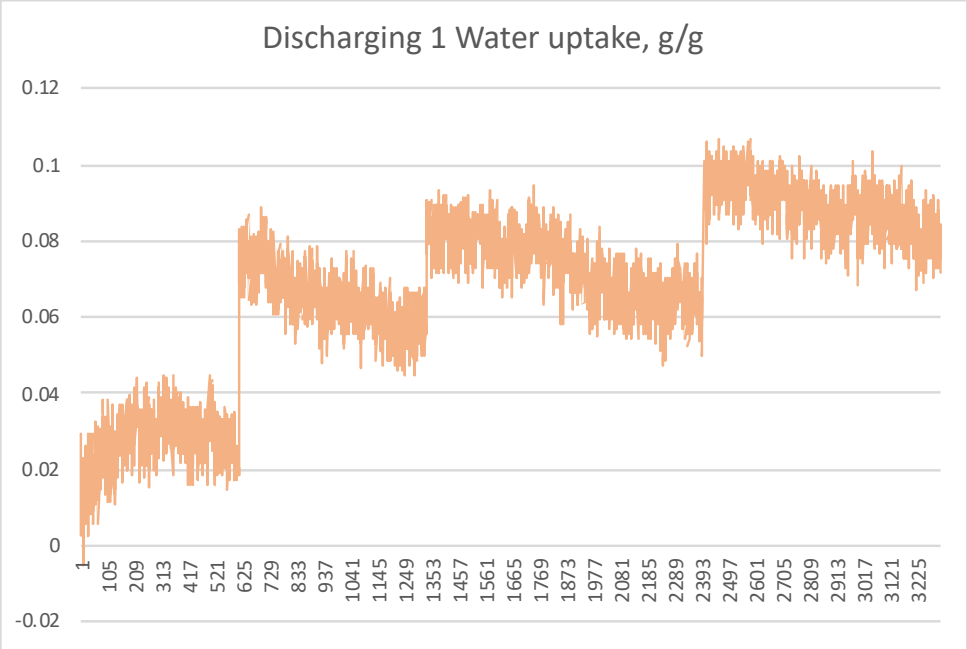


Figure 6-19 V-MgSO4-LiCl water uptake change with times in the 1st discharging process.

Charging process started at 10:45am and ended at 12:45 at 90 °C for two hours. The total weight of mesh tray with V-$MgSO_4$-LiCl was 656g (see Figure 6-20) after charging for 2 hours at 90 °C that means materials lost 12g of water vapor (see Figure 6-21). The charging period was the same as the 1st material test, however, water loss was much less than the 1st material, hence, the low regeneration efficiency of vermiculite with $MgSO_4$-LiCl was very low.



Figure 6-20 V-$MgSO_4$-LiCl in the mesh tray after charging for 2 hours.

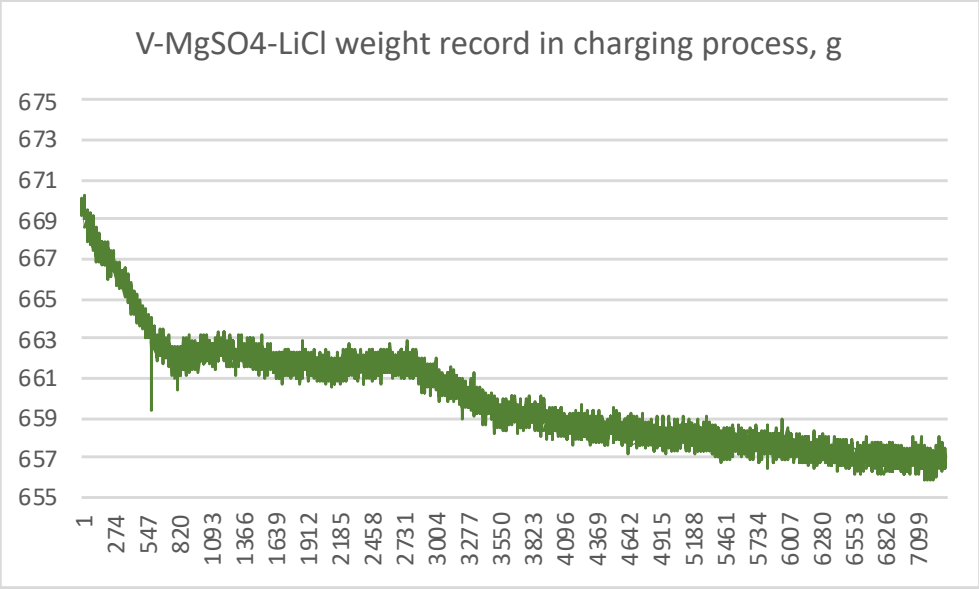


Figure 6-21 V-$MgSO_4$-LiCl weight change in the charging process.

Then after cooled down for 1 hour, the 2nd discharging process started at 13:20 and ended at 14:30pm for 1 hour reaction. The highest temperature reached 33.03 °C at 13:48pm after discharging process started 25 minutes (see Figure 6-22). And also, the air outlet temperature stayed above 30 °C for a very long time. The weight of v-$MgSO_4$-LiCl was 689g after the 2nd discharging cycle, and the total water uptake was 0.053g/g.

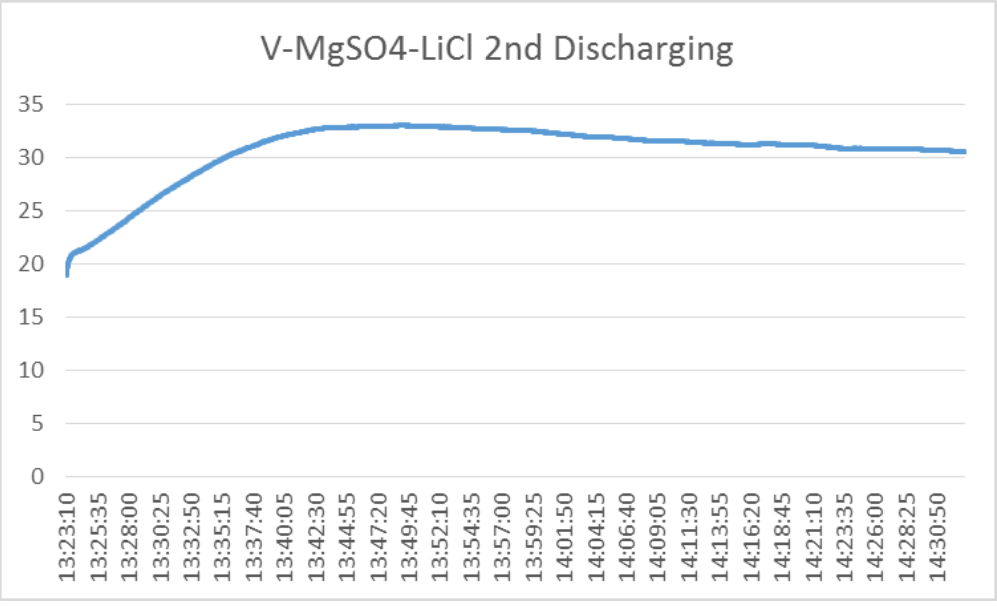


Figure 6-22 Temperature record of V-$MgSO_4$-LiCl in 2nd discharging process.

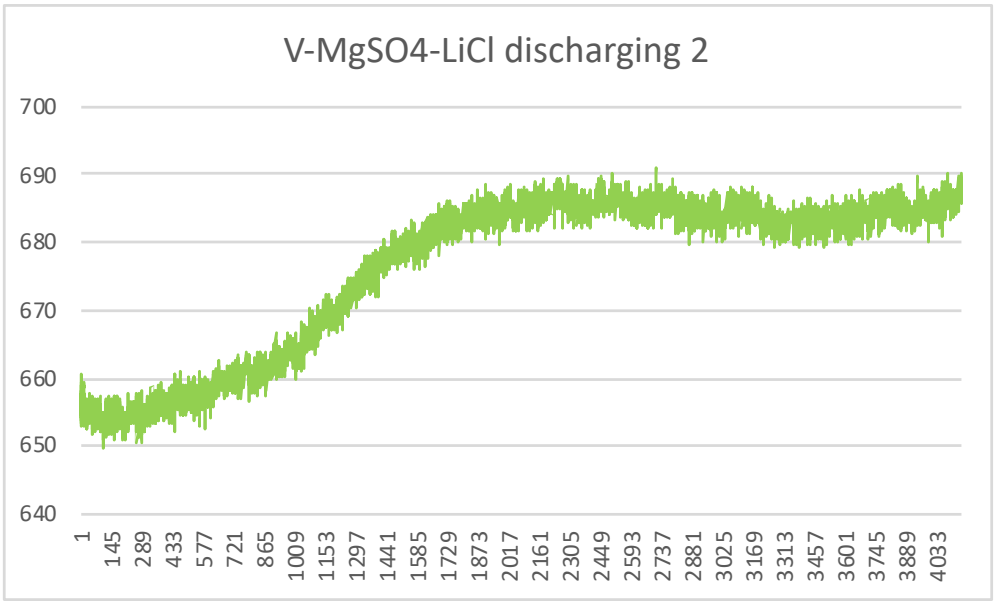


Figure 6-23 V-$MgSO_4$-LiCl weight change in the 2st discharging process.

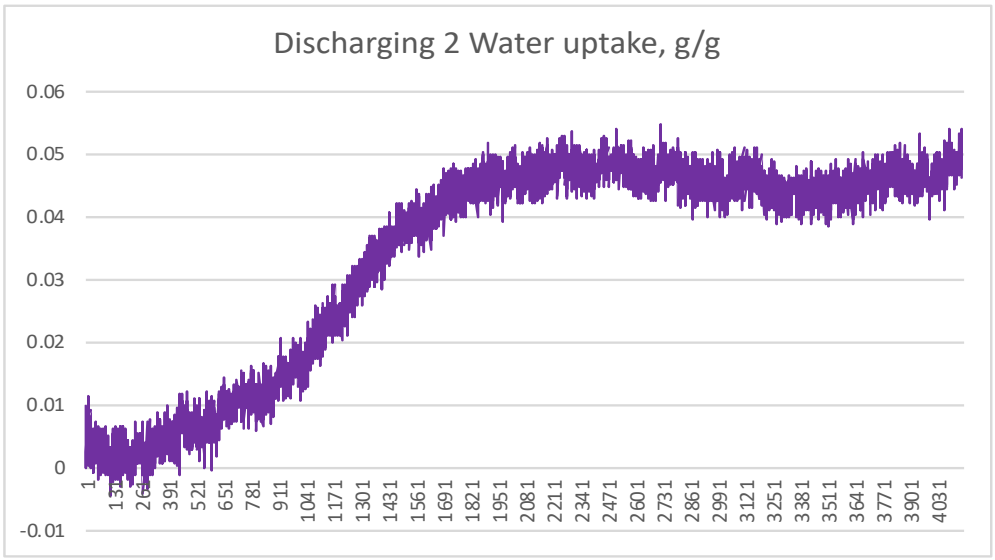


Figure 6-24 V-$MgSO_4$-LiCl water uptake change with times in the 2nd discharging process.

6.4.3 V-$MgSO_4$-$CaCl_2$ (weight ratio 1:1)

The 1st discharging cycle was started at 9:40am, mesh tray with materials were 600g, the process started at 9:40am and ended at 10:40am with the initial air inlet temperature at 20 °C.

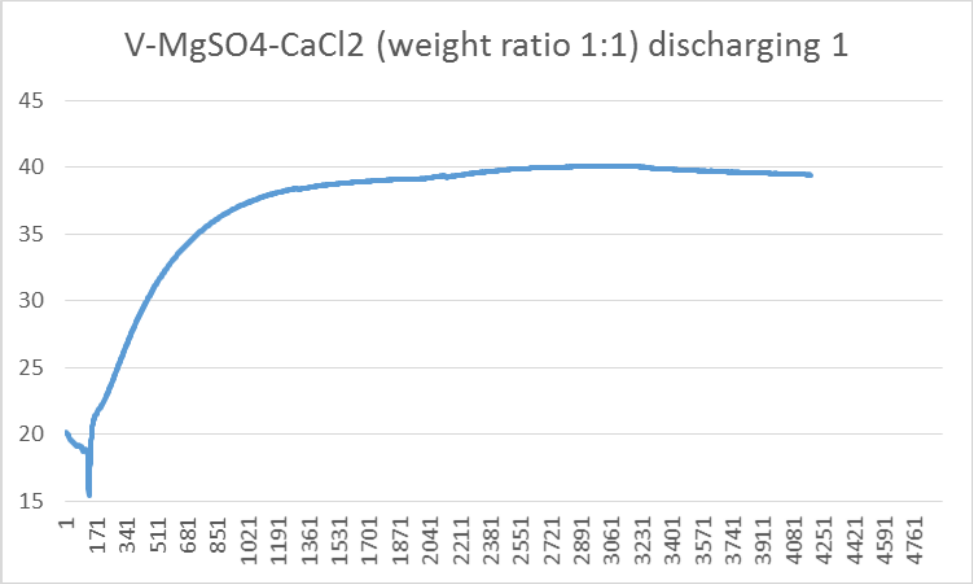


Figure 6-25 Temperature record of V-$MgSO_4$-$CaCl_2$ (weight ratio 1:1) in 1st discharging process.

At 10:25am, the air outlet temperature slowly reached 40 °C after 45 minutes. However, it can be seen in the Figure 6-25 that it can stay above 30 °C for a very long time period since 09:46am (6mins after teat started). After 1st discharging, the weight was 635g (see Figure 6-26) with 35g water vapor uptake and the total water uptake was 0.06g/g (see Figure 6-27).

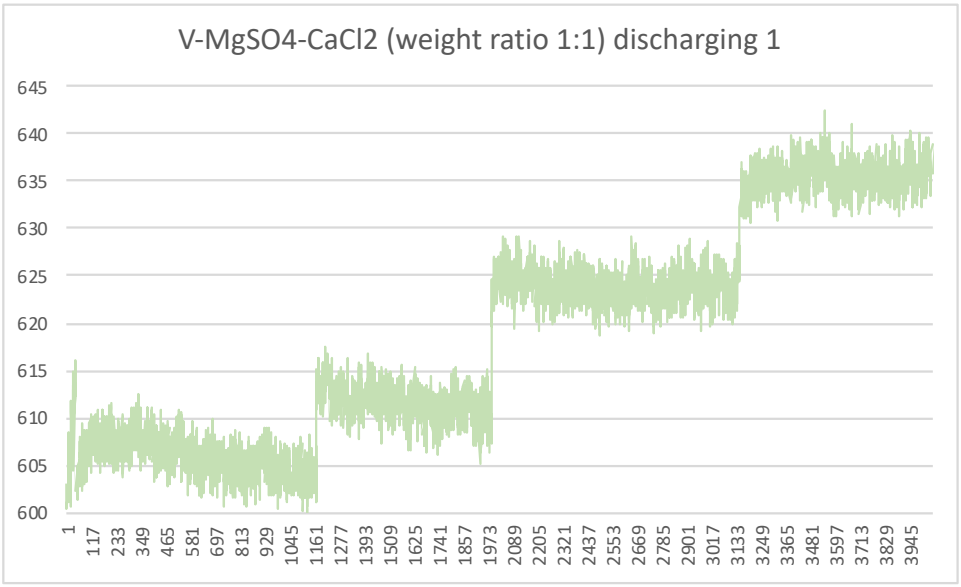


Figure 6-26 V-$MgSO_4$-$CaCl_2$ (weight ratio 1:1) weight change in the 1st discharging process.

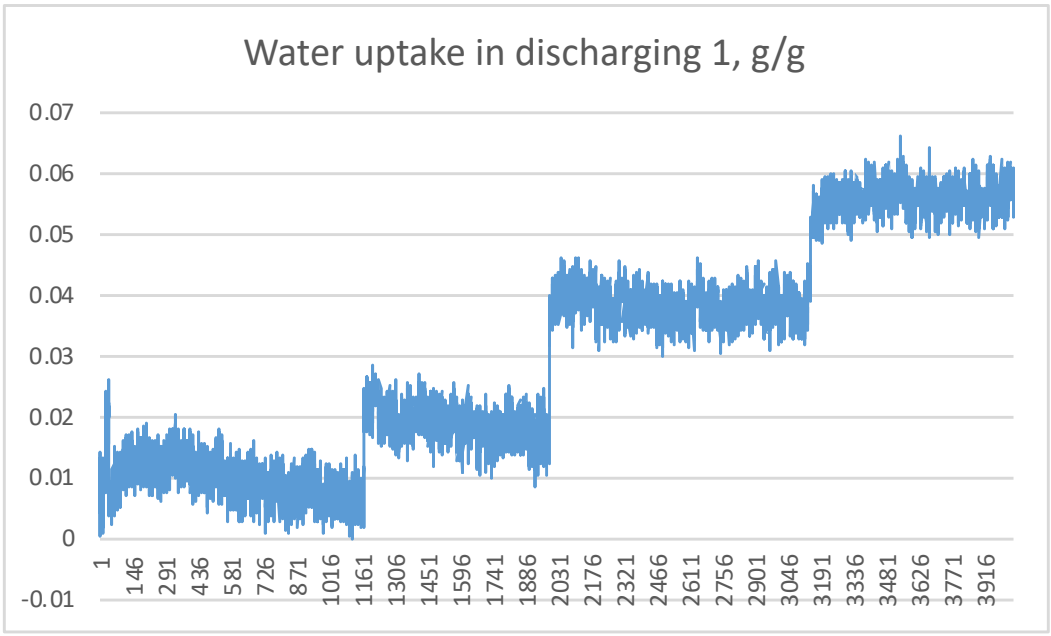


Figure 6-27 Water uptake in the 1st discharging process.

Charging process started at 10:51am and ends at 13:06pm at 90 °C for 2 hours. The initial weight was 635g. After 2 hours drying, the weight was 610g with 25g water loss (see Figure 6-28). In SDT-Q600 test in Chapter 4, we know that the V-MgSO4-CaCl2 has a very low regeneration temperature at 63 °C, this characteristic allows a faster charging process than other composites.

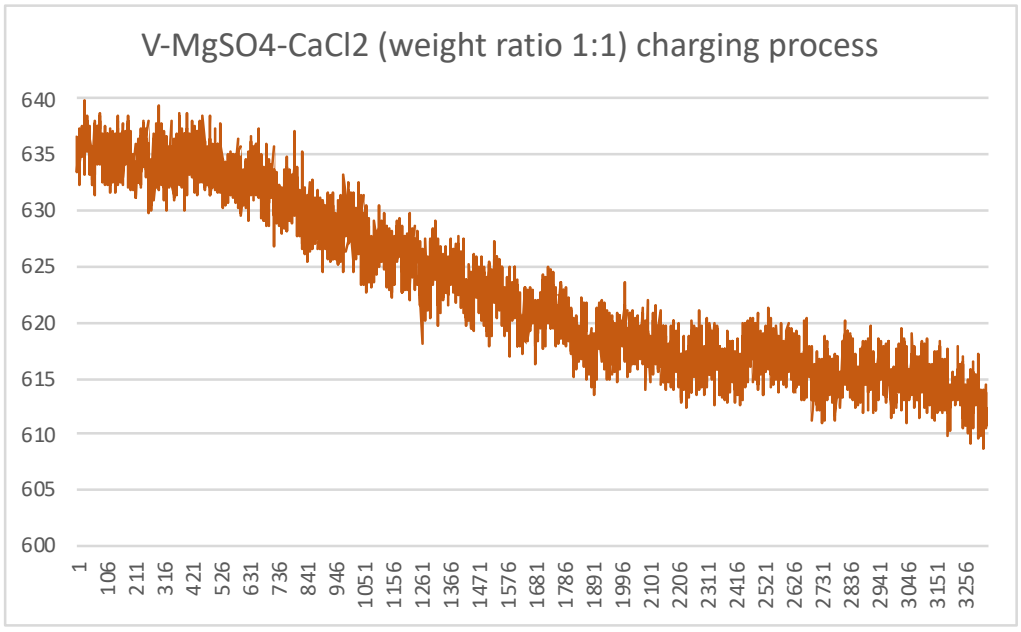


Figure 6-28 V-$MgSO_4$-$CaCl_2$ (weight ratio 1:1) weight change in the charging process.

Discharging 2 started at 13:55 and ended at 15:09 for 1 hour. The highest air outlet temperature increased to 35.5 °C in 18 minutes (see Figure 6-29). The weight changed from 610g to 659g with water uptake of 0.09g/g (see Figure 6-30 and Figure 6-31).

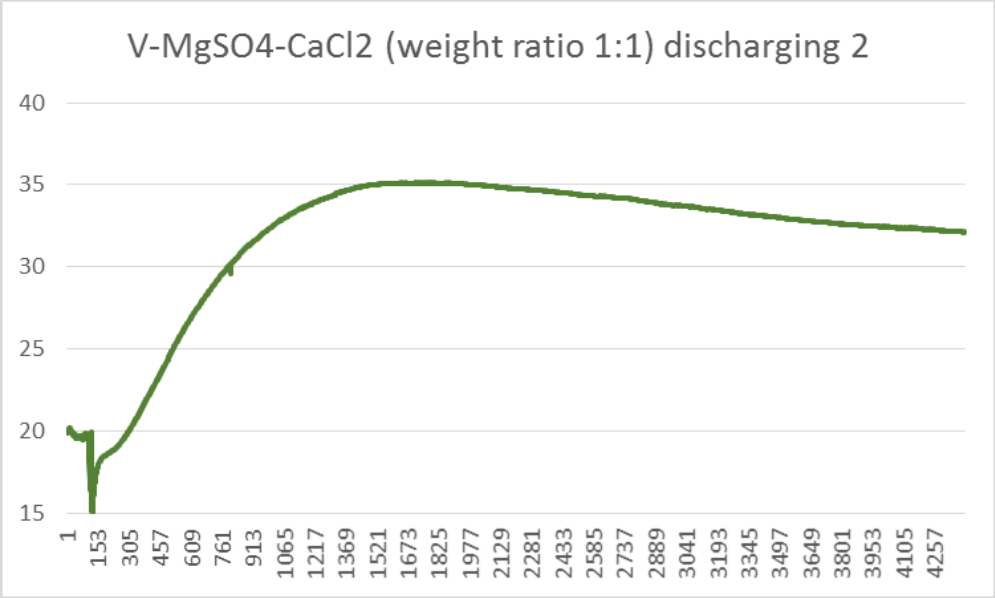


Figure 6-29 Temperature record of V-$MgSO_4$-$CaCl_2$ (weight ratio 1:1) in 2nd discharging process.

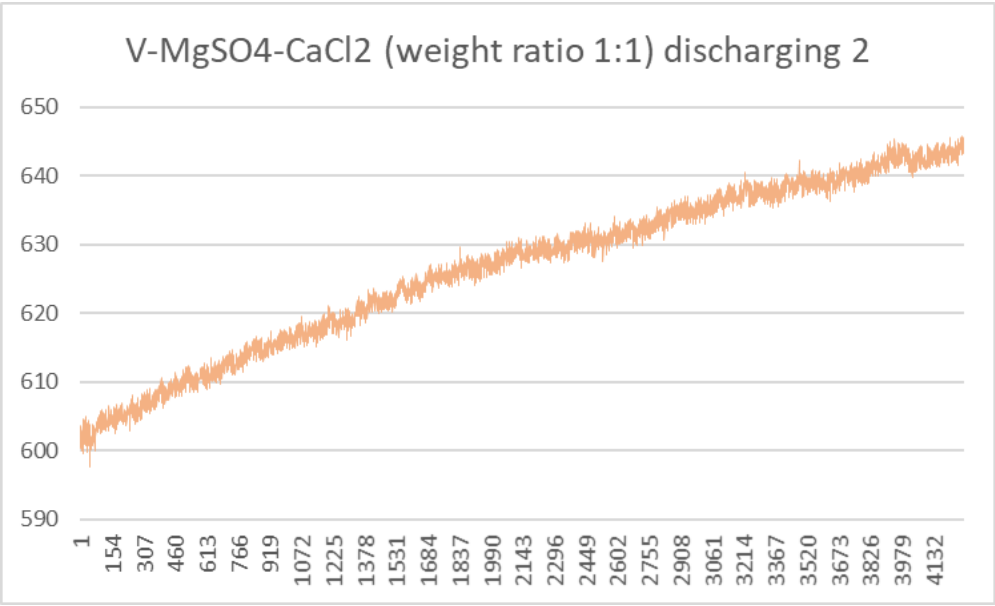


Figure 6-30 V-$MgSO_4$-$CaCl_2$ (weight ratio 1:1) weight change in the 2nd discharging process.

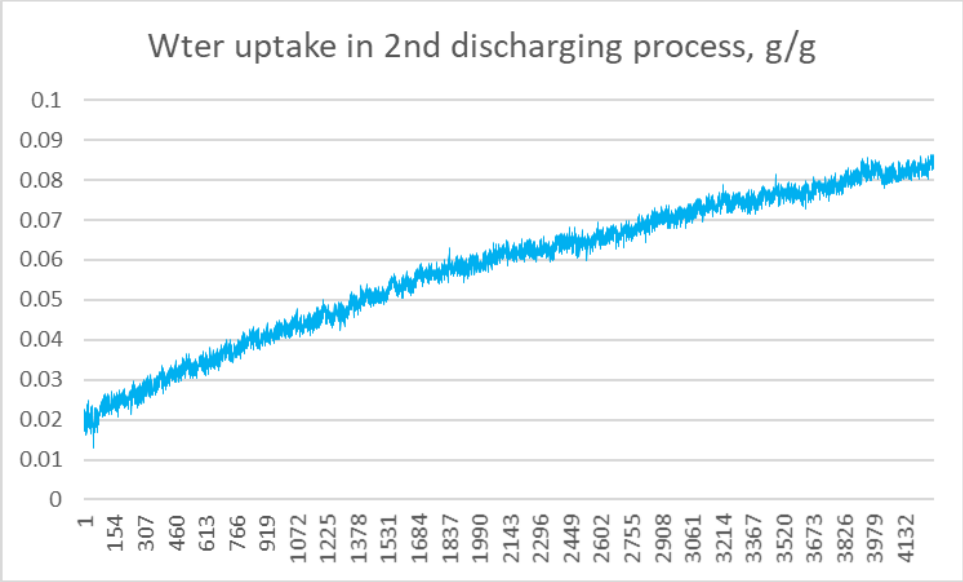


Figure 6-31 Water uptake in the 2nd discharging process.

6.4.4 V-$MgSO_4$-$CaCl_2$ (weight ratio 1:2)

Discharging 1 started at 11:22am, mesh tray with materials were 600g, the 1st discharging process started at 11:22am and end at 13:38pm with the initial air inlet temperature was 20 °C. The weight was 644 after 1st discharging process (see Figure 6-32 and Figure 6-34). And the total water uptake was 44g (0.076g/g) (see Figure 6-35). Based on Figure 6-33, it can be seen easily the highest temperature increased to 41.2 °C in 16 minutes, which was much higher than other composites. The air outlet temperature took about 10 minutes to reach 40 °C and remained above 40 °C for 2 hours.



Figure 6-32 V-$MgSO_4$-$CaCl_2$ in the mesh tray after 1st discharging process.

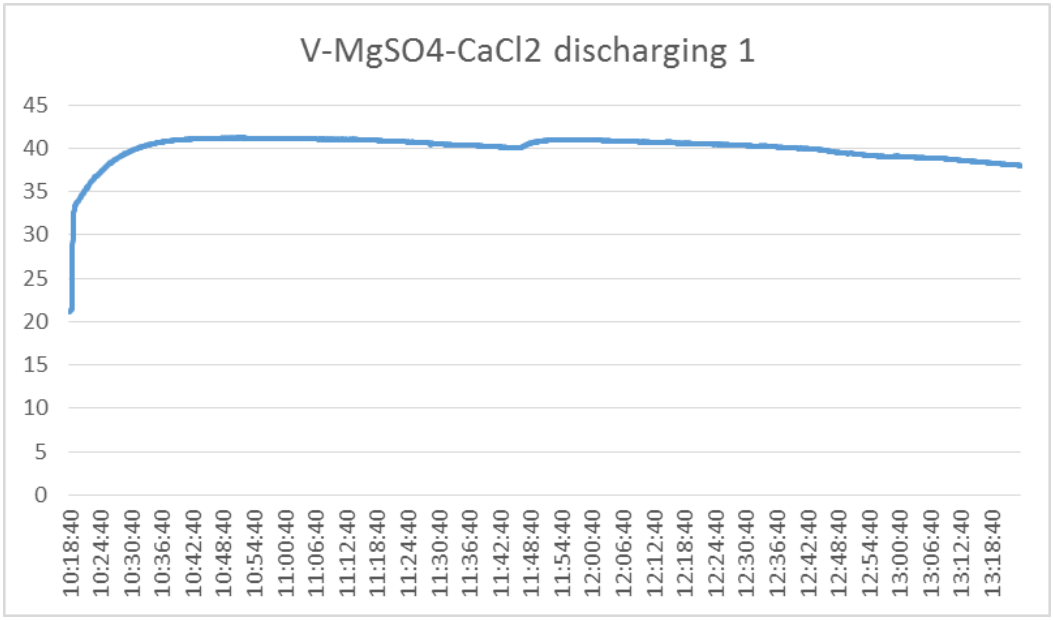


Figure 6-33 Temperature record of V-$MgSO_4$-$CaCl_2$ in 1st discharging process.

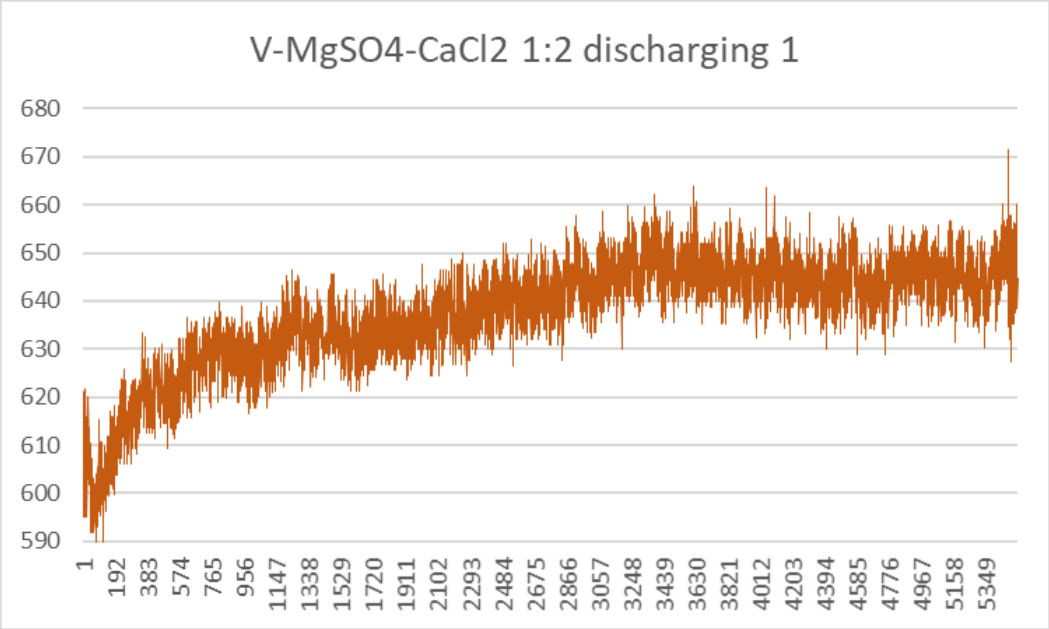


Figure 6-34 Weight changing record of V-MgSO4-CaCl2 in 1st discharging process.

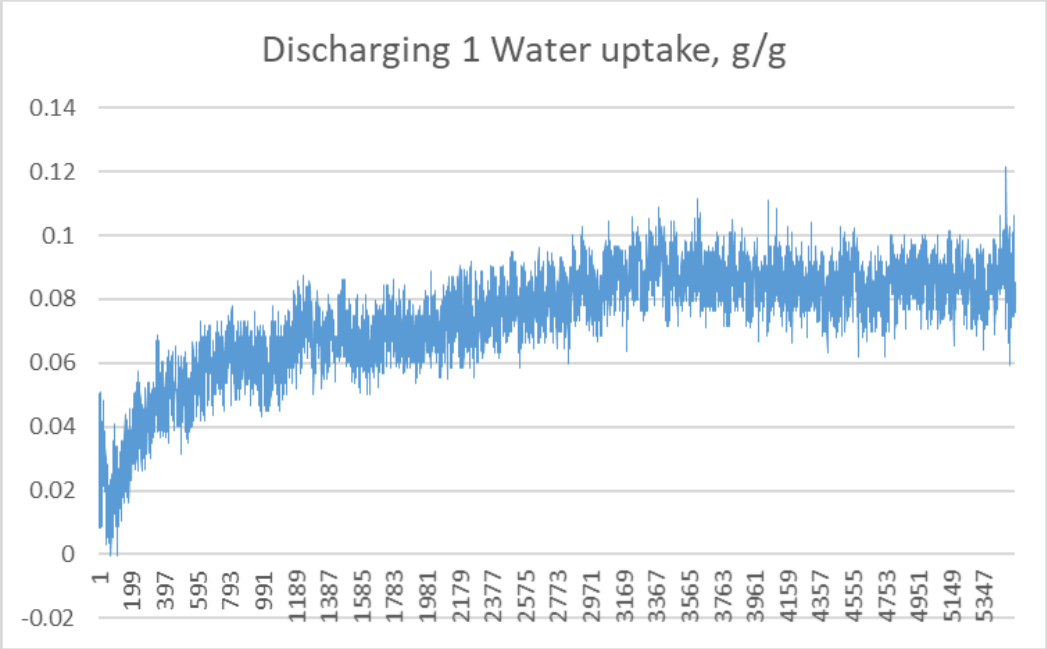


Figure 6-35 Water uptake of V-MgSO4-CaCl2 in 1st discharging process.

In the 2 hours charging process, air flow rate was 1.6m/s. Initial air flow temperature was 20 °C and charging temperature was 90 °C. The initial weight of the TES material was 644g. After drying for two hours the weight reduced to 611g (see Figure 6-36). The total water loss was 33g, which showed a very good regeneration performance.

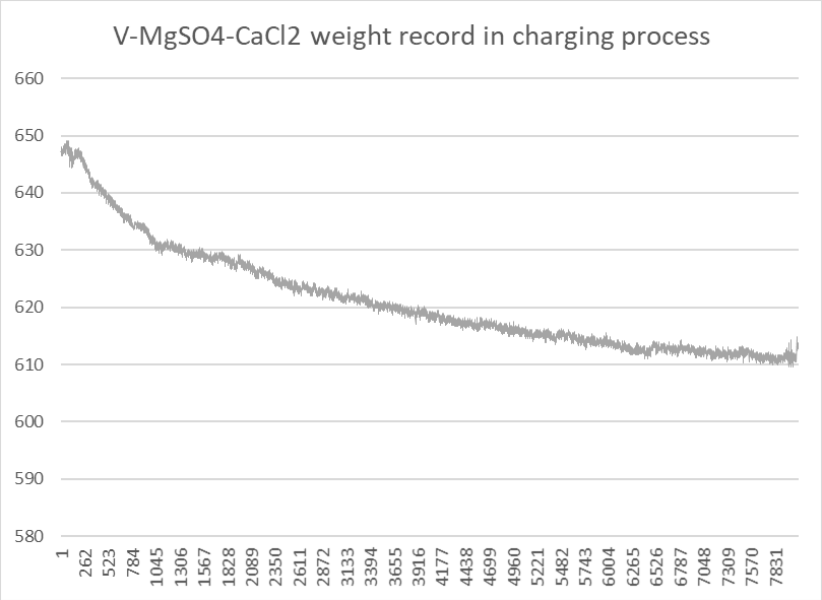


Figure 6-36 V-$MgSO_4$-$CaCl_2$ weight change in the charging process.

In the 2nd discharging process, the air outlet temperature reached peak at 46.1 °C in 15 minutes (see Figure 6-37). The highest temperature was 46.1 °C, which was higher than the 1st cycle. It took about 8 minutes to reach at 40 °C. It took about 14 minutes to reach at 45 °C and remained at above 45 °C for 20 minutes. This was the highest temperature provided by our tests TES materials. The air outlet temperature stayed above 40 °C for one hour and it remained above 35 °C for more than 2.5 hours.

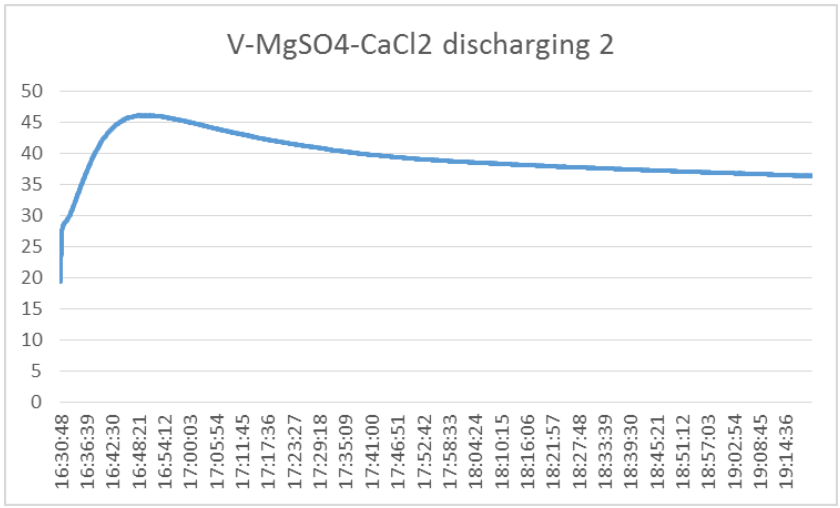


Figure 6-37 Temperature record of V-$MgSO_4$-$CaCl_2$ in 2nd discharging process.

In the 2nd discharging cycle, the process period was lasted for more than two hours, so the total water uptake was about 78g (0.137g/g) (see Figure 6-38 and Figure 6-39). Because in other materials test, the 2nd discharging process was 1 hour, hence, by the end of the 1st hour, the water uptake was 651g (0.07g/g), which means that the sorption ability was still high, and the material was suitable for reused.

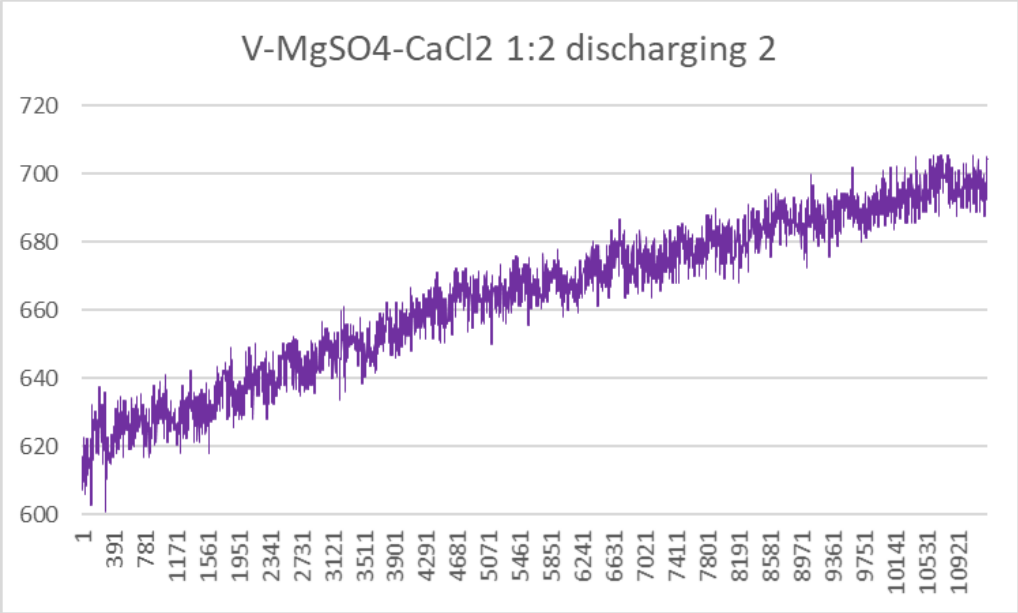


Figure 6-38 V-MgSO4-$CaCl_2$ water uptake change with times in the 2nd discharging process.

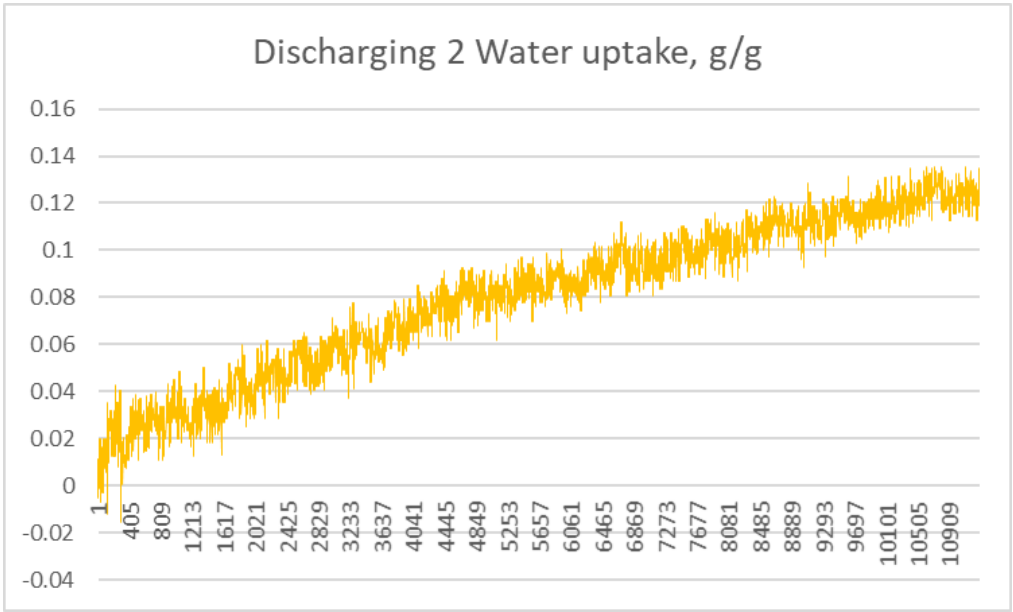


Figure 6-39 V-MgSO4-$CaCl_2$ water uptake change with times in the 2nd discharging process.

6.5 CALIBRATION

Two load cells should be calibrated before taking testing. In this calibration, 5 different mass were used on the LoadCell (0g, 23g, 25g, 58g and 80g).

Table 6-1 Thermochemical energy storage test rig calibration.

	Real weight, g	***LoadCell 1, g***	***LoadCell 2, g***
Calibration 1	0	-0.04	0.29
Calibration 2	23	-0.08	0.26
Calibration 3	25	-0.08	0.26
Calibration 4	58	-0.12	0.21
Calibration 5	80	-0.15	0.19
Formula	**X: load cell reading; Y: real number.**	**-719x-31.43=y**	**227.494-789.05x=y**

6.6 ANALYSIS

A number of thermochemical energy storage (TES) salts and matrix were chosen for an open loop THS system. These materials store energy by being dehydrated and release that energy when rehydrated. TES materials (Exothermic materials for heating and endothermic materials for cooling) are adsorbent/desiccant in the system.

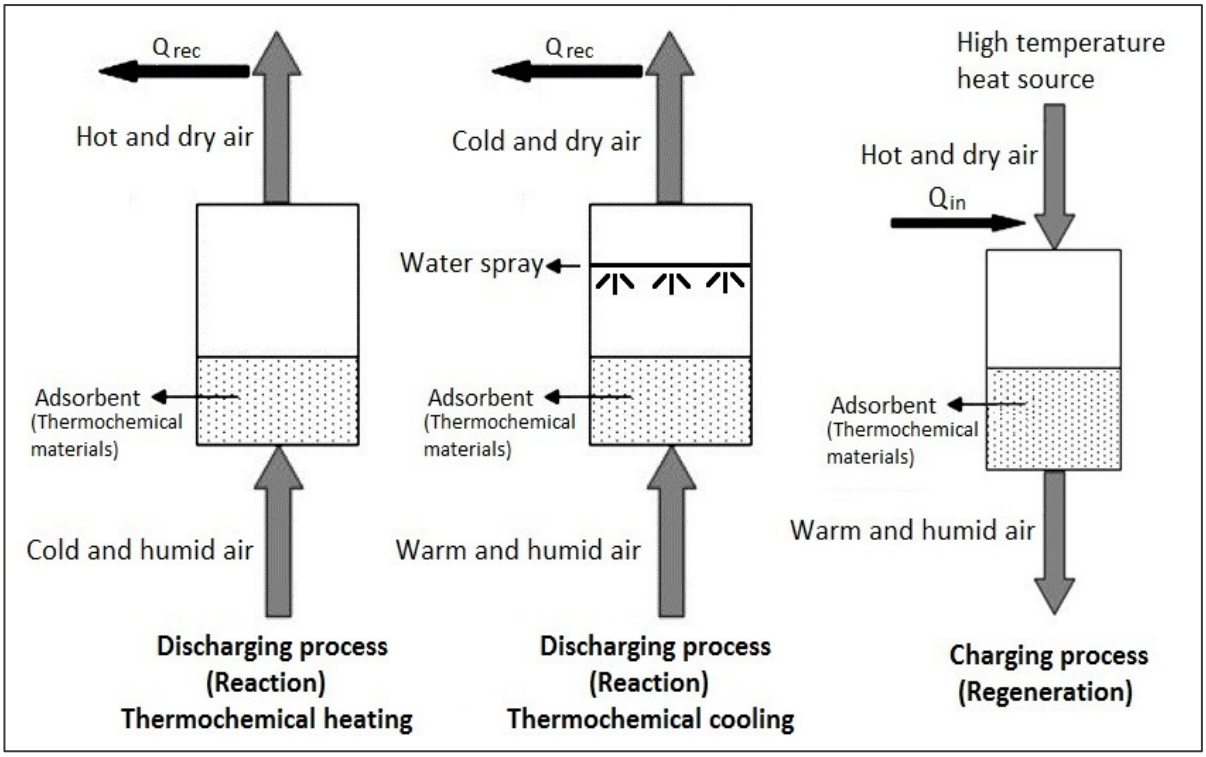


Figure 6-40 Charging and discharging process in open thermochemical energy storage system.

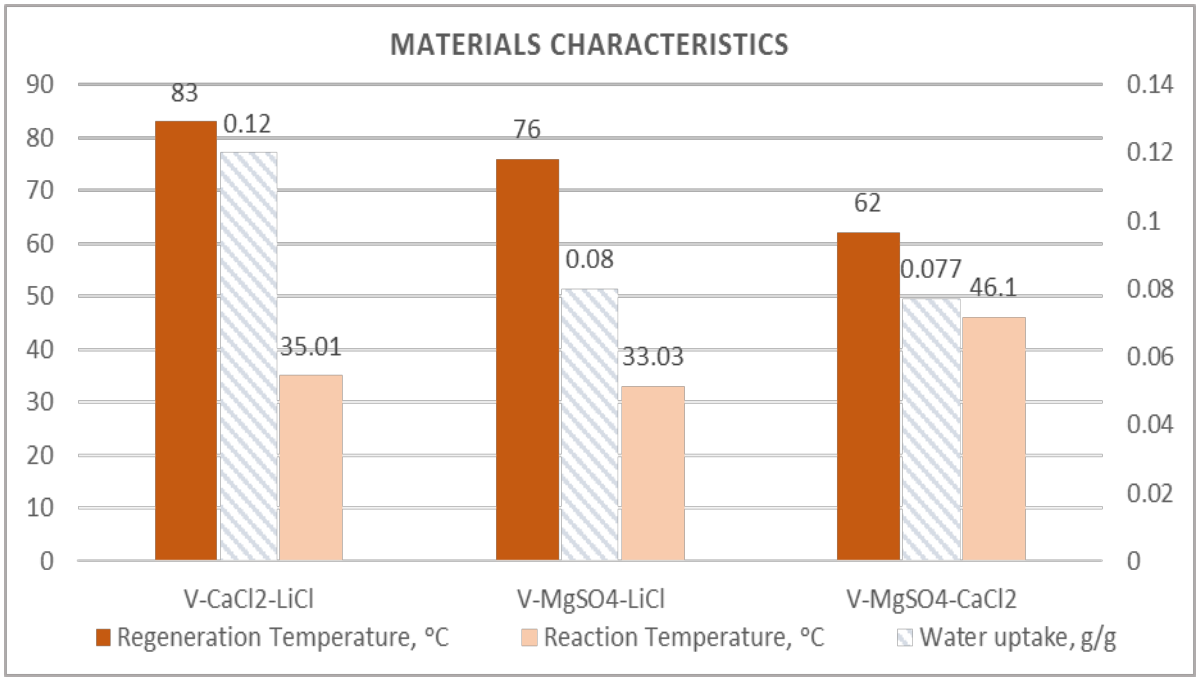


Figure 6-41 Different materials characteristics.

Chemical reaction (Hydration reaction):

$CaCl_2 + 6H_2O \rightarrow CaCl_2 \cdot 6H_2O + Heat$

$LiCl + 5H_2O \rightarrow LiCl{\cdot}5H_2O + Heat$

$MgSO_4 + 7H_2O \rightarrow MgSO_4{\cdot}7H_2O + Heat$

Thermal power and efficiency:

$P_{aver} = Q_{out}/\Delta T$

$\eta = P_{aver}/P_{store}$

$$COP = \frac{\text{Useful heat production}}{\text{Heat consumption}} = \frac{Q_{out}}{Q_{in}}$$

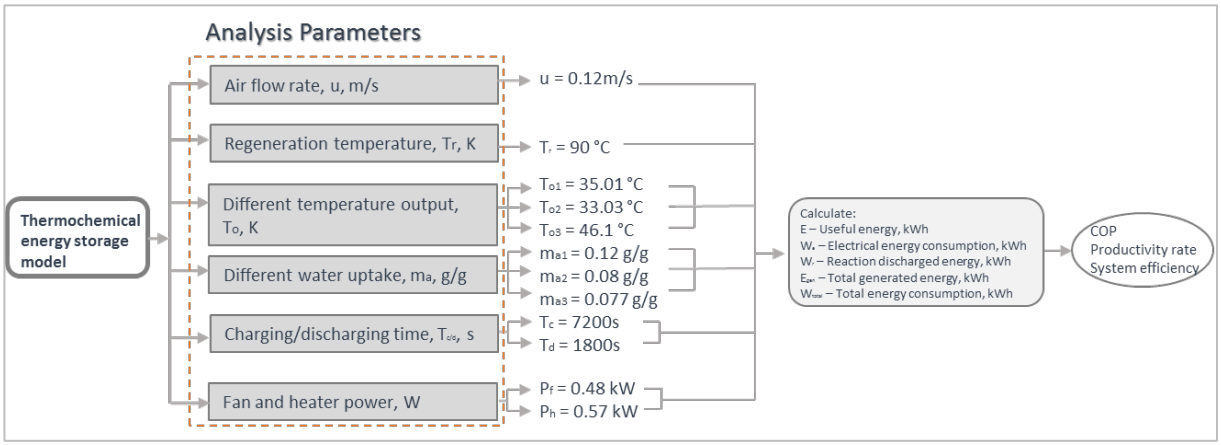


Figure 6-42 Flow chart of numerical model illustrating the analysis parameter.

Coefficient of performance (COP) of this TES model system is a ratio of useful heating provided to work required.

$$COP = \frac{useful\ energy}{electrical\ energy\ consumption}$$

Productivity rate (PR) of this TES model system is a ratio of the useful heating provided to the reaction discharged energy.

$$PR = \frac{useful\ energy}{Reaction\ discharged\ energy}$$

System efficiency (η) is a ratio of the total generated energy to the total energy consumption.

$$\eta = \frac{Total\ generated\ energy}{Total\ energy\ consumption}$$

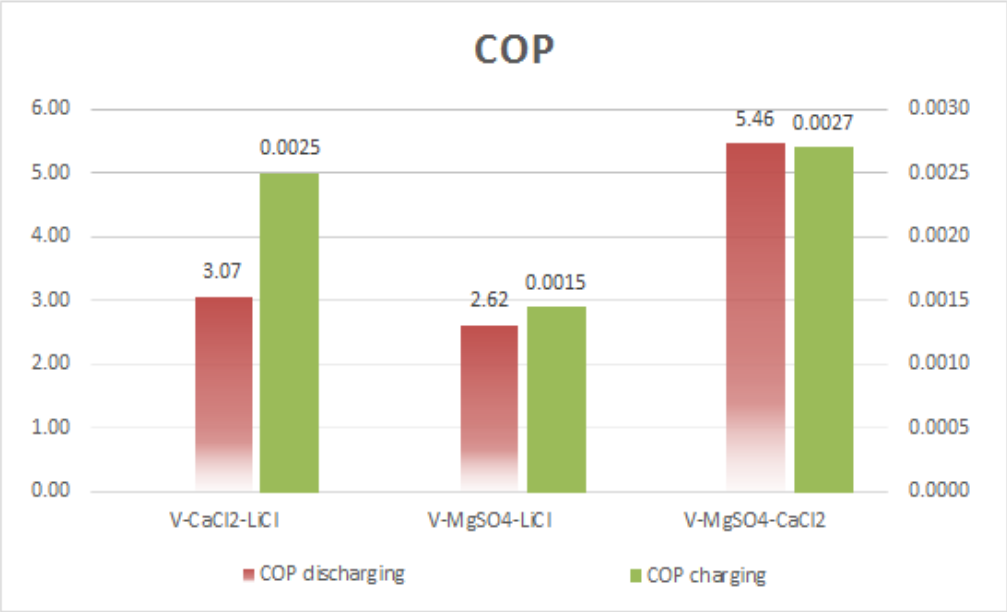


Figure 6-43 Discharging and charging COP of each material.

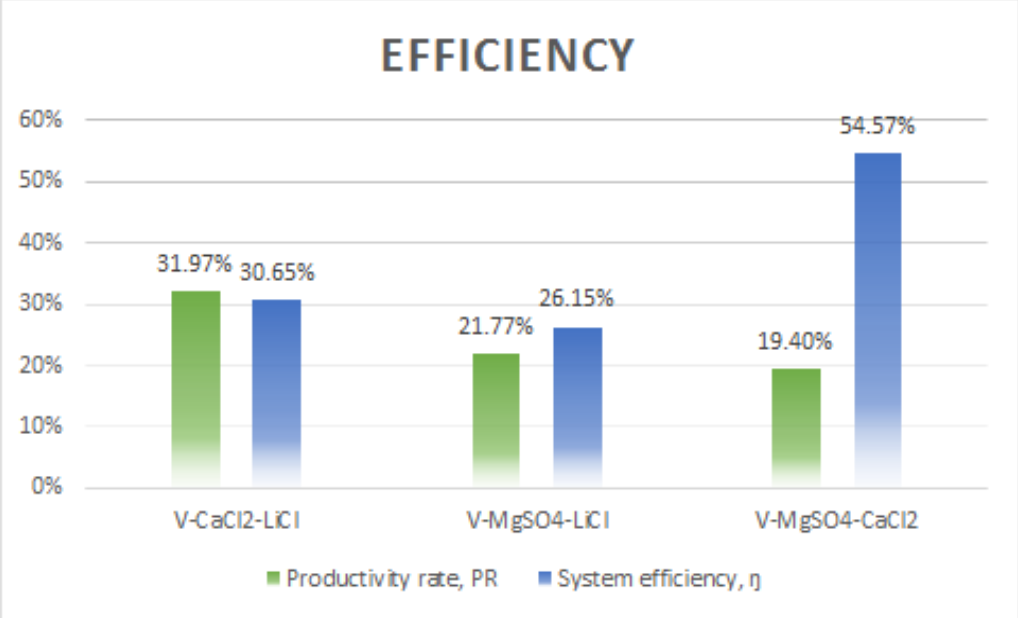


Figure 6-44 Productivity rate and system efficiency with different materials.

6.7 SUMMARY

V-$MgSO_4$-$CaCl_2$ had the highest energy density (1173.5kJ/kg) and the lowest regeneration temperature (63 °C). These two characteristics are the most crucial property required from the samples, it shows good potential for use in open THS systems.

V-$CaCl_2$-LiCl had the highest water uptake 0.12g/g whilst the other two had similar 0.08g/g. However, lowest regeneration temperature is an important characteristic, and also by considering reaction temperature, V-$MgSO_4$-$CaCl_2$ shows good potential for use in open THS systems.

Water uptake in this testing was very small because the mesh tray and reaction body did not seal properly. In the next step when we have the big test in the prototype, we fixed the issue to make sure moisture air can pass through all the testing materials.

Salt impregnation increased the bulk density.

V-$CaCl_2$-LiCl display higher water uptake than V-$MgSO_4$-$CaCl_2$, but the higher regeneration temperature was not the expected.

However, continuous long time is needed to have the rig test due to a longer time for discharging and charging process required. It will be improved in the next step test in prototype.

7 THE PROTOTYPE OF AN OPEN CYCLE FOR THERMOCHEMICAL HEAT STORAGE SYSTEM

7.1 INTRODUCTION

In current years, more than 40% of energy consumption occurred in building system with 36% of greenhouse gas emissions. In the UK, a major of 63% energy end-use for space heating/cooling for a comfort building condition. Energy comes is to store generated energy at early time for later use. It comes in multiple forms, such as chemical energy, electrical potential energy, gravitation potential energy, radiation, latent heat and kinetic power. We got lots of solar energy in summer or at daytime, but we need more heating in winter or at night. An average house uses 20,000 kWh of energy for hot water and space heating a year, of which 16,000 kWh (i.e. 80%) is for space heating and 4,000 kWh is for hot water heating. Developing smart and integrated energy systems is crucial to transforming the UK local energy system to meet carbon reduction targets and achieve clean growth ambitions. That's the reason why we need an energy storage system. Thermochemical energy storage (TES) can be a promising advanced technology in addressing massive energy use for heating and cooling in building application. System can be an alternative to the conventional energy system because of the lower heat loss, higher energy density of the materials, more efficient and environmentally friendly, and offers an opportunity to deliver annual building heating requirement from energy captured on site. In the last chapter, novel open system of thermochemical energy has been shown, and different high energy density storage salts (e.g. $CaCl_2$, $MgSO_4$, $LiNO_3$, and $MgCl_2$) with host matrix such as vermiculite and advanced carbon were used as thermochemical heat storage (THS) materials. The aim of this project is characterizing different composite to find better performing materials with higher energy density, lower heat loss, next

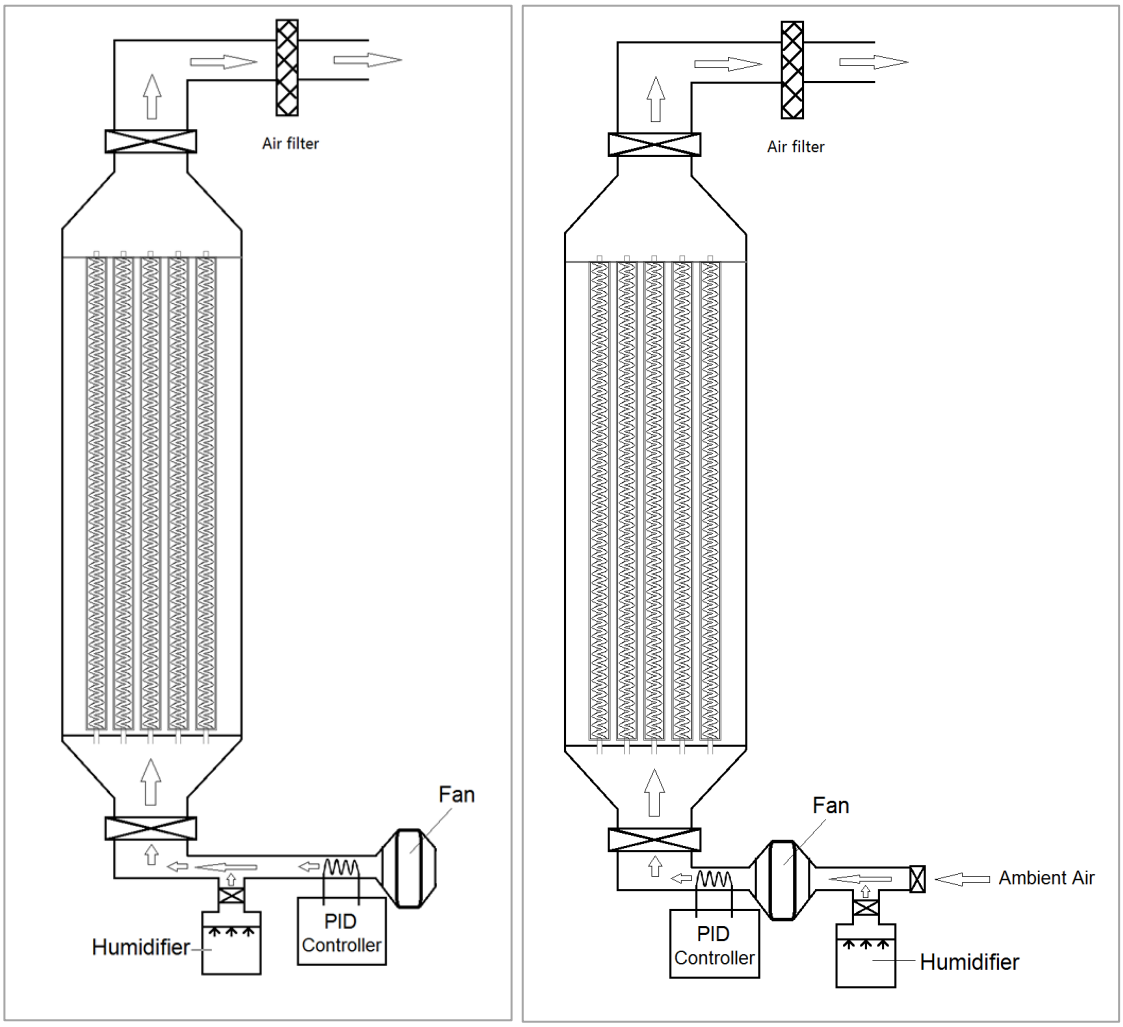
regeneration temperature, higher temperature lift in reaction process and higher system efficient.

In this project, an open thermochemical energy storage system was built for materials test which has been described in last chapter. This was a simple test rig in lab, we use a fan with heater as the low temperature heat source for regeneration. Humidifier used for moisture air supply. Thermochemical energy storage materials put in the drawer for testing and thermocouples were installed before and after the materials drawer to analyse temperature different. We have tested several composites and the basic chemical reactions are shown here to explain how it works. These salts impregnated composites materials are used as the TES materials, and the energy density were analysed to identify the optimal material. Some modification has been done on this result indicate that vermiculite-based composite with $MgSO_4$ and $CaCl_2$ as energy storage spices showed the best performance in the system and presented the optimal option. V-$MgSO_4$-$CaCl_2$ was selected because of its high energy density, low regeneration temperature and strong adhesion. And for the SEM photos, salts are attached with vermiculite and the salts solution can make a larger contact surface. That means it can absorb more moisture for reaction. These characteristics should be taken into consideration when we choose good thermochemical energy storage materials, such as high energy density, low regeneration temperature and high moisture uptake. In the TES materials test, because there is some gap between the material drawer and reaction body, moisture cannot go throw the materials completely, that's why we have a lower water uptake.

In the real prototype, we have fixed the issue. Figure 7-1(a) shows the designed prototype system which was tested in lab under real climatic conditions. A novel tube with fins heat exchange system is proposed for the TES system to solve the issue of

contact reaction of moisture air and the TES materials. The TES tank (reaction body) contains composite TES material granules distributed between fins on the tube, which serves as the embedded heat exchanger for internal heating/cooling. Compared with other conventional heat exchangers, the fins heat exchangers lead to significantly increased surface area and heat transfer. The fins on the mesh tube can increase the contact surface between materials and air to improve the charging and discharging efficiency.

In the charging process, fan and heater will provide hot air (90 °C) to the TES materials in reaction tank to dry/regenerate TES materials inside. Dry hot air was provided to the reaction body through mesh tube to the TES materials. The outlet humid air from TES reaction body will be released. (In the future work, we will reuse this part of heat for waste heat recovery system.) In the test of the modified prototype, I changed the place of humidifier and the fan to increase the inlet humidity level to 90%RH (see Figure 7-1(b)). And the modified prototype offers a higher accuracy and efficiency than the 1st one. In the reaction process, the fan will extract moisture air and blow into the reaction body to supply a stable humid air at a continuous relative humidity level of 90% for the TES materials. In the next stage, we will modify the new prototype to use as TES cooling supply system with solar driven.



(a) (b)

Figure 7-1 (a)The detail of TES open cycle prototype; (b) the detail of modified TES open cycle prototype

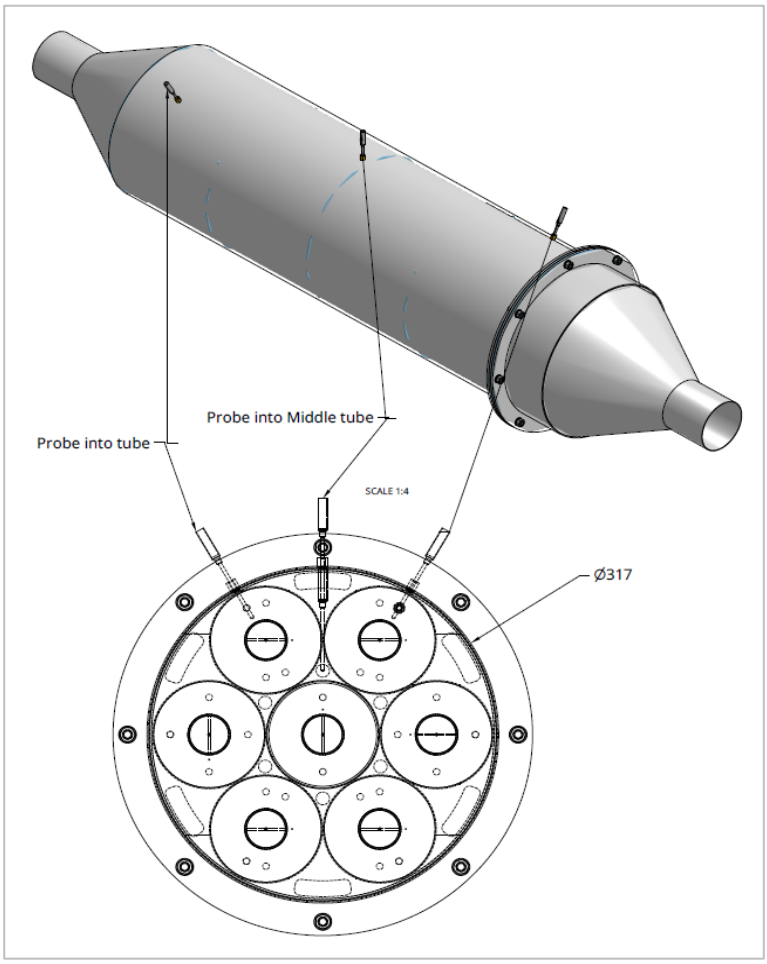


Figure 7-2 The reaction chamber and the holding plate.

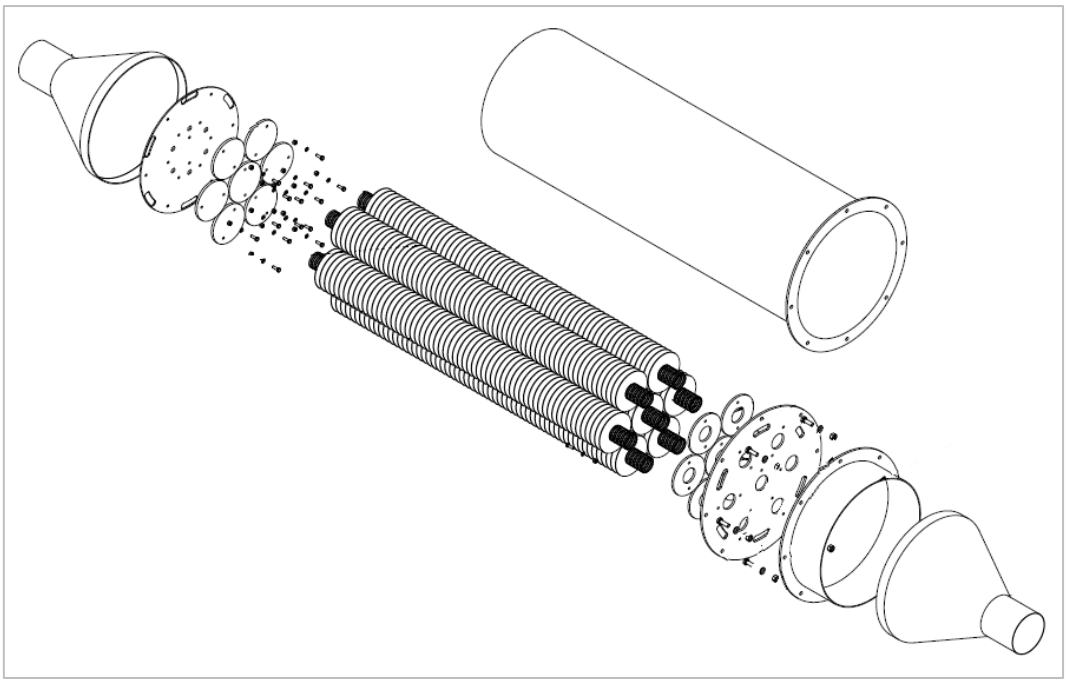


Figure 7-3 The inside detail of the prototype.

7.2 Experiment Designs for the Prototype of Open Thermochemical Heat Storage System

The energy storage capacity of ideal material and prototype level was tested under typical operating conditions of daily and seasonal heat storage cycles. According to the system characteristics (ref: Experimental characterization of the LiCl/vermiculite composite for sorption heat storage applications), the cycle defined as seasonal storage can be considered applicable for the cold winter, so that the heating demand can be stored by the excess of solar energy in summer. Moreover, the system can also work as daily energy storage system in winter in where the solar energy is intense enough to be stored during daytime and used for space heating at night. The daily storage system can be used in areas at warm climate.

7.2.1 Experiment rig set-up

This test rig system is consisted of the aluminium reactor, an air blower, a heat exchanger, an air humidifier, aluminium pipes and humidity and thermocouple sensors (see Figure 7-4). The main purpose was to test the selected materials for thermochemical energy system and analyse what materials prove to yield best results. The materials tested in the 1st step included vermiculate based composites with different salts (SIM): MgSO4-LiCl, $MgSO_4$-$CaCl_2$, and $CaCl_2$-LiCl. Each testing consisted of discharging and charging measuring. V-$MgSO_4$-$CaCl_2$ was selected as the best thermochemical heat storage material for the testing in the prototype. Some parameters of the vermiculite based mixture was shown in the Table 5-7.

A vertical cylinder tank was used as the reaction body, a fan with heater used for providing warm air (90 °C) in regeneration process. A proportional–integral–derivative controller (PID controller) was installed after the fan heater to control the

hot air temperature in case of overheating. A humidifier supplied moisture air for reaction during discharging process. Seven tubes with fins were installed inside the reaction body, all the materials (16kg) were filled inside the fins, there were many holes on the tubes to let the moisture air go through the tube and release to the materials. Moisture air went through the materials and exhausted through the air outlet tube.

In the discharging process, moisture air (90%RH, and air flow rate was 1.6m/s) was blew into the reaction body and through the TES materials from bottom to top. TES materials (V-$MgSO_4$-$CaCl_2$) absorbed moisture and dried the inlet air and released heat at the same time. Warm and dried air was supplied for space heating. In charging process, the heater was used as a low temperature heat source (90 °C) as the regeneration temperature of V-$MgSO_4$-$CaCl_2$ was 63 °C. The inlet air flow rate was the same as it was in discharging process. Warm and dried air was blowing to the reaction body to dry/regenerate TES materials. Then the warm and humid air will be exhausted to outside room. (In future work, the heat release in regeneration process will be considered for waste heat recovery to save more energy.)

Chemical reaction (Hydration reaction):

$CaCl_2 + 6H_2O \rightarrow CaCl_2 \cdot 6H_2O + Heat$

$MgSO_4 + 7H_2O \rightarrow MgSO_4 \cdot 7H_2O + Heat$

The 16kg composite sorbent vermiculite-$MgSO_4$-$CaCl_2$ was synthesized using a wet impregnation method, combining the $MgSO_4$ and $CaCl_2$ saturated solutions with microporous vermiculite matrix. The status of the mixture of $MgSO_4$ and $CaCl_2$ saturated solution was semisolid. The sticky semisolid can better adhere to the porous of vermiculite. However, too much semisolid salts mixture may lead to large

crystallization when dried or in regeneration process because more salts may leak out from the pore of the host matrix. Moreover, much salts may cause the retardation of the sorption dynamics because of ‘blocking effect’.

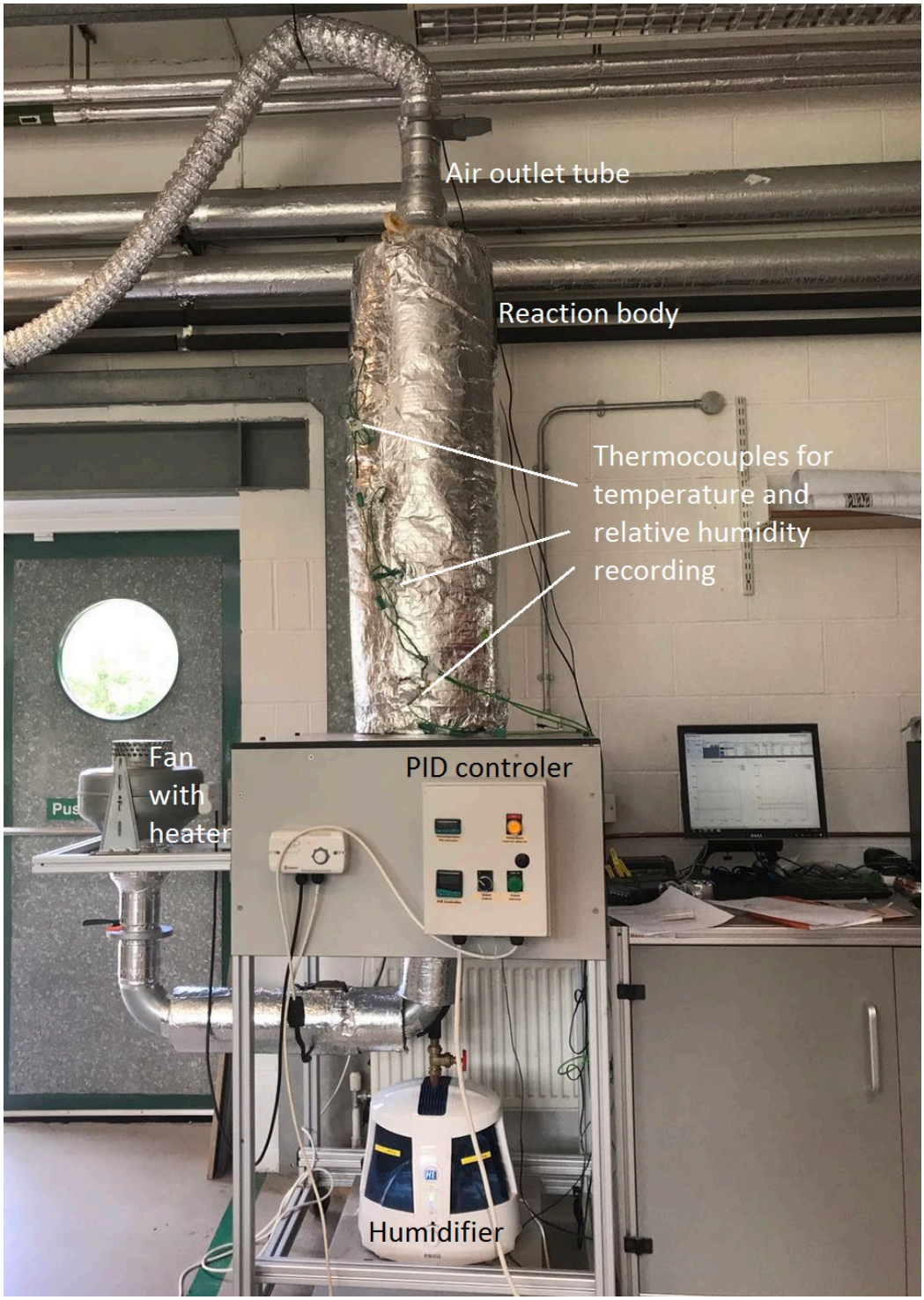


Figure 7-4 Open system for thermochemical energy storage materials test rig.

All the detail information of components of the test rig are shown below:

Table 7-1 Components information.

Components	Specifications	Purpose
Extract air Fan (diameter = 15 cm)	Air flow rate: 1.6 m/s Power: 470 W	For air inlet.
Humidifier	Power: 35 W	To provide moisture for the THS material.
Electrical heating element	505 W	To heat and dry the air before the reactor inlet
PID controller		To control charging temperature, which was 90ºC for this testing.
Thermocouple sensors		To monitor the temperature and relative humidity changing during the operation.
THS material	$MgSO_4$-$CaCl_2$, weight ratio is 1:2	Used for thermochemical energy storage to store energy inside as an energy storage media.
Aluminium (casing) reactor	Aluminium reactor with the well insulation	The reactor where discharging and charging occurs.

	Regeneration T: 90°C	
Pipes	Aluminium pipes with the well insulation	To direct the airflow and minimise heat losses.

7.2.2 Results and analysis

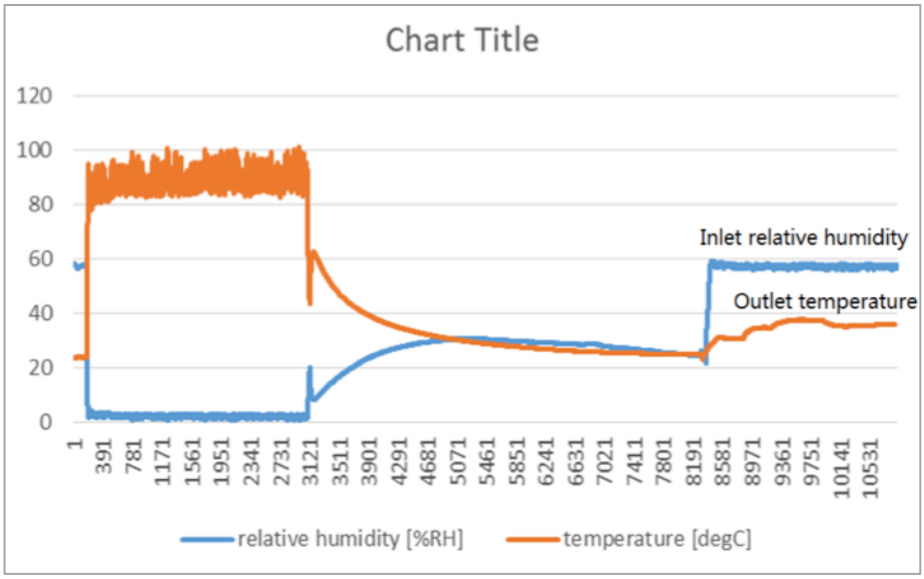


Figure 7-5 Temperature an relative humidity record in charging and discharging process of the prototype.

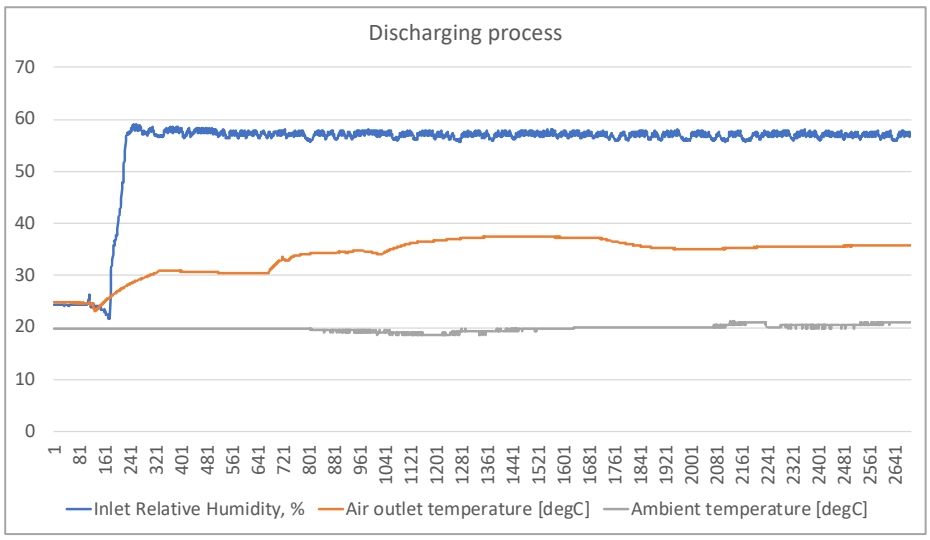


Figure 7-6 Air inlet relative humidity and air outlet temperature record.

According to the record readings, results showed that the V-MgSO4-CaCl2 temperature increased to the highest temperature at 37.44 °C after moisture supply in 22 minutes. And the temperature remained above 30 °C for 3 hours and 15 minutes (which didn't show a dropping temperature, so I assumed it can stay like that for quite a long time).

The fan velocity was 1.6 m/s, and the tube diameter was 0.14m (equals to $0.0154m^2$ * 1.6m/s * $1.29kg/m^3$ = 0.032kg/s, air density is $1.29kg/m^3$). The power of the fan was 470W and the heater power was 505W.

Specific heat capacity (Cp) of air is 1.006 kJ/kg°C.

Using heat transfer formula, for every second:

$$Qc = Cp * ma * \Delta T = m * Cp * (T_{outlet} - T_{ambient}) \qquad \text{Eq 4}$$

Qc = 1.006 kJ/kg°C * 0.032kg/s * ΔT

Total power input is P_T = Extract fan power input @ 1.6m/s + humidifier power input

The COP is the ratio of the generated heat to the total power input, the highest COP was 1.2 in this TES testing rig, the average COP was around 1.05 (Figure 7-7):

$$COP = \frac{Q_{useful}}{P_T} = \frac{m*Cp*(T_{outlet}-T_{ambient})}{P_{fan}+P_{humidifier}} \qquad \text{Eq 5}$$

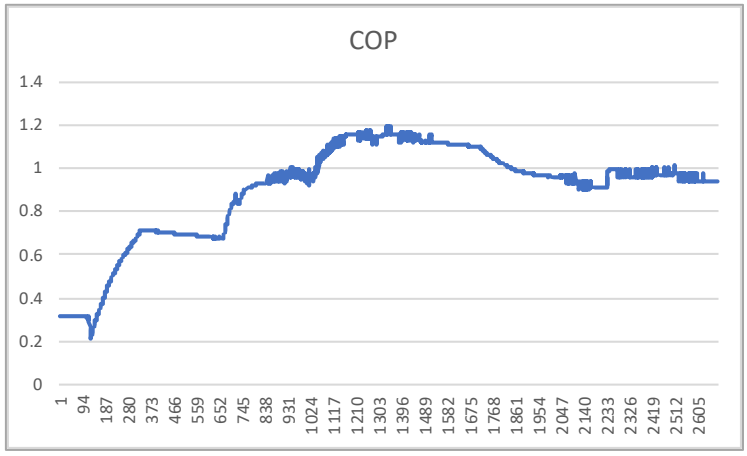


Figure 7-7 COP of discharging/reaction process.

7.2.3 Summary of the Real Prototype

The highest temperature was 37.44 °C, which did not reach the high temperature we expected (above 40 °C). Because the hole under the bottom of the reactor is too small that the moisture air cannot go through the rig completely, some of the moisture air escape from the gap of the humidifier, so the humidity level cannot reach 90%. In the next step, we will expend the hole to make them larger for the moisture air going through the tube to inject into the materials.

7.3 The Modified Prototype and the Result

7.3.1 The description of the modified prototype

The reaction body of the modified prototype rig is the same as the original one. But the humidifier of the new modified rig was placed in front of the extract fan to increase the relative humidity level in the reaction/discharging process (see Figure 7-8).

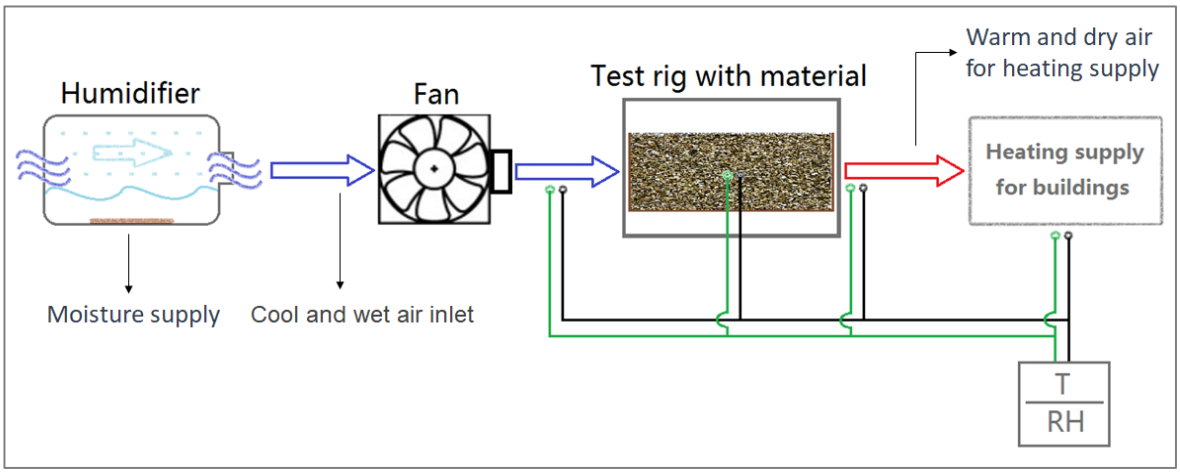


Figure 7-8 The modified prototype discharging process.

The new experimental cycle of the modified prototype was conducted at air flow rate of 1.6m/s (equals to 0.032kg/s, the air density is 1.29kg/m^3). The prototype was tested for two reaction cycles. In the desiccant chamber 16kg Vermiculite with $MgSO_4$-$CaCl_2$ (the ratio was 1:2, the same with the materials before rig modified) was

dried for 24 hours before test to make sure all the material was dried completely (90 °C air flow was blown into the reaction body until the outlet air relative humidity level was the same as the inlet air relative humidity level). Then all the tubes were closed to make sure there was no moisture absorbed, and the rig was cooled down for one day. During the experiments, the whole process was as followed: discharging process – charging process – discharging process.

In the discharging process, air is blown/extracted with a centrifugal fan and the air flow rate was adjusted with speed controller. Humidifier was placed in front of the extract fan to extract the front moisture and send it to the reactor. This was a very good way to increase the humidity level in the reaction chamber, compared with the original prototype. Blown moisture air was forced to pass through the TES materials (V-$MgSO_4$-$CaCl_2$) inside the chamber. The process continues till the outlet air temperature was the same with inlet air temperature. In charging/regeneration process, air blown into reaction chamber at a regeneration temperature of 90 °C, the TES material in the chamber started losing its absorbed moisture. And the charging process continues until the relative humidity level of the outlet air tended to be similar with the inlet air relative humidity. Then the prototype was cooled down for one day before another cycle discharging process. The humidifier, extract fan and heater were driven by electricity, which will be replaced by renewable energy source in the future work.

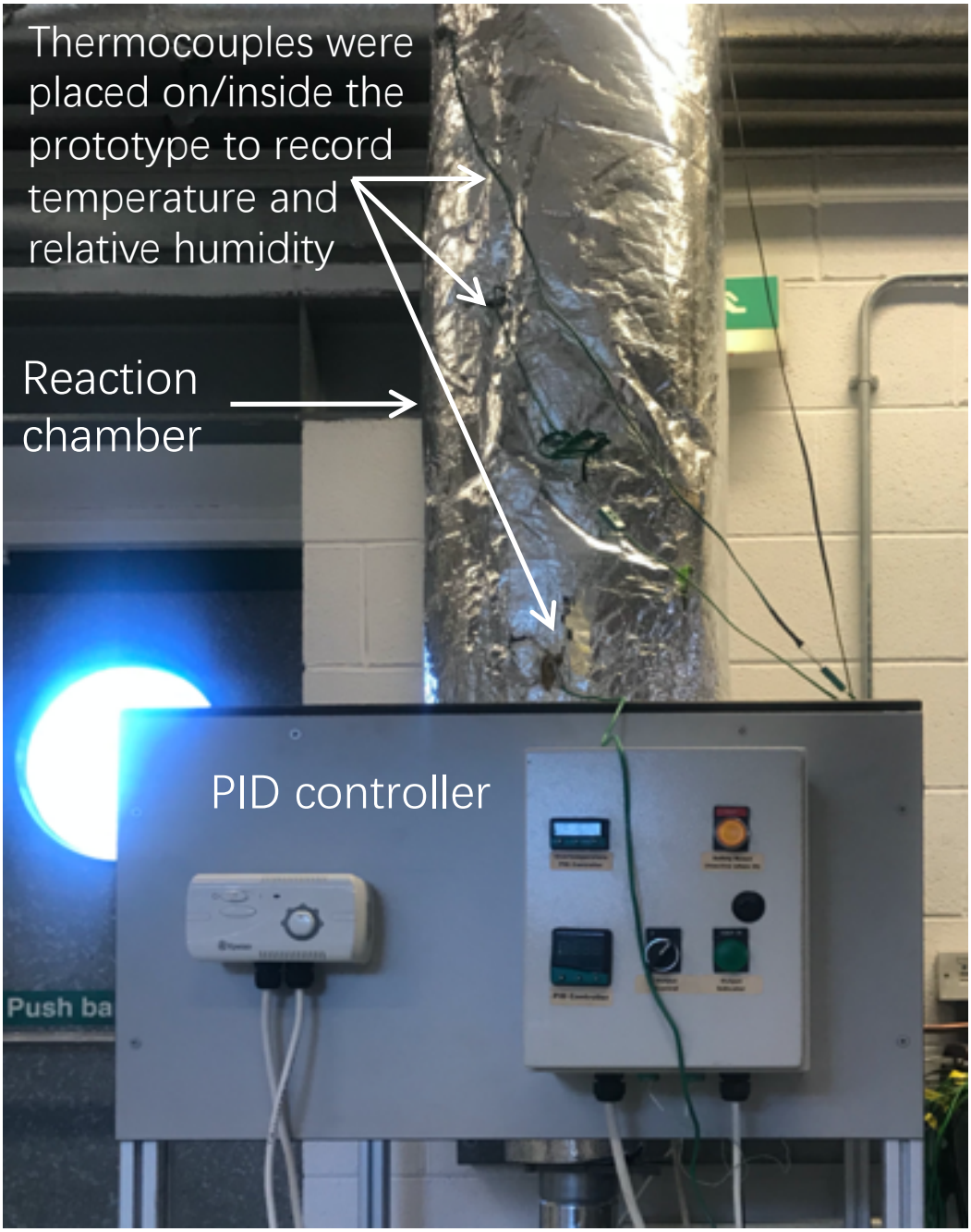


Figure 7-9 Modified prototype reaction chamber and PID controller.

The reaction chamber and PID controller stayed the same. The setting temperature for PID controller reduced a bit to make sure the inlet air temperature stayed at 90 °C because it was closer to the inlet tube after modified. The air flow rate was the same as 1.6m/s.



Figure 7-10 PID controller and two dataloggers (one for temperature record and one for relative humidifier record).

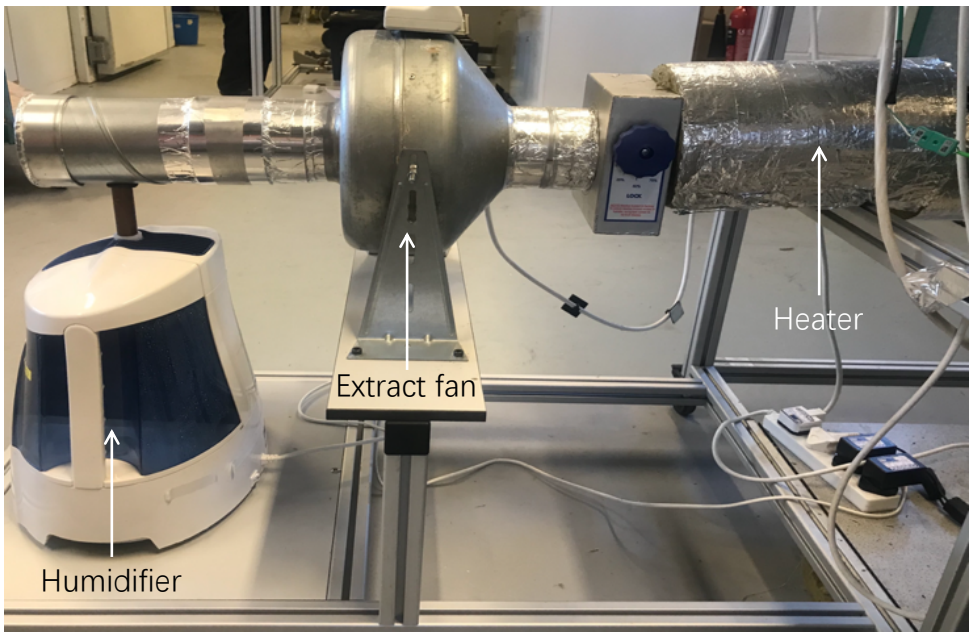


Figure 7-11 The modified components.

The centrifugal fan was placed after humidifier to extract moisture through the fan to increase inlet air relative humidity level to 90%. The system was run for twice before testing to confirm the inlet air relative humidity level can be lifted to the desired level.

7.3.2 Result and analysis

The temperature records of the discharging process tests of modified TES prototype were presented in Figure 7-12 and Figure 7-13, respectively. As it can be seen in Figure 7-12, the discharging process took 6.5 hours in total, due to the absorption

process of the TES materials in reaction chamber, the initial temperature increased quickly to 42.8 °C in 38 minutes, after that, the air outlet temperature showed a gradual drop over 6 hours. We assumed that 35 °C is a suitable temperature for air space heating system. The hot air supplying temperature stayed above 35 °C for 3 hours, and it stayed above 30 °C for 4 hours 10 minutes. According to Figure 7-13, the system air outlet temperature showed a sharp increase at the beginning, it reached the peak temperature at 43.1 °C in 45 minutes, then dropped slowly to room temperature in 5 hours. The heating supply temperature remained above 35 °C for 133 minutes and it stayed above 30 °C for 3 hours. In cycle 2, the heating output was less than cycle 1 because the charging process may not completely after the 1st reaction process. And also, another reason was because the air input temperature (ambient air temperature) was lower during the 2nd cycle discharging period, the ambient temperature (initial temperature) can affect the heat release temperature from the TES materials.

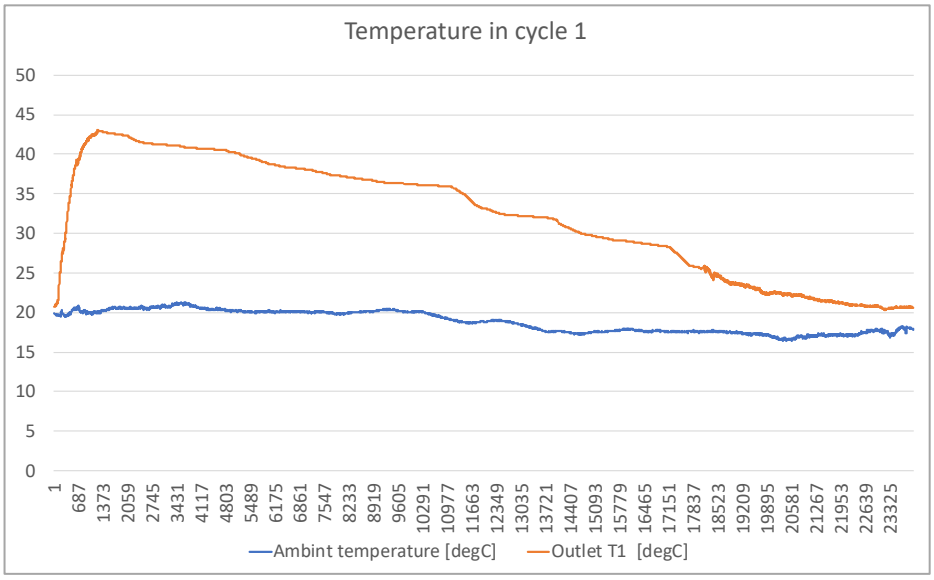


Figure 7-12 Temperature record for discharging process test in cycle 1.

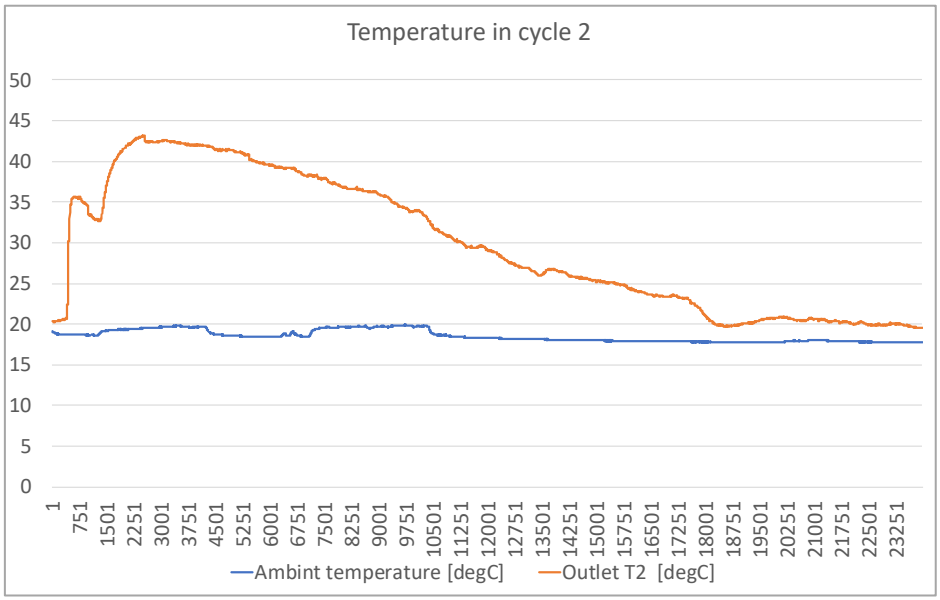


Figure 7-13 Temperature record for discharging process test in cycle 2.

The relative humidity level variation record in cycle 1 and 2 were shown in Figure 7-14 and Figure 7-15, respectively. Caused by the absorption process, the air outlet relative humidity level was increasing, however, because the TES materials were act as desiccant, the moisture was absorbed by the TES materials which led to a dry hot air supply (hot and dry air outlet). In the 1st cycle, the initial air outlet relative humidity was about 15%, and after 6.5 hours reaction/absorption process, it slightly increased to 20%, which was still lower than the ambient air relative humidity level (about 40%). In the 2nd reaction cycle, the initial air outlet relative humidity was 20.5% and after 6.5 hours processing, the air outlet relative humidity level grew to 27.5%. The initial air outlet relative humidity level was a little higher than it was in the 1st cycle, because TES material was not 100% dried in the charging/regeneration process after the 1st cycle reaction.

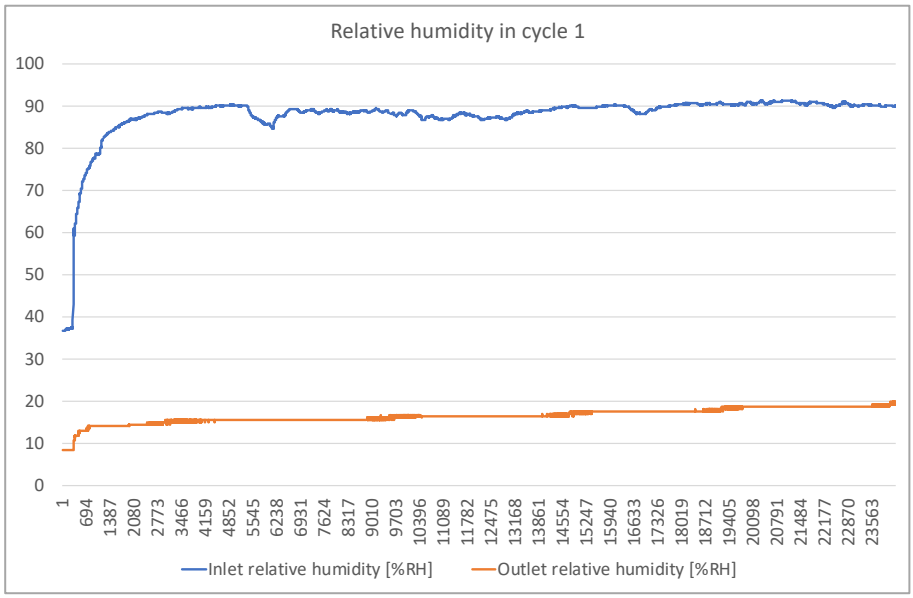


Figure 7-14 Air inlet and outlet relative humidity variation in cycle 1.

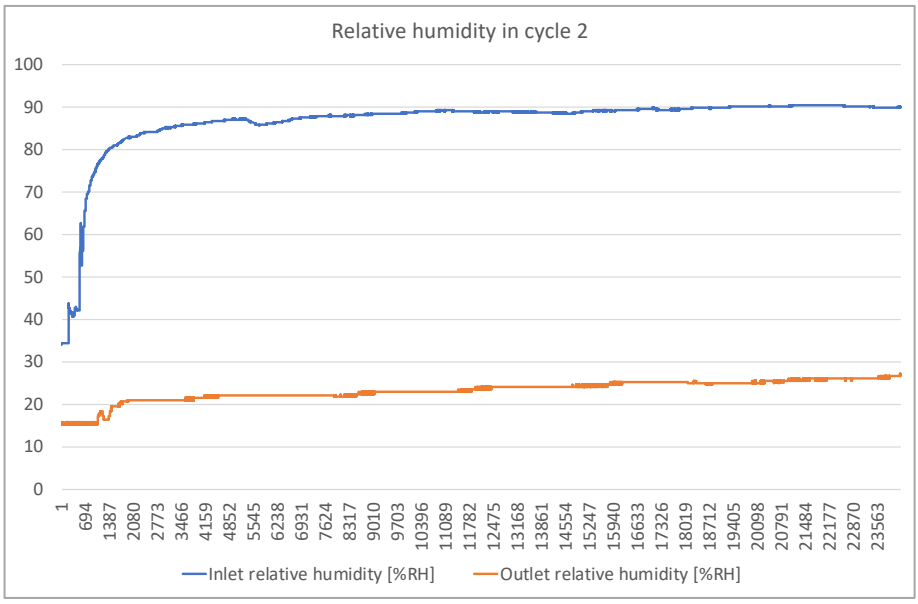


Figure 7-15 Air inlet and outlet relative humidity variation in cycle 2.

Water content is an important indicator for materials performance evaluation in the whole system. To calculate the TES material moisture content, the following formulas will be used, and the detail of water content in each cycle will be shown in Figure 7-16:

$$Ln(P_{ws}/P_c) = T_c/T \times (a_1 \times \vartheta + a_2 \times \vartheta^{1.5} + a_3 \times \vartheta^3 + a_4 \times \vartheta^{3.5} + a_5 \times \vartheta^4 + a_6 \times \vartheta^{7.5}) \quad \text{Eq 6}$$

— P_{ws} is saturated water vapor pressure, MPa;

— Pc is critical pressure equal to 22.064 MPa;

— T is the air inlet temperature, 256K (19 °C);

— Tc is critical temperature equal to 647.096 K;

— $\vartheta = (1 - T/T_c)$;

— $a_1 = -7.85951783$, $a_2 = 1.84408259$, $a_3 = -11.7866497$, $a_4 = 22.6807411$, $a_5 = -15.9618719$, $a_6 = 1.80122502$.

$$P_w = RH \times P_{ws}/100 \qquad \text{Eq 7}$$

— P_w is water vapor pressure, MPa;

— RH is relative humidity (%);

— P_{ws} is saturated water vapor pressure, MPa.

$$W, g/kg = 621.97 \times P_w/(P - P_w) \qquad \text{Eq 8}$$

— P_w is water vapor pressure, MPa;

— P is ambient pressure, MPa.

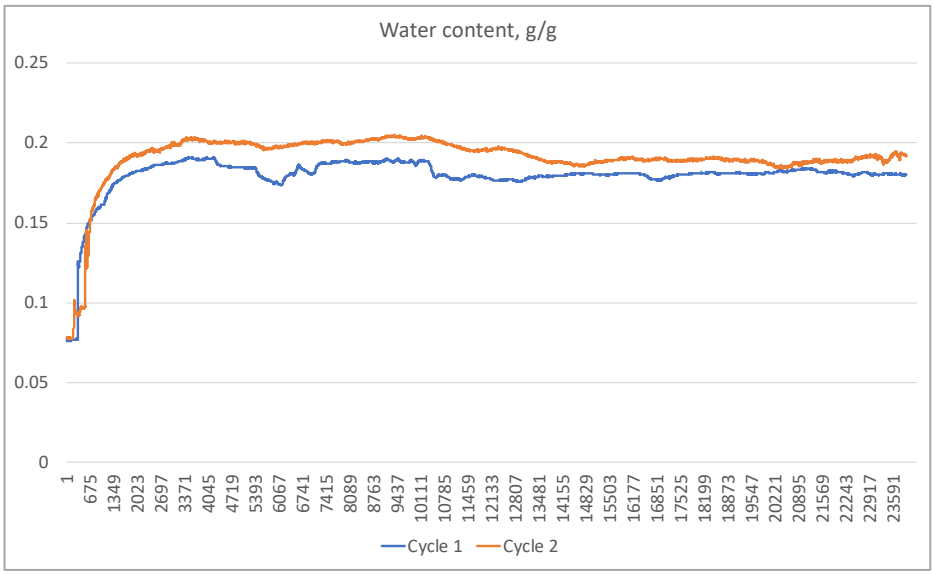


Figure 7-16 Water content in discharging process of cycle 1 and cycle 2.

Based on Figure 7-16, the water content range of cycle 1 was 0.18-0.21, and it was 0.155-0.186 in the 2nd cycle. Compared with the sorption testing result in Chapter 4, the result of modified prototype is very similar with the one in sorption testing. And also, the water content in 2nd cycle was less than the one in the 1st cycle because the charging process was not completely, and the ambient temperature was lower than it was in the 1st cycle.

The air mass flow rate was 0.00162 kg/s, it was the same as the original prototype. So, it equals to 4.5m^3/hour. The power of the fan was the same as 470W. The specific heat capacity (Cp) of air is 1.006 kJ/kg°C.

Using heat transfer formula, for every second: $Qc = Cp*ma*\Delta T$

The total reaction/discharging process took 6.5 hours (23400 seconds).

In Figure 7-17, COP of the prototype in discharging process was calculated as the useful heating release (Q_{useful}) to the total electrical power consumption (fan and humidifier, P_T = 505W in total). The highest COP value of cycle 1 was about 1.48 and the it was 1.51 in the 2nd cycle. The COP value was reducing as the heating supply temperature dropping. In the tests, the ambient temperature variation and the system heat loss will affect the COP and system efficiency.

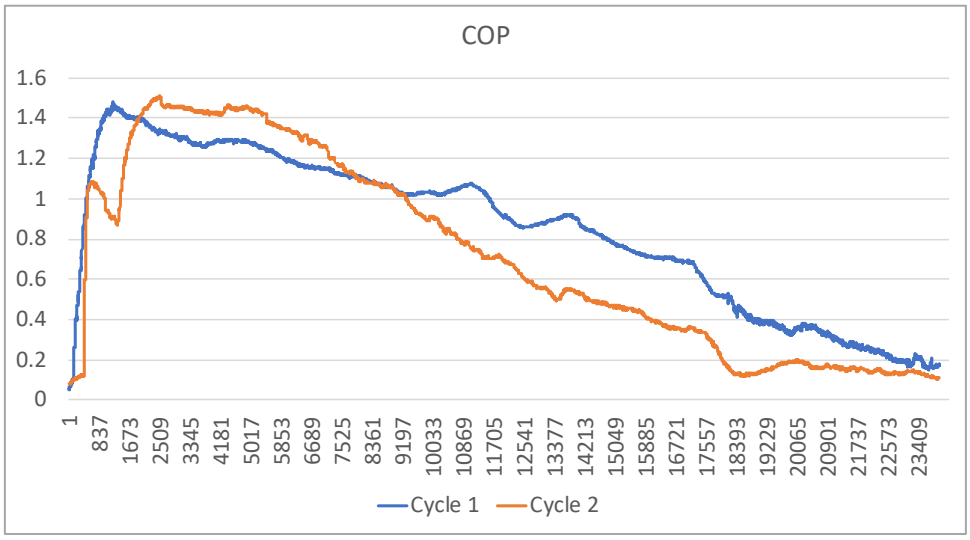


Figure 7-17 COP variations in each discharging cycle.

Some parameter performances have been worked out (see Table 7-2). The total stored energy was calculated as the sum of energy output. The overall COP of the system was worked out as the ration of total useful energy output to the total electricity consumption. The system efficiency was defined as the ratio of total stored energy to the theoretical stored energy (analysed by SDT-Q600, Chapter 4).

Table 7-2 Some parameter performance of the system.

	Cycle 1	Cycle 2
Stored energy, kWh	2.88	2.42
System overall COP	0.85	0.72
System efficiency, η	0.55	0.46

In the charging/regeneration process, 90 °C hot air was blown into the reaction chamber at an air flow rate of 1.6m/s. The initial relative humidity was about the same with ambient RH. System was supplied with a continuous hot air until the air outlet

relative humidity level tended to be similar with the air inlet relative humidity level. The whole charging process took about 6.6 hours. In the discharging process, the water content was about 0.18-0.2g/g, we assumed that the total water content of the 16 kg TES material was about 3.2kg. The approximate moisture flow rate was about 0.133g/s. According to the heat transfer formula and using data in Figure 7-18 to Figure 7-20, COP of charging process was worked out and shown in Figure 7-21, the system overall COP in charging/regeneration process was 0.021.

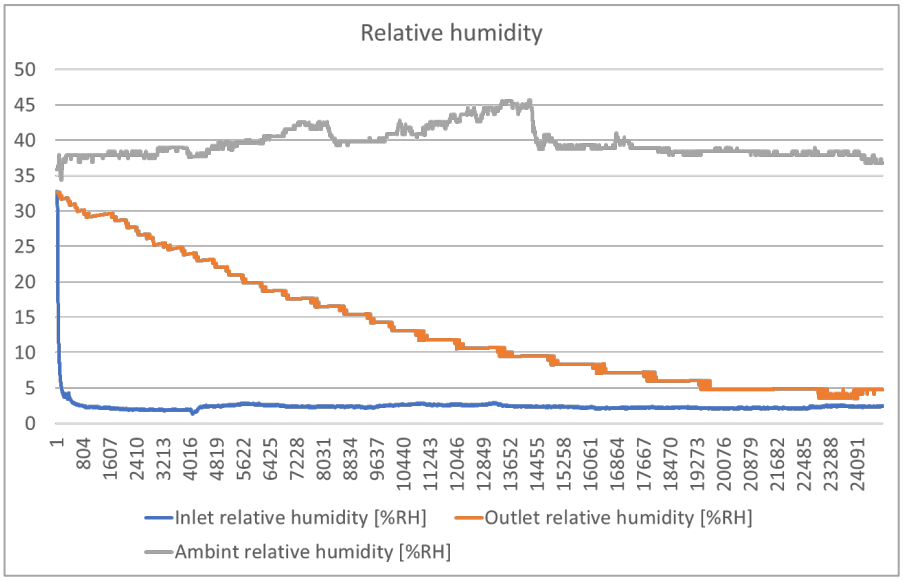


Figure 7-18 Relative humidity level in charging/regeneration process.

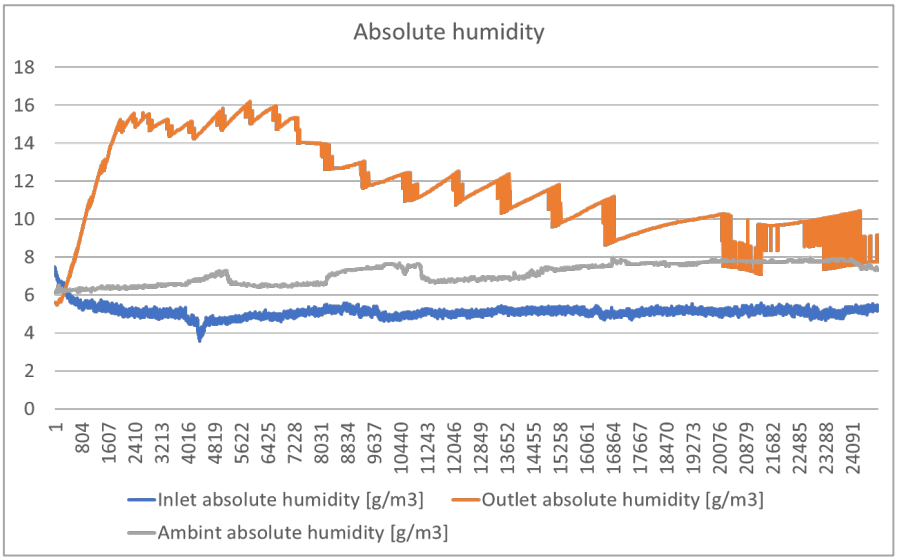


Figure 7-19 Absolute humidity in charging process.

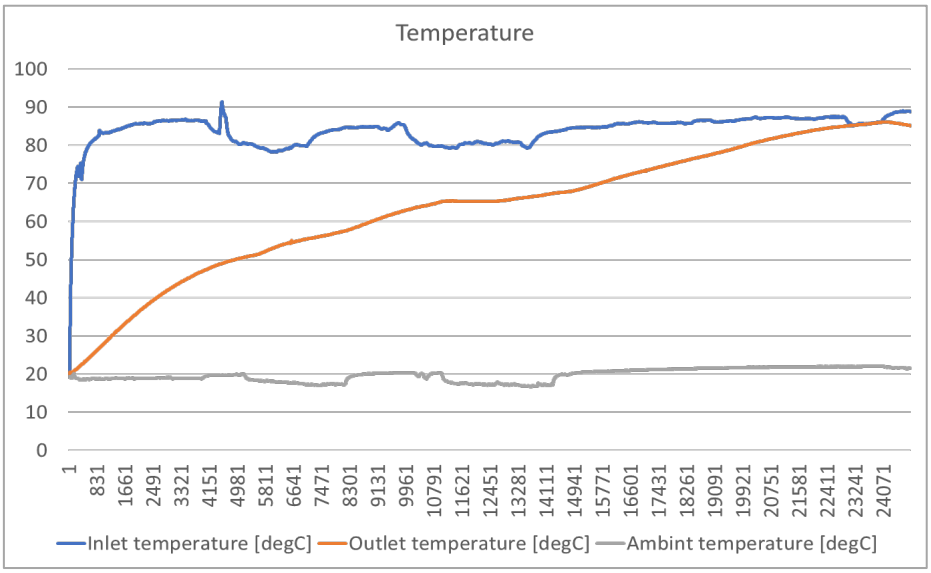


Figure 7-20 Temperature variation in charging process.

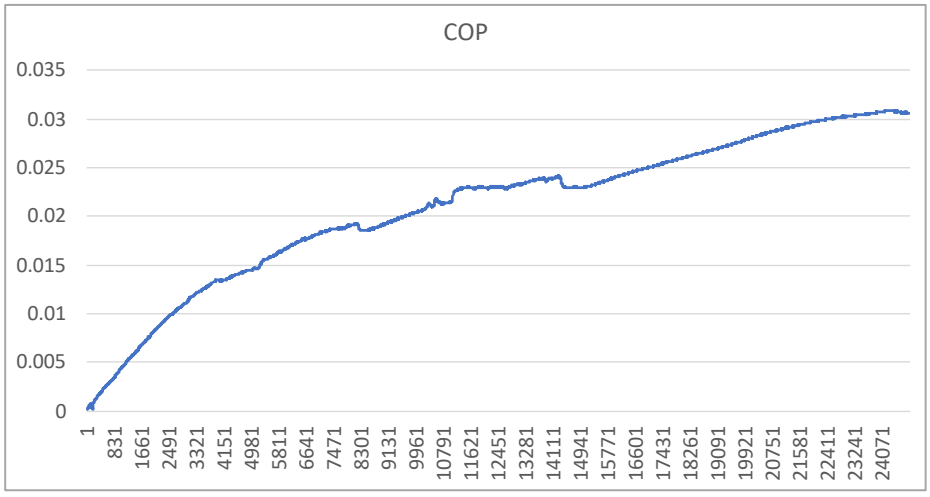


Figure 7-21 COP in charging/regeneration process.

7.4 SUMMARY

In this Chapter a novel TES prototype was numerically and experimentally investigated. In the 1st test with prototype, 16 kg V-$MgSO_4$-$CaCl_2$ was placed in the reactor. After one cycle test, the highest outlet temperature was 37.44 °C with reaction COP of 1.05-1.2, which did not reach the high temperature we expected (above 40 °C). The inlet relative humidity level was about 60% and the outlet relative humidity level was about 17%, which means that the TES materials have a very good

water uptake capacity. Because the hole under the bottom of the reactor is too small that the moisture air cannot go through the rig completely, some of the moisture air escape from the gap of the humidifier, so the humidity level cannot reach 90%.

In the 2nd test with prototype, the hole on the bottom was expended to make them larger for the moisture air going through the tube to inject into the materials. The flat pan in the bottom of the rig was used to provide the moisture transfer and fix the tubes inside the rig test body. More holes can supply more moisture air to rise the relative humidity level. Hence, a flat pan with more holes will be replaced the old one to provide more access for moisture air goes pass the reaction body. Moreover, after the 1st test in the prototype, humidifier was installed in front of the fan for the centrifugal fan to extract moisture air to lift the relative humidity level and reduce moisture leakage. As a result, the air outlet temperature can reach 43.1 °C and total 6 hours heating supply can be 2.88 kWh with COP of 1-1.51. For short-term TES storage, the system can easily provide enough heating demand for house. In the future work, renewable energy sources should be replaced the electricity power input to achieve zero-carbon requirement in building application. Some economic and environmental analysis will be done in the next chapter based on the prototype.

8 ECONOMIC AND ENVIRONMENTAL ANALYSIS

8.1 INTRODUCTION

Currently, fossil fuels are the main energy source in EU28, 78% of total supply to the building heat market (the electric heating accounts for 12%) [228]. The total building sector heat market constitutes an energy volume of approximately 13.1 EJ. Almost half of the final energy consumed is used as heat in the UK. It is mainly used for space heating (60%) and hot water (15%) in domestic and commercial buildings. The global market for energy storage is expected to grow at a CAGR of 19.8% during the forecast period of 2019-2024 [229]. The energy storage installations will multiply exponentially, from a modest 9GW/17GWh deployed as of 2018 to 1095GW/2850GWh by 2040 [230]. The residential sector is expected to account for the largest share in the energy storage market. Factors such as growing renewable energy sector, supportive government policies and schemes for energy storage systems (ESS) and improving energy storage economics are expected to be major drivers for the energy storage market in the coming years. To increase the utilization rate of renewable power sources, the energy storage systems are increasingly adopted. Energy storage will become a practical alternative to new-build energy and electricity generation. Combining thermochemical energy storage with solar PV/thermal system or any other kind of sustainable energy sources can significantly reduce CO_2 emissions and delivers a low LCoE solution. TES system presents the opportunity to meet Building Emissions Ratings and Target Emissions Ratings with relative easy. The system is a compact, inter-seasonally, loss-less thermochemical energy storage system that can be integrated into local energy systems with low cost, high efficiency, ease of production and installation. This indicates significant future market potential, especially as TES system is a potentially cost effective, versatile

and efficient inter-seasonal energy storage, which can be driven by many kinds of sustainable/renewable energy sources.

8.2 ECONOMIC ANALYSIS

The experimental results and analysis have shown that thermochemical energy storage system is intelligent and suitable for home and commercial applications from the technique view, and it can be easily integrated with any kinds of sustainable energy sources. A preliminary economic analysis of this TES system has been carried out in order to understand its commercial viability. Thermochemical energy storage system delivers a low operational cost solution by enabling sustainable technologies to be deployed into large established markets removing barriers to legislative energy efficiency improvements. Moreover, the development of the thermochemical energy storage concept has global applicability. The key features - low cost, high efficiency, low maintenance, ease of production and installation - will stimulate the thermochemical energy storage market, increasing the strategic role in the UK economy. This study assumes a lifetime of 20 years for the entire TES system. Moreover, the UK government's incentives and inflation rates were not considered in the calculations.

8.2.1 Capital cost and payback period

The capital cost for proposed solar TES system is shown in Table 8-1. The composite material Vermiculite with $MgSO_4$ and $CaCl_2$ will be used in the domestic heating system to provide 3kW (it is based on the peak energy consumption of a typical house in the UK; the heat loss for a typical UK house should be between 60-100 W/m^2, so we chose $80W/m^2$; and we used DegreeDays method to calculate the total heating

days will be 2159 hours/90 days a year), therefore, 92.1 kg of material was required based on the building heat load. Then final capital cost will be calculated as followed.

Table 8-1 Capital cost for TES systems

Equipment	Cost, £
TES material (92.1kg) (Vermiculite: 30.5kg, $MgSO_4$: 9.4kg, $CaCl_2$: 52kg)	(Vermiculite: £239.4 $MgSO_4$: £181 $CaCl_2$: £711) Total: £1131.4 (Fisher Scientific, 2019)
Material container	300 (PAK, 2019)
Insulation	130 (Kinspan, 2019)
Ducting pipes, fittings, vents	350 (PAK, 2019)
Fan	82 (ElectricalDirect, 2019)
Humidifier	92 (LIVIVO, 2019)
Total Cost (excluding loabour)	2085.4
Labour (10% of total)	208.54
VAT (20%)	458.8
Total	2752.7

Compared to the natural gas central space heating system (with boiler efficiency of 86%), cost of domestic TES system saved can be calculated by the heat demand of a typical 3 bedroom house in the UK with space heating consumption is 10428kWh/year (121kWh/m^2/year). The space heating period is assumed to from October to April. The gas price is 3.578p/kWh, and the electricity price is 18.19p/kWh. Therefore, the annual running costs saved by using a solar assisted thermochemical energy storage system are:

$$Cost\ of\ TES\ system\ saved = (10428 \times 0.03578)/0.86 = £433.85$$

$$The\ payback\ period = 2752.7/433.85 = 6.4\ years$$

8.2.2 Life cycle cost saving

The net present value (NPV) is used for evaluation of the profitability of the novel TES system. Net present value NPV is a capital budgeting formula used to calculate the difference between the cash inflows and outflows of a project or potential investment. In other words, it is used to evaluate the amount of investment compared to the cost of adjusting for the time value of money [231, 232]. In this study, Net Present Value (NPV) was used to evaluate if the investment of the novel TES system was valuable. In this evaluation, a lifetime of 20 years for the entire TES system was assumed, and the UK government's incentives and inflation rates were not considered. The NPV formula *Eq 9* adds up all future cash flows from an investment, discounts it using a discount rate, and then subtracts the initial investment.

$$NPV = \sum_{t-1}^{T} \frac{C_t}{(1+r)^t} - C_0 \qquad Eq\ 9$$

The meaning of each symbol is as follows:

C_t = net cash inflow during the period

C_O = initial investment

r = discount rate

t = number of cycles

To explain with non-mathematical equations: The NPV is obtained by subtracting the PV of the initial investment from the PV of the costs generated by future investments. This will discount future costs generated during the life of the investment with current costs spent on the investment, so investors can compare the potential return on an investment to its initial cost.

$$NPV = Present\ Value\ of\ Future\ Cash\ Flows - Present\ Value\ of\ Initial\ Investment\ costs \qquad Eq\ 10$$

Table 8-2 shows the net present value (NPV) for the 20-year system service period. The capital cost of the TES system was £2752.7. The annual discount rate is 3.7% [233]. The gas inflation rate was 2.2% in 2019. Annual heating load was 10428kWh and the price of gas was 3.578p/kWh.

The positive value appears in the 16th year (£69.42) and NPV value is £668.25 in the 20th year.

Table 8-2 The net present value (NPV) analysis method calculation.

Year	Ci, £	NPV, £
1	201.65	-2558.24
2	206.88	-2365.86
3	212.11	-2175.65
4	217.34	-1987.71
5	222.57	-1802.11
6	227.80	-1618.92
7	233.03	-1438.22
8	238.27	-1260.05
9	243.50	-1084.47

10	248.73	-911.51
11	253.96	-741.22
12	259.19	-573.62
13	264.42	-408.74
14	269.65	-246.60
15	274.88	-87.21
16	280.11	69.42
17	285.34	223.28
18	290.57	374.37
19	295.80	522.69
20	301.03	668.25

Internal rate of return (IRR) can be obtained when net present value (NPV) equals to zero, then the IRR is calculated as 7.56%. The annual discount rate is 3.7%, which is less than the IRR (7.56%). Hence, 20 years lifetime is reasonable for this novel TES system.

8.3 ENVIRONMENTAL ANALYSIS

Environmental issue is a hot topic in the world. The UK government's advisory Committee on Climate Change recommended "net zero" greenhouse gases by 2050. The domestic sector currently accounts for about 30% of UK's energy consumption and 25% of greenhouse gas emissions, a result of dependency on fossil fuels particularly for space heating and hot water. To increase the proportion of renewable energy using can reduce the use of fossil fuels. Thermochemical energy storage system using sustainable technologies will result in energy savings and reduction in GHG emissions caused by the domestic and commercial sector and this will lead to benefits to the public health. This novel TES system is a green and sustainable energy storage system. To investigate the environmental benefit of utilizing TES system instead of conventional source of energy for space heating, environmental analysis was conducted by estimating CO_2 emission reductions.

According to the UK government report on emission conversion factors for greenhouse gas, the CO_2 conversion can be calculated using the following equation:

$$Carbon\ Dioxide\ Emission\ (kg \cdot CO2/year) = Natural\ gas\ (kWh/year) \times Emission\ conversion\ factors\ for\ CO2$$

Eq 11

Where, CO_2 conversion factor is 0.2049 for natural gas and for a typical UK house the annual gas consumption is 10428kWh/year. The annual total CO_2 saving is calculated as follow:

Carbon dioxide emission (kg) = 10428kWh/year * 0.2049 = 2136.7kg

Therefore, the total CO_2 saving by using this TES system in UK house is about 2136.7kg every year.

8.4 SUMMARY

According to the capital costs and the novel TES system energy and CO_2 savings, the payback period of the TES system is 6.4 years. In consideration of a 20 years lifetime for the entire TES system, using NPV analysis method to work out the positive value appears in the 16th year (£69.42) and NPV value is £668.25 in the 20th year. Therefore, the novel TES system is attractive to use for space heating and is worth investing. The annual market discount rate is 3.7% currently, and the IRR of the system is 7.56% which is higher than the market discount, hence, it is desirable for 20 years of system life. In the environmental aspect, the novel TES system shows a large reduction on CO_2 emissions (2136.7kg/year) compared with conventional natural gas heating system. Consequently, the TES system will be an alternative to the current heating system, and it is a sustainable way to provide space heating for building applications.

9 CONCLUSION, RECOMMANDATIONS AND FUTURE WORKS

9.1 SUMMARY OF THE WORK

The main purpose of the research was to access the application and economic feasibility of thermochemical energy storage system using novel TES materials in building applications under UK climates condition. This thermochemical energy storage technology works as a 'heat storage battery' to store the energy generated by any kind of heat source (for example, solar, wind, tide and biomass, or waste heat recovery technology), and the stored heat in the TES materials can be used when required. The development of TES materials is one of the focus of this project. Through previous studies, some candidate materials have been identified. The main objective is to investigate the characteristics and performance of the new composites TES materials in order to access the application feasibility of TES system. Through simulation, experimentation and analysis, some new TES composites were developed and used in test rig and prototypes for further performances analysis. Through testing and improvement, the new TES system can bring efficient space heating and cooling to the building applications. The system has a low energy requirement as renewable/sustainable energy can be stored as thermochemical energy. The main driver behind the research is to save fossil fuel consumption and CO_2 emissions in household space heating. TES system is a promising method to improve the energy efficiency and proportion of renewable resources utilization for space heating. The main objective is to investigate the characteristics and performance of the new composites TES materials in order to access the application feasibility of TES system.

9.2 CONCLUSIONS

The aim of the research in this thesis is to design, develop and evaluate a high performance short-term thermochemical energy storage system for building sectors. The test rig system and prototype have been designed and tested in lab with a good result. Initially, comprehensive literature review has been carried out on the following aspects: existing thermal heat storage technology, thermal storage materials, and thermochemical energy storage technologies.

In the literature review, the classification of energy storage technologies has been learnt and the advantages of thermochemical energy storage technology compared to other energy storage methods (sensible heat storage and latent heat storage) have been studied. In the sensible heat storage method, the medium used for heat storage can be liquid water, hot water can be used directly, or it can be used for room heating. Latent heat storage is accomplished through phase change materials (Phase Change Materials, PCMs), which is the medium that stores thermal energy. Thermochemical energy storage has the largest energy storage density of the three (about 10 times the sensible heat storage and 5 times the latent heat storage) and realizes short-term / long-term and seasonal storage of thermal energy through electrostatic attraction between chemical bonds. However, it is currently difficult to break through due to issues such as safety, conversion efficiency, and economics. Most thermochemical heat storage material systems are in the early R & D stage, and there is still a long time before large-scale commercialization. As a widely used phase change material (PCM) storage technology, some details and current applications are given in Chapter 2. PCM heat storage is currently the focus of research in the field of energy storage. PCMs are mainly divided into organic phase change materials and inorganic phase change materials. Organic PCMs are

characterized by large phase change enthalpy and low subcooling, but poor high temperature stability, low thermal conductivity, and high cost. The temperature of the hot water changes during operation. Thermochemical energy storage principle, technologies and some recent advances have been presented. The recent research focus on the development of the absorption and adsorption working pair and the optimal materials and composites with the following characteristics: high energy storage density; low charging or regeneration temperature; high water or sorbate uptake (g sorbate/ g sorbent); and suitability for the application.

In chapter 4, some initial experiments have been done to investigate the performances and characteristics of TES materials and selected the optimal TES materials for the next step testing. Energy density analysis shows that the vermiculite and salt mixture is a promising candidate for THS system compared to the single salt. The energy density of a composite material is typically higher than a single salt. Vermiculite with $MgSO_4$-$CaCl_2$ showed a highest energy density among TES composites with the energy density obtained from DSC analysis was as high as 1173.5 kJ/kg, and the regeneration temperature was as low as 63 °C, which were the key features of TES composites. However, although the performance of each single salt in the vermiculite with $MgSO_4$-$LiNO_3$-$MgCl_2$ was good, the performance of the composite showed greatly deficient. For thermochemical cool storage materials, vermiculite with urea was selected as a candidate of TES cooling material due to its good energy density (727.85 kJ/kg) and relative low regeneration temperature at 54.5 °C. Sorption test was taken to study the water uptake. V-$MgSO_4$-$CaCl_2$ and V-$MgSO_4$-LiCl showed better sorption performance with higher water uptake of 2g/g and 2.5g/g, respectively. As a result, three composites (V-$CaCl_2$-LiCl, V-$MgSO_4$-LiCl

and V-$MgSO_4$-$CaCl_2$) were selected to be tested in the lab-scaled rig. The computer simulations of the TES system sizing were based on the initial test results.

Two initial computer simulations have been done based on the tests results of Chapter 4. The 1st simulation was using Integrated Environmental Solutions Virtual Environment (IES-VE) software to simulate heating and cooling load in a low-carbon house in the UK, and the 2nd one was a solar evacuated tubes collector TES system to analyse the feasibility of the thermochemical energy storage system in building applications. A typical low-carbon 3-bedroom house was simulated with heating and cooling load of 1091kWh/year and 1982.6kWh/year, respectively. The results showed that compared with latent heat storage and sensible heat storage, because of the high energy density of TES materials, TES systems for heating and cooling of house is more effective and feasible. And also, solar evacuated tube collector with TES materials can be another choice for a limited roof space to provide short-term energy storage.

In the 1st rig test in Chapter 6, V-$CaCl_2$-LiCl showed the highest water uptake 0.12g/g in the 1st discharging cycle, however, in the 2nd discharging process the system performance was much lower. The water uptake of V-$MgSO_4$-LiCl was about 0.1g/g, which was good performance. But in the charging process, the water loss was very low, which means that the regeneration efficiency was lower than others. V-$MgSO_4$-$CaCl_2$ shows good potential for use in open THS systems, because although the water uptake was less than other two composites, the air outlet temperature can reach as high as 40 °C. Then the V-$MgSO_4$-$CaCl_2$ with different salt ratio has been tested as well. And the it presented the best performance with the highest air outlet temperature of 41.2 °C. Surprisingly, the highest air outlet temperature rose to 46.1 °C and the water uptake stayed very similar with discharging cycle 1. As a result,

V-$MgSO_4$-$CaCl_2$ with ratio of 1:1:2 was chosen as the testing TES material in prototype.

16 kg V-$MgSO_4$-$CaCl_2$ was placed in a TES prototype was numerically and experimentally investigated. In the original prototype, the system showed poor performance because of some design flaws. The relative humidity cannot reach the designed level. The highest air outlet temperature was 37.44 °C with reaction COP of 1.05-1.2. In the 2nd cycle test, the prototype has been modified by changing the holding plate and placing humidifier in front of centrifugal fan. As a result, the air outlet temperature was as high as 43.1 °C to supply 2.88 kWh heating energy with COP of 1-1.51. It will be suitable for short-term TES storage as the system can easily provide enough heating demand for house.

By analysing the capital cost of the proposed system and the annual energy savings compared to natural gas central heating systems, the solar TES system shows a quick payback period of 6.4 years. Moreover, through analysis of the net present value (NPV) and the internal rate of return (IRR), the proposed TES system is feasible considering the system's service life of 20 years. In the environmental aspect, the novel TES system shows a large reduction on CO_2 emissions (2136.7kg/year) compared with conventional natural gas heating system. Consequently, the TES system will be an alternative to the current heating system, and it is a sustainable way to provide space heating for building applications.

Technically and economically the system has proved to yield great results which are likely to improve in the future, making it only a matter of time when these systems will be installed within the houses in the UK and worldwide.

There are some limitation of work, for example, the laboratory condition is not the same as the real environment may cause the inaccurate results of the experiments;

the time limited may cause less time for the whole cycle tests; there is no renewable resources connected with the prototype for power supply in regeneration process. The limitation of the work will be taken into consideration in the future work to give more accurate results.

9.3 RECOMMENDATION AND FUTURE WORK

The simple concept of the open-cycle THS system has many advantages. For example, the required energy storage materials are cheap; because the regeneration temperature is low, the reaction device can be connected to various low-temperature renewable energy heat sources, such as wind, solar or especially the waste heat recovery system in the industrial application; and the entire operation is carried out under atmospheric pressure without risk of high pressure. In this project, we found that the airtightness of the entire system will directly affect the temperature of the space heating provided. This problem needs to be overcome in future work. The TES materials used in the system have low heat transfer conductivity, so the heat transfer of the system is not very good. In the future work, we should find ways to improve the thermal conductivity of the entire reactor/TES materials.

9.3.1 Development of the open TES system with solar PV driven

This research has been studied the novel high capacity thermochemical energy storage system. The open thermochemical absorption energy storage system has been tested, and it worked well. In the next step, solar collector will be integrated in the thermochemical energy storage system to provide heating in regeneration process. The combined mode of solar collector and thermochemical absorption energy storage system will capture solar energy by evacuated tube collector and transfer heat energy to thermochemical absorption system in the

regeneration/charging process, dehydration reaction occurs and water will be driven out from materials to complete energy storage process. In the discharging process, moisture is from a humidifier provided to the reaction chamber will be driven by solar PV panel, materials will absorb moisture and release heat for space heating. In addition, waste heat recovery is a potential heat source that can be used in TES systems. In recent years, this area has received attention because of its high potential for improving energy efficiency and reducing carbon dioxide (CO_2). TES materials can store waste heat from the industrial sector and then use heat in buildings or industry for heating. Ground or air source heat pumps can be used as low temperature heat sources in the system as well. Renewables sources such as solar and wind energy could be stored in the form of heat and electricity. Excess power generated by PV/thermal panels could be electricity supply to houses or used for charging electrical vehicles. The new system with renewable sources will lead to significant energy savings (>50%) and CO_2 emissions reduction, with a maximum payback of 5 years.

9.3.2 Proposed solar driven thermochemical energy storage system (SeasonalStorage)

By the end of August 2019, total solar capacity of 13,275.5MW is achieved across 1,012,896 installations across the UK. UK has become a major global player and there's still much potential to be tapped. Recent studies suggest that covering 61% of south-facing commercial roofs with solar PV could provide all the energy needed for the UK businesses to save enterprises at least £30,000/year on energy bills. Factors such as growing renewable energy sector, supportive government policies and schemes for energy storage systems and improving energy storage economics are expected to be major drivers for the energy storage market in the coming years.

To increase the utilisation rate of renewable energy sources, energy storage systems are increasingly adopted. Energy storage will become a practical alternative to new-build energy and electricity generation. By combining thermochemical energy storage with solar PV/thermal technology, the proposed SeasonalStorage can significantly reduce CO_2 emissions and deliver a low LCoE solution. SeasonalStorage presents the opportunity to meet Building Emissions Ratings and Target Emissions Ratings as solar energy can be effectively stored with thermochemical materials in the forms of heat and electricity and excessive electrical power will charge electric vehicles to cater for the growing electrical cars usage. SeasonalStorage can run standalone or be integrated into local energy systems with low cost, high efficiency, ease of production and installation.

SeasonalStorage system using closed cycle has been proposed in our next stage to address the drawbacks related to other two common types of thermochemical energy storage (TES) systems. The first type is vacuum-sealed TES systems under high vacuum, within which a small amount of non-condensable gases could dramatically reduce or even stop the thermochemical sorption process. The vacuum-sealed TES system is expensive as it requires pressure vessels which can stand a high level of vacuum. Sealing of connection pipes and heat exchangers within the system is also challenging. As the performance of the reactor decreases dramatically with non-condensable gases, a vacuum pump is required to completely de-air the sealed thermochemical material.

In comparison, the second type is typical open TES system operated at the ambient pressure with air as heat transfer media. The thermochemical material granules can be packed in an inexpensive metal or plastic container. However, the open TES system can only obtain a temperature rise of less than 20°C in a discharging process.

This is because the thermal capacity of air flow is significantly high compared to the thermochemical reaction heat, which is produced by sorption of moisture from air flow. For the similar reason, in the charging process of thermochemical materials, air flow has to be raised to a high temperature of above 100°C in order to deliver sufficient heat. Fan power consumption may be also significant due to large air flow rate.

To address the above-mentioned drawbacks, a closed air loop TES system with internal heating/cooling and a controlled pressure is proposed in order to achieve a higher temperature rise across the thermochemical reactor. Unlike vacuum-sealed system, the closed air loop TES system does not require pressure vessels and other associated complexity.

9.3.3 Long Term Thermochemical Energy Storage System

The world's current demand for electricity is growing rapidly. According to the International Energy Agency's estimates, an additional 250 GW of electricity will be needed each year to meet commercial and domestic electricity requirement from now until 2050. The promotion of renewable energy technology can meet the demand for clean energy, but mismatch between demand and supply is an issue that has always existed, and it is also the main problem we need to solve. The long-term TES system can provide a cost-effective solution linking zero carbon renewable thermal energy and district energy systems with high energy density, low heat loss, low regeneration temperature and a low storage volume requirement. By providing effective long-term heat storage, it contributes to creating intelligent energy systems and meeting the UK obligations to climate-related issues by reducing GHG emissions. Novel composite adsorbents are essential for providing high energy density and effective thermochemical reaction that allows long term heat storage for building heating to

meet carbon reduction targets and achieve clean growth ambitions. Therefore, there is an urgent need to develop an efficient and sustainable long-term energy storage technology to make full use of green and clean energy.

The renewable resources driven TES system enables long term heat storage demands of commercial and industrial building applications through a smart renewable energy storage system using environmental-friendly thermochemical materials and facilitates higher renewable energy penetration by mitigating the time gap between energy generation and demand. This will be beneficial to industry including renewables, building services and construction as well as society.

Large scale longer-term energy storage technologies that can effectively store energy for several months will be the research and development direction of future energy storage technologies. Most of today's energy storage devices use fixed-beds as reactors and material storage. When long-term energy storage is required, larger quantities of energy storage materials are needed. Since the increase in bed thickness greatly limits the reaction capacity, it is impossible to scale up any fixed bed reactor to store heat for a long time, because the reaction capacity and gas flow rate of the fixed-bed reactor will be uneven and the pressure drop will become high. In order to realise and implement long-term and large-scale TES system provision in residential, commercial and industrial buildings, non-removable material storage tray in fixed-bed reaction unit can be replaced with removable fabrics. Encapsulating the TES material inside the movable fabric makes it thinner to increase the contact surface area between the air flow and the TES material, thereby improving the reaction efficiency to achieve long-term energy storage. At the same time, since most of the TES materials used are non-metallic materials, how to improve the heat transfer of TES materials is also a topic worth exploring and researching in the future.

REFERENCES

1. Aydin, D., S.P. Casey, and S. Riffat, *The latest advancements on thermochemical heat storage systems.* Renewable and Sustainable Energy Reviews, 2015. **41**: p. 356-367.
2. Gorlov, A., *Tidal energy.* Academic, London, 2001: p. 2955-2960.
3. Yu, N., R. Wang, and L. Wang, *Sorption thermal storage for solar energy.* Progress in Energy and Combustion Science, 2013. **39**(5): p. 489-514.
4. Pinel, P., et al., *A review of available methods for seasonal storage of solar thermal energy in residential applications.* Renewable and Sustainable Energy Reviews, 2011. **15**(7): p. 3341-3359.
5. Zalba, B., et al., *Review on thermal energy storage with phase change: materials, heat transfer analysis and applications.* Applied thermal engineering, 2003. **23**(3): p. 251-283.
6. Sharma, A., et al., *Review on thermal energy storage with phase change materials and applications.* Renewable and Sustainable energy reviews, 2009. **13**(2): p. 318-345.
7. Pardo, P., et al., *A review on high temperature thermochemical heat energy storage.* Renewable and Sustainable Energy Reviews, 2014. **32**: p. 591-610.
8. Ervin, G., *Solar heat storage using chemical reactions.* Journal of solid state chemistry, 1977. **22**(1): p. 51-61.
9. N'tsoukpoe, K.E., et al., *A review on long-term sorption solar energy storage.* Renewable and Sustainable Energy Reviews, 2009. **13**(9): p. 2385-2396.
10. McBain, J.W., *XCIX. The mechanism of the adsorption ("sorption") of hydrogen by carbon.* The London, Edinburgh, and Dublin Philosophical Magazine and Journal of Science, 1909. **18**(108): p. 916-935.
11. Department for Business, E.I.S., *Digest of United Kingdom Energy Statistics (DUKES) 2019: main chapters and annexes A to D*, in *National Statistics, GOV.UK*. 2019.
12. Change, D.o.E.C., *European Energy Efficiency trends – Household energy consumption*, in *Official Statistics - Household energy consumption*. 2018.
13. transmission, G.g.a.e., *Future Energy Scenarios*. 2019.
14. The UK Department for Business, E.a.I.S.B., *UPDATED ENERGY AND EMISSIONS PROJECTIONS 2016*. 2017, GOV: London.
15. Cabeza, L.F., *Advances in thermal energy storage systems: Methods and applications. , 2014.* Elsevier, 2014.
16. Arce P., M.M., Gil A., Oró E., Cabeza LF., *Overall of thermal energy storage (TES) potential energy saving and climate change mitigation in Spain and Europe.* Applied Energy, 2011. **88**: p. 2764-2774.
17. Aydin, D., S.P. Casey, and S. Riffat, *The latest advancements on thermochemical heat storage systems.* Renewable and Sustainable Energy Reviews, 2015. **41**: p. 356-367 %@ 1364-0321.
18. Kato, Y., *Chemical energy conversion technologies for efficient energy use.* Thermal Energy Storage for Sustainable Energy Consumption: Fundamentals, Case Studies and Design, 2007. **234**: p. 377.
19. Venkatarathnam, G. and S.S. Murthy, *Refrigerants for vapour compression refrigeration systems.* Resonance, 2012. **17**(2): p. 139-162 %@ 0971-8044.

20. Hasnain, S.M., *Review on sustainable thermal energy storage technologies, Part I: heat storage materials and techniques.* Energy conversion and management, 1998. **39**(11): p. 1127-1138 %@ 0196-8904.
21. Dalley, S., *Mari and Karana: two old Babylonian cities*. Vol. 21. 2002: Gorgias Press LLC.
22. James, P.J., N. Thorpe, and I. Thorpe, *Ancient inventions*. 1995: Random House Digital, Inc.
23. Dincer, I., *On thermal energy storage systems and applications in buildings.* Energy and buildings, 2002. **34**(4): p. 377-388.
24. Hepbasli, A. and Y. Kalinci, *A review of heat pump water heating systems.* Renewable and Sustainable Energy Reviews, 2009. **13**(6-7): p. 1211-1229 %@ 1364-0321.
25. Lee, K.S., *Underground thermal energy storage*, in *Underground Thermal Energy Storage*. 2013, Springer. p. 15-26.
26. Zhang, X. and I.X. Dincer, *Energy solutions to combat global warming*. 2017: Springer.
27. Hasnain, S., *Review on sustainable thermal energy storage technologies, Part I: heat storage materials and techniques.* Energy conversion and management, 1998. **39**(11): p. 1127-1138.
28. Dheep, G.R. and A. Sreekumar, *Influence of nanomaterials on properties of latent heat solar thermal energy storage materials–A review.* Energy conversion and management, 2014. **83**: p. 133-148.
29. Sarbu, I. and C. Sebarchievici, *A comprehensive review of thermal energy storage.* Sustainability, 2018. **10**(1): p. 191.
30. Wang, R. and X. Zhai, *Handbook of energy systems in green buildings*. 2018: Springer.
31. Nallusamy, N., S. Sampath, and R. Velraj, *Experimental investigation on a combined sensible and latent heat storage system integrated with constant/varying (solar) heat sources.* Renewable Energy, 2007. **32**(7): p. 1206-1227.
32. Li, C. and R.Z. Wang, *Building integrated energy storage opportunities in China.* Renewable and Sustainable Energy Reviews, 2012. **16**(8): p. 6191-6211 %@ 1364-0321.
33. Demirbas, M.F., *Thermal energy storage and phase change materials: an overview.* Energy Sources, Part B: Economics, Planning, and Policy, 2006. **1**(1): p. 85-95 %@ 1556-7249.
34. Mishra, A., A. Shukla, and A. Sharma, *Latent heat storage through phase change materials.* Resonance, 2015. **20**(6): p. 532-541 %@ 0971-8044.
35. Mondal, S., *Phase change materials for smart textiles–An overview.* Applied thermal engineering, 2008. **28**(11-12): p. 1536-1550 %@ 1359-4311.
36. Ustinov, E.A., *Improved modeling of two-dimensional transitions in dense phases on crystalline surfaces. Krypton–graphite system.* The Journal of chemical physics, 2015. **142**(7): p. 074701 %@ 0021-9606.
37. Mazman, M., et al., *Utilization of phase change materials in solar domestic hot water systems.* Renewable energy, 2009. **34**(6): p. 1639-1643 %@ 0960-1481.
38. Chen, M.M. and F.Q. Zhao. *Research and application of phase change energy storage technology in construction and buildings materials*. 2014. Trans Tech Publ.
39. Sharma, A., et al., *Review on thermal energy storage with phase change materials and applications.* Renewable and Sustainable energy reviews, 2009. **13**(2): p. 318-345 %@ 1364-0321.

40. Yan, T., et al., *A review of promising candidate reactions for chemical heat storage.* Renewable and Sustainable Energy Reviews, 2015. **43**: p. 13-31 %@ 1364-0321.
41. Ibrahim, H., A. Ilinca, and J. Perron, *Energy storage systems—Characteristics and comparisons.* Renewable and sustainable energy reviews, 2008. **12**(5): p. 1221-1250 %@ 1364-0321.
42. Zhang, Y.N., R.Z. Wang, and T.X. Li, *Thermochemical characterizations of high-stable activated alumina/LiCl composites with multistage sorption process for thermal storage.* Energy, 2018. **156**: p. 240-249 %@ 0360-5442.
43. Wu, J. and X.F. Long, *Research progress of solar thermochemical energy storage.* International Journal of Energy Research, 2015. **39**(7): p. 869-888 %@ 0363-907X.
44. Su, W., J. Darkwa, and G. Kokogiannakis, *Review of solid–liquid phase change materials and their encapsulation technologies.* Renewable and Sustainable Energy Reviews, 2015. **48**: p. 373-391 %@ 1364-0321.
45. Kośny, J., *PCM-enhanced building components: an application of phase change materials in building envelopes and internal structures*. 2015: Springer.
46. Zhang, Y., et al., *Form-stable phase change materials with high phase change enthalpy from the composite of paraffin and cross-linking phase change structure.* Applied energy, 2016. **184**: p. 241-246 %@ 0306-2619.
47. Zhang, Z. and X. Fang, *Study on paraffin/expanded graphite composite phase change thermal energy storage material.* Energy Conversion and Management, 2006. **47**(3): p. 303-310.
48. Khan, M.M.A., R. Saidur, and F.A. Al-Sulaiman, *A review for phase change materials (PCMs) in solar absorption refrigeration systems.* Renewable and sustainable energy reviews, 2017. **76**: p. 105-137 %@ 1364-0321.
49. Kenisarin, M. and K. Mahkamov, *Solar energy storage using phase change materials.* Renewable and sustainable energy reviews, 2007. **11**(9): p. 1913-1965.
50. Wei, F., et al., *A Novel Thermal Energy Storage System in Smart Building Based on Phase Change Material.* IEEE Transactions on Smart Grid, 2018. **10**(3): p. 2846-2857.
51. Castell, A. and C. Solé, *Design of latent heat storage systems using phase change materials (PCMs)*, in *Advances in Thermal Energy Storage Systems*. 2015, Elsevier. p. 285-305.
52. Verma, P. and S.K. Singal, *Review of mathematical modeling on latent heat thermal energy storage systems using phase-change material.* Renewable and sustainable energy reviews, 2008. **12**(4): p. 999-1031 %@ 1364-0321.
53. Frigione, M., M. Lettieri, and A. Sarcinella, *Phase Change Materials for Energy Efficiency in Buildings and Their Use in Mortars.* Materials, 2019. **12**(8): p. 1260.
54. Gassar, A. and G. Yun, *Energy saving potential of PCMs in buildings under future climate conditions.* Applied Sciences, 2017. **7**(12): p. 1219.
55. Torgal, F.P., et al., *Nearly zero energy building refurbishment: A multidisciplinary approach*. 2013: Springer Science & Business Media.
56. Shim, H., E. McCullough, and B. Jones, *Using phase change materials in clothing.* Textile Research Journal, 2001. **71**(6): p. 495-502.
57. Chen, H.-j., et al., *Attapulgite based LiCl composite adsorbents for cooling and air conditioning applications.* Applied Thermal Engineering, 2008. **28**(17-18): p. 2187-2193 %@ 1359-4311.
58. Lane, G.A., H.E. Rossow, and A.S. Teot, *Reversible phase change composition for storing thermal energy*. 1986, Google Patents.

59. Milian, Y.E., et al., *A review on encapsulation techniques for inorganic phase change materials and the influence on their thermophysical properties.* Renewable and Sustainable Energy Reviews, 2017. **73**: p. 983-999 %@ 1364-0321.
60. Wu, S., et al., *Thermal conductivity enhancement on phase change materials for thermal energy storage: A review.* Energy Storage Materials %@ 2405-8297, 2019.
61. Lin, Y., et al., *Review on thermal conductivity enhancement, thermal properties and applications of phase change materials in thermal energy storage.* Renewable and sustainable energy reviews, 2018. **82**: p. 2730-2742 %@ 1364-0321.
62. Lele, A.F., *A Thermochemical Heat Storage System for Households: Combined Investigations of Thermal Transfers Coupled to Chemical Reactions*. 2016: Springer.
63. Lombardi, L., E. Carnevale, and A. Corti, *A review of technologies and performances of thermal treatment systems for energy recovery from waste.* Waste management, 2015. **37**: p. 26-44 %@ 0956-053X.
64. Ammar, Y., et al., *Low grade thermal energy sources and uses from the process industry in the UK.* Applied Energy, 2012. **89**(1): p. 3-20 %@ 0306-2619.
65. *The Future of Heating: Meeting the challenge.* 2016, Department of Energy & Climate Change: London.
66. Dechert, S., *Energy Storage Companies*, in *Clean Technica*. 2015.
67. Dige, P., *Thermal Energy Storage Market*. 2013, Technology Segment.
68. *Thermal Energy Storage Market (Technology - Sensible Heat, Latent Heat, and Thermochemical; End Use - Commercial and Industrial, Utilities, and Residential) - Global Industry Analysis, Size, Share, Growth, Trends, and Forecast 2014 - 2020*, in *Transparency Market Research*. 2015.
69. WANG Zhihui, K.M., YANG Xixian, LIU Xuecheng, HE Zhaohong, OSAKA Yugo, HUANG Hongyu, *Research Progress on Thermochemical Heat Storage System.* ADVANCES IN NEW AND RENEWABLE ENERGY, 2015. **3**(4): p. 289-298.
70. Kerskes H, M.B., Bertsch F. *Development of a thermo-chemical energy storage for solar thermal applications*. 2011. Kassel, Germany: Solar World Congress Proceedings.
71. Aydin D, C.S., Riffat S, *The latest advancements on thermochemical heat storage systems.* Renewable and Sustainable Energy Reviews, 2015. **41**: p. 356-367.
72. Wentworth, W. and E. Chen, *Simple thermal decomposition reactions for storage of solar thermal energy.* Solar Energy, 1976. **18**(3): p. 205-214.
73. Bales, C. *Chemical and sorption heat storage*. in *Proceedings of DANVAK Seminar, DANVAK Seminar (Solar Heating Systems–Combisystems-Heat Storage), November*. 2006.
74. Hadorn, J., *Thermal energy storage for solar and low energy buildings, State of the art by IEA Solar Heating and Cooling Task 32. Typeset by Servei de Publicacions (UdL)*. 2005, ISBN 84-8409-877-X.
75. Casey S, A.D., Riffat S, Elvins J, *Salt impregnated desiccant matrices for 'open' thermochemical energy storage - Hygrothermal cyclic behaviour and energetic analysis by physical experimentation.* Energy and Buildings, 2015. **92**: p. 128-139.
76. Posern, K. and C. Kaps, *Calorimetric studies of thermochemical heat storage materials based on mixtures of MgSO4 and MgCl2.* Thermochimica Acta, 2010. **502**(1–2): p. 73-76.
77. Abedin, A.H. and M.A. Rosen, *Closed and open thermochemical energy storage: energy-and exergy-based comparisons.* Energy, 2012. **41**(1): p. 83-92.

78. P, R.J., *Storage of thermal energy by means of an absorption cycle.* NASA STI/Recon Technical Report N, 1987. **88**.
79. Hadorn J C, S.G.B.B.C. *IEA solar heating and cooling programme task 32: advanced storage concepts for solar and low energy buildings*. 2006. Ecostock 2006-The 10th International Conference on Thermal Energy Storage.
80. Yang B, C.L., Ge Y, et al, *Exergy performance analyses of an irreversible two-stage intercooled regenerative reheated closed Brayton CHP plant.* International Journal of Exergy, 2014. **14**(4): p. 459-483.
81. Quinnell, J. and J. Davidson, *Heat and mass transfer during heating of a hybrid absorption/sensible storage tank.* Solar Energy, 2014. **104**: p. 19-28.
82. J.A. Quinnell, J.H.D., J. Burch, *Liquid calcium chloride solar storage: concept and analysis.* Journal of Solar Energy Engineering, 2011. **133**(1).
83. Woods J, P.J., Kozubal E, et al, *Design and experimental characterization of a membrane-based absorption heat pump.* Journal of membrane science, 2011. **378**(1): p. 85-94.
84. Woods J, K.E., *A desiccant-enhanced evaporative air conditioner: numerical model and experiments.* Energy Conversion and Management, 2013. **65**: p. 208-220.
85. A. Allouhi, T.K., A.Jamil, P. Bruel, Y. Mourad, Y. Zeraouli, *Solar driven cooling systems:An up dated review.* Renewable and Sustainable Energy Reviews, 2015. **44**: p. 159-181.
86. Worsøe-Schmidt, *Solar refrigeration for developing countries using a solid absorption cycle.* International Journal Ambient Energy, 1983. **4**: p. 115-24.
87. Park Y, K.J., Lee H., *Physical properties of the lithium bromide propanediol water system.* Int Journal Refrigeration, 1997. **20**: p. 319-325.
88. Ayala R, H.C., Holland F., *Ammonia/lithium nitrate absorption/compression refrigeration cycle - Part II Experimental.* ApplTherEng, 1998. **18**: p. 661-670.
89. F Agyenim, I.K., M Rhodes, *Design and experimental testing of the performance of an outdoor LiBr/H2O solar thermal absorption cooling system with a cold store.* Solar Energy, 2010. **84**(5): p. 735-744.
90. Anyanwu, E., *Review of solid adsorption solar refrigerator I: an overview of the refrigeration cycle.* Energy conversion and Management, 2003. **44**(2): p. 301-312.
91. Ullah, K., et al., *A review of solar thermal refrigeration and cooling methods.* Renewable and Sustainable Energy Reviews, 2013. **24**: p. 499-513.
92. Sakoda, A. and M. Suzuki, *Fundamental study on solar powered adsorption cooling system.* Journal of chemical engineering of Japan, 1984. **17**(1): p. 52-57.
93. Zhang, L.Z. and L. Wang, *Performance estimation of an adsorption cooling system for automobile waste heat recovery.* Applied Thermal Engineering, 1997. **17**(12): p. 1127-1139.
94. Sami, S. and C. Tribes, *An improved model for predicting the dynamic behaviour of adsorption systems.* Applied Thermal Engineering, 1996. **16**(2): p. 149-161.
95. Gartler G, J.D., Purkarthofer G, et al. *Development of a high energy density sorption storage system*. 2004. Freiburg, Germany: The EuroSun Conference.
96. A., H., *Adsorption systems for TES—design and demonstration projects.* Thermal energy storage for sustainable energy consumption, 2007: p. 409-427.
97. H., K., *DANVAK seminar (solar heating systems – Combisystems – heat storage).* Seasonal sorption heat storage, 2006.

98. Askalany, A.A., et al., *An overview on adsorption pairs for cooling.* Renewable and Sustainable Energy Reviews, 2013. **19**: p. 565-572.
99. Abbott, A.P., et al., *Novel solvent properties of choline chloride/urea mixtures.* Chemical Communications, 2003(1): p. 70-71.
100. D.S. Kim, C.A.F., *Solar refrigeration options-a state-of-the-art review.* International Journal of Refrigeration, 2008. **31**: p. 3-15.
101. Theo Elmer, M.W., Shenyi Wu, Saffa Riffat, *An experimental study of a novel integrated desiccant air conditioning system for building applications.* Energy and Buildings, 2016. **111**: p. 434-445.
102. Z. Duan, C.Z., Xingxing Zhang, Mahmud Mustafa, Xudong Zhao, Behrang Alimohammadisagvand, Ala Hasan, *Indirect evaporative cooling: past, present and future potentials.* Renewable Sustainable Energy Reviews, 2012. **16**(9): p. 6823-6850.
103. Hauer, A. *Thermal energy storage with zeolite for heating and cooling applications*. in *Proceedings of 3rd Workshop of Annex*. 2002.
104. J, B.-R., *Solar cooling using an open-cycle adsorption system with adiabatical mass transfer and external heat exchange.* Solar energy, 1985. **35**(1): p. 93-104.
105. Aristov, Y.I., *New family of solid sorbents for adsorptive cooling: material scientist approach.* Journal of Engineering Thermophysics, 2007. **16**(2): p. 63-72.
106. H Abedin, A. and M. A Rosen, *A critical review of thermochemical energy storage systems.* The Open Renewable Energy Journal, 2011. **4**(1).
107. Zondag, H., et al., *Prototype thermochemical heat storage with open reactor system.* Applied energy, 2013. **109**: p. 360-365.
108. Sahlot, M. and S.B. Riffat, *Desiccant cooling systems: a review.* International Journal of Low-Carbon Technologies, 2016. **11**(4): p. 489-505.
109. Zhang, Y.N., et al., *Development and thermochemical characterizations of vermiculite/SrBr2 composite sorbents for low-temperature heat storage.* Energy, 2016. **115, Part 1**: p. 120-128.
110. Jänchen, J. and H. Stach, *Adsorption properties of porous materials for solar thermal energy storage and heat pump applications.* Energy Procedia, 2012. **30**: p. 289-293.
111. Lim, K., J. Che, and J. Lee, *Experimental study on adsorption characteristics of a water and silica-gel based thermal energy storage (TES) system.* Applied Thermal Engineering, 2017. **110**: p. 80-88.
112. Bahrami, K.C.C.C.Y.H.C.M. *Heat And Mass Transfer Characteristics Of A Zeolite 13x/Cacl2 Composite Adsorbent In Adsorption Cooling Systems*. in *Proceedings of the ASME 2012 6th International Conference on Energy Sustainability & 10th Fuel Cell Science, Engineering and Technology Conference ESFuelCell 2012*
. 2012. San Diego, CA, USA.
113. Li, H., et al., *Design and synthesis of an exceptionally stable and highly porous metal-organic framework.* Nature, 1999. **402**(6759): p. 276-279.
114. Kyotani, T., et al., *Formation of new type of porous carbon by carbonization in zeolite nanochannels.* Chemistry of materials, 1997. **9**(2): p. 609-615.
115. Hamamoto, Y., et al., *Study on adsorption refrigeration cycle utilizing activated carbon fibers. Part 2. Cycle performance evaluation.* International Journal of Refrigeration, 2006. **29**(2): p. 315-327.
116. Tso, C.Y. and C.Y.H. Chao, *Activated carbon, silica-gel and calcium chloride composite adsorbents for energy efficient solar adsorption cooling and dehumidification systems.* International Journal of Refrigeration, 2012. **35**(6): p. 1626-1638.

117. Wu, Y. and T. Wang, *Hydrated salts/expanded graphite composite with high thermal conductivity as a shape-stabilized phase change material for thermal energy storage.* Energy Conversion and Management, 2015. **101**: p. 164-171.
118. Du, L. and S.C. Jana, *Highly conductive epoxy/graphite composites for bipolar plates in proton exchange membrane fuel cells.* Journal of Power Sources, 2007. **172**(2): p. 734-741.
119. Glaznev, I., et al., *Composites CaCl2/SBA-15 for adsorptive transformation of low temperature heat: Pore size effect.* International Journal of Refrigeration, 2011. **34**(5): p. 1244-1250.
120. Chen, C.-C., J.-S. Do, and Y. Gu, *Immobilization of HRP in Mesoporous Silica and Its Application for the Construction of Polyaniline Modified Hydrogen Peroxide Biosensor.* Sensors, 2009. **9**(6): p. 4635.
121. Carrero, A., et al., *Hydrogen production through glycerol steam reforming using Co catalysts supported on SBA-15 doped with Zr, Ce and La.* Journal of Energy Chemistry, 2017. **26**(1): p. 42-48.
122. Hamamoto, Y., et al., *Study on adsorption refrigeration cycle utilizing activated carbon fibers. Part 1. Adsorption characteristics.* International Journal of Refrigeration, 2006. **29**(2): p. 305-314.
123. Wang, A., et al., *Mineralization of an azo dye Acid Red 14 by electro-Fenton's reagent using an activated carbon fiber cathode.* Dyes and Pigments, 2005. **65**(3): p. 227-233.
124. Tatsidjodoung, P., et al., *Experimental and numerical investigations of a zeolite 13X/water reactor for solar heat storage in buildings.* Energy Conversion and Management, 2016. **108**: p. 488-500.
125. Rao, G.P.C., et al., *Sorption of cadmium and zinc from aqueous solutions by zeolite 4A, zeolite 13X and bentonite.* Journal of environmental management, 2006. **81**(3): p. 265-272.
126. Liu, H., K. Nagano, and J. Togawa, *A composite material made of mesoporous siliceous shale impregnated with lithium chloride for an open sorption thermal energy storage system.* Solar Energy, 2015. **111**: p. 186-200.
127. Gordeeva, L.G. and Y.I. Aristov, *Composites ‘salt inside porous matrix’ for adsorption heat transformation: a current state-of-the-art and new trends.* International Journal of Low-Carbon Technologies, 2012.
128. Bourikas, K., C. Kordulis, and A. Lycourghiotis, *The Role of the Liquid‐Solid Interface in the Preparation of Supported Catalysts.* Catalysis Reviews, 2006. **48**(4): p. 363-444.
129. Gong, L.X., et al., *Adsorption Equilibrium of Water on a Composite Adsorbent Employing Lithium Chloride in Silica Gel.* Journal of Chemical & Engineering Data, 2010. **55**(8): p. 2920-2923.
130. Aristov, Y.I., et al., *Selective water sorbents for multiple applications, 1. CaCl2 confined in mesopores of silica gel: Sorption properties.* Reaction Kinetics and Catalysis Letters, 1996. **59**(2): p. 325-333.
131. Gordeeva, L.G., et al., *Composites “lithium halides in silica gel pores”: Methanol sorption equilibrium.* Microporous and Mesoporous Materials, 2008. **112**(1–3): p. 254-261.
132. de Jong, A.-J., et al., *Thermochemical heat storage–from reaction storage density to system storage density.* Energy Procedia, 2016. **91**: p. 128-137.
133. Craig, B., *DS Anderson Handbook of corrosion data.* ASM International, USA, 1995.

134. Warnqvist, B., *Comments on thermochemical data and fusion temperature for pure sodium sulfide.* Thermochimica Acta, 1980. **37**(3): p. 343-345.
135. Roelands, M., et al., *Preparation & characterization of sodium sulfide hydrates for application in thermochemical storage systems.* Energy Procedia, 2015. **70**: p. 257-266.
136. Jiang, J., et al., *Hydrogen sulfide—mechanisms of toxicity and development of an antidote.* Scientific reports, 2016. **6**: p. 20831.
137. Donkers, P., et al., *A review of salt hydrates for seasonal heat storage in domestic applications.* Applied Energy, 2017. **199**: p. 45-68.
138. Isbell, R., *The Australian soil classification*. 2016: CSIRO publishing.
139. Boer R, H.W.G., Veldhuis J B J, et al. *Solid-sorption cooling with integrated thermal storage-the SWEAT prototype*. in *The 3rd International Heat Powered Cycles Conference (HPC 2004)*. 2004. Larnaca, Cyprus.
140. Ranade S M, L.M.C., Prengle H W., *Chemical storage of solar energy kinetics of heterogeneous SO3 and H2O reaction—Reaction analysis and reactor design.* Solar energy, 1990. **44**(6): p. 321-332.
141. Wongsuwan W, K.S., Neveu P, et al, *A review of chemical heat pump technology and applications.* Applied Thermal Engineering, 2001. **21**(15): p. 1489-1519.
142. Ibrahim M, S.K., Daud W R W, et al, *Solar chemical heat pump drying system for tropical region.* WSEAS Transactions on Environment and Development, 2009. **5**(5): p. 404-413.
143. Ogura H, Y.T., Kage H, et al, *Effects of heat exchange condition on hot air production by a chemical heat pump dryer using CaO/H 2 O/Ca (OH) 2 reaction[J]. .* Chemical Engineering Journal, 2002. **86**(1): p. 3-10.
144. Mauran, S., H. Lahmidi, and V. Goetz, *Solar heating and cooling by a thermochemical process. First experiments of a prototype storing 60kWh by a solid/gas reaction.* Solar Energy, 2008. **82**(7): p. 623-636.
145. Sharonov V E, A.Y.I., *Chemical and adsorption heat pumps: comments on the second law efficiency.* Chemical Engineering Journal, 2008. **136**(2): p. 419-424.
146. Kim S T, R.J., Kato Y, *Reactivity enhancement of chemical materials used in packed bed reactor of chemical heat pump.* Progress in Nuclear Energy, 2011. **53**(7): p. 1027-1033.
147. Kim S T, R.J., Kato Y., *The optimization of mixing ratio of expanded graphite mixed chemical heat storage material for magnesium oxide/water chemical heat pump.* Applied Thermal Engineering, 2014. **66**(1): p. 274-281.
148. Myagmarjav O, R.J., Kato Y, *Lithium bromide-mediated reaction performance enhancement of a chemical heat-storage material for magnesium oxide/water chemical heat pumps.* Applied Thermal Engineering, 2014. **63**(1): p. 170-176.
149. Buker, M.S. and S.B. Riffat, *Recent developments in solar assisted liquid desiccant evaporative cooling technology—A review.* Energy and Buildings, 2015. **96**: p. 95-108.
150. Cuce, P.M. and S. Riffat, *A state of the art review of evaporative cooling systems for building applications.* Renewable and Sustainable Energy Reviews, 2016. **54**: p. 1240-1249.
151. Zhao, X., et al., *Feasibility study of a novel dew point air conditioning system for China building application.* Building and Environment, 2009. **44**(9): p. 1990-1999.
152. Maisotsenko, V., et al., *Method and plate apparatus for dew point evaporative cooler*. 2003, Google Patents.

153. Amer, O., R. Boukhanouf, and H. Ibrahim, *A review of evaporative cooling technologies.* International journal of environmental science and development, 2015. **6**(2): p. 111.
154. Zheng, X., T. Ge, and R. Wang, *Recent progress on desiccant materials for solid desiccant cooling systems.* Energy, 2014. **74**: p. 280-294.
155. Baniyounes, A.M., et al., *An overview of solar assisted air conditioning in Queensland's subtropical regions, Australia.* Renewable and Sustainable Energy Reviews, 2013. **26**: p. 781-804.
156. Elmer, T., et al., *An experimental study of a novel integrated desiccant air conditioning system for building applications.* Energy and Buildings, 2016. **111**: p. 434-445.
157. Bergida, D.D.L.R., *Cooling agent for cold packs and food and beverage containers*. 2017: US.
158. Collins, P., *Self-Cooling Beverage Can*. 2011: US.
159. Cuce P M, R.S., *A state of the art review of evaporative cooling systems for building applications.* Renewable and Sustainable Energy Reviews, 2016. **54**: p. 1240-1249.
160. L, K., *New evaporative cooling systems: an emerging solution for homes in hot dry climates with modest cooling loads.* SWEEP, 2007. **5**.
161. Zhang H, S.Y., Hongxing Y, *Enhanced performance of air-cooled chillers using evaporative cooling.* Building Services Engineering Research and Technology, 2000. **21**(4): p. 213-217.
162. Ibrahim E, S.L., Riffat S B, *Performance of porous ceramic evaporators for building cooling application.* Energy and Buildings, 2003. **35**(9): p. 941-949.
163. Taufiq B N, M.H.H., Mahlia T M I, *Exergy analysis of evaporative cooling for reducing energy use in a Malaysian building.* Desalination, 2007. **209**(1): p. 238-243.
164. Krüger E, C.E.G., Givoni B, *Effectiveness of indirect evaporative cooling and thermal mass in a hot arid climate.* Building and Environment, 2010. **45**(6): p. 1422-1433.
165. Maheshwari G P, A.-R.F., Suri R K, *Energy-saving potential of an indirect evaporative cooler.* Applied Energy, 2001. **69**(1): p. 69-76.
166. Hajidavalloo, *Application of evaporative cooling on the condenser of window-air-conditioner.* Applied Thermal Engineering, 2007. **27**(11): p. 1937-1943.
167. Camargo J R, E.C.D., *A mathematical model for direct and indirect evaporative cooling air conditioning systems.* BRAZILIAN CONGRESS OF THERMAL ENGINEERING AND SCIENCES, 2002. **9**.
168. Watt, J., *Evaporative air conditioning handbook*. 1963, New York: Springer Science & Business Media.
169. Riangvilaikul, B. and S. Kumar, *Numerical study of a novel dew point evaporative cooling system.* Energy and Buildings, 2010. **42**(11): p. 2241-2250.
170. Mahmood, M.H., et al., *Overview of the Maisotsenko cycle–A way towards dew point evaporative cooling.* Renewable and Sustainable Energy Reviews, 2016. **66**: p. 537-555.
171. Caliskan, H., et al., *Thermodynamic performance assessment of a novel air cooling cycle: Maisotsenko cycle.* International Journal of Refrigeration, 2011. **34**(4): p. 980-990.
172. T.S. Ge, J.C.X., *Review of solar-powered desiccant cooling systems.* Advances in Solar Heating and Cooling, 2016: p. 329-379.

173. N. Enteria, H.Y., A. Mochida, R. Takaki, A. Satake, R. Yoshie, *Construction and initial operation of the combined solar thermal and electric desiccant cooling system.* Solar Energy, 2009. **83**: p. 1300-1311.
174. S. Jain, P.K.B., *Performance analysis of liquid desiccant dehumidification systems.* International Journal of Refrigeration, 2007. **30**(5): p. 861-872.
175. Abdulrahman Th. Mohammada, S.B.M., K. Sopian, Abduljalil A. Al-abidi, *Review: Survey of the control strategy of liquid desiccant systems.* Renewable and Sustainable Energy Reviews, 2016. **58**: p. 250-258.
176. M. Mujahid Rafique, P.G., Luai M. Al-Hadhrami, and Shafiqur Rehman, *Energy, Exergy and Anergy Analysis of a Solar Desiccant Cooling System.* Journal of Clean Energy Technologies, 2016. **4**(1): p. 78-83.
177. Bales, C., et al., *Thermal properties of materials for thermo-chemical storage of solar heat.* A Report of IEA Solar Heating and Cooling programme–Task, 2005. **32**.
178. Y. Zhao, Y.J.D., T.S. Ge, H.H. Wang, R.Z. Wang, *A high performance desiccant dehumidification unit using solid desiccant coated heat exchanger with heat recovery.* Energy and Buildings, 2016. **116**: p. 583-592.
179. Muzaffar Ali, V.V., , Nadeem Ahmed Sheikh, , Hafiz M. Ali, *Performance investigation of solid desiccant evaporative cooling system configurations in different climatic zones.* Energy Conversion and Management, 2015. **97**: p. 323-339.
180. Stefano De Antonellis, C.M.J., Luca Molinaroli, *Simulation, performance analysis and optimization of desiccant wheels.* Energy and Buildings, 2010. **42**(9): p. 1386-1393.
181. CEL Nóbrega, N.B., *An Introduction to Solid Desiccant Cooling Technology*, in *Desiccant-Assisted Cooling*. 2014, Springer London: London. p. 1-23.
182. G. Panaras, E.M., V. Belessiotis, *Solid desiccant air-conditioning systems – Design parameters.* Energy, 2011. **36**(5): p. 2399-2406.
183. Rouquerol J, R.F., Llewellyn P, *Adsorption by powders and porous solids: principles, methodology and applications*. 2013: Academic press.
184. Weilong Wang, L.W., Zhong Li , Yutang Fang , Jing Ding & Jing Xiao, *Reviews An Overview of Adsorbents in the Rotary Desiccant Dehumidifier for Air Dehumidification.* AnInternation Journal of Drying Technology, 2013. **31**(12): p. 1334-1345.
185. X. Zheng, T.S.G., R.Z. Wang, *Recent progress on desiccant materials for solid desiccant cooling systems.* Energy, 2014. **74**: p. 280-294.
186. Cohen, P.S. and S.M. Cohen, *Wöhler's synthesis of urea: how do the textbooks report it?* J. Chem. Educ, 1996. **73**(9): p. 883.
187. Bundy, L.G., *Managing Urea-Containing Fertilizers.* University of Wisconsin, 2001.
188. L, G.R., *Urea cold pack having an inner bag provided with a perforated seal*. 1976: U.S.
189. Kruckman J, C.J., *Dry Instant Cold Pack and Method of Use: U.S. Patent Application*. 2016: U.S.
190. Gunhan, T., et al., *Experimental exergetic performance evaluation of a novel solar assisted LiCl–H 2 O absorption cooling system.* Energy and Buildings, 2014. **68**: p. 138-146.
191. Diarce, G., et al., *The sodium nitrate–urea binary mixture as a phase change material for medium temperature thermal energy storage. Part I: Determination of the phase diagram and main thermal properties.* Solar Energy Materials and Solar Cells, 2016.
192. Ge, T., et al., *Experimental study on a two-stage rotary desiccant cooling system.* International Journal of Refrigeration, 2009. **32**(3): p. 498-508.

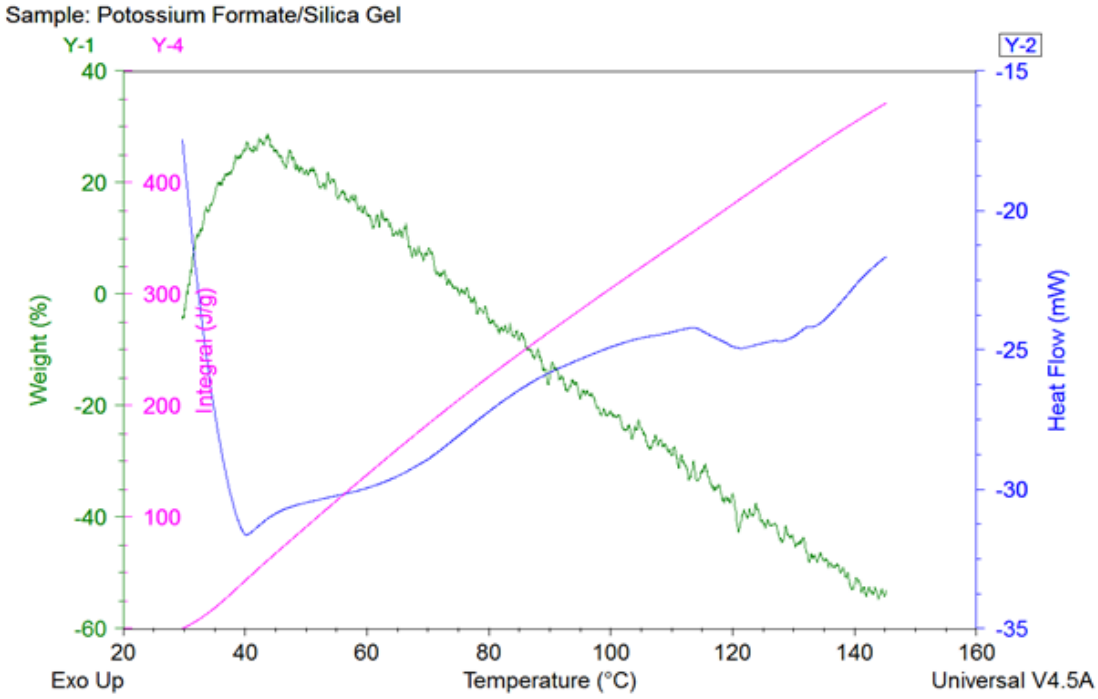
193. Gordeeva, L.G., et al., *Composite sorbent of methanol "lithium chloride in mesoporous silica gel" for adsorption cooling machines: performance and stability evaluation.* Industrial & Engineering Chemistry Research, 2009. **48**(13): p. 6197-6202.
194. Gordeeva, L.G. and Y.I. Aristov, *Composite sorbent of methanol "LiCl in mesoporous silica gel" for adsorption cooling: dynamic optimization.* Energy, 2011. **36**(2): p. 1273-1279.
195. Zhang, X. and L. Qiu, *Moisture transport and adsorption on silica gel–calcium chloride composite adsorbents.* Energy Conversion and Management, 2007. **48**(1): p. 320-326.
196. Huang, H., et al., *Development research on composite adsorbents applied in adsorption heat pump.* Applied Thermal Engineering, 2010. **30**(10): p. 1193-1198.
197. Cortés, F.B., et al., *Water sorption on silica-and zeolite-supported hygroscopic salts for cooling system applications.* Energy Conversion and Management, 2012. **53**(1): p. 219-223.
198. Aristov, Y.I., et al., *Reallocation of adsorption and desorption times for optimisation of cooling cycles.* International Journal of refrigeration, 2012. **35**(3): p. 525-531.
199. Sukhyy, K.M., et al., *Structure and adsorption properties of the composites 'silica gel–sodium sulphate', obtained by sol–gel method.* Applied Thermal Engineering, 2014. **64**(1): p. 408-412.
200. Ponomarenko, I., et al., *Synthesis and water sorption properties of a new composite "CaCl 2 confined into SBA-15 pores".* Microporous and Mesoporous Materials, 2010. **129**(1): p. 243-250.
201. Zheng, X., et al., *Performance study of SAPO-34 and FAPO-34 desiccants for desiccant coated heat exchanger systems.* Energy, 2015. **93**: p. 88-94.
202. Glaznev, I., et al., *Composites CaCl 2/SBA-15 for adsorptive transformation of low temperature heat: pore size effect.* International journal of refrigeration, 2011. **34**(5): p. 1244-1250.
203. Pei, L. and L. Zhang, *Preparation and selective adsorption of core–shell desiccant for heat and moisture recovery.* Colloids and Surfaces A: Physicochemical and Engineering Aspects, 2012. **406**: p. 68-74.
204. Nakabayashi, S., et al., *Improvement of water vapor adsorption ability of natural mesoporous material by impregnating with chloride salts for development of a new desiccant filter.* Adsorption, 2011. **17**(4): p. 675-686.
205. Sapienza, A., et al., *Adsorption chilling driven by low temperature heat: new adsorbent and cycle optimization.* Applied Thermal Engineering, 2012. **32**: p. 141-146.
206. Zheng, X., R. Wang, and T. Ge, *Experimental study and performance predication of carbon based composite desiccants for desiccant coated heat exchangers.* International Journal of Refrigeration, 2016. **72**: p. 124-131.
207. Wang, J., R. Wang, and L. Wang, *Water vapor sorption performance of ACF-CaCl 2 and silica gel-CaCl 2 composite adsorbents.* Applied Thermal Engineering, 2016. **100**: p. 893-901.
208. Tian, H., et al., *Preparation of binary eutectic chloride/expanded graphite as high-temperature thermal energy storage materials.* Solar Energy Materials and Solar Cells, 2016. **149**: p. 187-194.
209. Sharafian, A., et al., *Performance analysis of a novel expansion valve and control valves designed for a waste heat-driven two-adsorber bed adsorption cooling system.* Applied Thermal Engineering, 2016. **100**: p. 1119-1129.

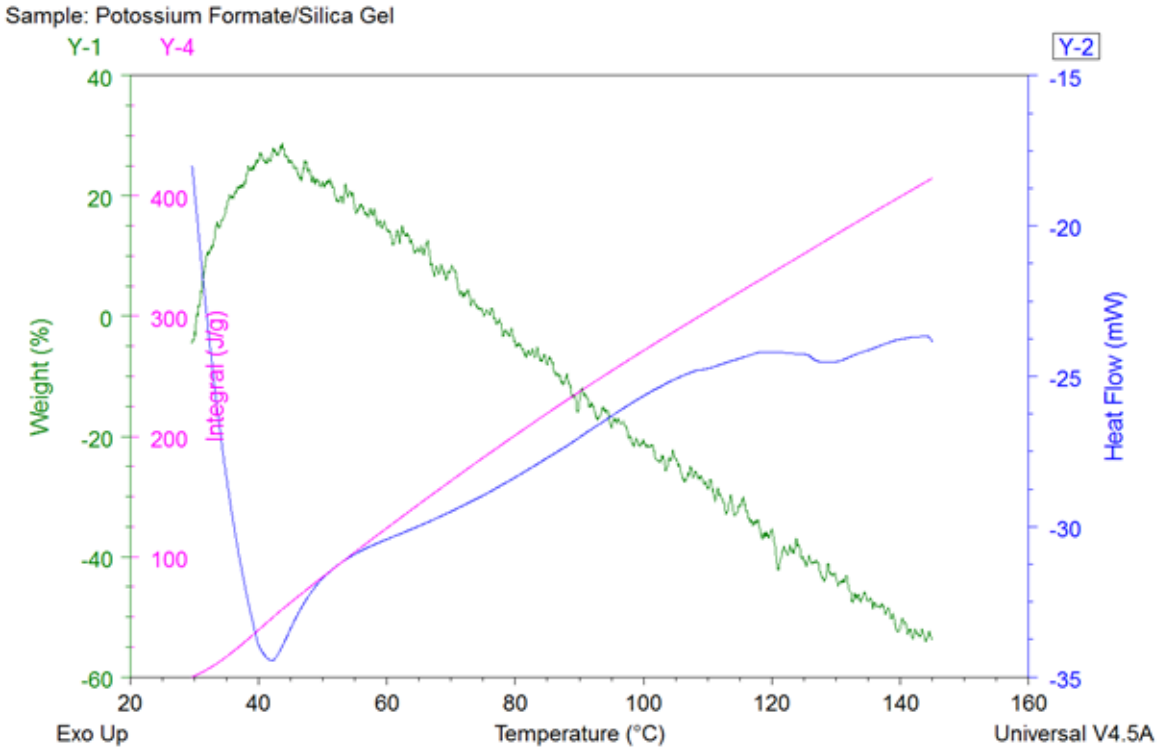
210. Elsayed, E., et al., *Aluminium fumarate and CPO-27 (Ni) MOFs: characterization and thermodynamic analysis for adsorption heat pump applications.* Applied Thermal Engineering, 2016. **99**: p. 802-812.
211. Kim, S.-I., et al., *Metal–organic frameworks with high working capacities and cyclic hydrothermal stabilities for fresh water production.* Chemical Engineering Journal, 2016. **286**: p. 467-475.
212. Muiambo, H.F., *Preparation and properties of flame retarded vermiculite composites*. 2015, University of Pretoria.
213. Longo, G.A. and A. Gasparella, *Experimental measurement of thermophysical properties of H2O/KCOOH (potassium formate) desiccant.* International Journal of Refrigeration, 2016. **62**: p. 106-113.
214. Le Pierrès, N., et al., *Long-term solar heat storage process by absorption with the KCOOH/H2O couple: Experimental investigation.* Energy, 2017. **141**: p. 1313-1323.
215. Luo, Y., et al. *Experimental and Numerical Study on the Dehumidification Performance of KCOOH Solution*. in *Multidisciplinary Digital Publishing Institute Proceedings*. 2018.
216. Wen, T., et al., *Thermal properties study and performance investigation of potassium formate solution in a falling film dehumidifier/regenerator.* International Journal of Heat and Mass Transfer, 2019. **134**: p. 131-142.
217. Longo, G.A. and A. Gasparella, *Experimental and theoretical analysis of heat and mass transfer in a packed column dehumidifier/regenerator with liquid desiccant.* International Journal of Heat and Mass Transfer, 2005. **48**(25-26): p. 5240-5254.
218. Jradi, M. and S. Riffat, *Energy performance of an innovative liquid desiccant dehumidification system with a counter-flow heat and mass exchanger using potassium formate.* Renewable Bioresources, 2014. **2**(1): p. 5.
219. Riffat, S., S. James, and C. Wong, *Experimental analysis of the absorption and desorption rates of HCOOK/H2O and LiBr/H2O.* International journal of energy research, 1998. **22**(12): p. 1099-1103.
220. Afonso, C.F., *Recent advances in building air conditioning systems.* Applied Thermal Engineering, 2006. **26**(16): p. 1961-1971.
221. Salyer, I.O., *Compositions for thermal energy storage or thermal energy generation*. 1996, Google Patents.
222. Gangopadhyay, R. and S. Das, *Ammonia leakage from refrigeration plant and the management practice.* Process Safety Progress, 2008. **27**(1): p. 15-20.
223. Azeem, B., et al., *Review on materials & methods to produce controlled release coated urea fertilizer.* Journal of controlled release, 2014. **181**: p. 11-21.
224. 123, *aaa.* renewable energy, 2015. **48**: p. 128-136.
225. Intini M, G.M., White S, et al, *Experimental analysis and numerical modelling of an AQSOA zeolite desiccant wheel.* Applied Thermal Engineering, 2015. **80**: p. 20-30.
226. Qiong Li, W.G., Wenxian Lin, Tao Liu, Yougang Zhang, Xiang Ding, Xiaoqiao Huang, Wuming Liu, *Experiment and Simulation Study on Convective Heat Transfer of All-glass Evacuated Tube Solar Collector*, in *Renewable Energy*. 2020.
227. Abdul Waheed Badar, R.B., Felix Ziegler, *Experimental and theoretical evaluation of the overall heat loss coefficient of vacuum tubes of a solar collector*, in *Applied Thermal Engineering*. 2019. p. 315-325.

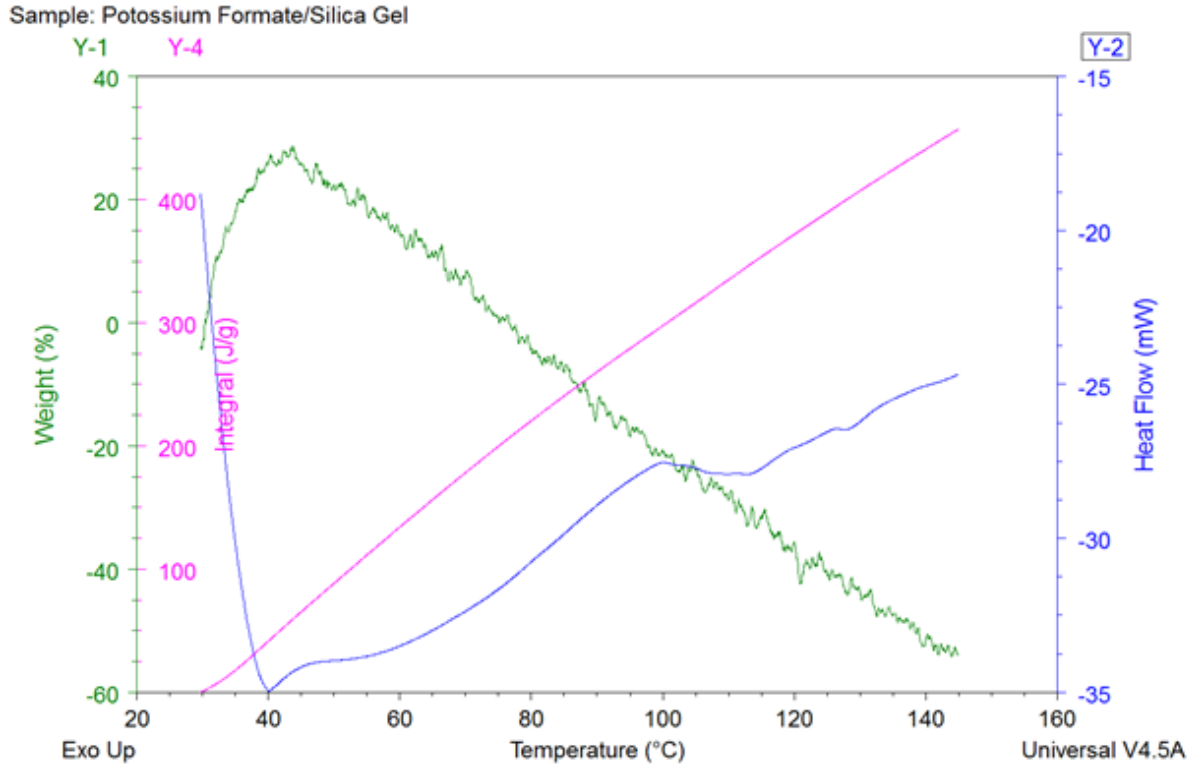
228. Colmenar-Santos, A., et al., *District heating and cogeneration in the EU-28: Current situation, potential and proposed energy strategy for its generalisation.* Renewable and Sustainable Energy Reviews, 2016. **62**: p. 621-639.
229. BYD Co. Ltd, G.Y.C.e.a., *Energy Storage Market - Growth, Trends, and Forecast (2020 - 2025).* Energy Storage, 2020.
230. Henze, V., *Energy Storage Investments Boom As Battery Costs Halve in the Next Decade.* BloombergNEF, 2019.
231. Osborne, M.J., *A resolution to the NPV–IRR debate?* The Quarterly Review of Economics and Finance, 2010. **50**(2): p. 234-239.
232. Wetekamp, W. *Net Present Value (NPV) as a tool supporting effective project management*. in *Proceedings of the 6th IEEE International Conference on Intelligent Data Acquisition and Advanced Computing Systems*. 2011. IEEE.
233. Jan Steinbach, D.S., *Discount rates in energy system analysis.* Buildings Performance Institute Europe (BPIE), 2015.

APPENDIX A: TA INSTRUMENT ANALYSIS RUNNING RESULTS FOR SDT-Q600

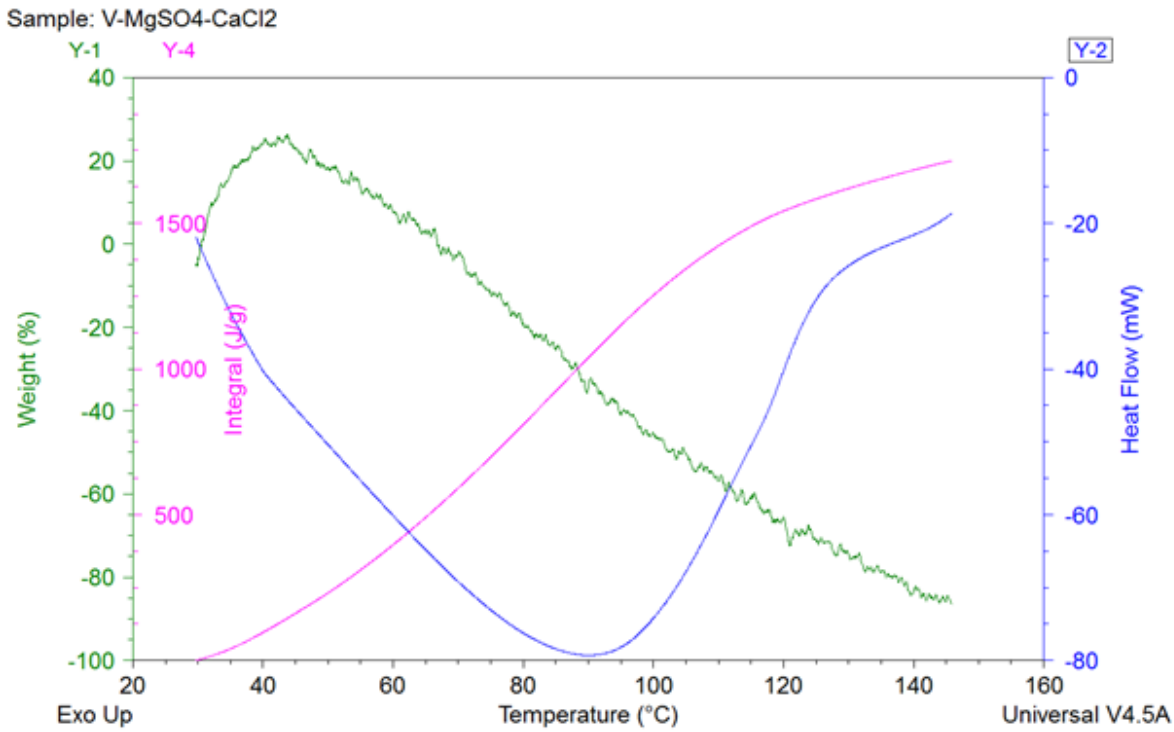
a. PF-SG



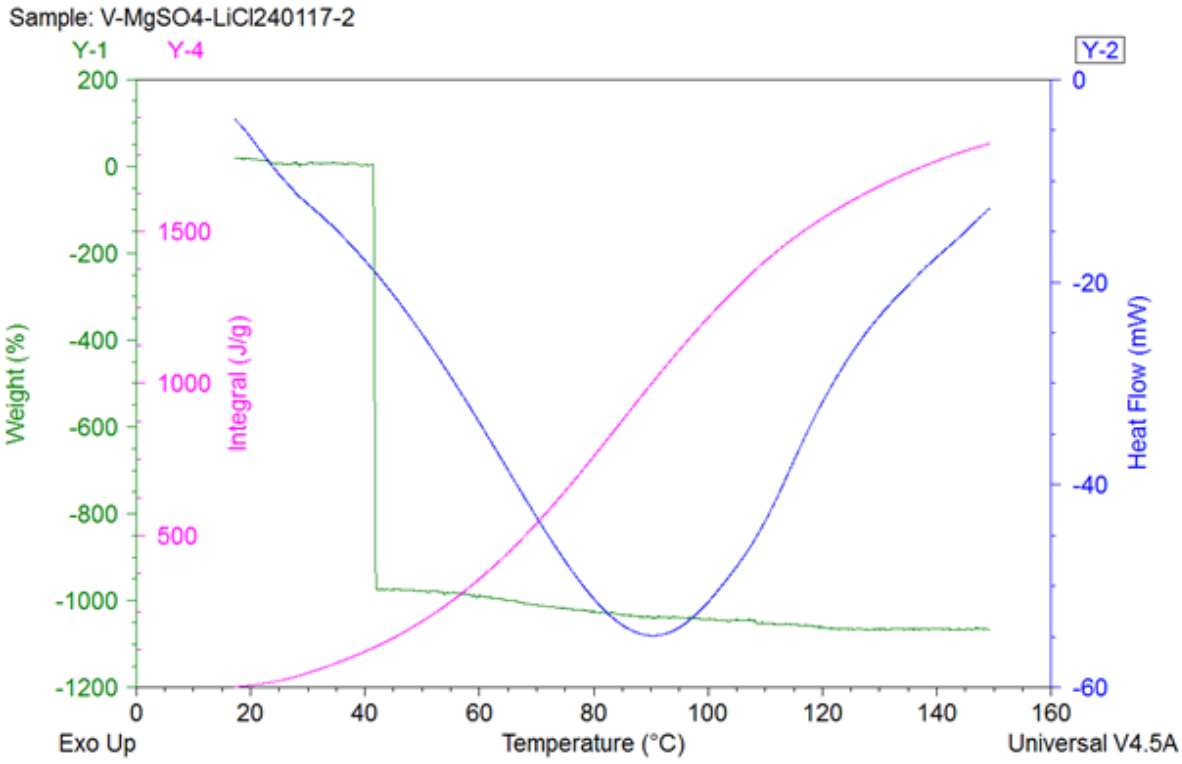


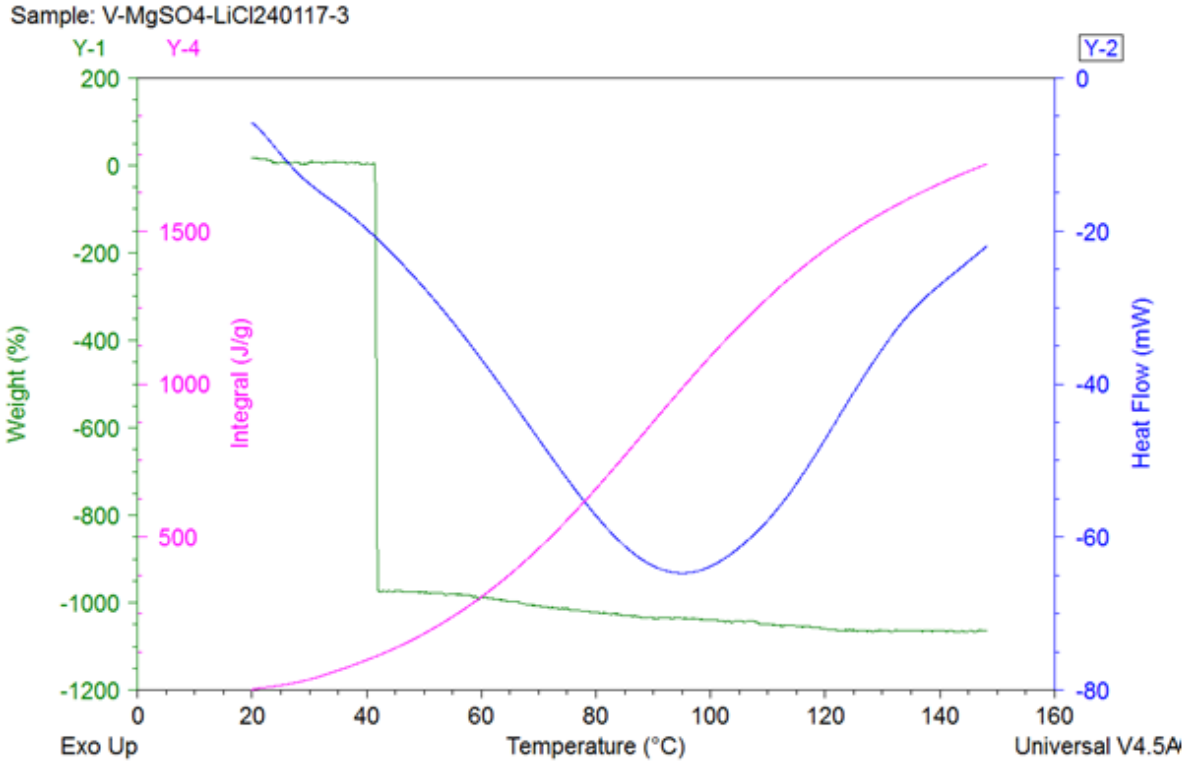


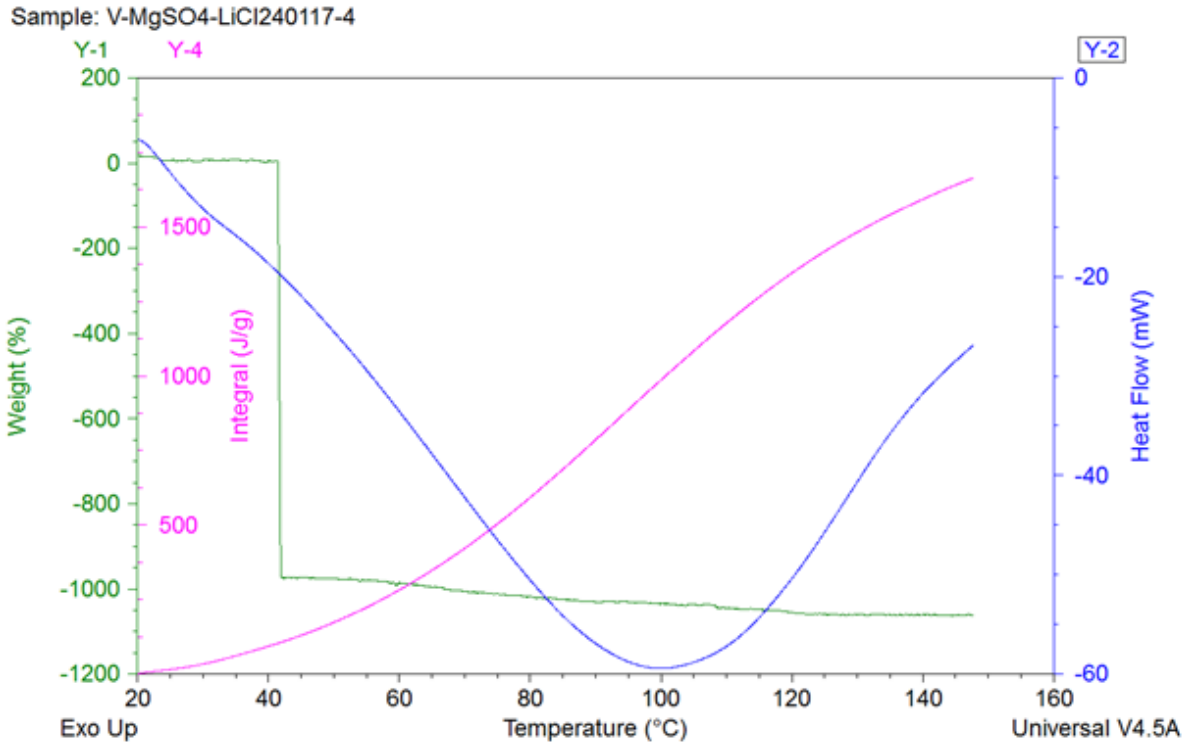
b. V-$MgSO_4$-$CaCl_2$ (1:2)



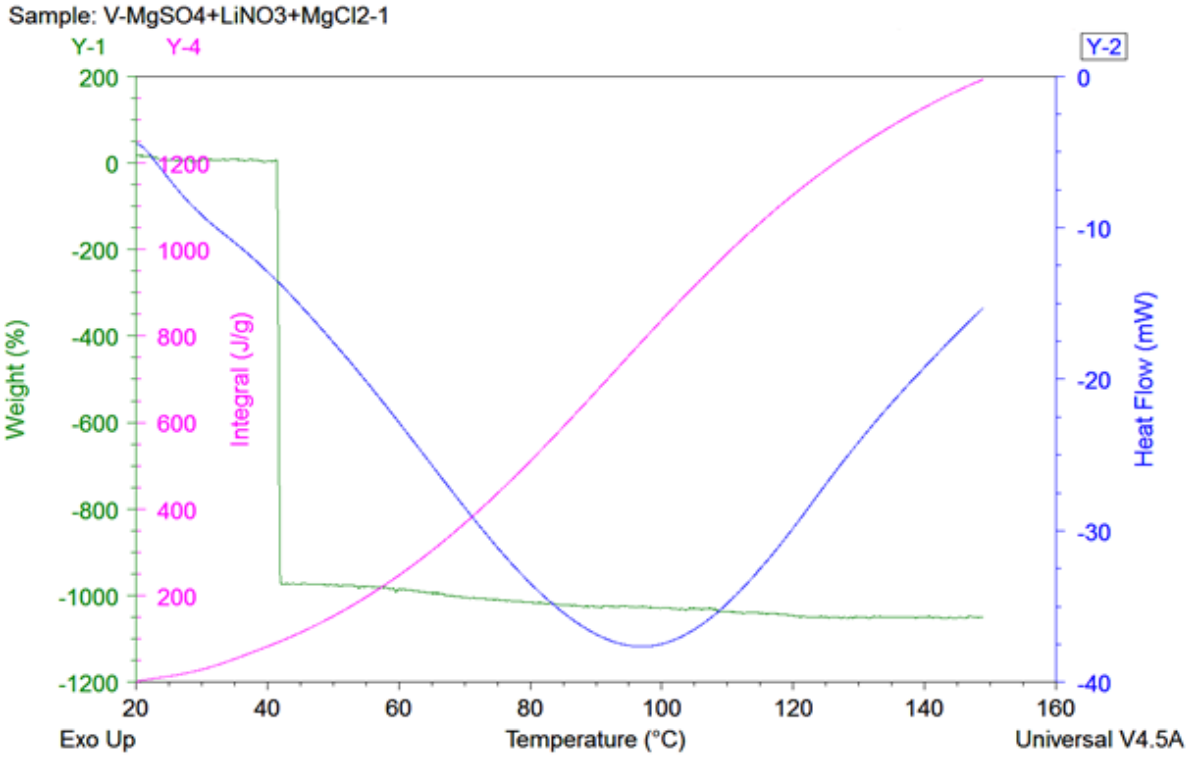
c. V-$MgSO_4$-LiCl

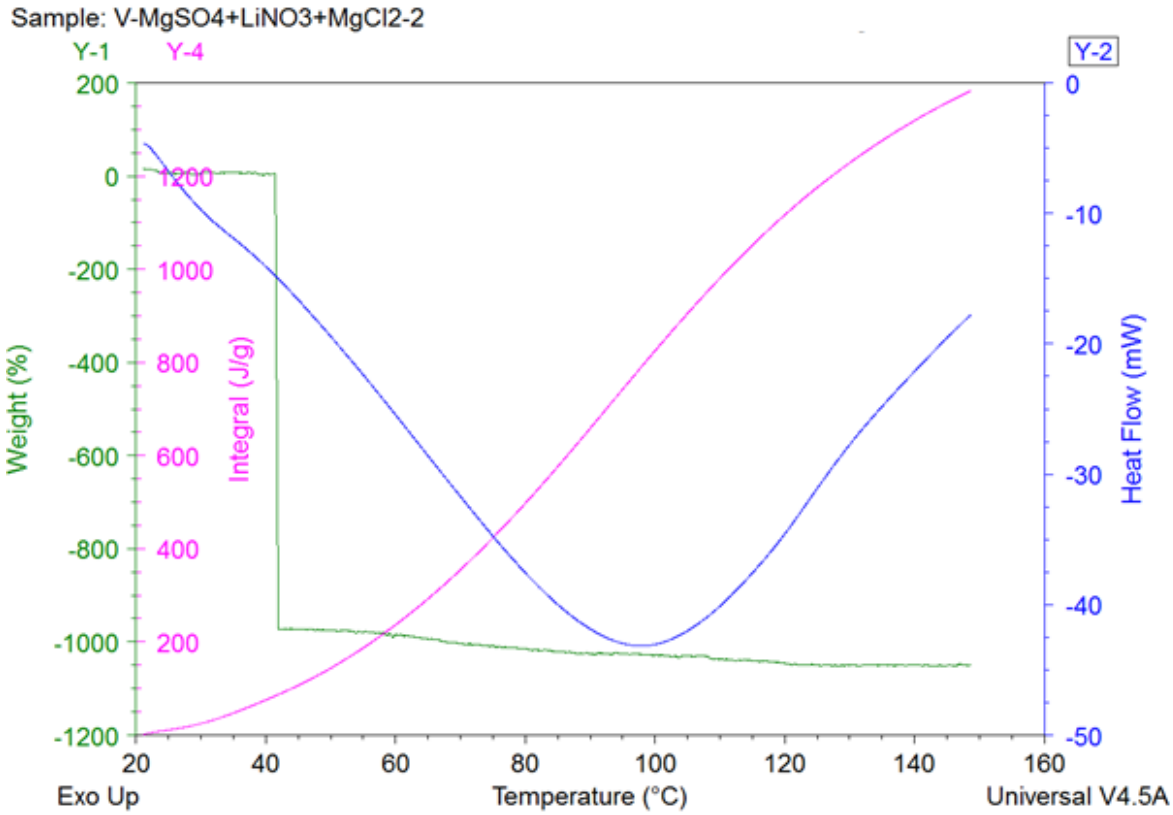


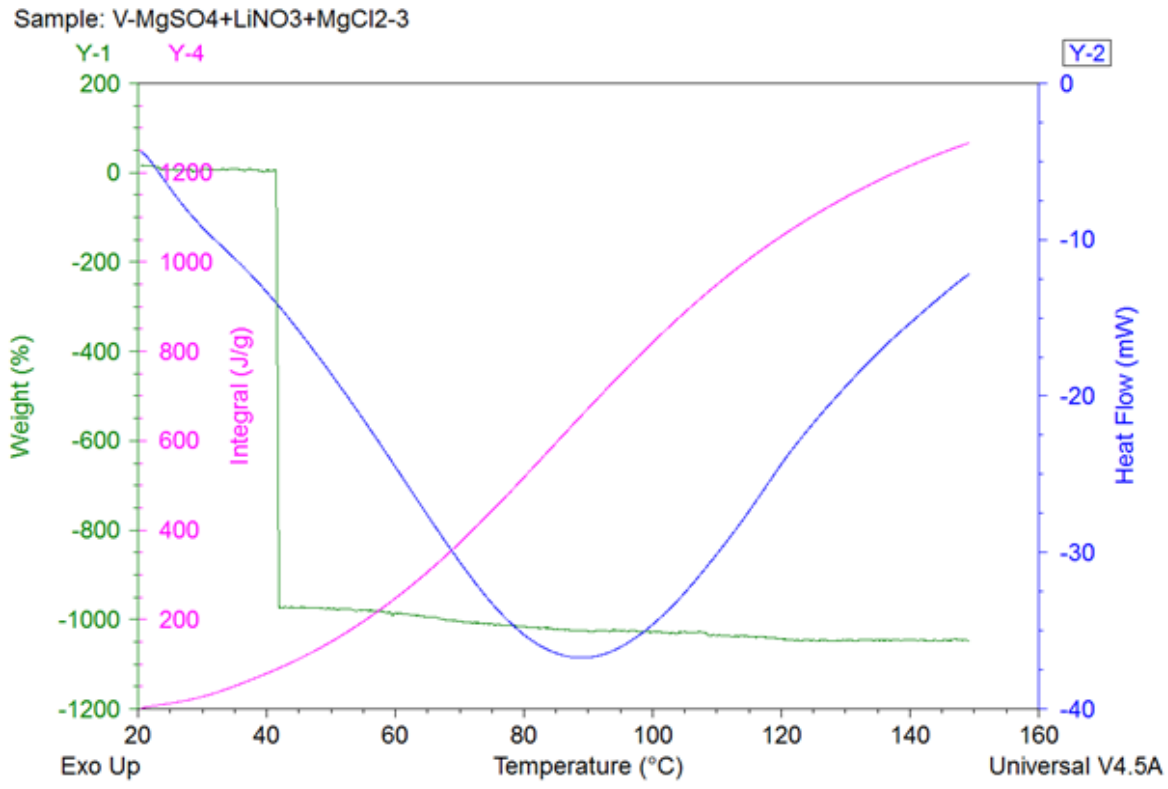




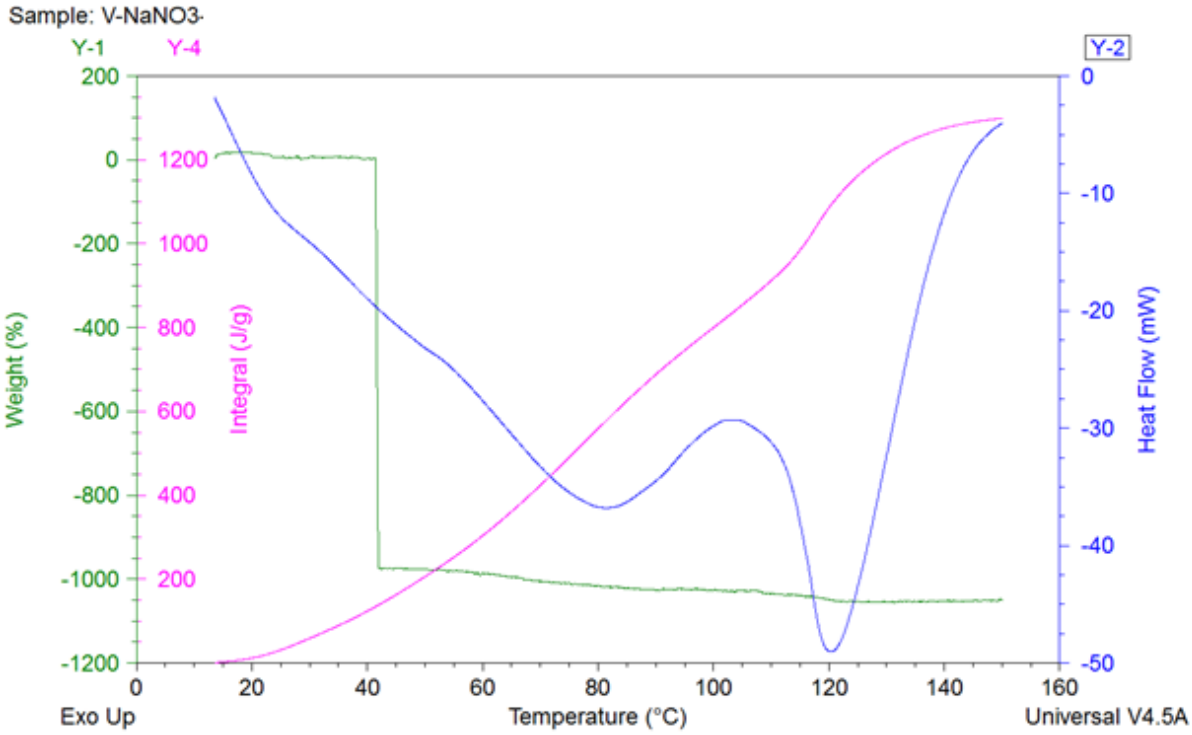
d. V-$MgSO_4$-$LiNO_3$-$MgCl_2$

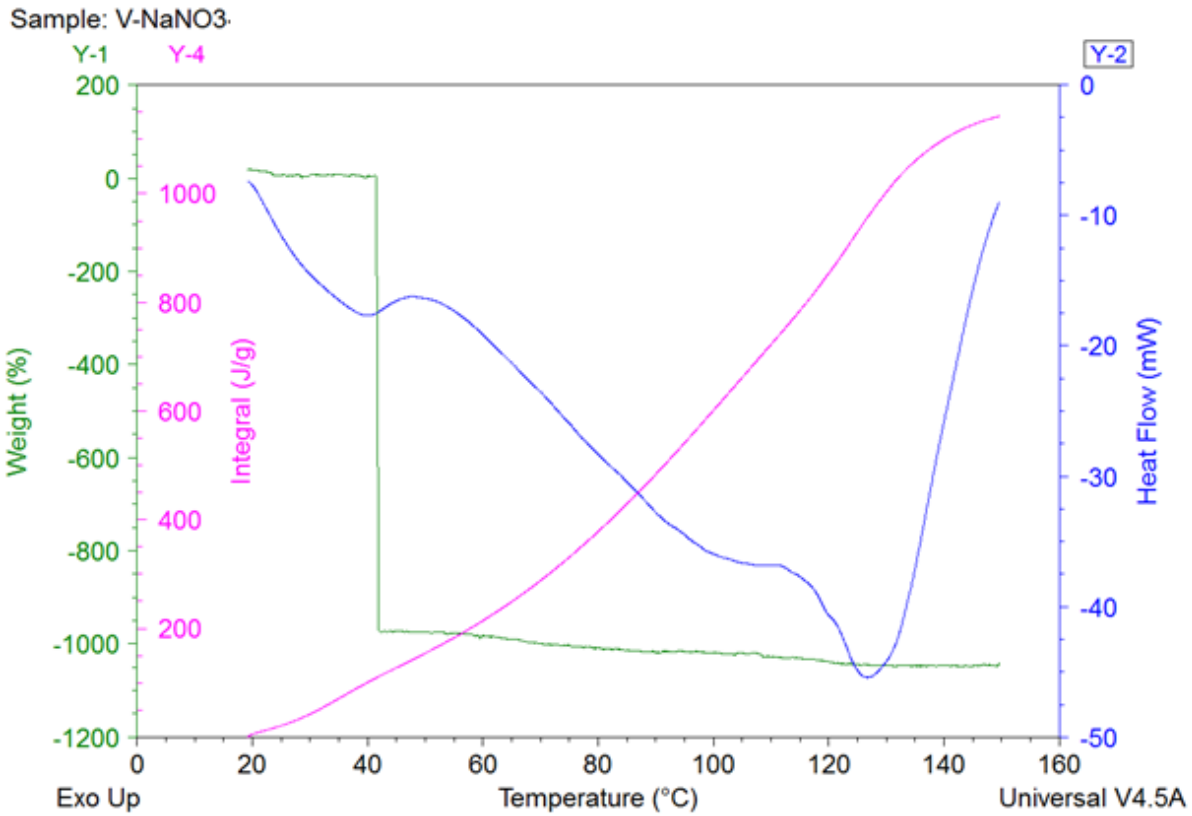


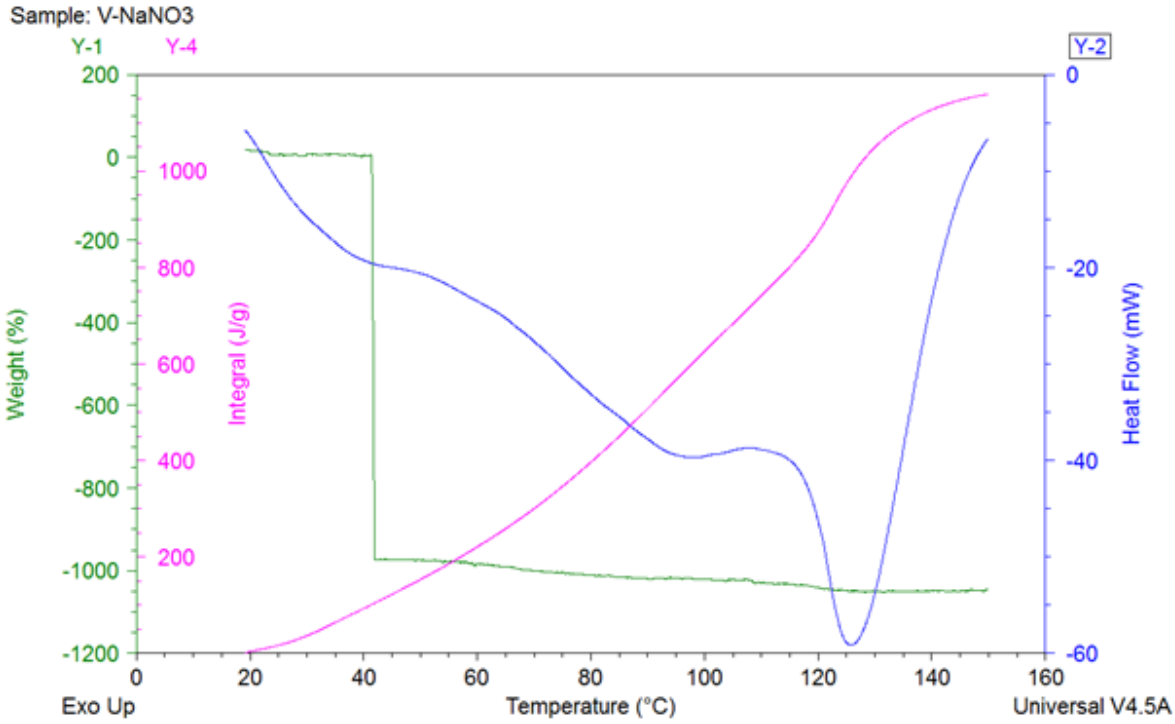

Sample: V-MgSO4+LiNO3+MgCl2-2
Y-1
Y-4
Y-2
Weight (%)
Integral (J/g)
Heat Flow (mW)
Exo Up
Temperature (°C)
Universal V4.5A

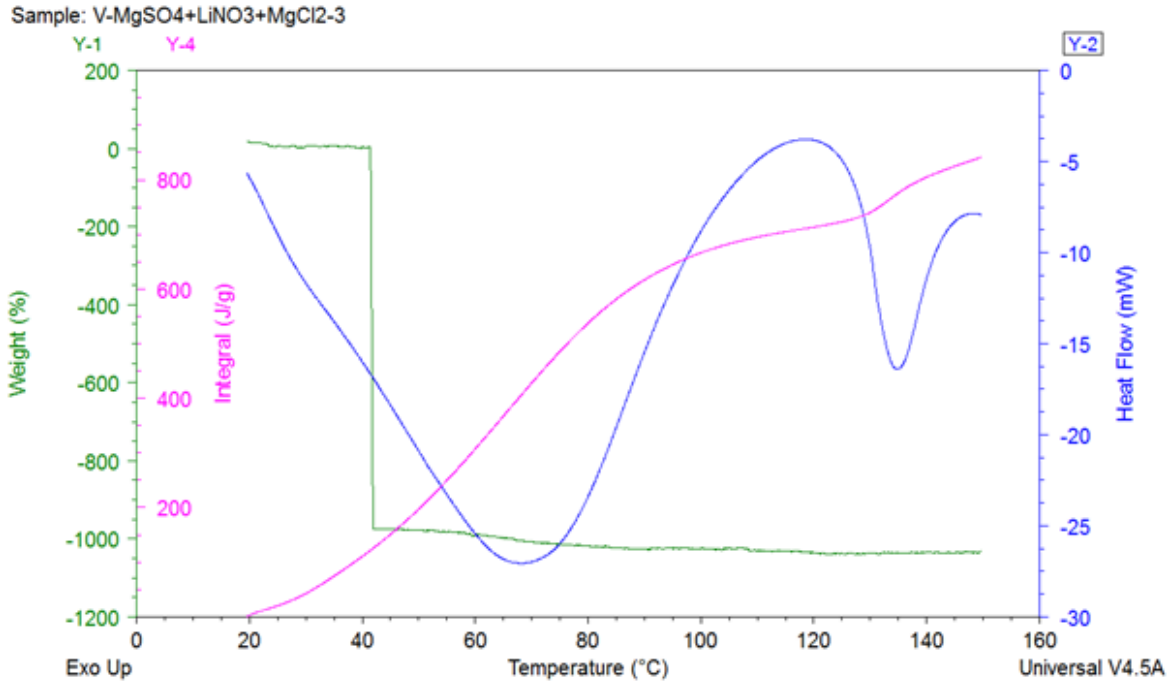

Sample: V-MgSO4+LiNO3+MgCl2-3
Y-1
Y-4
Y-2
Weight (%)
Integral (J/g)
Heat Flow (mW)
Exo Up
Temperature (°C)
Universal V4.5A

e. V-NaNO3

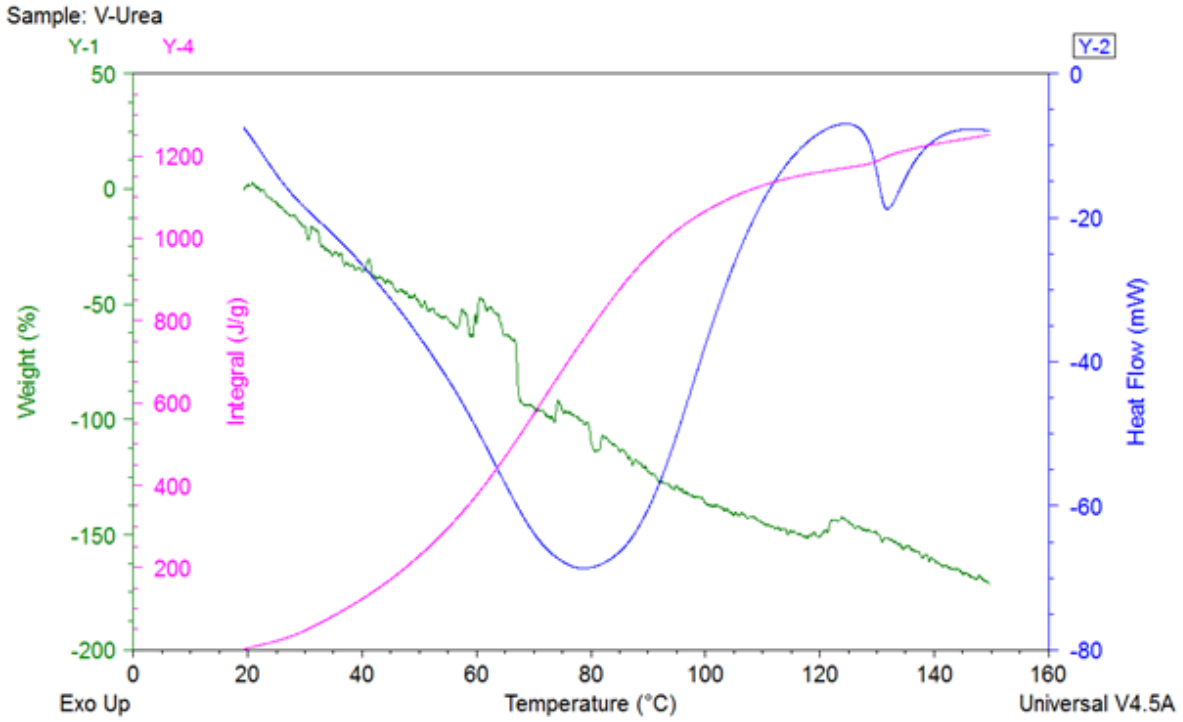

Sample: V-NaNO3-
Y-1
Y-4
Y-2
Weight (%)
Integral (J/g)
Heat Flow (mW)
Exo Up
Temperature (°C)
Universal V4.5A

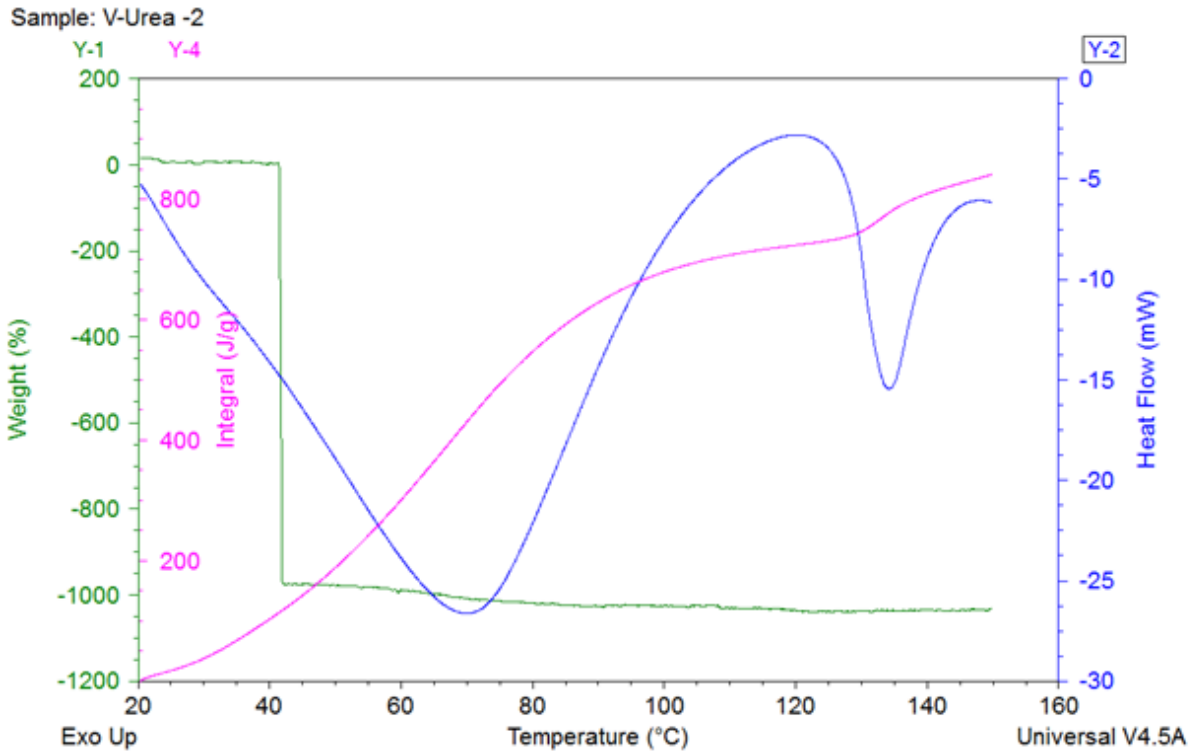

Sample: V-NaNO3-
Y-1
Y-4
Y-2
Weight (%)
Integral (J/g)
Heat Flow (mW)
Exo Up
Temperature (°C)
Universal V4.5A

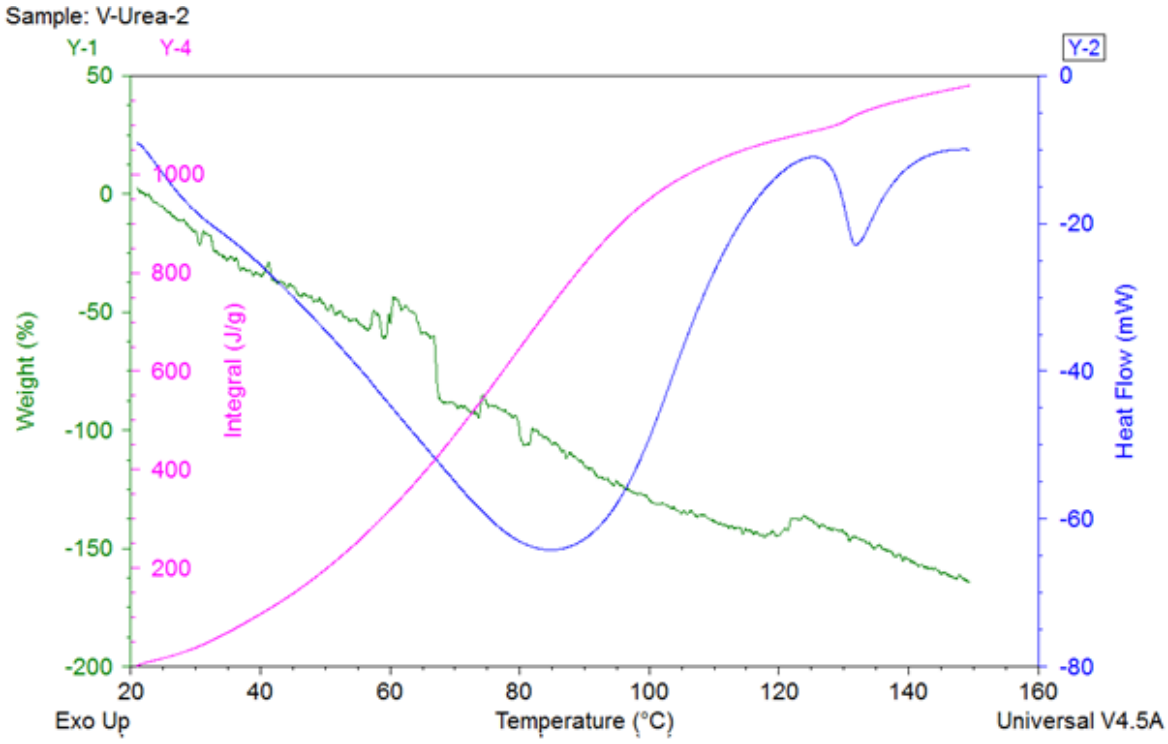

Sample: V-NaNO3
Y-1
Y-4
Y-2
Weight (%)
Integral (J/g)
Heat Flow (mW)
Exo Up
Temperature (°C)
Universal V4.5A


Sample: V-MgSO4+LiNO3+MgCl2-3
Y-1
Y-4
Y-2
Weight (%)
Integral (J/g)
Heat Flow (mW)
Exo Up
Temperature (°C)
Universal V4.5A

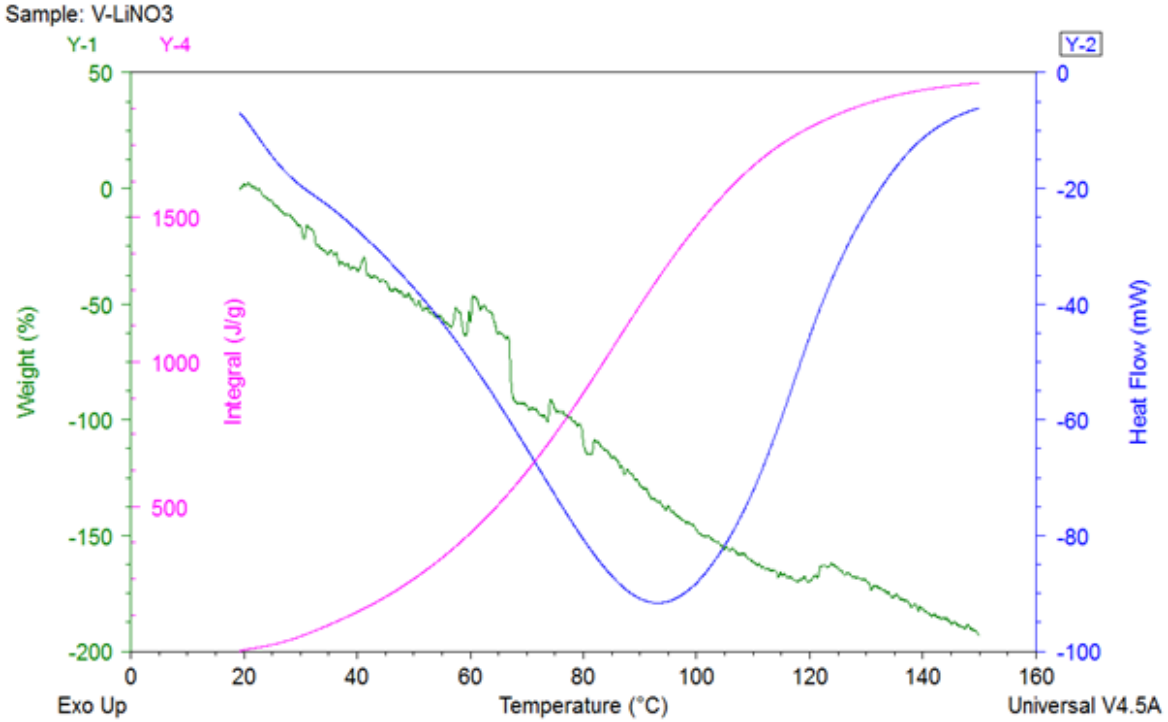
f. V-Urea


Sample: V-Urea
Y-1
Y-4
Y-2
Weight (%)
Integral (J/g)
Heat Flow (mW)
Exo Up
Temperature (°C)
Universal V4.5A

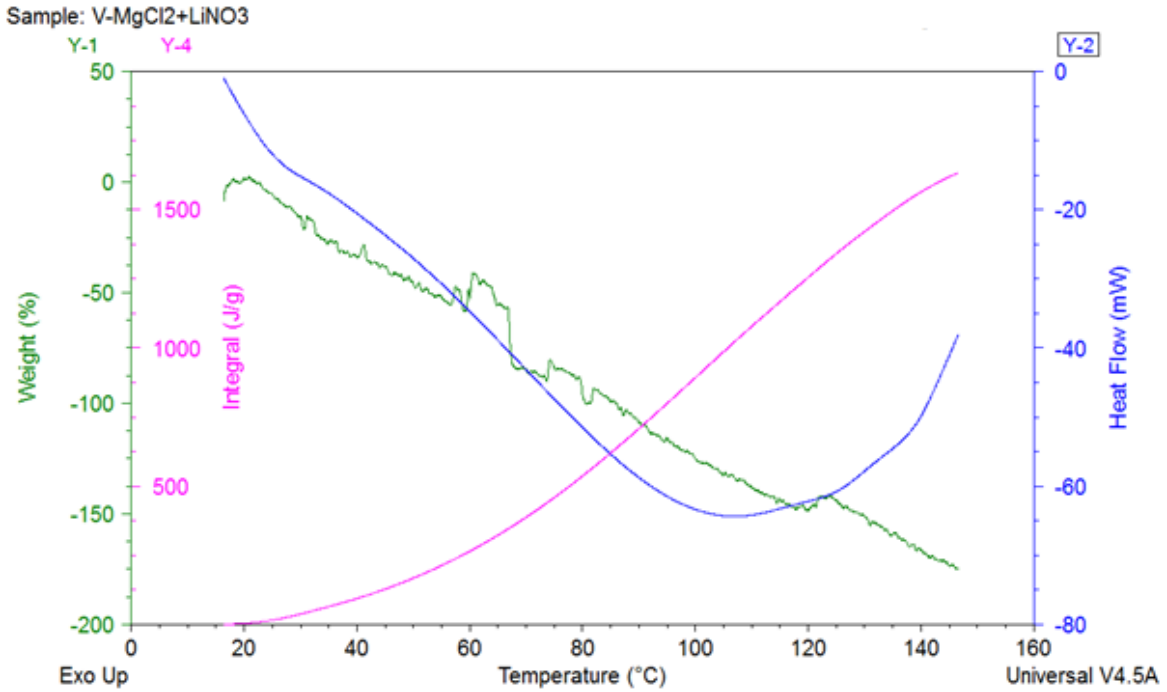

Sample: V-Urea -2
Y-1
Y-4
Y-2
Weight (%)
Integral (J/g)
Heat Flow (mW)
Exo Up
Temperature (°C)
Universal V4.5A

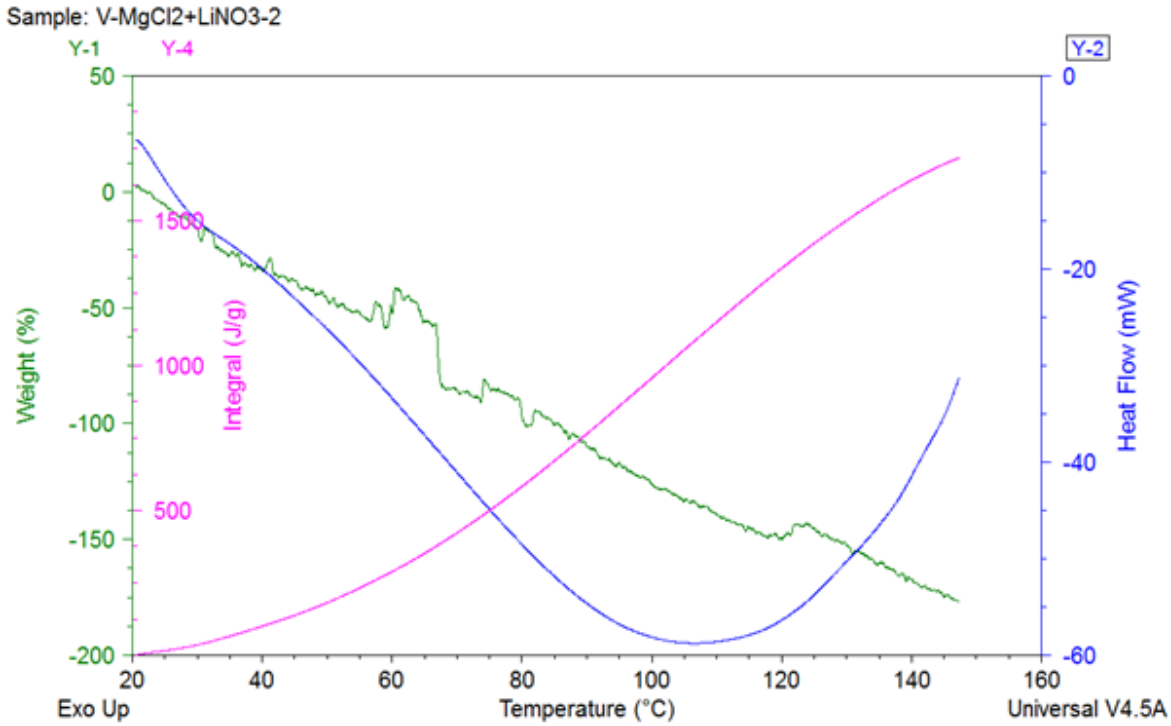

Sample: V-Urea-2
Y-1
Y-4
Y-2
Weight (%)
Integral (J/g)
Heat Flow (mW)
Exo Up
Temperature (°C)
Universal V4.5A

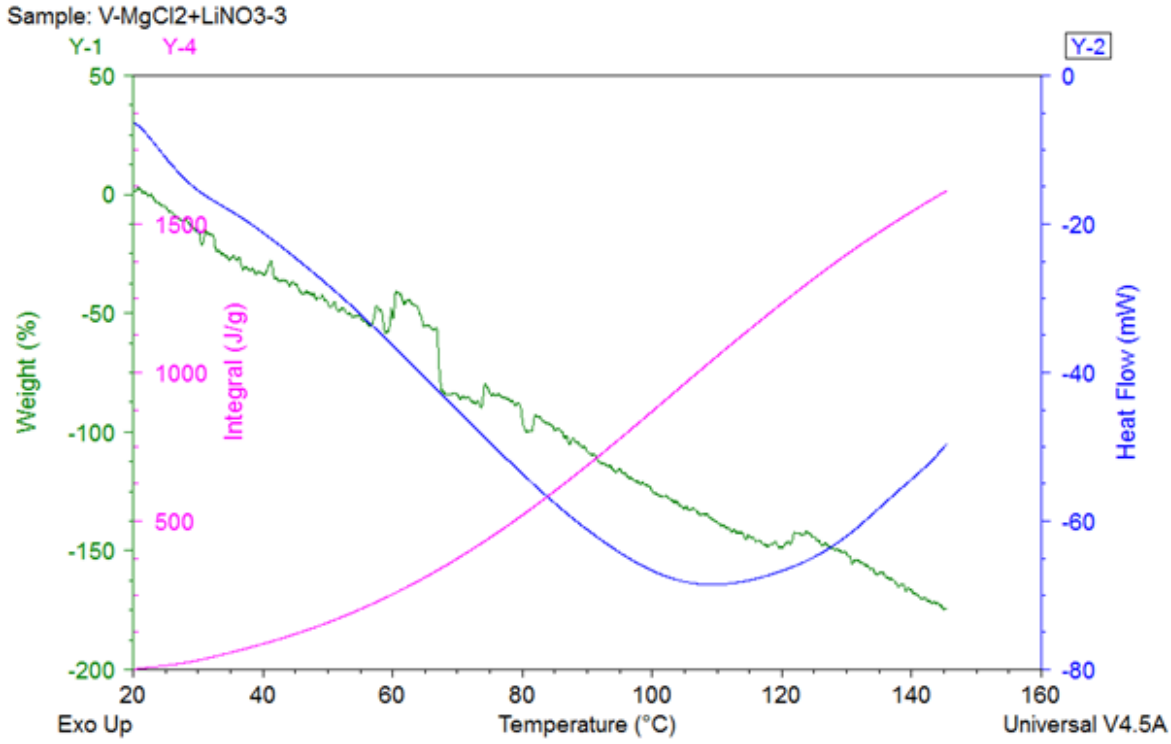
g. V-LiNO3


Sample: V-LiNO3
Y-1
Y-4
Y-2
Weight (%)
Integral (J/g)
Heat Flow (mW)
Exo Up
Temperature (°C)
Universal V4.5A

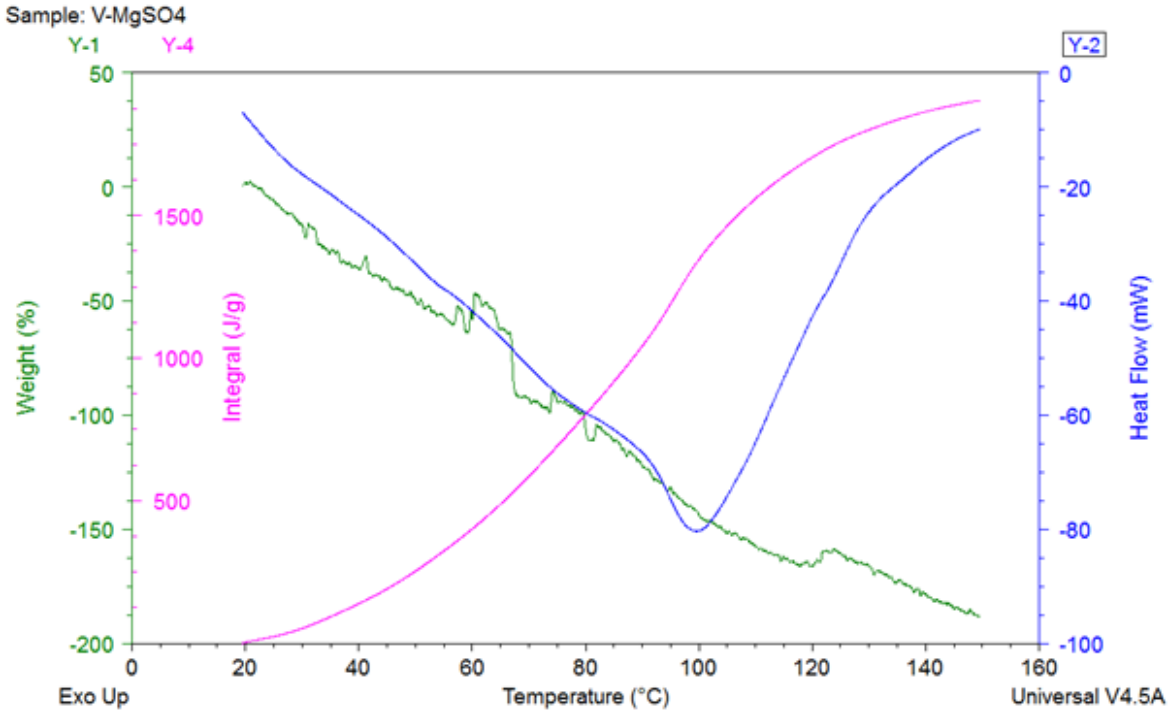
h. V-$MgCl_2$-$LiNO_3$



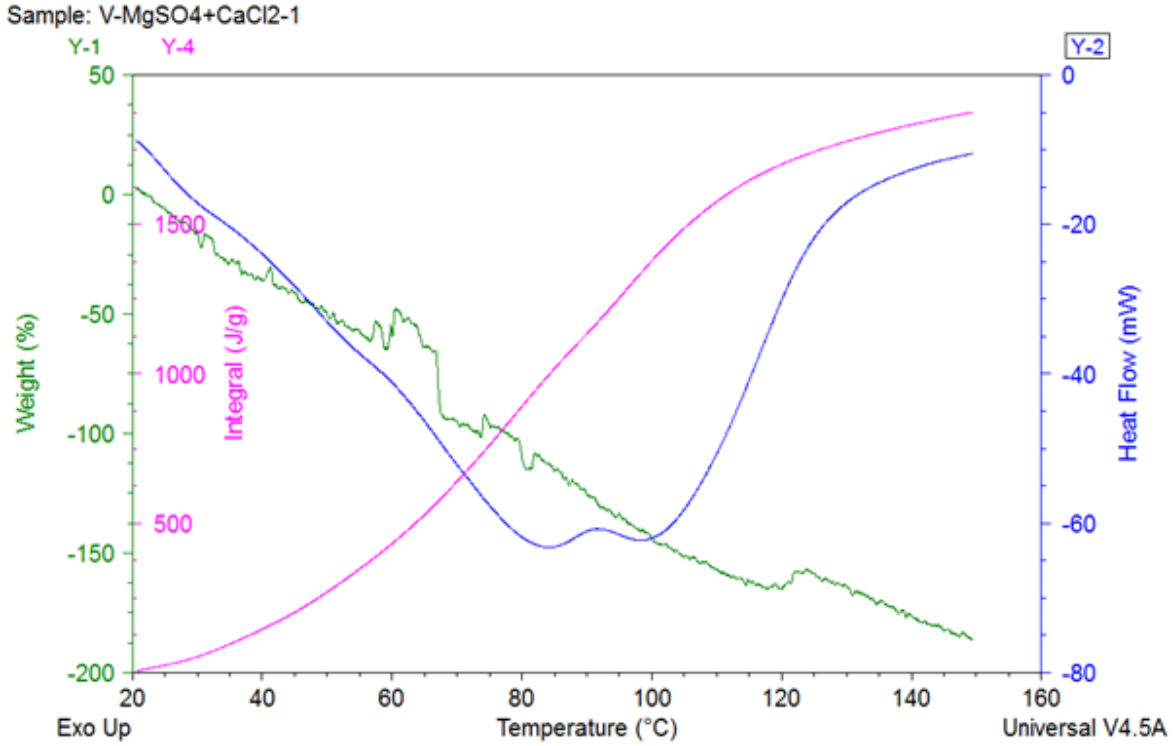


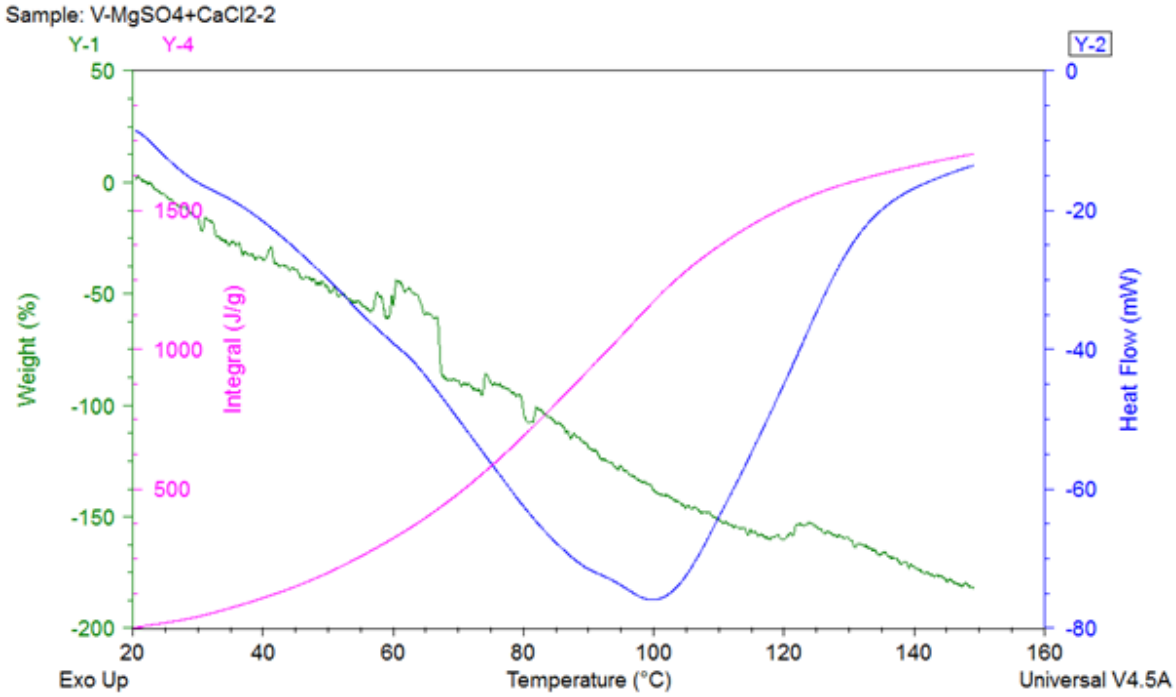

Sample: V-MgCl2+LiNO3-3
Y-1
Y-4
Y-2
Weight (%)
Integral (J/g)
Heat Flow (mW)
Exo Up
Temperature (°C)
Universal V4.5A

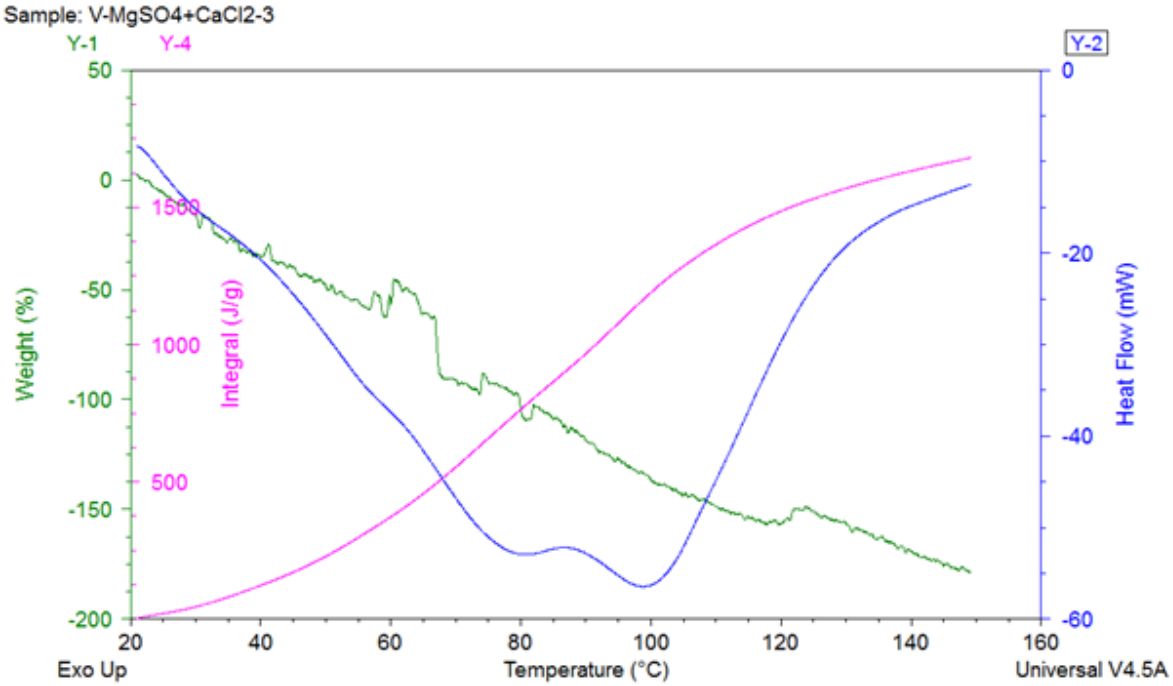
i. V-$MgSO_4$


Sample: V-MgSO4
Y-1
Y-4
Y-2
Weight (%)
Integral (J/g)
Heat Flow (mW)
Exo Up
Temperature (°C)
Universal V4.5A

j. V-$MgSO_4$-$CaCl_2$

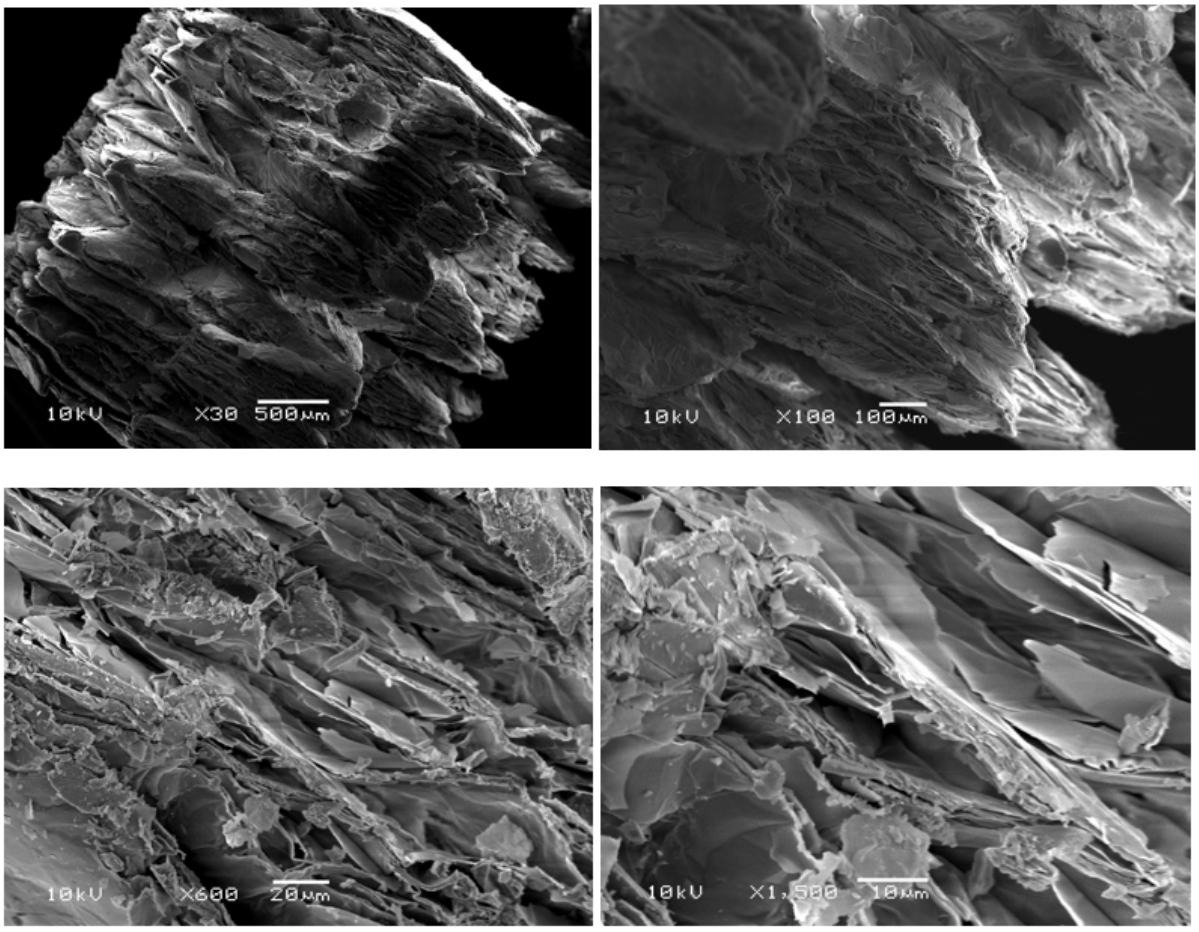




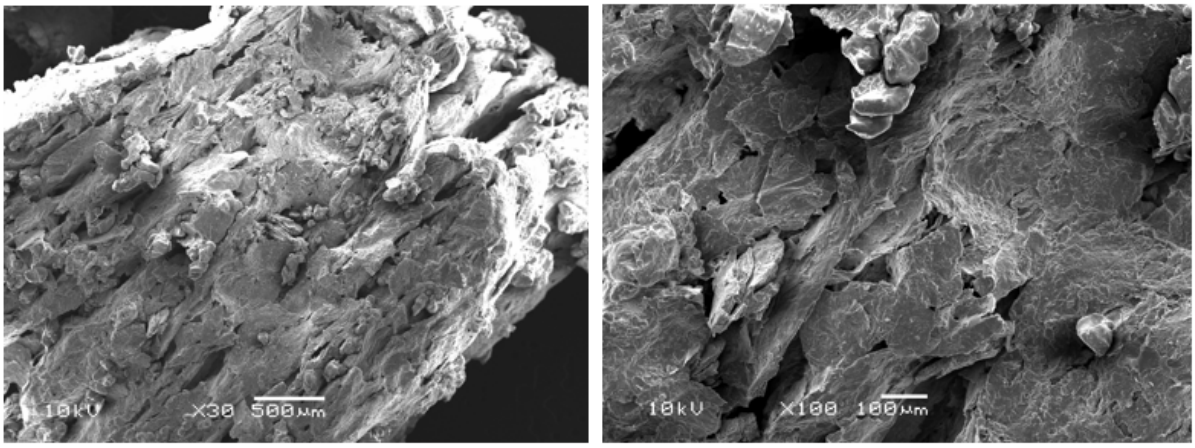

Sample: V-MgSO4+CaCl2-3
Y-1
Y-4
Y-2
50
0
-50
-100
-150
-200
1500
1000
500
Weight (%)
Integral (J/g)
0
-20
-40
-60
Heat Flow (mW)
20
40
60
80
100
120
140
160
Exo Up
Temperature (°C)
Universal V4.5A

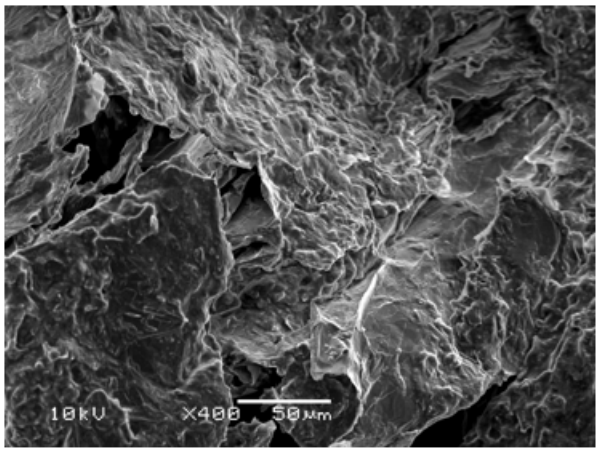
APPENDIX B: SCANNING ELECTRON MICROSCOPY PHOTOS

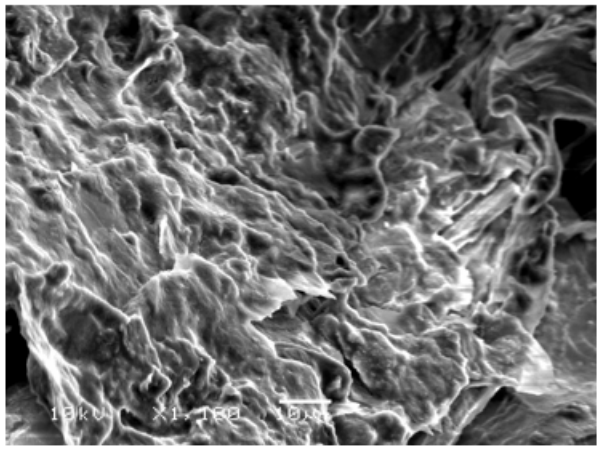
Vermiculite



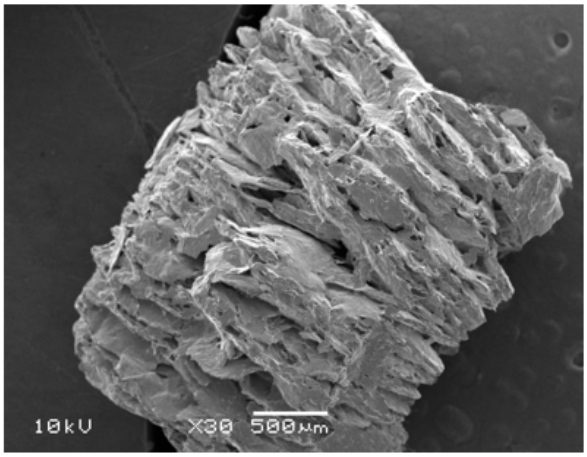
V-$MgSO_4$-$MgCl_2$

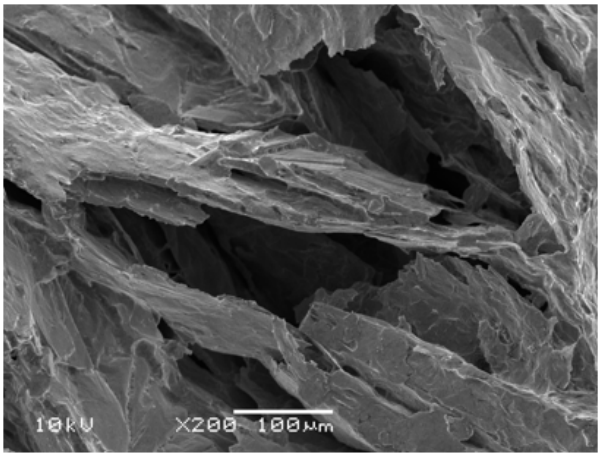


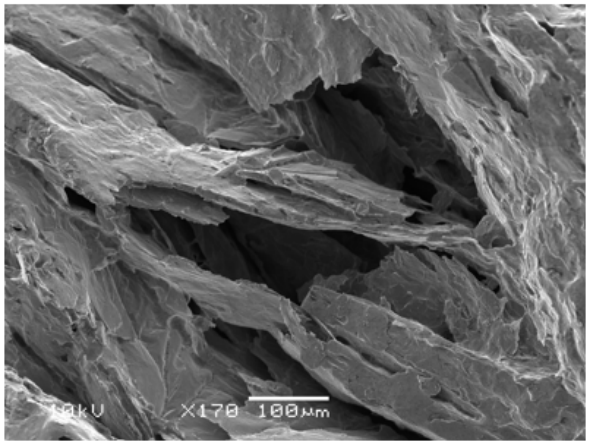

10kV X400 50µm

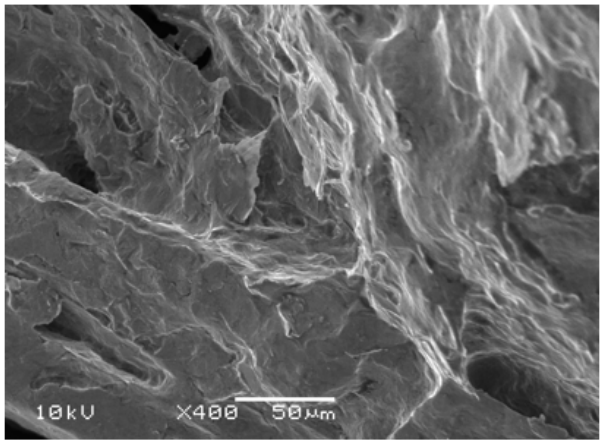


V-$CaCl_2$-LiCl

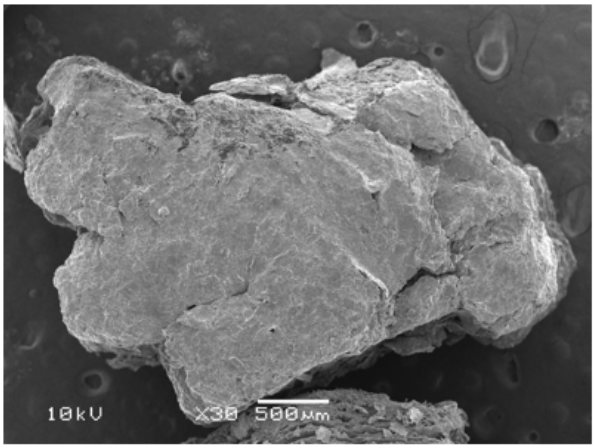

10kV X30 500µm

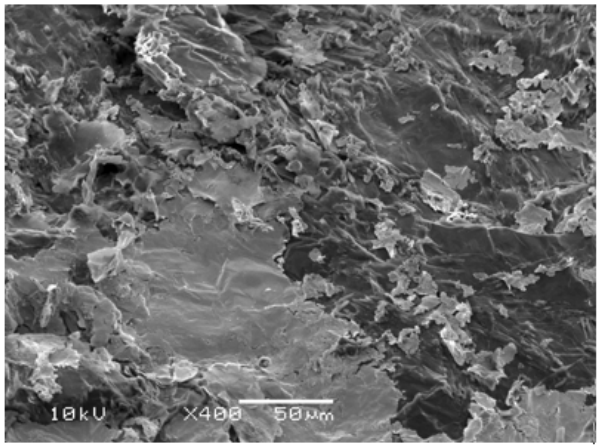

10kV X200 100µm


X170 100µm

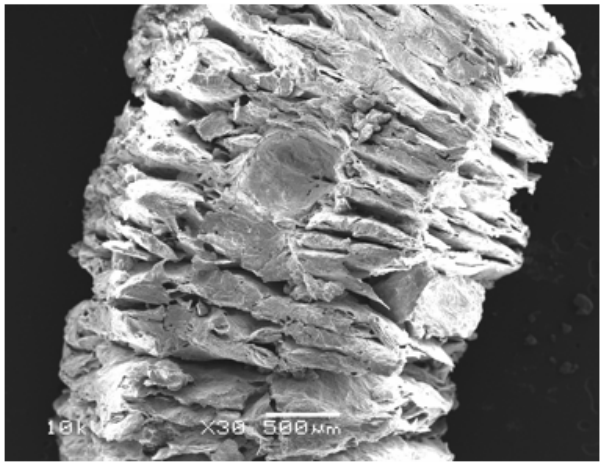

10kV X400 50µm

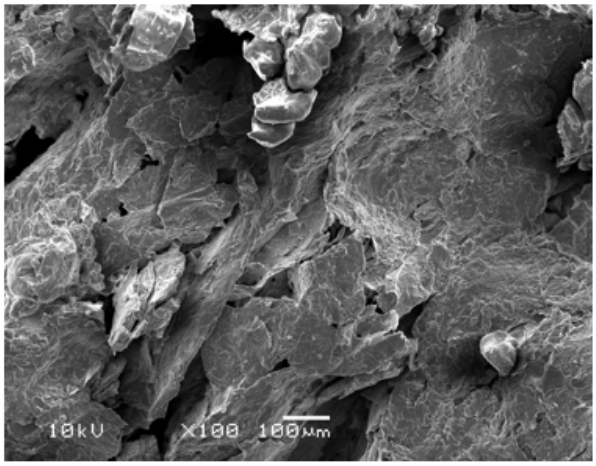
V-$LiNO_3$

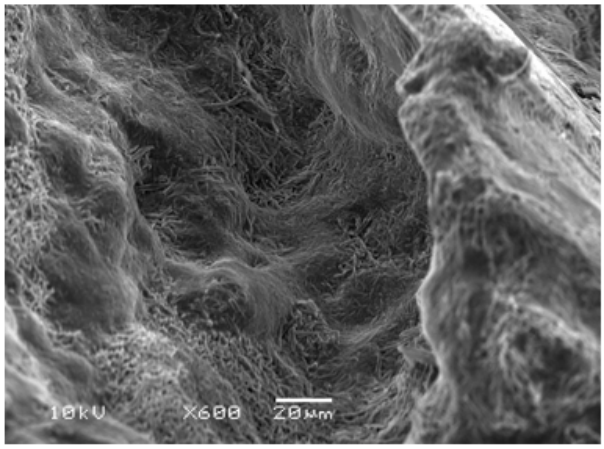


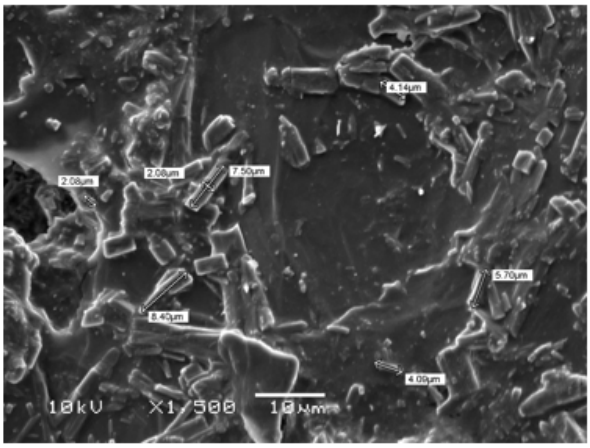


V-$MgSO_4$-$CaCl_2$

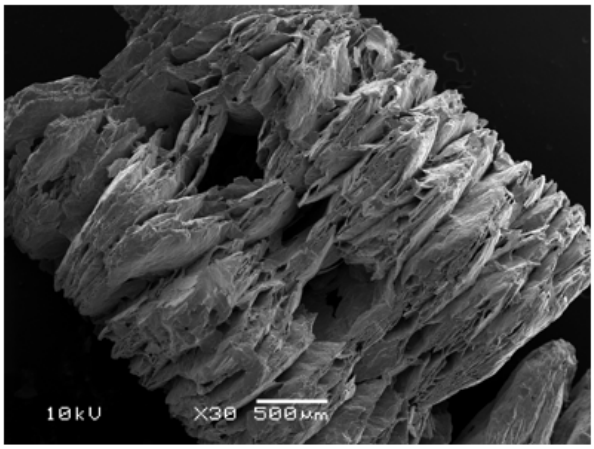


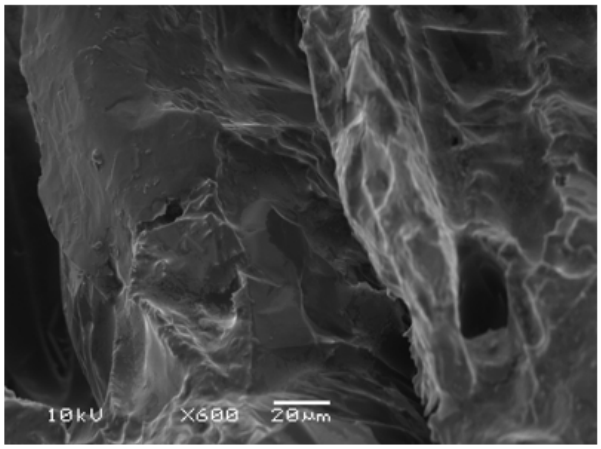




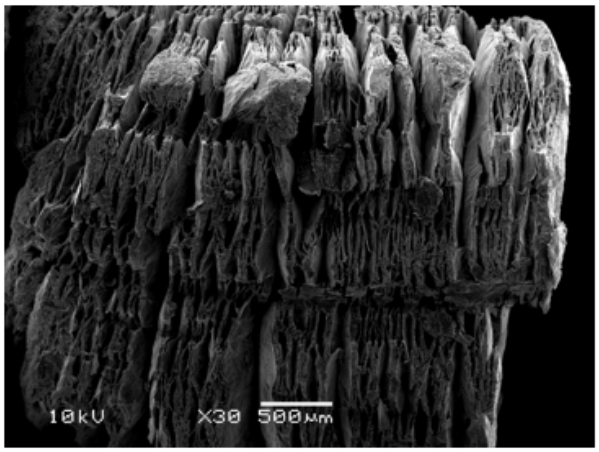


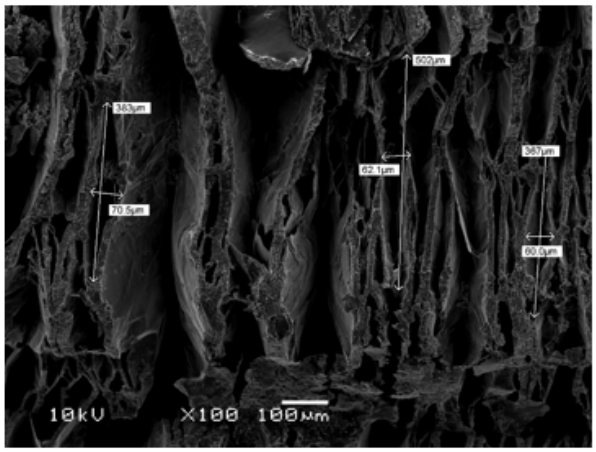
V-$CaCl_2$-$LiNO_3$

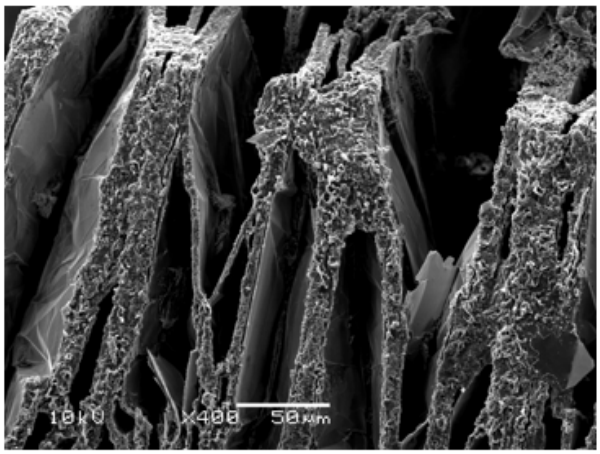


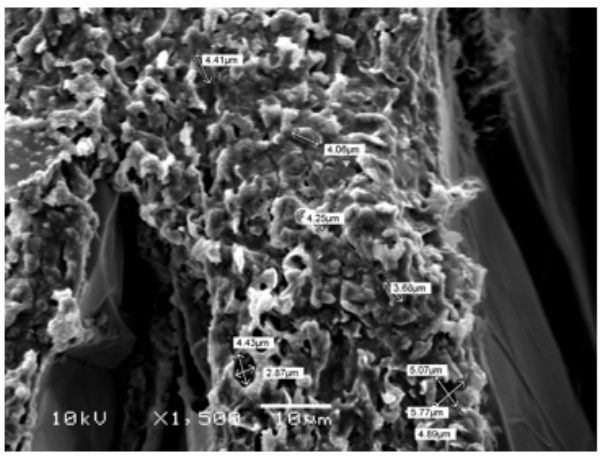


V-$MgSO_4$-$LiNO_3$









V-Urea

